MINERALIZATION IN THE KARMOY OPHIOLITE, SOUTHWEST NORWAY

JAMES L. SCOTT

NOTICE

The quality of this microform is heavily dependent upon the quality of the original thesis submitted for microfilming. Every effort has been made to ensure the highest quality of reproduction possible.

If pages are missing, contact the university which granted the degree.

Some pages may have indistinct print especially if the original pages were typed with a poor typewriter ribbon or if the university sent us an inferior photocopy.

Reproduction in full or in part of this microform is governed by the Canadian Copyright Act, R.S.C. 1970, c. C-30, and subsequent amendments.

AVIS

La qualité de cette microforme dépend grandement de la qualité de la thèse soumise au microfilmage. Nous avons tout fait pour assurer une qualité supérieure de reproduction.

S'il manque des pages, veuillez communiquer avec l'université qui a conféré le grade.

La qualité d'impression de certaines pages peut laisser à désirer, surtout si les pages originales ont été dactylographiées à l'aide d'un ruban usé ou si l'université nous a fait parvenir une photocopie de qualité inférieure.

La reproduction, même partielle, de cette microforme est soumise à la Loi canadienne sur le droit d'auteur, SRC 1970, c. C-30, et ses amendements subséquents.

MINERALIZATION IN THE KARMOY OPHIOLITE, SOUTHWEST NORWAY

by

James L. Scott

A thesis submitted in partial fulfillment of the requirements

for the degree of Master of Science

Department of Earth Sciences

Memorial University of Newfoundland

April, 1992

St. John's, Newfoundland

ISBN 0-315-73300-4

Canada

"I was trained to rape Mother Earth, and I fell in love with her instead."

Anon.

Frontispiece: Top- a view overlooking the Visnes Kobberverk.
Bottom- a panorama of the Feoy mine dump area.

Abstract

The Karmoy ophiolite is a remnant of Early Ordovician oceanic crust which is thought to have formed in a supra-subduction zone environment, and undergone development in a back-arc basin before its final emplacement on the Baltic craton. The uppermost sections of this ophiolite are exposed in the study area; the rock types are gabbros, sheeted dykes, plagiogranites, and lesser amounts of pillow lavas, diorites, volcaniclastic sediments, and breccias.

Contained within these rocks are two sulfide deposits, the Visnes massive Fe-Cu-Zn sulfide deposit and the Feoy massive Fe-Cu-Ni-PGE sulfide deposit. While they are spatially quite closely related, these deposits record two distinctly different periods of mineralization during the evolution of the ophiolite complex.

The Visnes deposit formed as a result of sub-seafloor alteration of basaltic rocks of the Visnes High Level Complex. Rocks of this complex are altered to spilites on a regional scale. Geochemically, alteration of the sheeted dykes is defined by: a relative loss of K2O, CaO, MnO, Al2O3, MgO, Cr, Ni, Cu, Zn, Pb and Sr; a relative gain of TiO2, Fe2O3, Na2O and Zr, and; variable changes in P2O5 and SiO2 relative to unaltered rocks from similar tectonic environments.

More local zones of intense alteration and mineralization within the sheeted dykes are called "epidosite zones", and these represent flowthrough zones for highly corrosive, magma-influenced hydrothermal fluids. "Epidotites", or deuterically formed rocks composed of nearly 100% coarse crystalline epidote, are closely associated with such zones, and their presence suggests that the hydrothermal fluids responsible for formation of epidosite zones may well have had a direct magmatic water input. However, oxygen isotope evidence from epidotites and plagiogranites suggest that the magmatic fluids may ultimately have been derived from magma-chamber assimilation of seawater-altered roof rocks.

The Feoy deposit is a small, orthomagmatic Ni-sulfide body which appears to have very few known analogues elsewhere in the world. Petrogenetic modelling using Platinum Group Element (PGE) abundances and sulfur isotopes indicates that the sulfides precipitated from an already-depleted partial melt during its ascent from a mantle source. The deposit is predominantly a massive pyrrhotite/chalcopyrite deposit with minor pyrite and pentlandite. It is unique in its high concentrations of Platinum Group Minerals (PGM's); this is a reflection of the PGE-enriched nature of the residual sulfide fraction present in an already-depleted (previously melted) mantle parent.

The co-magmatic silicate host rocks for the Feoy deposit are high-Mg basalt dykes, and these contain Ni-sulfides interstitial to silicate minerals. The host rocks can be petrogenetically modelled using PGE's, and as expected show PGE patterns indicative

of formation from a second stage melt, or from partial melting of an already-depleted mantle.

The Feoy deposit formed later than the Visnes deposit; rocks associated with the Visnes deposit are spilitized, and are dated at ca. 493ma (using Pb/Pb Zircon dating techniques); rocks associated with the Feoy deposit (high-Mg dykes, Type 2 plagiogranites and clinopyroxene-phyric intrusions in the Feoy area) are not spilitized, and are dated at ca. 470ma.

All rocks in the study area are variably altered and deformed. It appears that such deformation post-dates formation of both sulfide deposits as well, since they have both been mobilized along shear zones. Also, volcaniclastic sediments of the Torvastad Group, which are compositionally and genetically related to late clinopyroxene-phyric intrusions in the area, and which represent a period of arc-basin formation following arc-volcanism, are themselves quite deformed and cut by shear zones.

The occurrence of tourmaline-bearing breccias in the Feoy area is an intriguing addition to the study of late deformation features. Breccia, containing rounded Ni-sulfide and tourmalinite fragments in a hydrothermal cement matrix, is found in the Feoy area. Textural, isotopic and chemical analysis of the breccia and tourmaline strongly suggests that it formed as a result of the forceful intrusion of a hydrous granitic body into the surrounding country rocks. This may well represent part of the nearby West Karmoy Igneous Complex, which is a large granitic pluton that intrudes all rocks of the Karmoy ophiolite. Indeed, shear zone formation in the study area may also be related to this late, post-emplacement event.

Acknowledgements

Firstly, I thank Dr. J. Malpas for his continuous guidance during my undergraduate and graduate years, for his generous financial support of this project, and for his ongoing friendship. Without his help, this project could not have been completed.

R.B. Pedersen was a great help and a good friend during my field work in Norway. Thanks also go to Ann-Helen Rydland and her family for their generous hospitality during this time.

The assistence of G.Andrews, D. Healey, B. Gosse, Dr. F. Longstaffe, T. Brace, D. Williams, and B. Buckingham in analysis and compilation of chemical data, drafting and typing, is gratefully acknowledged.

Thanks also to Norsk Hydro for allowing access to old drill core and mine maps of the Visnes deposit.

Finally, I thank my family and my soon-to-be wife for making everything easier for me.

Table of contents

Frontispiece . . . . . Page i
Abstract. . . . . Page ii
Acknowledgements . . . . . Page iv
Table of contents. . . . . Page v
List of plates. . . . . Page viii
List of figures. . . . . Page xv
List of tables. . . . . Page xvii
List of appendices. . . . . Page xix
References . . . . . Page 200
Appendices . . . . . Page 209

Part A: Introduction, geology and petrology

Chapter 1: Introduction

1.1: Location and access. . . . . Page 1
1.2: Physiography and climate. . . . . Page 3
1.3: Previous work. . . . . Page 3
1.4: Aims of the present study. . . . . Page 5
1.5: Methods. . . . . Page 8
1.6: Terminology. . . . . Page 12
1.7: General geology of the Karmoy Ophiolite. . . . . Page 13
1.7.1: The East Karmoy Igneous Complex. . . . . Page 16
1.7.2: The Veavagen Igneous Complex. . . . . Page 16
1.7.3: The Visnes High Level Complex. . . . . Page 17
1.7.4: Regional patterns of deformation and metamorphism. . . . . Page 20

Chapter 2: Geology and petrology of the Visnes and Feoy regions

2.1: Introduction. . . . . Page 24
2.2: Sheeted dykes (the "Visnes dykes"), and associated rocks of the Karmoy Ophiolite . . . . . Page 26
2.2.1: The Visnes dykes. . . . . Page 26
2.2.2: Pillow lavas. . . . . Page 34
2.2.3: Gabbro. . . . . Page 40
2.2.4: Type 1 plagiogranite. . . . . Page 45
2.3: Type 2 plagiogranite. . . . . Page 50
2.4: High-Mg dykes, diorite, and related clinopyroxene-phyric intrusions . . . . . Page 53

2.4.1: High-Mg dykes. . . . . Page 53
2.4.2: Diorites. . . . . Page 57
2.4.3: Clinopyroxene-phyric intrusion. . . . . Page 59
2.5: Sediments. . . . . Page 59
2.6: Epidotites. . . . . Page 60
2.7: Late metamorphism and deformation features in the study area . . . . . Page 60
2.8: Summary and discussion of field relationships and petrology . . . . . Page 71

Chapter 3: The Visnes Fe-Cu-Zn massive sulfide deposit

3.1: Introduction . . . . . Page 74
3.2: Historical perspective. . . . . Page 78
3.3: Structural and stratigraphic relationships . . . . . Page 77
3.4: Metal content of the Visnes sulfides. . . . . Page 78
3.5: Ore petrology and geology. . . . . Page 81
3.6: Summary . . . . . Page 90

Chapter 4: The Feoy Fe-Cu-Ni-PGE sulfide deposit

4.1: Introduction. . . . . Page 93
4.2: Ore geology and petrography. . . . . Page 94
4.3: Metamorphism and deformation associated with the Feoy Ni sulfides . . . . . Page 111
4.3.1: Breccias. . . . . Page 111
4.3.2: Tourmaline and tourmalinite. . . . . Page 116
4.3.3: Leaching of PGE's from the Feoy Ni-sulfides. . . . . Page 122
4.3.4: Metamorphic textures in the Feoy Ni-sulfides. . . . . Page 123
4.4: Comparison of the Feoy and Visnes sulfide deposits . . . . . Page 126

Part B: Major oxide, trace element, PGE, oxygen and sulfur isotope chemistry

Chapter 5: Alteration geochemistry of the Visnes dykes

5.1: Introduction and literature review. . . . . Page 129
5.2: Alteration geochemistry. . . . . Page 130

Chapter 6: The origin and oxygen-isotopic tenor of epidotites and Type 1 plagiogranites, and their bearing on formation of the Visnes massive sulfide deposit

6.1: Literature review. . . . . Page 136
6.2: Oxygen isotopes from epidotites and Type 1 plagiogranites
. . . . . Page 141
6.3: Summary. . . . . Page 144

Chapter 7: PGE's, trace elements, sulfur isotopes, and their relationships to the petrogenesis of the Feoy Ni-sulfides and their host rocks

7.1: Introduction. . . . . Page 147
7.2: Classification of the Feoy Ni-sulfide deposit. . . . . Page 148
7.3: Petrogenetic considerations from other Ni-sulfide deposits
. . . . . Page 152
7.4: The geochemistry, PGE and sulfur-isotopic tenor of the Feoy Ni-sulfides and their host rocks. . . . . Page 163
7.4.1: Sulfur isotopes. . . . . Page 163
7.4.2: Ore geochemistry. . . . . Page 166
7.4.3: Co-magmatic host rock geochemistry. . . . . Page 174
7.5: Summary and discussion. . . . . Page 177

Chapter 8: Major oxide and oxygen isotope chemistry, and the origin of tourmaline and breccia occurrences in the Feoy area

8.1: Introduction: The origin of tourmaline. . . . . Page 180
8.2: Tourmaline field relationships. . . . . Page 181
8.3: Major element chemistry. . . . . Page 181
8.4: Oxygen isotopes. . . . . Page 186
8.5: The origin of the Feoy breccia. . . . . Page 190

Chapter 9: Summary and conclusions . . . . . Page 197

List of plates

Frontispiece: Top- a view overlooking the Visnes Kobberverk
Bottom- a panorama of the Feoy mine dump area. . . . . Page 1 .

Chapter 2

Plate 2.1: Alteration assemblages in the Visnes dykes. Epidote is dark green; chlorite is light green; quartz and albite are white; note also the black sphene and the small needles of apatite (magnification: 40X; plane polarized light, ppl)
. . . . . Page 29.

Plate 2.2: Alteration assemblages in "epidosite" zones in the Visnes dykes. Epidote is yellow brown; quartz is white; chlorite is green; pyrite is black (magnification: 40X; ppl). . . . . Page 29.

Plate 2.3: Alteration assemblages in "epidosites". Mineralogy as in Plate 2.2 (Magnification: 40X; ppl). . . . . Page 31.

Plate 2.4: Altered Visnes dyke sample showing relict clinopyroxene which is nearly completely altered to ferro-actinolite (magnification: 40X; crossed nicols, cn).
. . . . . Page 31.

Plate 2.5: A selectively mineralized and epidotized dyke, or "epidosite zone" from the Fiskdammen area of Visnes. The surrounding country rock is neither mineralized nor heavily altered. . . . . Page 32.

Plate 2.6: Epidote and quartz veins, or "streamers", running parallel to the strike of sheeted dykes in the Visnes region. . . . . Page 32.

Plate 2.7: Epidotite veins or "streamers" cutting basalt dykes in the Visnes region. Note the hammer handle for scale. . . . . Page 33.

Plate 2.8: Epidotite "streamers" running parallel to the strike of sheeted basalt dykes in the Dyrnes area of Visnes. Note hammer handle for scale.
. . . . . Page 33.

Plate 2.9: Plastically deformed Type 1 plagiogranite xenoliths in basalt dyke in the Dyrnes area of Visnes. Xenoliths are about 0.5m in length. . . . . Page 35.

Plate 2.10: Plastically deformed Type 1 plagiogranite xenolith in a basic dyke. Dyrnes, Visnes. . . . . Page 35.

Plate 2.11: Plastically deformed epidotite xenolith in the Dyrnes area of Visnes. . . . . Page 36.

Plate 2.12: Plastically deformed epidotite xenolith in Dyrnes area, Visnes. Note the tiny trail of epidotite "spherules" which rims the xenolith nearest the hammer. . . . . Page 36.

Plate 2.13: An outcrop of pillow lavas in the Visnes region. . . . . Page 38.

Plate 2.14: Outcrop of pillow breccia in plagiogranitic matrix. From one of the nearby offshore skerries in the Visnes area. . . . . Page 38.

Plate 2.15: Highly altered, corroded and mineralized pillow lavas in a matrix of quartz and epidote. From the Visnes area. . . . . Page 39.

Plate 2.16: Highly altered pillow lavas rimmed by quartz and epidote. From the northern Visnes area. . . . . Page 39.

Plate 2.17: Epidotite "segregations" in pegmatitic gabbro. Note the gradational nature of the contact between the coarse grained epidotite and the surrounding gabbro. From the Feoy area. . . . . Page 41.

Plate 2.18: Epidotite "segregations" in coarse to pegmatitic hornblende gabbro. From the Feoy area. . . . . Page 41.

Plate 2.19: Stockwork-type pyrite and chalcopyrite veins which cut melanocratic gabbro. Taken from the Visnes region. . . . . Page 43.

Plate 2.20: Stockwork-type pyrite and chalcopyrite veinlets which cut melanocratic gabbro. Taken from the Visnes region. . . . . Page 43.

Plate 2.21: Plagioclase phenocrysts in gabbro pegmatite. The plagioclase has well developed core to rim saussuritization, and is set in a matrix of quartz and albite intergrowth (magnification: 40X; ppl). . . . . Page 44.

Plate 2.22: Plate 2.21 photographed under crossed nicols to illustrate nucleation of the quartz-albite intergrowths on the rim of the plagioclase phenocryst (magnification: 40X; cn). . . . . Page 44.

Plate 2.23: Photomicrograph of graphic quartz-albite intergrowth (magnification: 40X; cn). . . . . Page 47.

Plate 2.24: Diorite dyke crosscutting Type 1 plagiogranite in the Fiskdammen area, Visnes region. Note the presence of abundant immiscible "spherules" within the diorite dyke . . . . . Page 47.

Plate 2.25: Epidotite veins rimming the contact between plagiogranite and diorite in the Fiskdammen area, Visnes. The contact between the epidotite and plagiogranite here is quite sharp. . . . . Page 48.

Plate 2.26: Photomicrograph of the "spherules" seen in Plate 2.24. The core of the spherules is composed of quartz-albite intergrowths, while the dark brown rim is composed of coarse epidote (magnification: 40X; ppl). . . . . Page 48.

Plate 2.27: Same as Plate 2.26 photographed under crossed nicols (magnification: 40X; cn). . . . . Page 49.

Plate 2.28: Photomicrograph of Type 2 plagiogranite illustrating fluxioned quartz-albite groundmass with an overprint of biotite and hornblende (magnification: 40X; cn). . . . . Page 49

Plate 2.29: Metamorphic biotite overprint on Type 2 plagiogranite (magnification: 40X; ppl). . . . . Page 52.

Plate 2.30: High-Mg dyke sample illustrating Ni-sulfides "interstitial" to actinolite (after clinopyroxene)-chlorite groundmass (magnification: 40X; ppl) . . . . . Page 52.

Plate 2.31: Large (up to 3cm) tourmaline crystals along microfractures, cracks and dyke margins in basic dykes. From the Feoy area. . . . . Page 55.

Plate 2.32: Quartz and tourmaline filling tension gashes in basic dykes in the Feoy area. . . . . Page 55.

Plate 2.33: Large (up to 2cm in length) actinolite porphyroblasts in a groundmass of chlorite and actinolite. From a high-Mg dyke sample from the Feoy area (magnification: 20X; ppl). . . . . Page 56

Plate 2.34: Photomicrograph illustrating alteration assemblage in diorites from the Visnes area. Note abundant actinolite (yellow/brown), and chlorite (green) (magnification: 20X; cn). . . . . Page 56.

Plate 2.35: Photomicrograph of epidotite "segregation" in gabbro pegmatite from the Feoy area. Note the relatively fresh, coarse grained and euhedral epidote crystals in an unaltered interstitial quartz matrix (magnification: 30X;cn) . . . . . Page 62

Chapter 3

Plate 3.1: A view of the remains of the old smelting house in the Visnes area. . . . . Page 76.

Plate 3.2: Hand sample of massive, banded pyrite-sphalerite-chalcopyrite ore from the Visnes Kobberverk. . . . . Page 76.

Plate 3.3: Photomicrograph of sample in Plate 3.2. Note pyrite cubes (white) with interstitial chalcopyrite (yellow) and sphalerite (grey) (magnification: 10X; reflected light, rl). . . . . Page 82.

Plate 3.4: Hand sample of massive, banded pyrite-sphalerite ore from Visnes Kobberverk. . . . . Page 82.

Plate 3.5: Photomicrograph of sample in Plate 3.4. Note the embayment of pyrite cubes (white) by sphalerite (grey) (magnification: 10X; rl). . . . . Page 83.

Plate 3.6: Annealed texture in massive pyrite from Visnes Kobberverk. Note yellow interstitial chalcopyrite (yellow) (magnification: 10X; rl). . . . . Page 83.

Plate 3.7: Tectonic fabric in massive sphalerite ore from Visnes Kobberverk. Sphalerite is light grey, and it is strongly alligned from left to right (magnification: 10X; rl). . . . . Page 85.

Plate 3.8: Actinolite-pyrite schist. Taken from main shear zone in the Visnes Kobberverk area (magnification: 10X; ppl). . . . . Page 85.

Plate 3.9: Fe-rich "Vasskis", which is thought to represent ancient seafloor chemical precipitates from "black smokers". The Vasskis is contained in a highly altered, silicified basalt dyke sample in this section (magnification: 10X; ppl) . . . . . Page 88.

Plate 3.10: Pyrite-chalcopyrite assemblages intensely veined and corroded by quartz. The chalcopyrite may have replaced the pyrite along cracks (magnification and scale at base of photograph). . . . . Page 88.

Plate 3.11: Hand sample of highly deformed, folded sphalerite layer (brown) in calcite. . . . . Page 91.

Plate 3.12: Photomicrograph of trace amounts of galena (Pb) in massive pyrite and sphalerite (sp) (magnification and scale at base of photograph). . . . . Page 91.

Chapter 4

Plate 4.1: Well developed annealed texture (with triple point grain boundary angles approaching 120 degrees) in massive, pyrrhotite ore from the Feoy area (magnification: 10X; reflected light, rl). . . . . Page 97.

Plate 4.2: Exsolution "flames" of pentlandite (cream coloured) in massive pyrrhotite (grey) and chalcopyrite (yellow) (magnification: 40X;rl). . . . . Page 97.

Plate 4.3: "Durchbewegung" texture, illustrating cataclastic deformation of pyrrhotite (white), along with abundant amphibole (black) (magnification and scale at base of photograph). . . . . Page 98.

Plate 4.4: Magnetite (dark grey), pyrite (light grey), and hematite (black) in massive pyrrhotite ore from Feoy. The magnetite has formed as a result of the decomposition of pyrite, while the hematite is an alteration product of magnetite (magnification and scale at the base of photograph). . . . . Page 98.

Plate 4.5: Remobilized chalcopyrite (yellow) interstitial to amphibole in highly deformed pyrrhotite-chalcopyrite ore sample from the Feoy area (magnification: 3.2X; rl). . . . . Page 100.

Plate 4.6: Pyrite porphyroblast rimmed and corroded by chalcopyrite (yellow) and magnetite (dark grey). Note the inclusions of chalcopyrite and magnetite in the pyrite porphyroblast (magnification: 3.2X; rl). . . . . Page 100.

Plate 4.7: Blocky, altered pentlandite crystals (dark grey, at center) in massive pyrrhotite-chalcopyrite ore from Feoy (magnification and scale at base of photograph). . . . . Page 103.

Plate 4.8: Highly altered pentlandite veins (dark grey with cream coloured cores) cutting and rimming massive pyrrhotite (light grey) (magnification and scale at base of photograph). . . . . Page 103.

Plate 4.9: Pentlandite which has been heavily altered to violarite. The dark brown violarite rims fresh, cream coloured cores of pentlandite. The surrounding material is pyrrhotite (white) and chalcopyrite (yellow) (magnification: 10X; rl). . . . . Page 104.

Plate 4.10: Tiny grain of chromite in a pyrite grain. This is in a massive pyrrhotite ore sample from Feoy (magnification and scale at base of pho tograph). . . . . Page 104.

Plate 4.11: A scanning electron photomicrograph of a Platinum Group Mineral (PGM), probably michenerite, in massive pyrrhotite from Feoy (magnification and scale at base of photograph). . . . . Page 107.

Plate 4.12: A euhedral grain of temagamite (Pd3HgTe3) in massive pyrrhotite from Feoy (magnification and scale at base of photograph). . . . . Page 107.

Plate 4.13: Temagamite grain (bright white, at center) in highly deformed amphibole (black)-pyrrhotite (white) assemblage (magnification and scale at base of photograph). . . . . Page 108.

Plate 4.14: Michenerite grain in massive pyrrhotite from Feoy (magnification and scale are at the base of photograph). . . . . Page 108.

Plate 4.15: Kotulskite (PdTe) and probable hessite (Ag2Te) grains in tourmaline-pyrrhotite assemblage from Feoy (magnification and scale at base of photograph). . . . . Page 109.

Plate 4.16: Photograph of Type A breccia from the Feoy mine dump. Note the large, rounded tourmalinite fragment at right, and the sub-rounded, massive pyrrhotite fragment at left (brown). At the top of this sample is an elongate fragment of Type 2 plagiogranite. The matrix material is mainly chlorite and calcite. Note the pen for scale. . . . . Page 109.

Plate 4.17: Type A breccia sample. The black areas at far left and far right are zones of tourmalinization. Close observation of the cement material in this sample reveals abundant tourmaline in the matrix. . . . . Page 113.

Plate 4.18: Quartz-tourmaline vein assemblages from the Feoy mine dump. Large (up to 3cm long), black, radially disposed tourmaline crystals are intergrown with coarse grained quartz in these samples. . . . . Page 113.

Plate 4.19: Photograph of Type B breccia from the Feoy mine dump. Note the massive pyrite fragments in a quartz-calcite (minor chlorite) matrix . . . . . Page 114.

Plate 4.20: Fresh, euhedral tourmaline crystals (dark and pale blue) set in a matrix of calcite (white) and chlorite (light green). Note the growth lines in the tourmaline at upper right (magnification: 20X; ppl). . . . . Page 114.

Plate 4.21: Schistose tourmalinite fragment. Sample consists of 100% tourmaline which has been deformed and metamorphosed to tourmaline schist. Note the dark band which is in the center of the photograph, which is a kink band (magnification: 20X; cn). . . . . Page 119.

Plate 4.22: Pyrrhotite along growth lines in tourmaline (magnification and scale are given at the base of photograph). . . . . Page 119.

Plate 4.23: Randomly orientated tourmaline from tourmalinite sample (magnification: 20X; ppl). . . . . Page 120.

Plate 4.24: Tourmaline (green) from tourmalinite sample being dissected by pyrrhotite and chalcopyrite (black) (magnification: 20X; ppl). . . . . Page 120.

Plate 4.25: Fresh, euhedral tourmaline set in a matrix of chalcopyrite and pyrrhotite (magnification and scale at base of photograph). . . . . Page 121.

Plate 4.26: Massive pyrrhotite-chalcopyrite ore sample from Feoy. Note the highly deformed nature of this sample, with strong chalcopyrite banding. Pen top for scale. . . . . Page 121.

Plate 4.27: Photomicrograph of amphibole porphyroblast being replaced by tourmaline (blue-white). From high-Mg dyke sample from Feoy (magnification: 20X; cn) . . . . . Page 125.

Plate 4.28: Tourmaline "sun", from Type A breccia sample from Feoy. Note abundant inclusions of pyrrhotite present in the tourmaline crystals (magnification: 20X; cn). . . . . Page 125.

List of figures

Chapter 1

Figure 1.1 (a and b): Location maps of Visnes and Feoy regions. . . . . Page 2

Figure 1.2: Geological map of the Karmoy Ophiolite Complex (Pedersen and Malpas, 1984). . . . . Page 14

Figure 1.3: Comparison of the Visnes (Type 1) and East Karmoy plagiogranites (Pedersen and Malpas, 1984). . . . . Page 19

Chapter 2

Figure 2.1 (a and b): Geological maps of the Visnes and Feoy areas. . . . . Page 25

Figure 2.2 (a and b): Comparison of epidotites of the study area with "epidosites" from Troodos (data from Aldiss, 1978), and with ideal epidote (data from Deer et al., 1963) compositions. . . . . Page 63

Figure 2.3: Sketch of epidotite vein containing a "rind" of euhedral pyrite cubes(pyrite cubes are represented by black dots). From an offshore skerrie in the Visnes region. . . . . Page 65

Chapter 5

Figures 5.1.1 to 5.1.10: Major oxides (in wt. %) versus Na2O/Na2O+CaO for: 1- the Visnes dykes; 2- the high-Mg dykes of Feoy; 3-typical unaltered island arc tholeiites (data from Basaltic Volcanism Study Project, 1981); 4- the field for 231 spilitized basalts of an island arc tholeiitic nature (data from Stevens, 1980); 5- an average of 66 typical unaltered MORB samples (data from Engel et al., 1965; Cann, 1969; Engel and Engel, 1970; Shido et al., 1971); 6- the average compositions of 32 typical unaltered boninites (data from Hamlyn and Keays, 1986). . . . . Page 131

Figures 5.2.1 to 5.2.8: Trace elements (in ppm) versus Na2O/Na2O+CaO for rock suites 1 through 6 in Figure 5.1 (symbols as in Figure 5.1). . . . . Page 132

Chapter 6

Figure 6.1: Comparison of continental granophyres with plagiogranites (data from Coleman and Peterman, 1975). . . . . Page 138

Chapter 7

Figure 7.1: Histogram of average sulfur isotope values from selected orthomagmatic Ni sulfide deposits (after Naldrett, 1981a; data for Bruvann is from Boyd and Mathieson, 1979; data for Feoy is from present study).
. . . . . Page 164

Figures 7.2(a and b): Cu, Ni, Pt and Pd relations for sulfides of the Feoy deposit, compared with data for Ni-sulfides from various other environments (data for all deposits except Visnes is from Naldrett, 1981a). . . . . Page 170

Figures 7.3 (a and b): C1-chondrite normalized PGE patterns for the Feoy sulfides, along with patterns for other Norwegian Ni-sulfide deposits, and patterns for Ni sulfides from various other tectonic environments (data for Norwegian deposits other than Feoy is from Barnes et al., 1987; data for Feoy is from the present study; data for all other deposits is from Naldrett and Duke, 1980). . . . . Page 173

Figure 7.4: Pd-Ir relations for high-Mg and Visnes dyke samples from the study area, along with fields for typical MORB and low-Ti Lavas (data for MORB and low Ti Lavas fields from Hamyln et al., 1985). . . . . Page 175

Chapter 8

Figure 8.1: Chemical disparity between tourmaline from Feoy and tourmaline from massive sulfide and granite related environments (data for all areas except Feoy from Taylor and Slack, 1984). . . . . Page 185

Figures 8.2 and 8.3: Oxygen isotope relations for tourmaline and quartz assemblages from the study area, along with data from massive sulfide and granite related environments (data from all areas except Feoy from Taylor and Slack, 1984).
. . . . . Page 188

Chapter 9

Figure 9.1: Schematic diagram with annotations illustrating the complex evolutionary history of the Feoy and Visnes sulfide deposits . . . . . Page 197

List of Tables

Chapter 2

Table 2.1: Comparison of whole rock major oxide, Cu, Zn, Ni and Cr analyses of the Visnes epidotites with "epidosites" from Troodos and Visnes, and with ideal epidote analyses from Deer, Howie and Zussman (1962) (data for Troodos rocks is from Aldiss, 1978). . . . . Page 66

Table 2.2: Summary of epidote and epidotite occurrences in the study area. . . . . Page 68

Chapter 3

Table 3.1: Whole rock geochemical analyses of selected ore samples from the Visnes massive sulfide deposit. . . . . Page 80

Chapter 4

Table 4.1: Platinum Group Minerals found in the Feoy Ni-sulfides. . . . . Page 110

Chapter 6

Table 6.1: Oxygen isotopic tenor of selected rocks from the Troodos ophiolite (data for Troodos samples is from Heaton and Sheppard, 1977), and from the Visnes region. . . . . Page 142

Table 6.2: Major oxide analyses of Type 1 plagiogranites from the Visnes region, along with selected analyses from Aldiss (1978) for plagiogranites from the Troodos ophiolite in Cyprus. . . . . Page 145

Chapter 7

Table 7.1: Classification of Ni-sulfide deposits from various geological environments (modified after Naldrett, 1981a). . . . . Page 149

Table 7.2: The geochemistry of massive Ni-sulfide samples from Feoy, along with data from several other Ni-sulfide deposits (data sources are the same as in Figure 7.1).

. . . . . Page 167

Chapter 8

Table 8.1: Electron microprobe analyses of tourmaline from the Feoy area (data from the present study), along with data from selected massive sulfide related tourmaline occurrences (data from Taylor and Slack, 1984).
. . . . . Page 182

Table 8.2: Chemical disparities between tourmaline from Feoy and tourmaline from granite-related (Portugese granite data from Neiva, 1974; English granite data from Power, 1968) and massive sulfide-related (data from Taylor and Slack, 1984) environments. . . . . Page 187

Table 8.3: Oxygen isotope values of tourmaline and quartz from Feoy.
. . . . . Page 187

Table 8.4: General characteristics of ore-related breccias in volcano plutonic arcs (after Sillitoe, 1985). . . . . Page 192

List of appendices

Appendix 1: Accuracy data for major element analyses of the Visnes dykes. . . . . Page 209

Appendix 2: Microprobe analyses of chlorite and amphibole from rocks of the study area. . . . . Page 211

Appendix 3: Major and trace element analyses of the Visnes dykes (1 to 23), the high-Mg dykes (24 to 28), and selected basalts from various tectonic environments (29 and 30 are typical unaltered island arc tholeiites, IAT; 31 to 33 are spilites of an IAT nature; 34 is average unaltered MORB composition; 35 is average unaltered boninite composition; data sources are given in text). . . . . Page 212

Appendix 4: Sample descriptions for rock samples which were used in the present study. . . . . Page 218

Part A: Introduction, geology and petrology

Chapter 1: Introduction

1.1: Location and access

The Visnes and Feoy regions are part of the island of Karmoy in southwest Norway (Figure 1.1). The town of Visnes is easily accessible by automobile and ferry, and is about three hours drive south from Bergen, the nearest city. The largest town in the immediate area is Haugesund, which is approximately 30km's drive from Visnes. There is a large airfield in the Visnes area which serves Haugesund, and daily flights are available to and from Bergen and Oslo.

The Visnes region is an area of approximately three square kilometers comprising the northwest section of the island of Karmoy (Figure 1.1.). The area has a population of about 2000, with small scale farming and fishing as the main industries. In earlier, more prosperous times, the Visnes copper mine was very productive, and the population was considerably larger. The copper mine has not been worked for over 15 years.

The Feoy area (Figure 1.1) includes a cluster of about 4 islands, with many more smaller skerries, situated about 1.5 km northwest of Visnes. Feoy is a sparsely populated fishing community which is accessible only by boat. The Feoy Ni-sulfide occurrence was mined on a small scale from the 1890's to the 1920's.

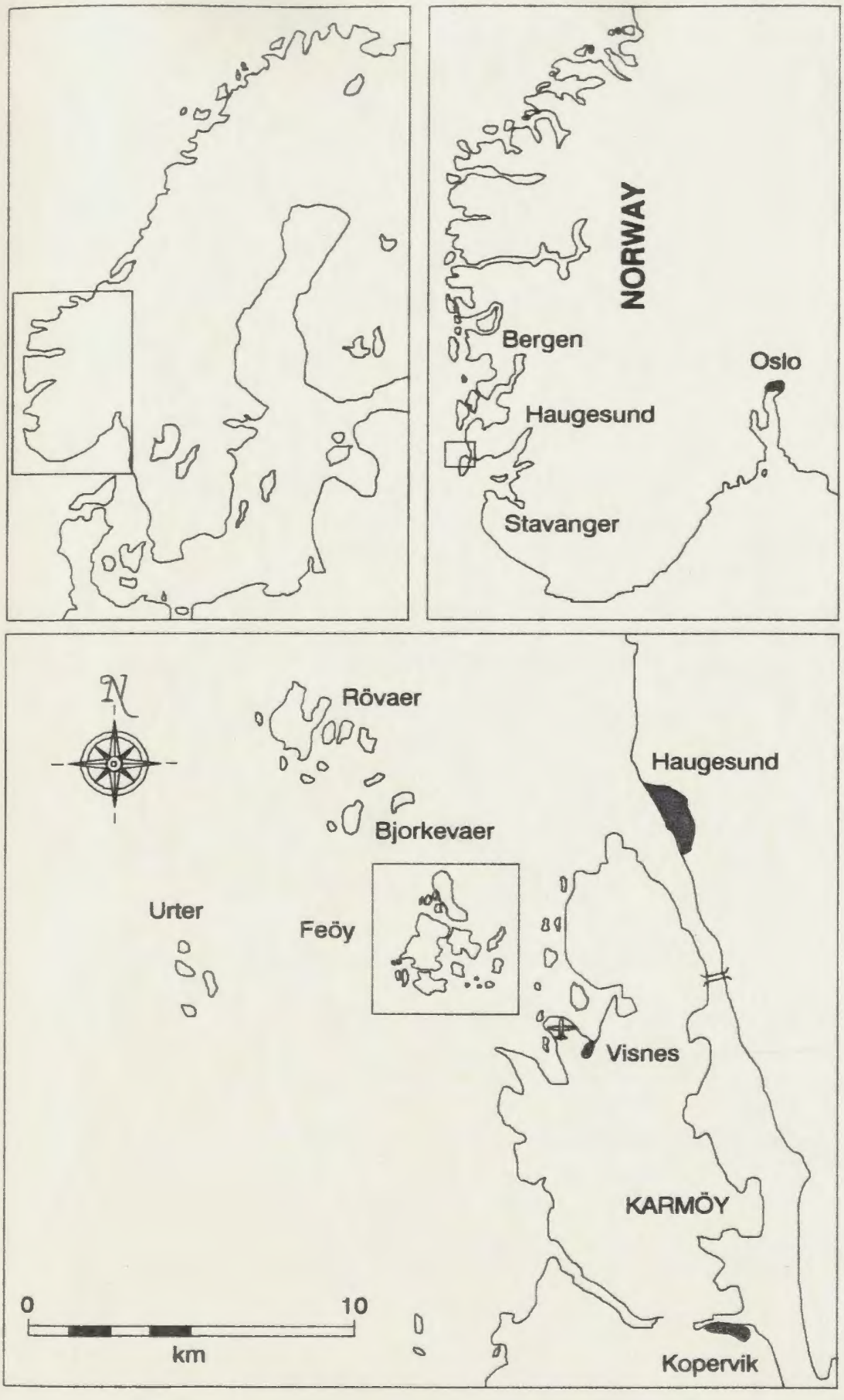

Figure 1.1: Location maps of the Visnes and Feoy areas.

1.2: Physiography and climate

The Visnes region is dominated by a rugged, coastal topography with extensive ling-covered barren grounds and excellent rock exposure along coastal areas. Further inland, exposure is reduced as grassy fields and evergreen stands become more frequent. Along the coast, numerous small (from 10 to 100m in width), vegetation free skerries serve as a protective barrier to the open North Atlantic Ocean.

The Feoy islands further offshore offer much better exposure than at Visnes, being relatively flat, treeless and wave washed. Field work in the Feoy area was facilitated by use of a Zodiak or light boat, as much of the best outcrop is on very small skerries.

1.3: Previous work

The first major geological study of the island of Karmoy had not been initiated until recent times, when Geis (1962) attempted to define the nature of the lava-greenstone/gabbro boundary. Geis concluded that the gabbros were of metamorphic, not igneous, origin, based on the lack of a clearly intrusive boundary with the surrounding rocks. Birkland (1975), on the other hand, suggested that the presence of layered crystalline rocks could only result from cooling of a magma.

Initial interpretation of the Karmoy ophiolite as such was made by Sturt and Thon (1978), a study which paved the way for subsequent reinterpretation of numerous other

mafic-ultramafic bodies throughout Norway as ophiolites. Since then, several detailed geochemical, geochronological and petrographic studies of these rocks have been completed (Sturt et al, 1979; Furnes et al, 1980; Pedersen, 1982; Pedersen and Malpas, 1984; Pedersen et al, 1987; Dunning and Pedersen, 1987; Pedersen and Hertogen, 1987).

The old Visnes copper mine is now owned by Norsk Hydro, and the facilities are presently being converted for use as an aluminum processing plant. As a result, many of the old mine reports and much of the accompanying drill core have been disposed of. However, the sulfide occurrence has been well documented over the years (eg., Per Singsaas, 1958; Vokes, 1968; Geis, 1962; Vokes and Gale, 1976).

The Ni-sulfide deposit of Feoy has not been thoroughly studied from an academic standpoint since its closure in the 1920's. In this respect the data presented on the Feoy Ni-sulfides are new, although Feoy was previously known to contain high contents of Platinum Group Elements (Foslie, 1938). Also, a recent review of Cu-Ni-sulfide deposits in Norway (Barnes et al., 1987) has documented elevated PGE values from Ni-sulfide grab samples in the study area. As a result of the lack of recent mining activity, it has been difficult to locate data from the mine's operative years. Consequently, the present study relies on an extensive sampling program on both Visnes and Feoy, and on field mapping by R.B. Pedersen (1982; 1986) and by this writer (1985, and present study).

1.4: Aims of the present study

Original interpretation of the Karmoy ophiolite implied late Caledonian obduction of a slice of oceanic crust which formed, along with the several sulfide occurrences, in a major ocean basin (Sturt and Thon, 1978). Since then, geochemical studies have indicated that the ophiolite may have a closer affiliation to a supra-subduction zone spreading center (Furnes et al., 1980; Furnes et al., 1982; Pedersen, 1982; Pedersen and Hertogen, 1987). More specifically it is now possible to trace the ophiolite's history from early spreading activity above a subduction zone (forming a sheeted dyke complex), to a later ensimatic-arc environment (with associated plagiogranitic intrusions), to final intrusion of highly magnesian, low-Ti basalt dykes (similar to rocks recovered from the Bonin Islands in the Western Pacific Ocean), diorites and clinopyroxene-phyric stocks. This interpretion is based both on field studies of the dyke rocks in the area, and on their geochemistry.

It had been previously assumed (Vokes, 1976; Vokes and Gale, 1976; Bjorlykke et al., 1980; Stevens et al., 1984) that Fe-Cu-Zn sulfide deposits in the Visnes area were similar to typical Cyprus-type cupriferous pyrite deposits, believed to be ancient analogues of those deposits currently forming in the "Black Smoker" environments of the Pacific and Atlantic oceans (Sillitoe, 1972; Spooner and Fyfe, 1973; Spooner, 1977; Cann et al., 1985/86; Richardson et al., 1987; Von Damm, 1988; Cowan and Cann, 1988; Kelley et al., in prep.). This interpretation was based on their stratigraphically high position in the ophiolite, and on the apparent MORB nature of the host rocks. In the case of the Feoy

Ni-sulfide body, its proximity to the Visnes orebody, its position within shear zones similar to those hosting the Visnes orebody (see Chapters 2 and 3), and the apparently similar geochemical affinity of its host rocks all suggested an interpretation as simply a deeper-rooted extension of the "high level" Visnes orebody (Scott, 1985). With the present state of knowledge, however, it is apparent that these interpretations need some revision and modification. That is, the Visnes deposit can now be shown to be genetically related to intrusion and subsequent alteration of a sheeted dyke complex above a subducting oceanic plate (see Chapters 2 and 3), while the Ni-sulfide deposit of Feoy can be shown to be temporally and genetically unique (see Chapters 4 and 7).

The aims of the present study then, are fourfold:

1- to present evidence showing that the two sulfide occurrences in the area (the Visnes Fe-Cu-Zn deposit and the Feoy Fe-Ni-Cu deposit) are unrelated to one another, other than spatially;

2- to postulate origins for these deposits in terms of their dependence (or lack thereof) on magmatic or hydrothermal activity, and in terms of the tectonic environment of formation, and also to examine links between alteration and mineralization;

3- to qualify those features (deformation, alteration and metamorphism) seen in the field which have had either direct genetic, or secondary (structural and metamorphic) effects and controls on sulfide formation in both deposits;

4- to use geochemical and isotopic data to support and expand upon conclusions derived from field and petrographic studies.

Chapters 3 and 4 examine the two sulfide deposits in the study area. They are essential components of this study, since they reflect the systematic evolution of magmatism and associated metallogeny within a subduction zone environment.

With reference to point 4 above, it is this writer's opinion that detailed geochemical and isotopic studies on rocks from an area with such a complex magmatic and tectonic history can be of most use when combined with observations made during classical field/petrographic work. Several authors (Sturt et al., 1979, 1980; Furnes et al., 1982, 1983; Pedersen, 1982; Pedersen and Hertogen, 1987) have discussed the geotectonic environment in which the main dyke and volcanic units of the Karmoy ophiolite formed. In the final analysis however, geochemical variation and discrimination diagrams have been unable to distinguish, without some ambiguity, between truly mid-oceanic and possible island-arc/back-arc signatures of these particular rocks. This is in part because of the variability and inconsistency in the degree of element mobility during intense alteration of the sheeted dyke complex in the study area. The mobility of certain trace elements, and major oxide changes during alteration, are discussed in Chapter 5.

While there are no completely unaltered rocks in the study area from which to make comparisons with the highly altered rocks, unaltered analogues from similar tectonic environments can be used to monitor relative chemical changes during alteration. Analysis of these alteration effects will allow a better understanding of the relationships between host rock modification and massive sulfide formation in the Visnes region.

Geochemical variation diagrams are used for the purpose of distinguishing the main chemical modifications in the host rocks for both sulfide deposits. As mentioned, the primary geochemical nature of these rocks has already been exhaustively studied. More recently, Pedersen and Hertogen (1987), Pedersen et al. (1987), and Dunning and Pedersen (1987) have provided evidence for an arc-related evolutionary cycle for the Karmoy ophiolite, based on extensive field work, REE geochemistry and geochronological studies. This involves initial arc volcanism, later arc-basin development and subsequent back-arc activity, and is similar to the model proposed by Crawford et al. (1981) for the evolution of the Mariana arc system in the Pacific Ocean.

The definition of tectonic environments using samples of the main sheeted dyke complex risks courting redundancy, simply because of their extremely altered nature. On the other hand, some valuable petrogenetic insight might be gained from PGE analysis of the less altered, late stage high-Mg, low-Ti dykes and associated Ni-sulfides of Feoy, since some studies (Naldrett and Duke, 1980; Hamyln and Keays, 1986; Keays et al., 1982; Hamyln et al., 1985) have successfully modelled similar rock types in terms of their PGE abundances. Therefore, some attempts are made in Chapter 7 to define the petrogenesis and tectonic environment of formation of these rocks, based on methods described by the above authors.

1.5: Methods

Mapping of the Visnes area was based on 1:5000 scale topographic maps (map numbers

AF032-5-1, 2, and 3), and from 1:50,000 aerial photographs (see Figure 2.1a). Maps are available from the offices of the Haugesund Geographical Survey in Haugesund. The map of the Feoy area (see Figure 2.1b) has been modified from a previous map produced by Pedersen (1987, pers. comm.).

Major element analyses of the Visnes and high-Mg dykes (see Chapter 5) were obtained by Atomic Absorption Spectrophotometry after HF-dissolution, using the method of Langmhyr and Paus (1968). Precision and accuracy data for major oxide analyses is given in Appendix 1.

Trace element analyses of both silicates and sulfides were obtained by X-Ray Fluorescence (XRF) analysis of pressed powder pellets, at Memorial University of Newfoundland (MUN). In terms of the precision of these data, the relative standard deviations of elements with K alpha lines (Ti through Nb in the periodic table) is 1% at 1000 ppm; at 0 concentration the standard deviation becomes 2 ppm. The agreement of determined versus accepted values of pressed powder pellet standards is considered very satisfactory (Longerich and Veinott, 1986). The limits of detection for the trace elements are: 2 ppm for Ni and Zr; 3 ppm for Nb and Cu; 4 ppm for Rb; 5 ppm for Cr Sr and Y; 6 ppm for V; 9 ppm for Zn, and 12 ppm for Pb (Longerich and Veinott, 1986). Major and Trace Element analyses of rock powder samples from this study are given in Appendix 3.

Electron microprobe analyses of 23 tourmaline samples from shear zones, and of selected chlorites and amphiboles from country rocks of the study area, were carried out on a Jeol JXA-50A Electron Probe Microanalyser, at Memorial University of Newfoundland, using an international clinopyroxene standard block (F-cpx) for instrument calibration. Acceptable working limits for deviations from actual values for each of the major oxides were: -0.02 to +0.1% for Na2O; -0.1 to +0.3% for MgO; -0.13 to +0.11% for Al2O3; -2.0 to +0.9% for SiO2; +0.01% for K2O; -0.38 to +0.25% for CaO; -0.1 to +0.07% for TiO2; +0.05% for Cr2O3; -0.1% for MnO; -0.2 to +0.02% for FeO; +0.07% for NiO; -2.03 to +0.83% for % total oxides. Data for the chlorites and amphiboles are given in Appendix 2; data for the tourmaline samples are given in Table 8.2.

Sulfur isotope ratios for pyrrhotite/chalcopyrite assemblages from the Feoy Ni-sulfides, and for sphalerite/pyrite assemblages from the Visnes Cu-Zn deposit were obtained from two sources: 1- samples F24a, V9, and V2 were analyzed commercially by Coastal Science Laboratories in Austin, Texas, on a Micromass Isotope Ratio Mass Spectrometer (Model 602D and 602E); 2- samples F56, F11, F33, V14 and F35 were analyzed at the University of Waterloo, Ontario. Sulfide fractions were separated manually, and sulfur isotope ratios were determined by extraction of SO2 using Cu2O oxidation at 1000 degrees Celsius, followed by analysis on a VG-Isogas Micromass 602E Spectrometer. Two internal standards with delta 34S values of 1.13 and 30.5 per mil were run before and after analysis of the Visnes and Feoy sulfide samples.

Oxygen isotope analyses were completed at the University of Alberta, using standard

BrF5 dissolution methods.

Platinum Group Element (PGE) contents, along with Gold (Au), were analyzed at Memorial University of Newfoundland from selected sulfide and silicate samples by the following method: 1- initial preconcentration of these metals into a Ni-sulfide bead by fire assay; 2- subsequent crushing, HCl dissolution of the bead, and precipitation of the PGE's and Au using a Tellurium solution and filter paper. Analysis of this final product by Inductively Coupled Plasma Mass Spectrometry (ICP/MS) provided results accurate at sensitivities of the order of 0.113 ppb for Ru, 0.016 ppb for Rh, 0.044 ppb for Pd, 0.444 ppb for Os, 0.214 ppb for Ir, 0.229 ppb for Pt, and 0.5 ppb for Au.

Platinum Group Minerals (PGM's) and sulfides were analysed on a Hitachi S570 Scanning Electron Microscope at Memorial University of Newfoundland. In determination of specific PGM phases, a semiquantitative stoichiometric method using X-Ray analysis was performed on a beam spot mode with a Tracer Northern 5500 Energy Dispersive X-Ray Analyser, Model 70152, with a spectral resolution of 145eV. Stoichiometric analysis ("SSQ") was carried out without standards, using a ZAF correction program to calculate element or oxide percentages.

Rock samples were taken from representative outcrops, from mine dumps, and from drill core samples in the case of some mineralized specimens from Visnes. Sample descriptions for selected rock samples used in this study are given in Appendix 4.

1.6: Terminology

In the study area, there are two genetically and temporally unique occurrences of felsic dyke rocks with a composition of typical low-K oceanic plagiogranites (Coleman and Peterman, 1975). For purposes of clarity, plagiogranitic segregations of the Visnes area associated with gabbros and basalt dykes of the sheeted complex are hereafter referred to as Type 1 Plagiogranites. Plagiogranitic to quartz dioritic dykes associated with later, ensimatic arc activity, and which are petrographically distinguished by a preponderance of quartz phenocrysts in an autobrecciated groundmass, are hereafter referred to as Type 2 Plagiogranites.

There are also two important groups of mafic dyke rocks in the study area, each of which have different geochemical signatures and field appearances. They also have different genetic and temporal relationships with respect to the Visnes and Feoy sulfide deposits. In this thesis the dykes are described as follows:

1- altered basic dykes of the sheeted complex, which are shown to be genetically related to the Visnes Fe-Cu-Zn sulfides, but which contain little or no Cr, are called the Visnes dykes. Some of the more intensely altered dyke samples are composed of simple epidote, quartz and chlorite alteration assemblages, with epidote predominating. This alteration style has been termed "epidosite" (Aldiss, 1978; Richardson et al., 1987);

2- very late, high MgO-Ni-Cr dykes which crosscut all other basalts in the area, and which can be shown to be genetically related to the Feoy Ni-sulfides, are called the high-Mg dykes.

In Chapters 2 and 6, the term "epidotite" is used to describe rocks composed of near 100% coarse crystalline epidote, without any evidence of having formed from secondary alteration of pre-existing lithologies. The term "epidosite", as mentioned, refers to heavily altered basalts of the Visnes dyke group. Geochemically, division between primary crystallized "epidotite" and secondary or replacement "epidosite" is clear (see Figure 2.2).

1.7: General geology of the Karmoy ophiolite

The Karmoy ophiolite in southwest Norway (Figure 1.2) is an almost complete and well exposed ophiolitic assemblage, and the present study area contains only a portion of the suite. This is the most southerly of Norway's ophiolite complexes, and was thought to have formed and been finally emplaced onto the Baltic Craton between the Late Precambrian Finmarkian and Middle Silurian Scandian orogenic events. In this sense it was assumed to be an older, Type 1 (Sturt et al., 1978) ophiolite which represents a slice of oceanic crust formed at a major ocean basin spreading center. However, Pb/Pb (Zircon) dates of 493Ma for the sheeted dyke-plagiogranite-gabbro sequence, 485+/-2Ma for the Type 2 plagiogranites, and 470 +9/-5Ma for late clinopyroxene--phyric intrusions in the area all indicate that the ophiolite is in fact younger than previously thought (Dunning and Pedersen, 1987). This, along with the discovery (Pedersen et al, 1987) of volcanic equivalents to late mafic intrusions (pyroclastic deposits and lava flows within the Torvastad Group of sediments), suggests that at least some of the rocks of this ophiolite formed in an Early Ordovician (Tremadoc) island-arc/back-arc/arc-basin

Figure 1.2: Geological map of the Karmoy Ophiolite Complex (Pedersen and Malpas, 1984).

GEOLOGICAL MAP OF KARMØY OPHIOLITE COMPLEX

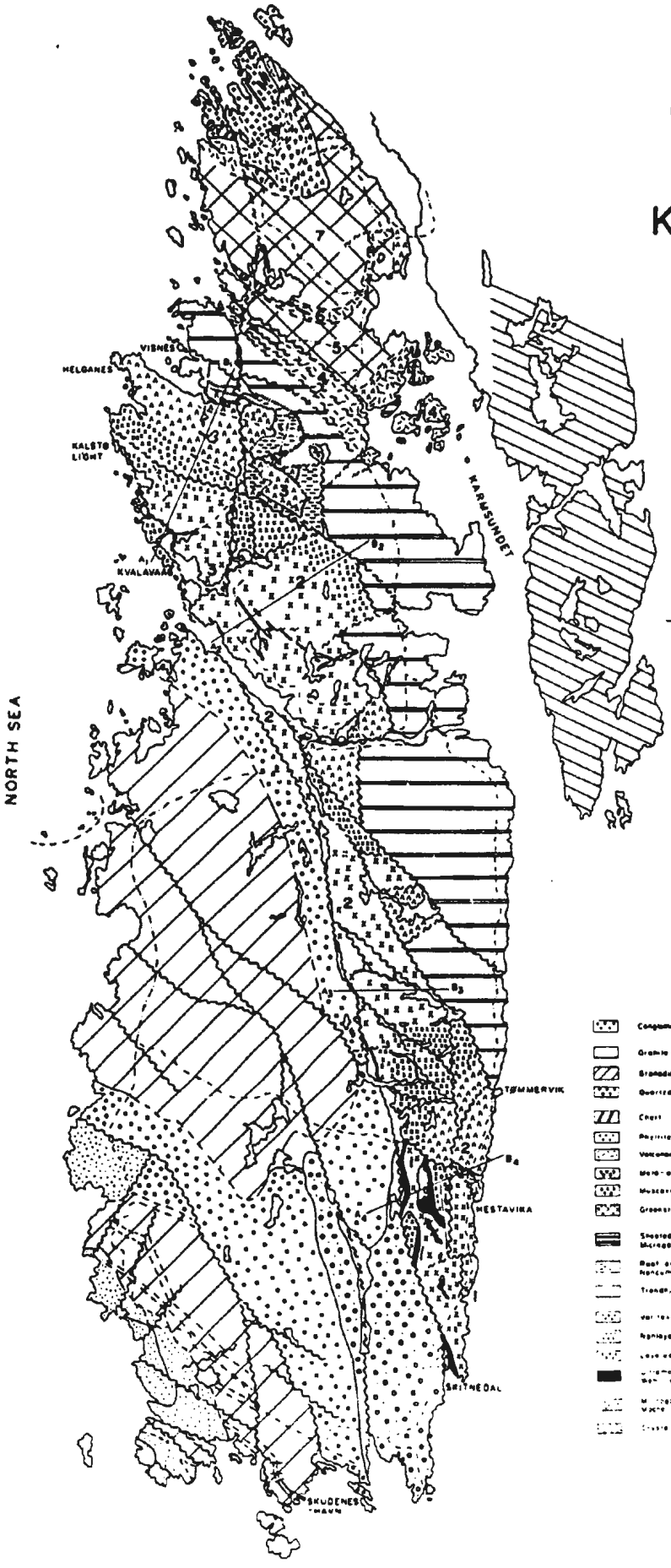

LOCATION MAP

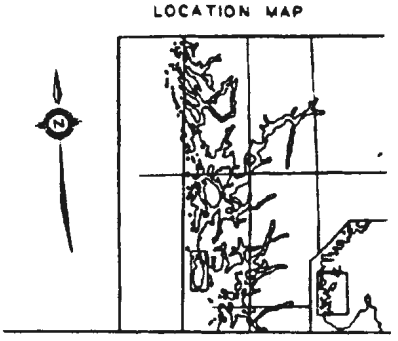

LEGEND

Geological boundary (defined, approximate)
Gradational geological boundary
Major shearzones (defined, approximate)
Minor shearzones (defined, approximate)

Post Ophiolite Rocks

THE SKUDENESET GROUP

THE WEST KARMØY IGNEOUS COMPLEX

The Cap Rocks To The Ophiolite

Conglomeratous Sandstones
Granite
Granodiorite
Quartzdiorite

THE TORVASTAD GROUP

8 HAALAND FORMATION
7 VIKINGSTAD GREENSTONE
6 HAUGAVAAG FORMATION
5 AVALDSNES GREENSTONE
4 VELLE FORMATION

Chert
Phyllite
Volcanoclastic sediments
Meta-andesite
Meta-dacite-rhyolite
Greenstone

Ophiolitic Rocks

THE VISNES GROUP

Sheeted dykes Dykes breccia Microgabbro Pillow-lava
Roof assemblage Microgabbro Nonlayered gabbro Dykes
Trondhjemite
Layered gabbro
Nonlayered gabbro
Layered gabbro
Ultramafic rocks (dunite-peridotite-pyroxenite)
Microgabbro Nonlayered gabbro Layered gabbro
Cumulate ultramafics

THE PLUTONIC ZONE

5 VISNES HIGH LEVEL COMPLEX
2 VEAVAAGEN IGNEOUS COMPLEX
1 EAST KARMØY IGNEOUS COMPLEX

Precambrian Basement

type of environment.

The Karmoy Ophiolite is intruded by a granitic pluton, the West Karmoy Igneous Complex (WKIC), which has been dated at ca. 450Ma by Rb/Sr methods (Priem and Torske, 1973). This means that final emplacement of the ophiolite had been completed at least by Upper Ordovician, Llandeilian times.

The Karmoy Ophiolite comprises a large plutonic body which grades upwards into an impressive sheeted dyke complex capped by a thin pillow lava unit. In the Visnes area, sheeted dykes and sparse pillow lavas are overlain by pyroclastic deposits of the Torvastad Group. In areas where granites of the WKIC intrude the ophiolite, the contact between the two is almost everywhere marked by extensive shearing which has produced quartz-augen gneisses.

On the basis of field relationships, the Karmoy Ophiolite has been divided into three major plutonic units (Sturt and Thon, 1978a):

1- The East Karmoy Igneous Complex (EKIC);

2- The Veavagen Igneous Complex (VIC);

3- The Visnes High Level Complex (VHLC), which constitutes the study area for this thesis.

1.7.1: The East Karmoy Igneous Complex

The EKIC is composed of relatively large bodies of cumulate ultramafic rocks which grade into layered and non-layered gabbros. In some areas these are cut by several generations of plagiogranitic intrusions.

This complex represents perhaps the oldest and lowermost section of the ophiolite, and has been subject to several generations of folding, faulting and high temperature shearing. The high temperature (amphibolite facies) shear zones are conspicuously cut by basic dykes with a low-Ti chemistry. In the field, plagiogranites are seen to be closely related to these high temperature shear zones, and are clearly rooted in amphibolite grade meta-gabbros found both along and adjacent to the shear zones. These plagiogranites are suggested to be a product of partial melting of the amphibolite gabbro (Pedersen and Malpas, 1984), and contrast sharply with ophiolitic plagiogranite of the Visnes region (Type 1), which is interpreted as a differentiate of a basic magma. They also contrast with plagiogranite dykes of the Feoy area (Type 2), which are related to much later, supra-subduction zone activity (Pedersen et al., 1987). Unfortunately, no dates are available for these rock types.

1.7.2: The Veavagen Igneous Complex

The VIC to the north, the largest of the three complexes, is composed of layered gabbros and lesser amounts of layered ultramafic rocks, as well as non-layered and varitextured

gabbros, which are intrusive into the EKIC. Layered gabbros are the most voluminous rock type, and are texturally similar to the gabbros of the EKIC. They occur in the northern sections of the VIC, and are structurally separated from the rest of the complex by a major shear zone between Veavagen and Kopervik.

Ultramafic rocks are found in layers up to 100m thick, and on a smaller scale exhibit rhythmic layering. As is typical of nearly all rocks in the Karmoy area, alteration is extensive, as well as faulting and shearing. Plagiogranites are also present, and occur as dykes and veins intruding microgabbro and varitextured gabbro. These dykes have approximately the same trend as the basic dykes which also cut this complex (strike north, dip 75-90 degrees east). Geochemically these plagiogranites are akin to those of the EKIC, once again suggestive of partial melting of metamorphosed gabbro (Pedersen and Malpas, 1984)(see Figure 1.3).

1.7.3: The Visnes High Level Complex

The VHLC in the northwestern part of the plutonic zone is composed of mainly gabbroic material and roof assemblage rocks (microgabbro, non-cumulate gabbro and dykes), with significant amounts of plagiogranite occurring in the upper (northern) sections. The complex has a gradational contact with the uppermost portion of the ophiolite, the Visnes Group (in the same area), which consists of sheeted dykes, dyke-breccia, microgabbro and pillow lavas. The VHLC is, like the EKIC and VIC, cut by several generations of basic dykes.

It is important here to examine the nature of plagiogranitic rocks (Type 1) occurring within this complex, since they are thought to represent a sandwich horizon, together with small patches of biotite diorite, between a roof zone of sheeted dykes, microgabbro and pegmatitic gabbros, and a floor of isotropic gabbros.

Compared with plagiogranites of the EKIC, which are considered partial melts of flaser gabbro, these plagiogranites have distinct geochemical signatures (Figure 1.3). They are found only in association with sheeted dykes or gabbros, and in some areas with biotite diorite and epidotite. Because of this, they were probably cogenetic with the original basaltic magma, and represent the latest stages of fractional crystallization of filter pressed interstitial liquid from the varitextured gabbros (Pedersen and Malpas, 1984). Their close association with epidotites has a significance which will be discussed in Chapters 2 and 6.

A 2km thick sequence of metabasalts forms part of the Visnes Group. These vary from aphanitic greenstones to dolerites (sometimes porphyritic), and are separated from the pillow lavas by large shear zones. Chilled margins are common in the dykes. Geochemically, these metabasalts possess three distinct characteristics (Furnes et al., 1980):

1- a consistent depletion in the LREE;

2- a large variation in incompatible and compatible element abundances;

3- large variations in some incompatible element ratios.

It is suggested by Furnes et al. (1980) that these large scale variations are a result of batch melting of a depleted mantle source. Later interpretation (Pedersen, 1982) suggests

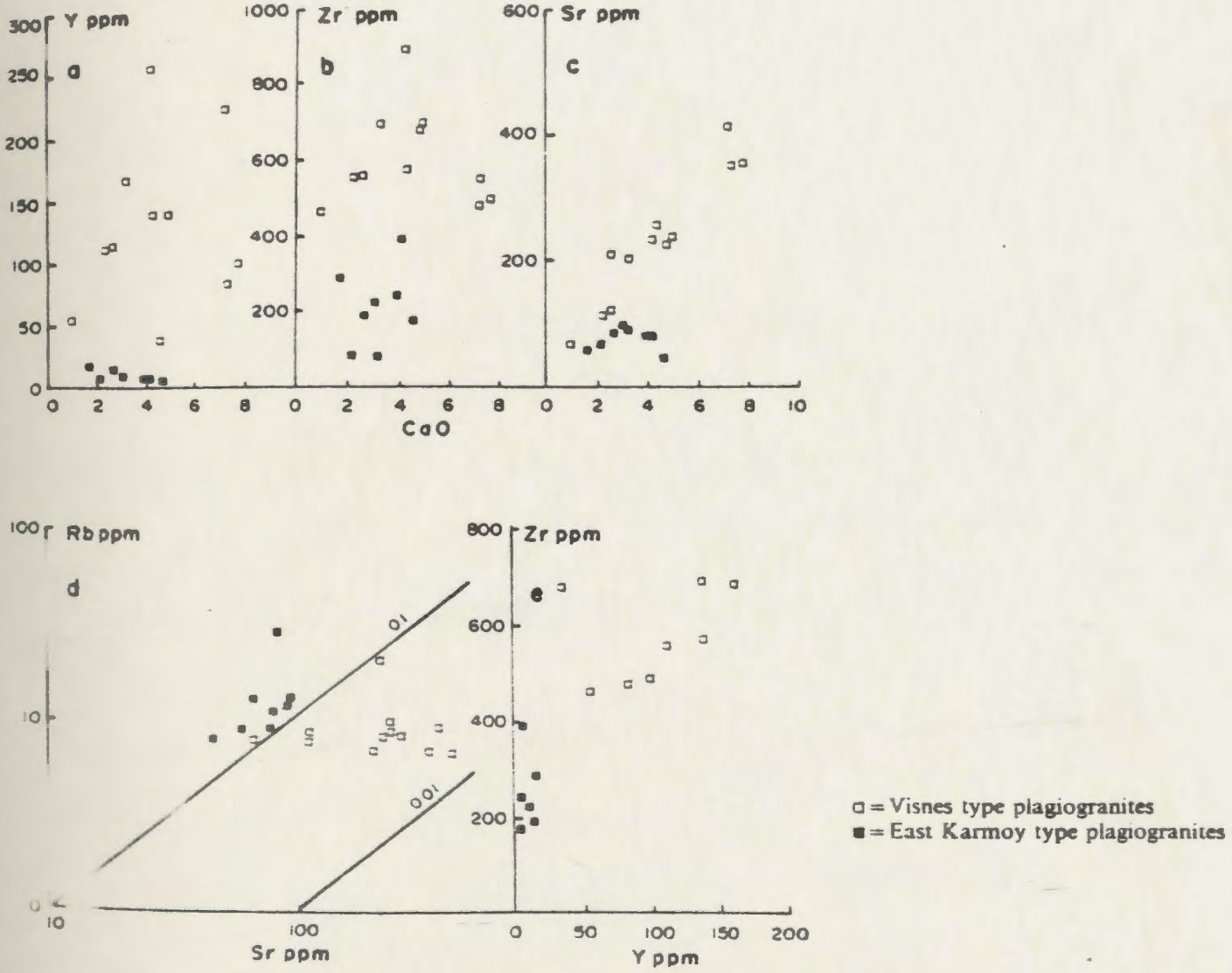

Figure 1.3: Comparison of the Visnes (Type 1) and East Karmoy plagiogranites (Pedersen and Malpas, 1984).

that these variations in trace element composition may be accounted for by deriving the basaltic liquid(s) from different sources and injecting them concurrently (i.e. a multiple magma chamber system). Some of these variations may be a result of seafloor alteration and mobility of supposedly "immobile" elements; geochemical and field data which bear on this problem are presented in Chapter 5, insofar as they relate to alteration and mineralization of the Visnes dykes.

1.7.4: Regional patterns of deformation and metamorphism

Rocks of the Karmoy Ophiolite have not escaped the effects of several periods of deformation and metamorphism associated with Caledonian orogenesis. In light of this, Sturt et al. (1979) divided the deformation and metamorphism in this area into three temporal divisions:

1- oceanic metamorphism and deformation (M0 and D0);

2- syn-emplacement metamorphism (M1), and

3- post-emplacement metamorphism and deformation (M2 and D2).

Metamorphism and deformation which occurred on the ocean floor predated the intrusion of low-Ti basalt dykes, and is a higher temperature process than later episodes; gabbroic rocks affected by M0 are metamorphosed up to amphibolite facies, and are related to plagiogranite generation by shear heating and subsequent partial melting of gabbro (Pedersen, 1982; Pedersen and Malpas, 1984). Associated amphibolitized shear zones

themselves cut deformed, layered gabbros, suggesting that multiple stage deformation occurred on the ocean floor.

Other, much lower temperature features in rocks of the study area which also formed in an ocean basin are: sub-seafloor alteration of the upper parts of the ophiolite; massive Fe-Cu-Zn sulfides of the Visnes deposit (see Chapter 2). However, these are clearly unrelated to high temperature M0 metamorphism, and so are considered as post-M0/pre-M1 features.

Because of the pervasively altered nature of almost all rocks in the Karmoy region, it is quite difficult to define the exact nature of syn-emplacement metamorphism (M1). However, it is clear that all metamorphism post-dating M0 is of a lower grade. Sturt et al. (1979) suggested that a regional penetrative cleavage, well developed in the uppermost parts of the ophiolite, formed during the latest stages of obduction of the ophiolite (S1).

Pedersen (1982) also described the effects of these three main stages of deformation and metamorphism within the Karmoy ophiolite, although there remain some ambiguities between delineated metamorphic episodes in this area. There has been no problem in interpretation of the high temperature, oceanic deformation and metamorphism patterns, but there is considerable overlap in the low-medium metamorphic grade periods of deformation and metamorphism which succeeded this first episode (on the ocean floor, as well as during and after ophiolite emplacement). Intense and multiple periods of fluid

circulation through the country rocks during this time has resulted in extensive to complete alteration of original parageneses.

The time of formation of the Visnes and Feoy sulfide deposits relative to these metamorphic and deformation episodes is delineated in the present study. Therefore, for purposes of convenience the present writer has found it necessary to modify previous classifications of deformation and metamorphism with respect to massive sulfide formation in the study area:

1- oceanic deformation and metamorphism which preceeded formation of the Visnes sulfides (M0);

2- oceanic metamorphism/deformation post-dating formation of the Visnes sulfides, but which pre-dated intrusion of high-Mg dykes, diorites, Type 2 plagiogranites, and the Ni-sulfides of Feoy. This is probably related to M1 metamorphism;

3- deformation and metamorphism which post-dated intrusion of the late dykes and other intrusives mentioned in 2 above, and also post-dated the Feoy Ni-sulfides (M2 and D2).

This classification is more relevant because it is correlatable with the current interpretation of the magmatic history of the Karmoy ophiolite, and also because it serves as a direct link between this magmatic history and the mineralization history.

The first phase(s) of metamorphism (M0) had apparently no bearing on formation of either sulfide body, and hence will not be expanded upon in this study. However, M0

metamorphism is discussed in detail by Pedersen (1982). Suffice it to say that it was evidently a much higher temperature/strain episode(s) than subsequent events, and may have been responsible for generation of plagiogranitic partial melts (the EKIC plagiogranites).

In conclusion, it is evident that the Karmoy ophiolite represents a very important component of Lower Paleozoic volcanic sequences in Norway. Over 20 other areas of greenstone, gabbro and plagiogranite have all been now interpreted as part of a once continuous and extensive oceanic crust that was later disseminated and emplaced onto the Baltic Craton during the evolution of the Caledonian orogenic cycle.

Chapter 2: Geology and petrology of the Visnes and Feoy regions

2.1: Introduction

The study area represents the uppermost section of the Karmoy ophiolite, ranging from isotropic and varitextured gabbros at the base, to sheeted dykes, plagiogranites and sparse pillow lavas at the top of the section. Pelagic sediments are not present in the map area, but volcaniclastic rocks of the Torvastad Group do outcrop in one coastal section near Digermulen. Figures 2.1a and b are geological maps of the Visnes and Feoy regions (see back pocket for 2.1.a).

The Visnes region is host to a large massive sulfide deposit which occurs along a major shear zone within the sheeted dyke complex. At one time the largest copper mine in northern Europe, the deposit exhibits several of the typical Cyprus-type massive sulfide characteristics, with the notable exception of its position in sheeted dykes rather than in pillow lavas. Likewise, on the nearby island of Feoy, a small massive Ni-sulfide body occurs along a large shear zone in close association with basic and plagiogranitic (Type 2) dykes, and gabbros.

The following sections describe the salient field and petrological features of rocks in the study area. Particular emphasis is given to those aspects of geology and petrology which bear some relevance to the Visnes and Feoy sulfide deposits. The geology and petrology of the Visnes and Feoy sulfide deposits themselves are discussed separately in Chapters

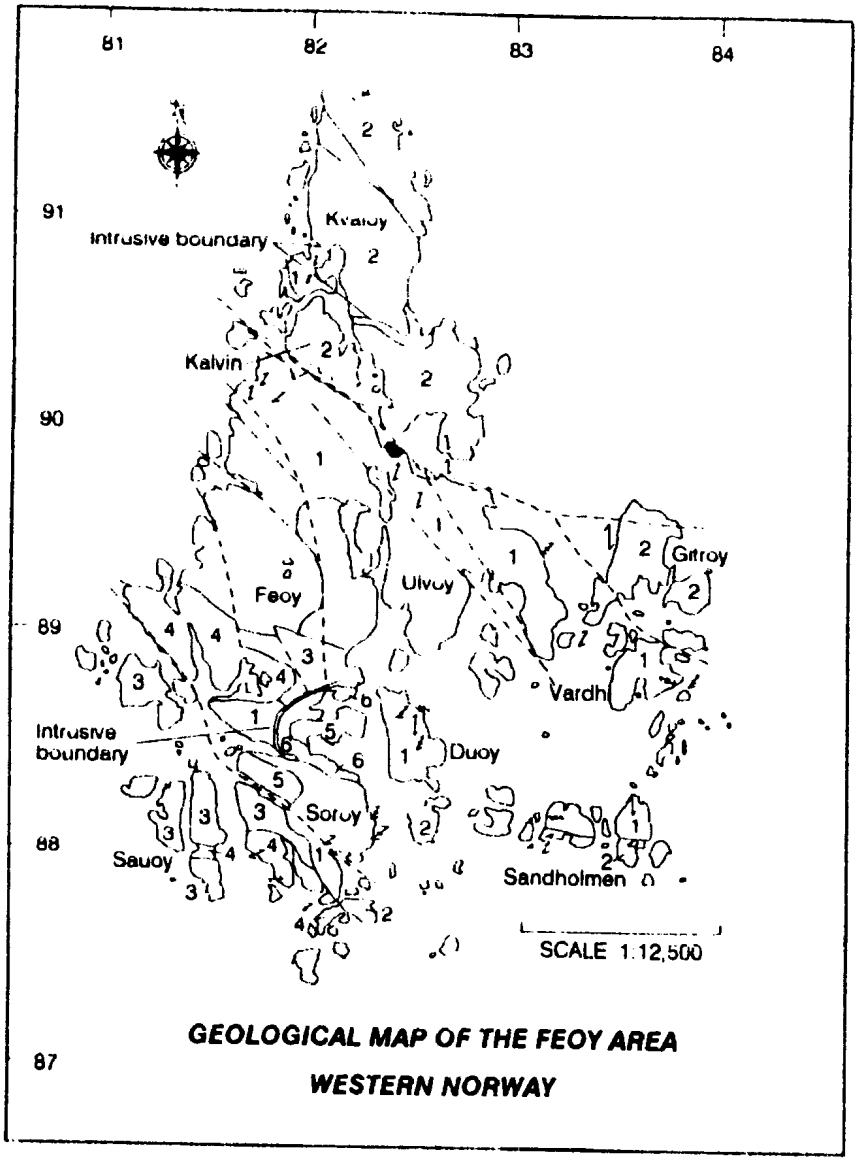

Figure 2.1a: Geological map of the Feoy area

3 and 4.

2.2: Sheeted dykes (the "Visnes dykes"), and associated rocks of the Karmoy Ophiolite

2.2.1: The Visnes dykes

The Visnes dykes constitute a thick (about 1.5km thickness) sheeted complex, and are often intermixed with plagiogranitic and gabbroic pods and screens. The dykes are by far the most abundant rock type in this area.

In some areas the sheeted complex is well exposed, as on the islands of Feoy and Ulvoy. Some dykes are primary biotite phyric, but most are aphyric, and all are extensively altered and/or recrystallized, so that original mineral parageneses are rare.

These dykes generally strike northwest and dip 75-90 degrees east (see Figure 2.1). Cross-cutting relationships are complex; two sets of basic dykes have been noted on the west coast (based on textures and chemistry), although field relationships locally indicate up to five generations of mafic intrusion, along with several generations of plagiogranite.

The Visnes dykes range in thickness from 5cm to 4m and in some places show chilled margins. Dykes within dykes are common, as are xenoliths of gabbro, plagiogranite and

epidotite, the latter having only been observed in the Dyrnes area (see Plates 2.9 to 2.12). Dykes are seen to cut isotropic and varitextured gabbro and Type 1 plagiogranite, but in other areas are themselves cut by gabbro and plagiogranite. The lower boundary of the Visnes dykes is a transition to pegmatitic, varitextured and isotropic gabbro and plagiogranite. Intrusive relationships are complex in this boundary zone, and have been studied in some detail by Pedersen (1986). The upper parts of the sheeted complex are in general sheared, are hosts to the Visnes ore deposit, and rarely show gradational relationships with highly altered and variably mineralized overlying pillow lavas.

Large shear zones cut the area in a conjugate pattern, and where they penetrate the sheeted dykes, the dyke structures are lost, and the rocks become simply homophanous greenschist. In other areas such as Fransehagen and Kvaloy, the Visnes dykes are more uniform, and dyke margins are clearly seen. Dykes are in some areas (eg. Sandholmen Island) parallel to the shear zones, suggesting that shearing may have originally propagated in a preferred direction parallel to the dyke strike.

As mentioned, the Visnes Dykes are host to the Visnes massive sulfide deposit. The main orebodies occur along steeply dipping greenschist facies shear zones wwhich cut the dykes in a N-S/E-W conjugate pattern (see map in back flap; also see Chapter 3).

Dykes of the sheeted complex also have an extremely well developed microfracture and vein system, and this becomes more intense with increasing proximity to the Visnes

orebodies. All dykes are net-veined to variable degrees with epidote and quartz, with lesser amounts of albite, and in some places calcite. Closer to the Visnes orebodies, disseminated pyrite is much more abundant in the country rocks, with lesser amounts of chalcopyrite, and rarely, sphalerite (the latter occurs only as veinlets).

In thin section, because of the pervasive alteration, most primary textures and mineralogies of the Visnes dykes have been obliterated and replaced by typical spilitic alteration assemblages. The Visnes dykes are variably altered to epidote, quartz, chlorite, albite, sphene, pyrite and apatite (in decreasing order of abundance) (Plate 2.1). Some dyke samples also contain appreciable amounts of calcite and actinolite. This classic "spilitic" alteration assemblage (Cann et al, 1985/86) is present in all rocks which are genetically related to formation of the sheeted complex. This excludes the high-Mg dykes, Type 2 plagiogranitic dykes, and plutonic rocks which have clearly different alteration mineralogies (see Sections 2.3 and 2.4). The differences in alteration styles that exist between these latter rock units and those of the VHLC allow petrographic distinctions to be made between them. Also, coupled with geochronologic data from Chapter 1 indicating an age difference of about 20m.y. between these rock units, it appears that there may have been two distinct episodes of alteration which were separated in time by at least 20m.y.

In thin section, chlorite in the Visnes dyke samples is always green-brown under crossed nicols, and contains blebs of sphene, suggesting that the chlorite may in fact be a replacement of Ti-rich biotite. This is supported by the presence of relict biotite within

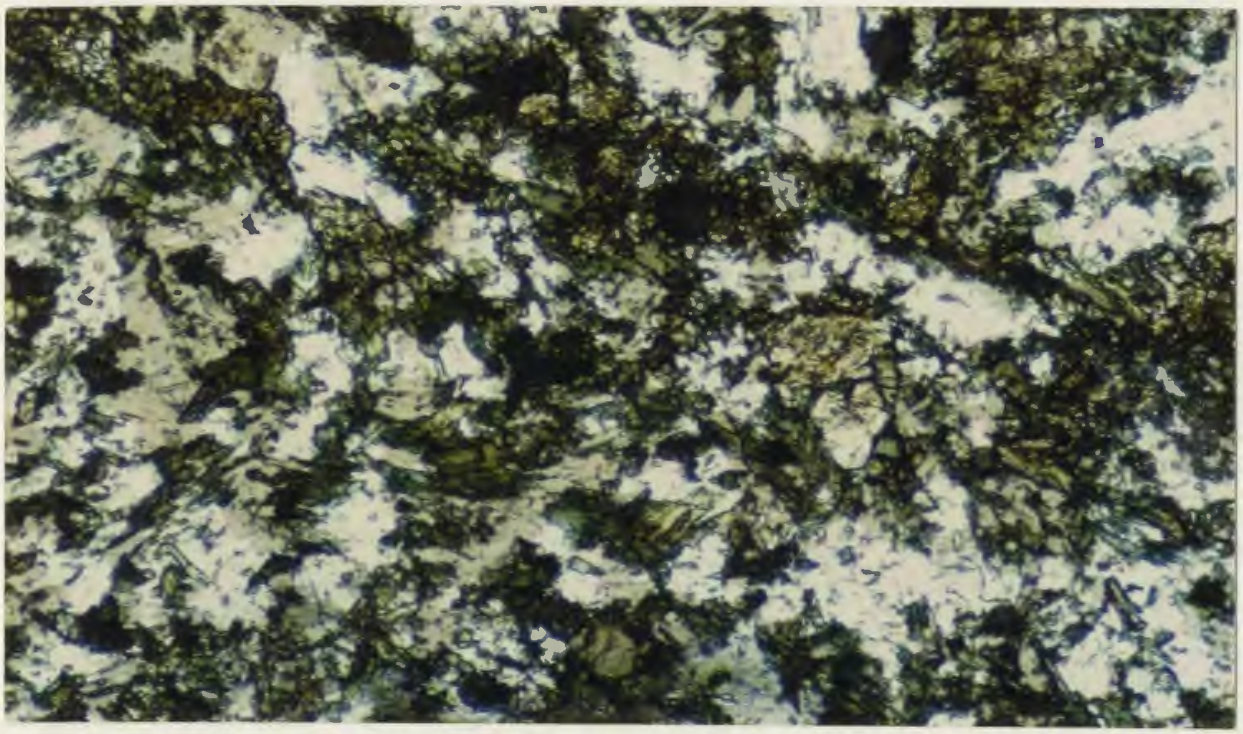

Plate 2.1: Alteration assemblages in the Visnes dykes. Epidote is dark green; chlorite is light green; quartz and albite are white; note also the black sphene and the small needles of apatite (magnification: 40X; plane polarized light, ppl).

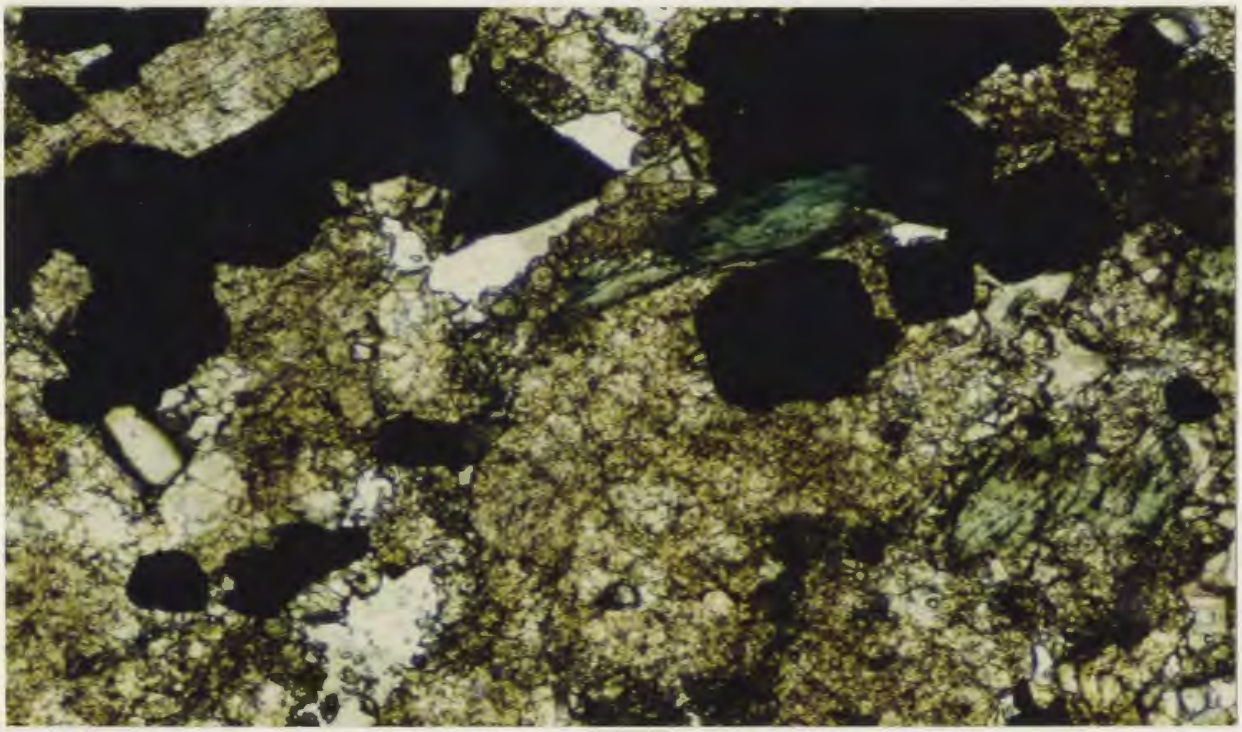

Plate 2.2: Alteration assemblages in "epidosite" zones in the Visnes dykes. Epidote is yellow brown; quartz is white; chlorite is green; pyrite is black (magnification: 40X; ppl).

the chlorite. The chlorite is, without exception, of the Fe-rich ripidolite variety (see Appendix 2 for microprobe analyses), is always fine grained, and often defines a strong schistosity within the dykes. Epidote in the Visnes dykes ranges from true epidote to clinozoisite/zoisite in composition, and forms from 10 to 60% of the modal analysis. The groundmass is always fine grained, and in many sections exhibits a sugary texture. Some of the more intensely altered Visnes dyke samples have a simple mineralogy of about 70 to 80% epidote, with lesser amounts of quartz, chlorite, sphene and pyrite (Plates 2.2 and 2.3). These are "epidosites", and represent the end products of intense hydrothermal alteration of basic dykes (Richardson et al., 1987; also, see below and Section 2.6).

Very rarely, less intensely altered samples of the Visnes dykes contain preserved primary igneous pyroxenes, which show a crude sub-ophitic texture. These pyroxenes are altered to ferro-actinolite (Plate 2.4).

In the Fiskdammen and Dyrnes areas (see Figure 2.1), important field relationships between the Visnes dykes, Type 1 plagiogranites and epidotites are seen. In Fiskdammen, a small dyke swarm cuts isotropic gabbro. Several of these dykes are heavily altered to epidosites, and are also heavily mineralized with pyrite and lesser amounts of chalcopyrite (Plate 2.5). Not only this, but they also contain small xenoliths of "epidotite". Accompanying these dykes are streamers of epidote and quartz (Plates 2.6 to 2.8). Immediately adjacent dykes are considerably less mineralized and less altered. Hydrothermal alteration fluids which were responsible for mineralization in these dykes were clearly enriched in Fe and Cu. Such areas appear to represent "flowthrough

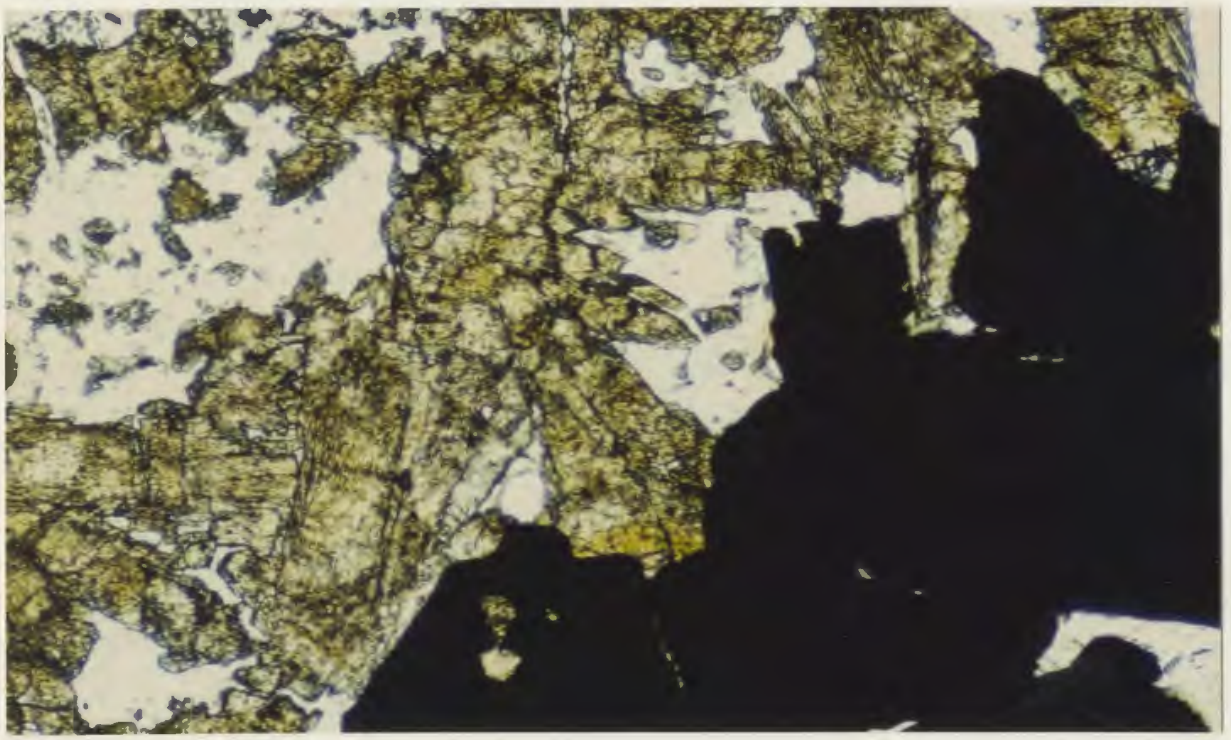

Plate 2.3: Alteration assemblages in "epidosites". Mineralogy as in Plate 2.2 (Magnification: 40X; ppl).

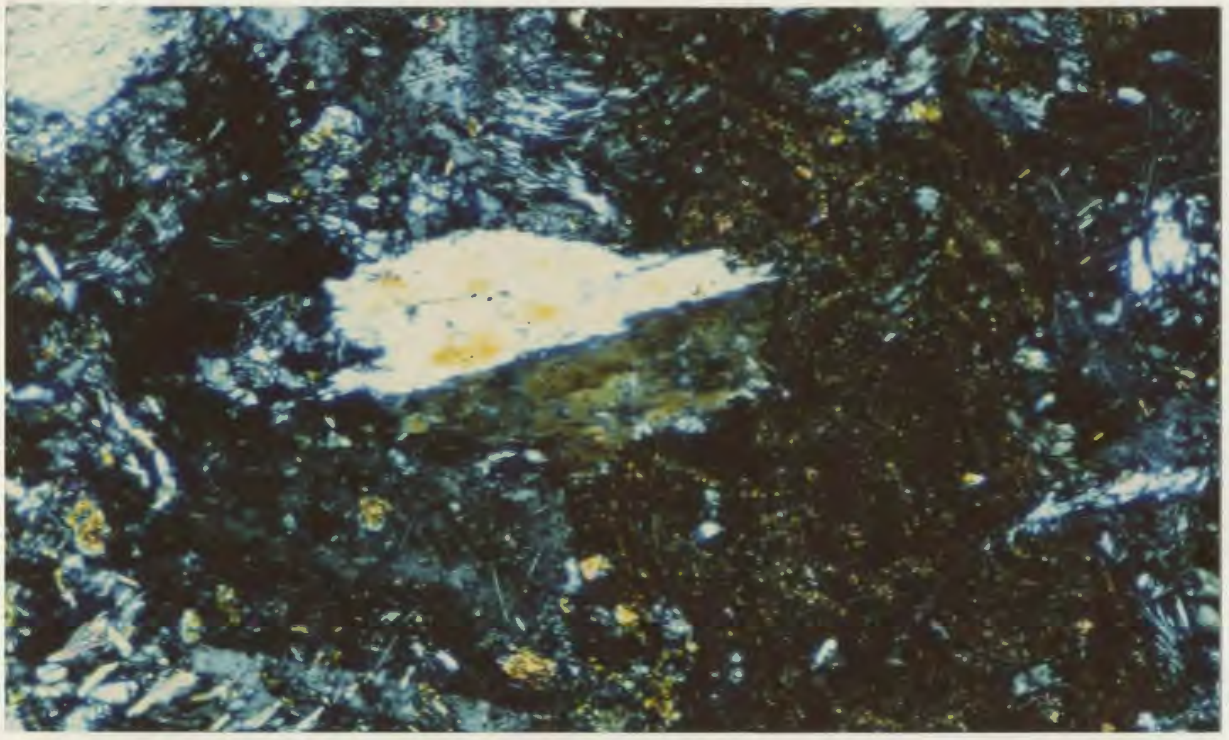

Plate 2.4: Altered Visnes dyke sample showing relict clinopyroxene which is nearly completely altered to ferro-actinolite (magnification: 40X; crossed nicols, cn).

Plate 2.5: A selectively mineralized and epidotized dyke, or "epidosite zone" from the Fiskdammen area of Visnes. The surrounding country rock is neither mineralized nor heavily altered.

Plate 2.6: Epidote and quartz veins, or "streamers", running parallel to the strike of sheeted dykes in the Visnes area.

Plate 2.7: Epidote veins or "streamers" cutting basalt dykes in the Visnes area. Note hammer handle for scale.

Plate 2.8: Epidote "streamers" running parallel to the strike of sheeted basalt dykes in the Dyrnes area of Visnes. Note hammer handle for scale.

zones" for ascending metal-rich hydrothermal solutions (Richardson et al, 1987).

In nearby Dyrnes, wide basalt dykes contain large (>0.25m) xenoliths of epidotite and Type 1 plagiogranite (Plates 2.9 to 2.12). The xenoliths have been deformed in a plastic fashion within the dykes (i.e. as if the xenoliths were not completely solidified upon inclusion). Surrounding the xenoliths are "streams" of epidote-quartz spherules alligned parallel to the flow direction of the dyke itself (see Plate 2.12), and the spherules have a "pinched off" appearance from the xenoliths. Also, close examination of the xenoliths and spherules indicates that there are distinct, sharp boundaries between the epidotite and the plagiogranite, suggesting a possible fluid immiscibility between the two. These observations suggest several things:

1- epidotites may have been cogenetic with the Type 1 plagiogranites, and are therefore primary magmatic rocks rather than alteration products;

2- magmatic liquid immiscibility may have exerted strong controls over epidotite and plagiogranite formation;

3- there was a continuation of basic magmatism shortly after formation of the epidotites and plagiogranites, since these occur as xenoliths in some of the Visnes dykes. A more comprehensive discussion of the plagiogranites and epidotites is presented in Sections 2.2.4 and 2.2.6 (respectively), and in Chapter 6.

2.2.2: Pillow lavas

In the Visnes area in general, relatively minor occurrences of variolitic pillow lavas and

Plate 2.9: Plastically deformed Type 1 plagiogranite xenoliths in basalt dyke in the Dyrnes area of Visnes. Xenoliths are about 0.5m in length.

Plate 2.10: Plastically deformed Type 1 plagiogranite xenolith in a basic dyke. Dyrnes, Visnes.

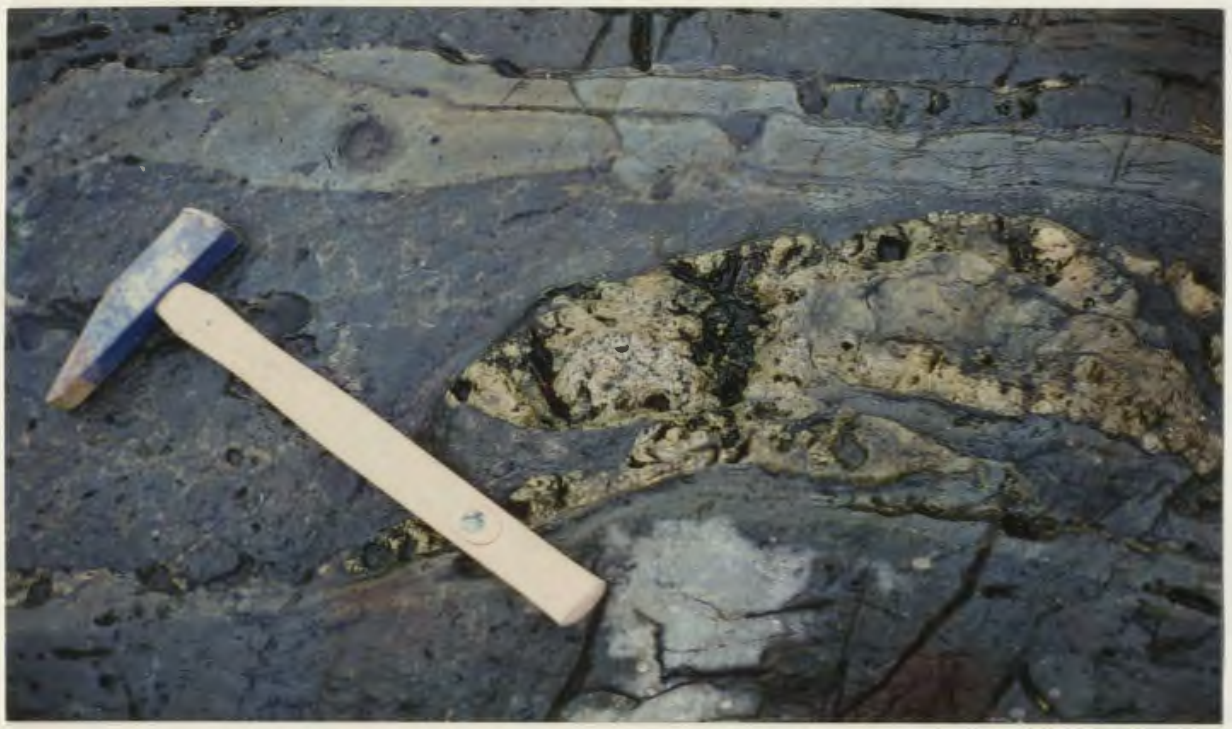

Plate 2.11: Plastically deformed epidotite xenolith in the Dyrnes area of Visnes.

Plate 2.12: Plastically deformed epidotite xenolith in Dyrnes area, Visnes. Note the tiny trail of epidotite "spherules" which rims the xenolith nearest the hammer.

pillow breccias are seen. Although there are few distinct pillow lava outcrops in the study area, a thick pillow lava sequence occurs just east of Visnes Kobberverk. The boundary between pillow lavas and sheeted dykes is marked by a large shear zone of 100 to 200m width. It is this same shear zone which hosts the Visnes massive sulfide deposit at a deeper stratigraphic and structural level.

In the study area in particular, pillow lavas occur mainly as minor screens within sheeted dykes, and as pillow breccia. However, pillow structures are well preserved on some of the nearby offshore skerries, and also on one outcrop near the old bridle path in Visnes (Plate 2.13). On these offshore skerries, pillow lavas pass downwards into extensive pillow and dyke breccias, and then into sheeted dykes. Brecciation is a result of intrusion of plagiogranite into the upper regions of the sheeted dyke complex (Plate 2.14). In other outcrops epidote and quartz rim the pillows. Where the pillows are rimmed by epidote and quartz, they are intensely corroded, rounded and mineralized with pyrite (Plates 2.15 and 2.16), and the groundmass assemblages are intensely altered. This is likely a result of circulation of corrosive hydrothermal fluids through the pillow lavas, and is a feature analogous to similar zones of alteration and mineralization in the Visnes dykes (see Section 2.2.1).

All pillow lavas appear quite altered in the field, and are variably pyritized. In thin section they are all totally altered to epidote-quartz-chlorite-sphene-pyrite alteration assemblages.

Plate 2.13: Outcrop of pillow lavas in the Visnes region.

Plate 2.14: Outcrop of pillow breccia in plagiogranitic matrix. From one of the nearby offshore skerries in the Visnes area.

Plate 2.17: Epidotite "segregations" in pegmatitic gabbro. Note the gradational nature of the contact between the coarse grained epidotite and the surrounding gabbro. From the Feoy area.

Plate 2.18: Epidotite "segregations" in coarse to pegmatitic hornblende gabbro. From the Feoy area.

2.2.3: Gabbro

Isotropic, varitextured and micro-gabbros are second only to the Visnes dykes in abundance within the study area. They are well exposed and are usually coarse grained with abundant pegmatitic patches. Although there are large textural variations in the field, poikilitic textures are quite obvious in the coarser, hornblende-rich varieties.

The gabbros are intimately associated with the sheeted complex and plagiogranites, or the "roof assemblage" (Pedersen, 1982). They are characterized in the field by highly variable textures, from coarse pegmatitic hornblende gabbros to microgabbroic varieties. They must have formed from fairly hydrous melts, as in some areas "segregations" of epidotite and amphibole of apparently deuteric origin are seen (Plates 2.17 and 2.18; also see Section 2.6).

Ellipsoidal plagiogranitic pods of 10-100m width are scattered in a random fashion throughout the main gabbroic body. Contacts between these rocks and the gabbros are equivocal, but appear to be primary and gradational.

Near the shear zones the gabbros, like the sheeted dykes, have been extensively altered to greenschist facies assemblages, and are also deformed. A foliation marked by a preferred orientation of secondary amphiboles is moderately developed on a regional scale.

Plate 2.17: Epidotite "segregations" in pegmatitic gabbro. Note the gradational nature of the contact between the coarse grained epidotite and the surrounding gabbro. From the Feoy area.

Plate 2.18: Epidotite "segregations" in coarse to pegmatitic hornblende gabbro. From the Feoy area.

A dominant feature of the gabbro in many areas is the presence of the same epidote-quartz netveins and groundmass alteration assemblages which are so evident in the sheeted dykes and pillow lavas. Epidote is again the most abundant of these alteration minerals.

It is in these gabbros that the only evidence of stockwork-type sulfide veining can be seen (Plates 2.19 and 2.20); sulfide mineralization in the gabbro occurs both as veins and disseminations, and as clusters of euhedral pyrite cubes in epidotite veins which cut the gabbro (see Figure 2.3).

In thin section, the gabbros are quite altered, and display granophyric texture. They are leucocratic, with a simple mineralogy of plagioclase (albite), hornblende, quartz, epidote, sphene, and minor apatite, pyrite and magnetite. The plagioclase is saussuritized and epidotized. These altered feldspars usually retain a euhedral form, however, and crystals can be quite large, up to 1.5cm. Some sections show large euhedral plagioclase phenocrysts with well developed core to rim saussuritization, set in an interstitial quartz-albite granophyric intergrowth; the intergrowth has nucleated on the phenocrysts themselves (Plates 2.21 and 2.22). This is an obvious reflection of the hypabyssal and volatile-rich nature of the magma during crystallization of these rocks.

Pyroxenes are rare, and are nearly everywhere pseudomorphed by actinolite. Amphiboles are primary Ca-rich hornblende and secondary actinolite (see Appendix 2), which suggests that the original pyroxene component was clinopyroxene. The primary

Plate 2.19: Stockwork-type pyrite and chalcopyrite veins cutting melanocratic gabbro. From the Visnes region.

Plate 2.20: Stockwork-type pyrite and chalcopyrite veins cutting melanocratic gabbro. From the Visnes region.

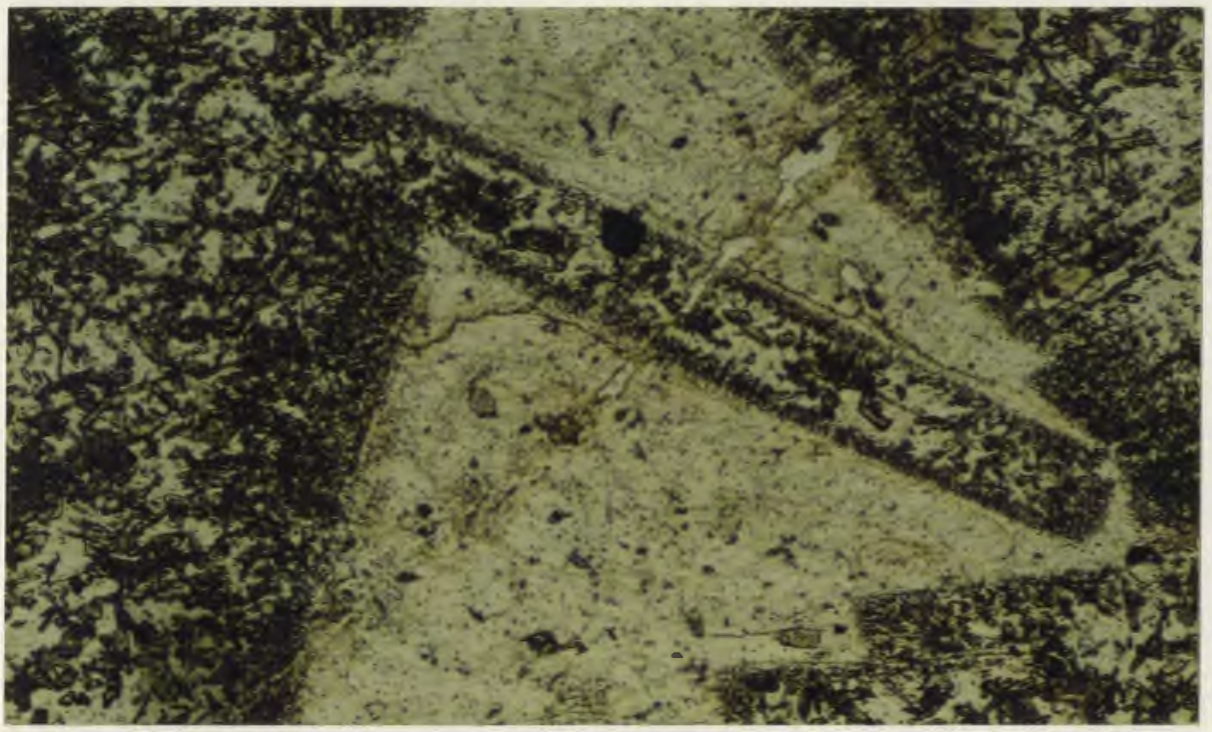

Plate 2.21: Plagioclase phenocrysts in gabbro pegmatite. The plagioclase has well developed core to rim saussuritization, and is set in a matrix of quartz and albite intergrowth (magnification: 40X; ppl).

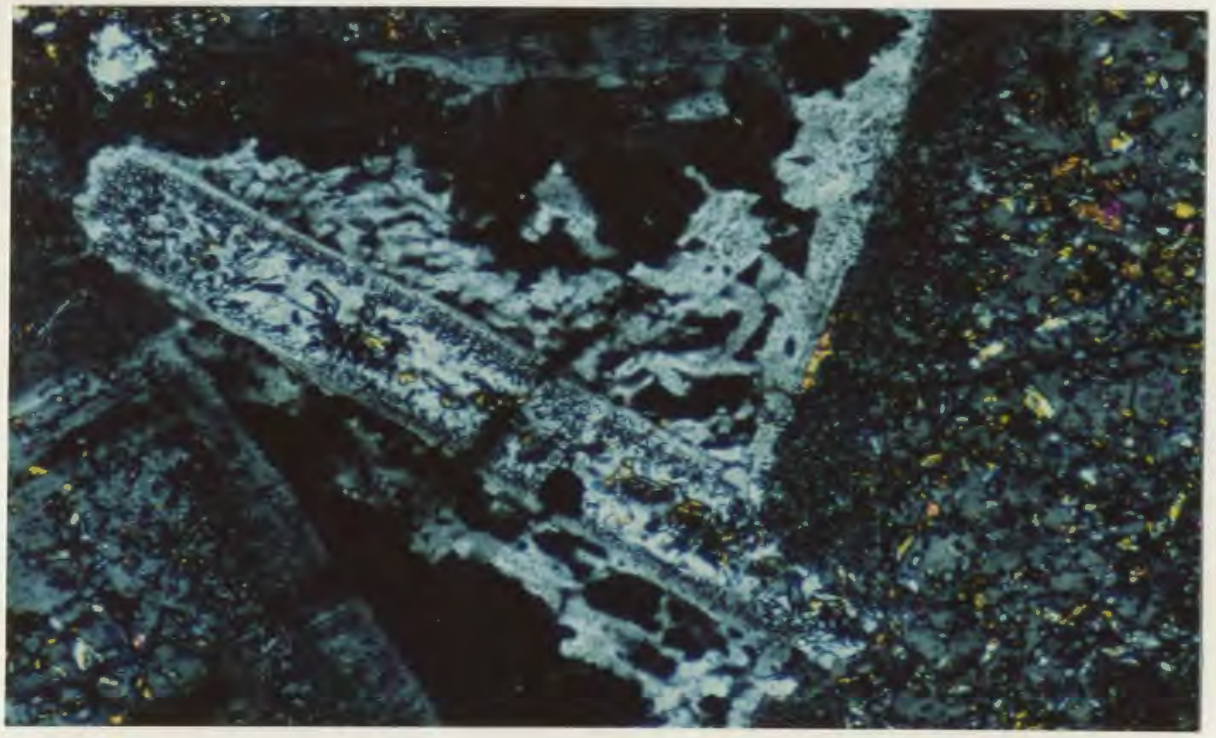

Plate 2.22: Plate 2.21 photographed under crossed nicols to illustrate nucleation of the quartz-albite intergrowths on the rim of the plagioclase phenocryst (magnification: 40X; cn).

hornblende phenocrysts can be large, up to 3cm long, and in some places poikilitically enclose plagioclase.

2.2.4: Type 1 plagiogranite

Although plagiogranitic rocks are distributed throughout the whole of the region, they are volumetrically not that significant, representing $< 10\%$ of all the hypabyssal rocks in Visnes and Feoy. The Visnes (Type 1) plagiogranites are considered as stratigraphic intermediates between the roof assemblage and the underlying isotropic gabbros, and are genetically distinct from both the plagiogranites of the EKIC and the Type 2 plagiogranites.

The main bodies of plagiogranite occur in the southern half of the Visnes map area in pods of 10-100m width, although there is a larger unit of approximately 500m in length in the southeast sector. In the northern section of Visnes, plagiogranite is restricted to small screens or dykes within the sheeted complex. Where dykes or gabbros are brecciated, as on some of the nearby skerries, the interclast matrix is invariably plagiogranitic, as indeed is much of the material that intrudes and brecciates pillow lavas on these islands.

The plagiogranites are predominantly albite and quartz; sericitization of the plagioclase is only minor. All quartz shows undulatory extinction with variable degrees of subgrain development. Graphic quartz-albite intergrowth, reflecting the hypabyssal nature of the

rock, is quite common (Plate 2.23). Euhedral hornblende is often present in minor amounts, as is actinolite, ferroactinolite, epidote and fragmentary biotite in variable amounts. Magnetite and pyrite occur in trace amounts in some places. The plagiogranites are on the whole relatively fresh, and feldspars are not turbid as they are in the gabbro and dyke samples.

In the Dyrnes and Fiskdammen areas, plagiogranite grades into biotite-diorite, and in this latter area a dioritic dyke cuts both plagiogranitic and gabbroic rocks (Plates 2.24 and 2.25). The presence of primary biotite in these rocks is believed to be a rare occurrence in ophiolitic terranes, and is of some importance in understanding the genesis of the assocciated plagiogranites in that it provides a link in the fractionation series from gabbro to silicic, very low-K end members (Pedersen and Malpas, 1984).

The biotite-diorite is composed of plagioclase, quartz, biotite, amphibole, magnetite, ilmenite, apatite and zircon. Felsic minerals comprise 60% of the rock, while biotite and amphibole are the predominent mafic minerals.

At Fiskdammen, the diorite has numerous small (0.5-2cm wide) globules distributed throughout it (Plates 2.26 and 2.27). Pedersen and Malpas (1984) have suggested that these globules, or spherules, could be products of liquid immiscibility. When a dioritic liquid was injected into a pocket of plagiogranitic liquid, the compositional differences between the two resulted in the development of an emulsified two-liquid mixture, which upon cooling produced the spherules.

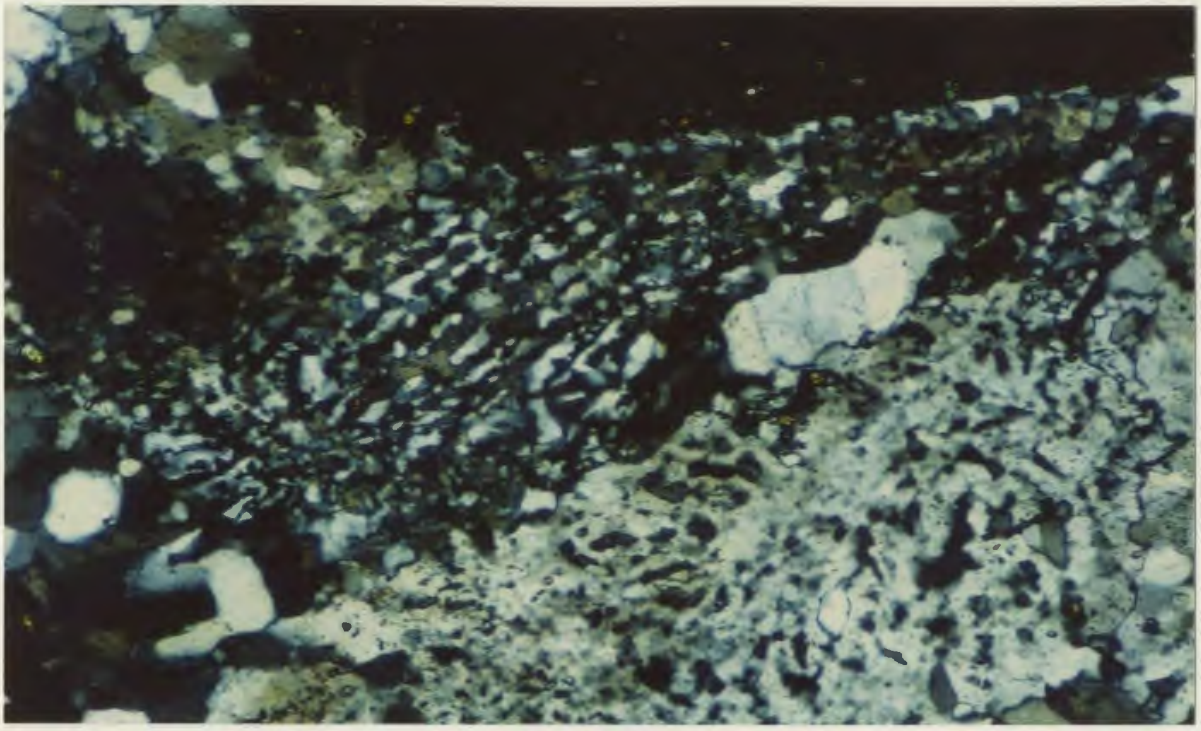

Plate 2.23: Photomicrograph of graphic quartz-albite intergrowth (mag.: 40X; cn).

Plate 2.24: Diorite dyke cutting Type 1 plagiogranite in the Fiskdammen area, Visnes. Note the presence of abundant immiscible "spherules" in the diorite dyke.

Plate 2.25: Epidotite veins (note green colored rock to the right of the hand) rimming the contact between plagiogranite (grey- below) and diorite (black- above) in the Fiskdammen area, Visnes. The contact between the epidotite and plagiogranite here is quite sharp.

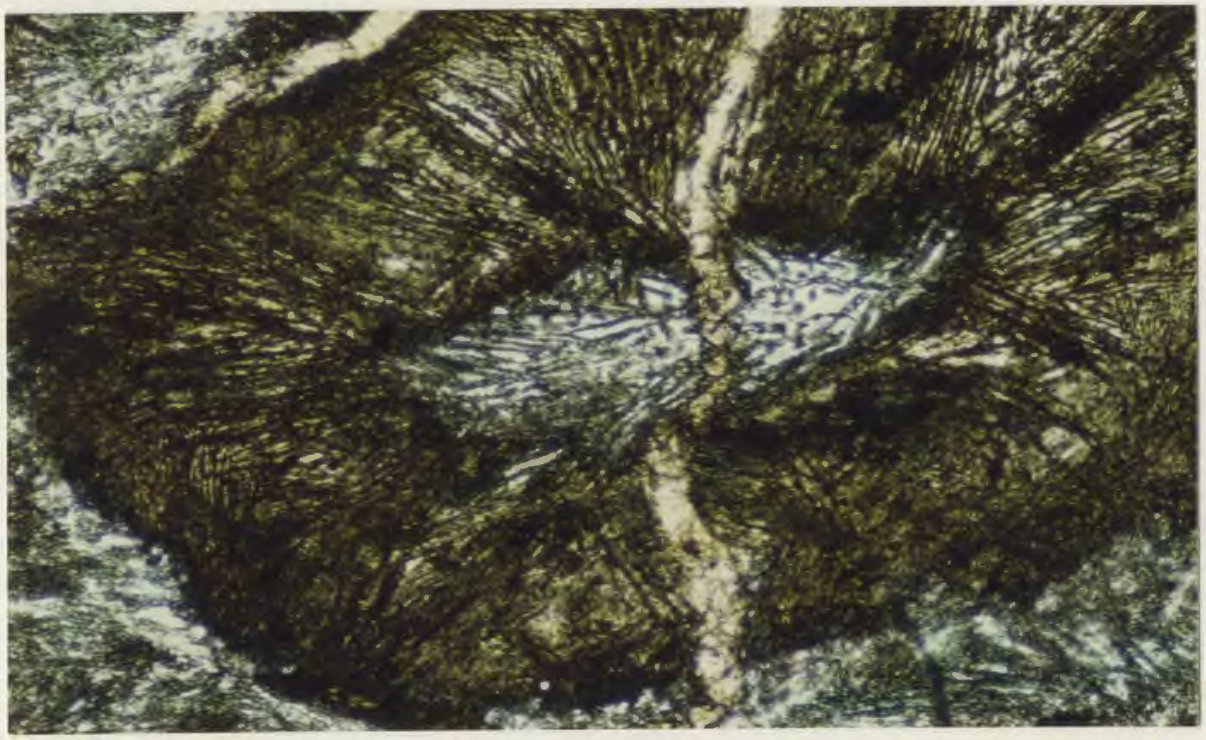

Plate 2.26: Photomicrograph of the "spherules" seen in Plate 2.24. The core of the spherules is composed of quartz-albite intergrowths, while the dark brown rim is composed of coarse epidote (magnification: 40X; ppl).

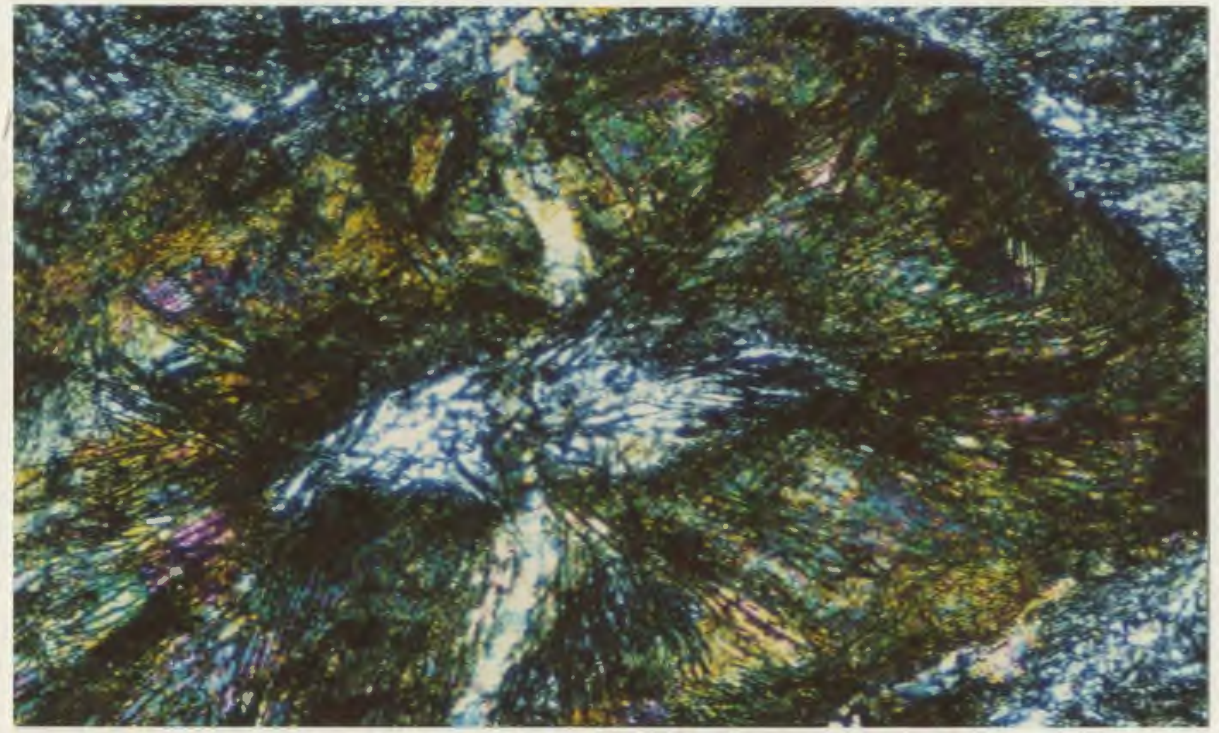

Plate 2.27: Plate 2.26 photographed under crossed nicols (magnification: 40X; cn).

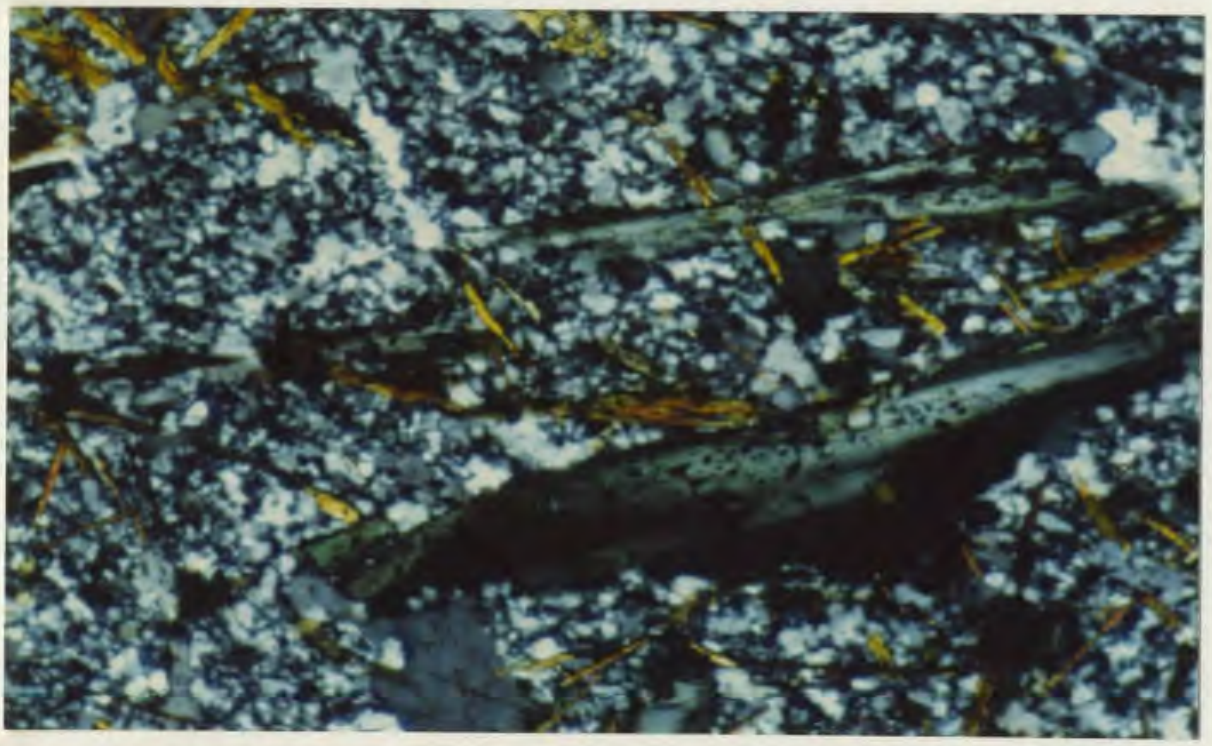

Plate 2.28: Photomicrograph of Type 2 plagiogranite illustrating fluxioned quartz-albite groundmass with an overprint of biotite (brown colored) and hornblende (grey colored) (magnification: 40X; cn).

The core of the spherules is plagiogranitic in composition, with quartz and albite intergrown in a radial pattern, exhibiting wavy extinction. The spherules are rimmed by a thick circular rind of coarse epidote.

There are several other possible explanations for this feature. It may be simply a result of spherulitic devitrification of a felsic dyke, or a quench texture. However, the diorite is a relatively coarse grained rock, and was therefore probably not quenched. If, on the other hand, this is an immiscibility texture as suggested above, the diorite and plagiogranite liquids may have emulsified as a result of simple differentiation mechanisms, or conversely the dioritic liquid may have been injected into the plagiogranite body, creating an emulsion (Pedersen and Malpas, 1984). The rind of coarse epidote suggests formation of the spherules under hydrous magmatic conditions.

2.3: Type 2 plagiogranite

A set of plagiogranitic or quartz dioritic dykes crosscuts rocks of the plutonic suite and associated sheeted complex in the study area. They are easily distinguishable from earlier formed plagiogranites on the basis of petrography and geochemistry. They are most abundant in the Feoy area, more specifically near the shear zone which hosts the Ni-sulfide body, suggesting that these dykes may possibly have intruded along fault zones.

The dykes generally trend about 65 degrees, but there are variations. They are

volumetrically insignificant, amounting to less than 5% of all dykes in the area.

In thin section, they have sugary microcrystalline textures, with a highly recrystallized and in places, a fluxioned groundmass (Plate 2.28). Plagioclase and quartz phenocrysts are all strained and show marginal subgrain development. In some samples autobrecciation is a dominant feature, with abundant fragmental quartz and plagioclase phenocrysts and glomerophenocrysts.

There is a late actinolite-hornblende-biotite overprint on the groundmass; actinolite is blue-green pleochroic, with a euhedral habit, while biotites are very fine grained, brown-pleochroic needles (Plate 2.29).

Near the Feoy Ni-sulfide occurrence, country rocks bordering a local shear zone have been mineralized by pyrrhotite, chalcopyrite and tourmaline. The mineralization occurs only on fracture surfaces of the rocks, and is confined to the area directly around the mine dump. This mineralization is likely a result of mobilization of the Feoy Ni-sulfides and circulation of boron-rich hydrothermal fluids along local shear zones during a period of metamorphism and deformation (see Chapters 4 and 7).

An important feature of these dykes is the lack of epidote alteration and netveining, a feature which was so prevalent in the rocks of earlier generations. This indicates that the Type 2 plagiogranites have escaped the spilitic alteration which intensely altered the

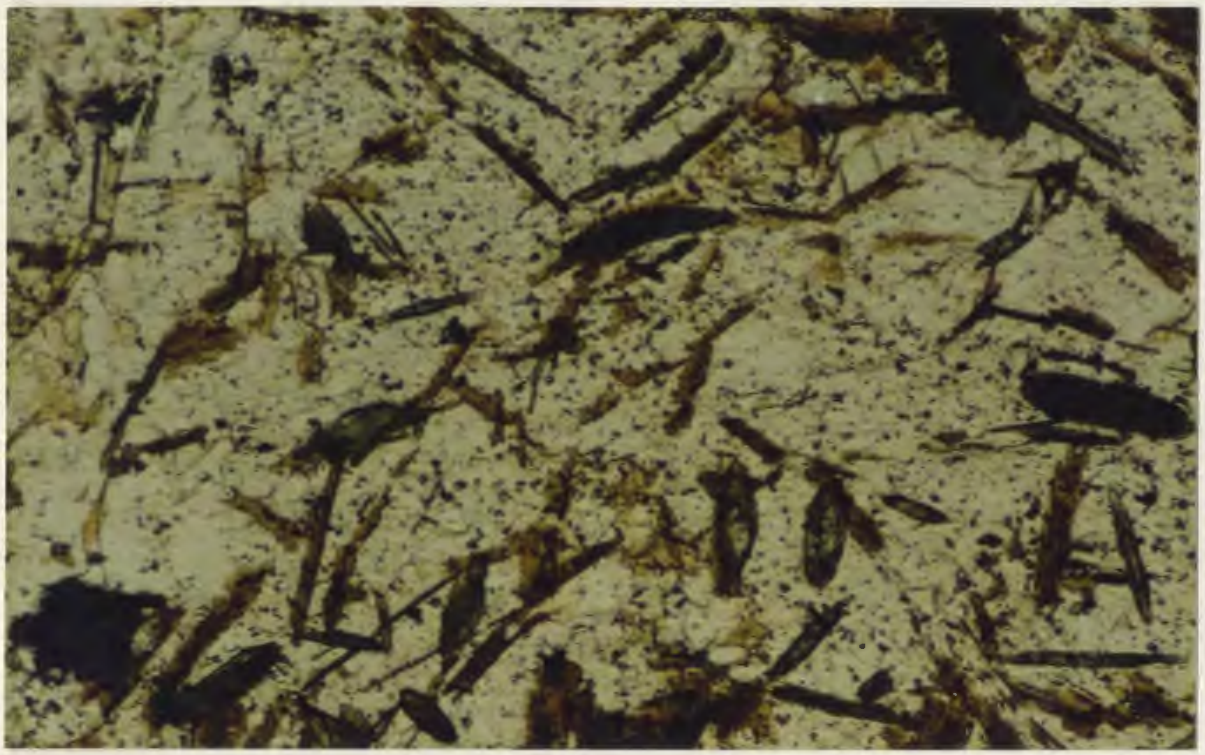

Plate 2.29: Metamorphic biotite overprint on Type 2 plagiogranite (magnification: 40X; ppl).

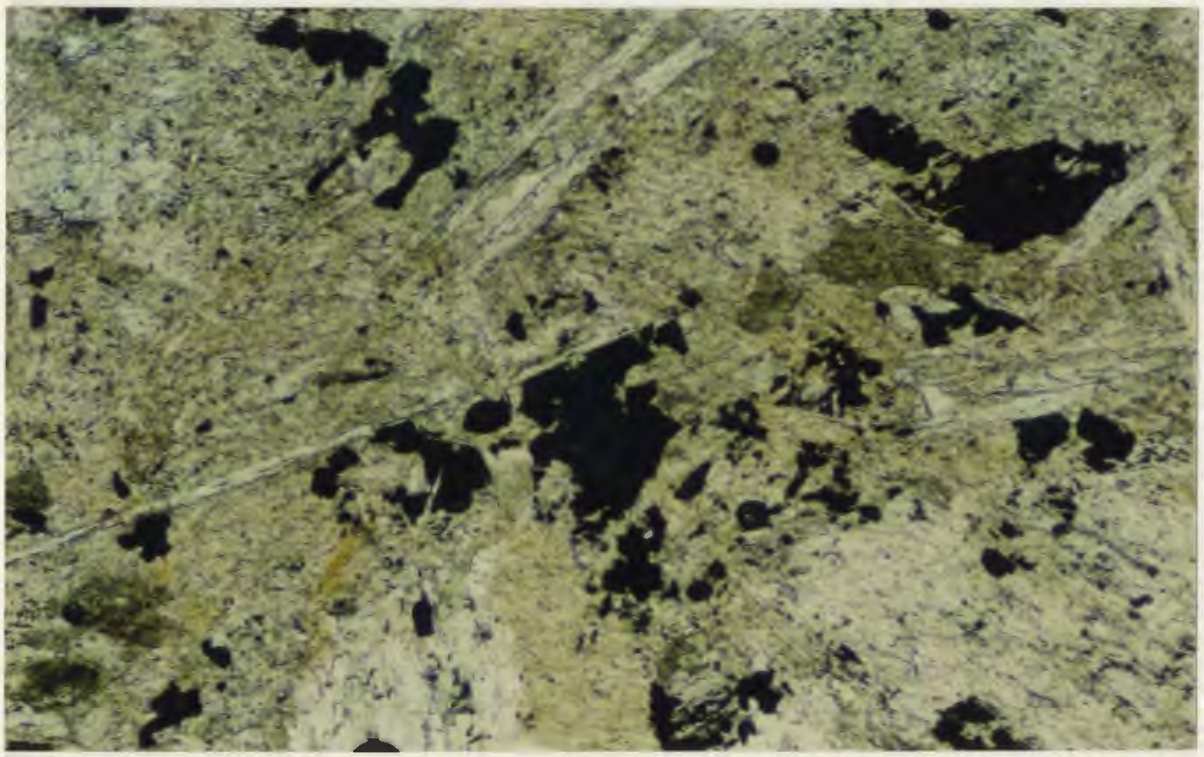

Plate 2.30: High-Mg dyke sample illustrating Ni-sulfides (pyrrhotite and pentlandite) "interstitial" to actinolite (grey and green colored) (after clinopyroxene) and chlorite groundmass (magnification: 40X; ppl).

Visnes dykes and pillow lavas. This is consistant with the current interpretation of the Type 2 plagiogranite dykes as products of late ensimatic arc activity (Dunning and Pedersen, 1987).

2.4: High-Mg dykes, associated diorite, and related clinopyroxene-phyric intrusions

2.4.1: High-Mg dykes

The latest stage of intrusive activity in the study area is evidenced by swarms of mafic-ultramafic dykes which are petrographically and geochemically unique, with a high-MgO, low-TiO2 chemistry, similar to basaltic rocks found in the Bonin Islands of the western Pacific Ocean (Crawford et al., 1981). They are later than basic dykes of the sheeted complex, because: 1- they generally crosscut the sheeted dykes at a high angle (roughly north-south); 2- they have been shown by Dunning and Pedersen (1987) to be geochemically related to very late clinopyroxene phyric intrusions in the area, and; 3- unmineralized and relatively unaltered high-Mg dykes are seen to cut highly altered, mineralized and epidotized dykes of the sheeted complex.

The high-Mg dykes are more competent than the other basalts, and have a darker green colour. They are aphyric, and in the direct area of the Feoy Ni-sulfide body they contain

abundant pyrrhotite and chalcopyrite. Nowhere do they contain any pyrite or sphalerite as do the Visnes dykes.

In thin section pyrrhotite and chalcopyrite can be seen to be interstitial to groundmass silicates (mainly amphiboles) (Plate 2.30). Nowhere else in the study area has pyrrhotite been found either interstitial to, or as veins in the country rocks. The presence of pyrrhotite interstitial to silicates, and its confinement to rocks in the Feoy mine dump area, is very important as it suggests that a genetic relationship exists between the high-Mg dykes and the Feoy Ni-sulfide body.

In some areas of Feoy, especially near the Ni-sulfide occurrence, high-Mg dykes contain tension gashes filled with coarse crystalline tourmaline and quartz (Plates 2.31 and 2.32). They are, however, distinctly less fractured than other dykes, and as mentioned do not contain any epidote-quartz netveining. They do not host any disseminated pyrite as do the Visnes dykes, gabbros and pillow lavas.

Although the dykes look relatively fresh in hand samples, when examined petrographically they reveal extensive alteration to lower amphibolite, tremolite-actinolite facies metamorphic assemblages. In thin section they are 90-100% chlorite-tremolite-/ferroactinolite (after clinopyroxene) which is often quite coarse grained. In some sections porphyroblastic amphibole growth is observed up to 2cm in length (Plate 2.33). Minor alteration constituents include talc, calcite, serpentine and tourmaline. Because much of the amphibole may have grown porphyroblastically from a finer grained parent groundmass (as opposed to incipient alteration of clinopyroxene phenocrysts), it

Plate 2.31: Large (up to 3cm) tourmaline crystals along microfractures, cracks and dyke margins in basic dykes. From the Feoy area.

Plate 2.32: Quartz and tourmaline filling tension gashes in basic dykes in the Feoy area.

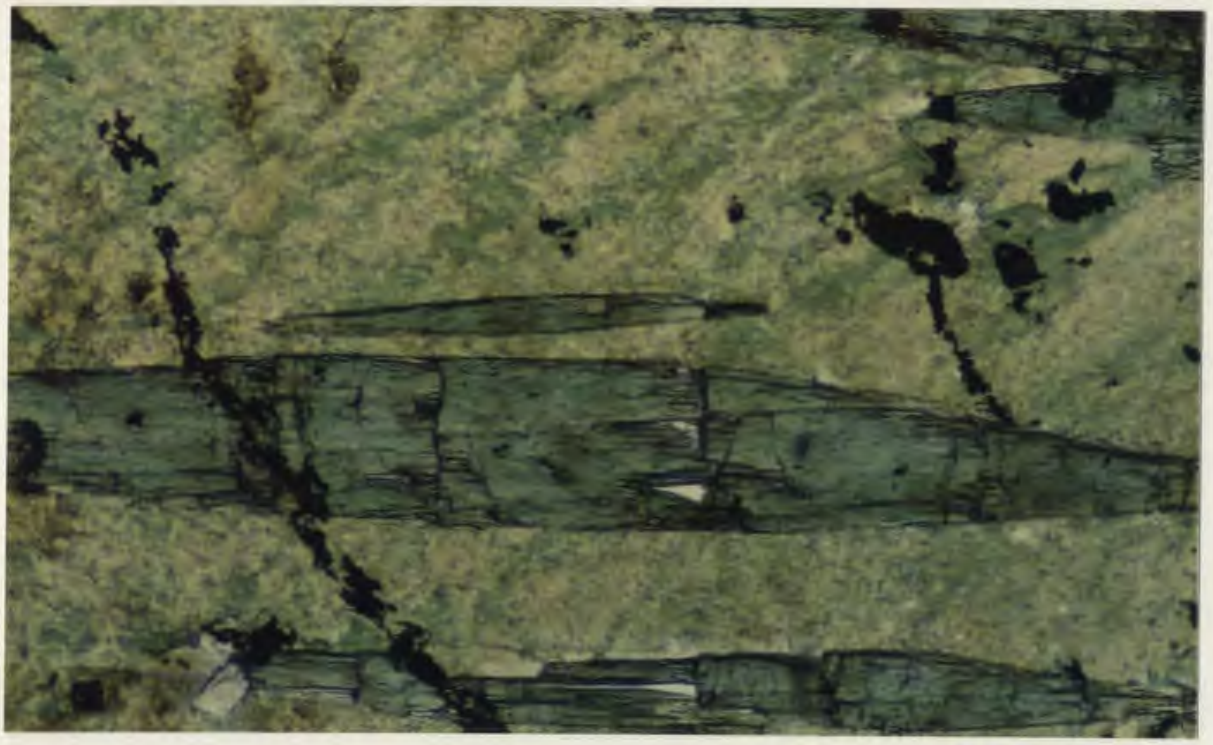

Plate 2.33: Large (up to 2cm in length) actinolite porphyroblasts in a groundmass of chlorite and actinolite. From a high-Mg dyke sample from the Feoy area (magnification: 40X; ppl).

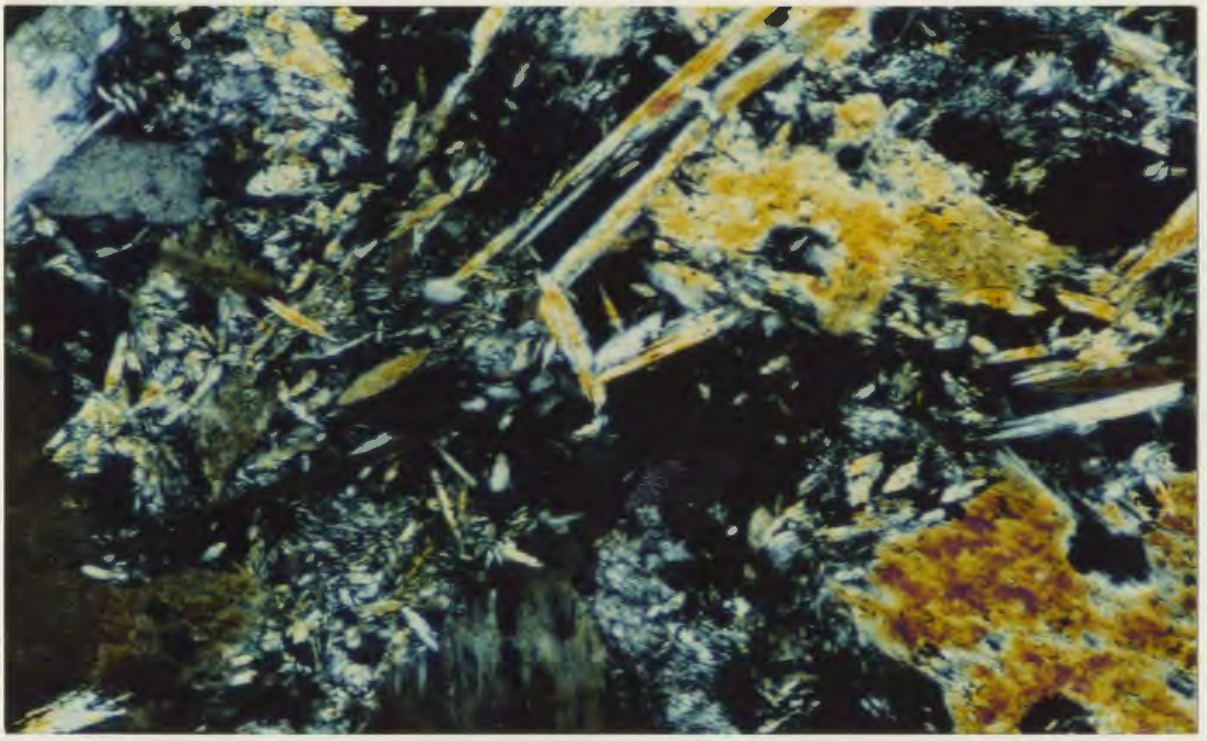

Plate 2.34: Photomicrograph illustrating alteration assemblage in diorites from the Visnes area. Note abundant actinolite (yellow/brown), and chlorite (green) (magnification: 40X; cn).

is impossible to tell whether these dykes were originally porphyritic or not.

The alteration and mineralization assemblages seen in the high-Mg dykes are distinctly different to those seen in the Visnes dykes. As mentioned, mineralization in the former rocks is in the form of pyrrhotite and chalcopyrite as interstitial phases to the silicate minerals, and is confined only to the Feoy mine dump area. Mineralization in the latter rocks is on a regional scale, and consists of disseminated pyrite, chalcopyrite, and rarely sphalerite; mineralization intensifies with increasing proximity to the main Visnes orebodies. These are important distinctions in that they suggest that the high-Mg dykes are related to the Feoy sulfide deposit, and that they are unrelated to the sulfide mineralization associated with the Visnes deposit.

2.4.2: Diorites

Two small (approximately 100 and 300m wide) diorite bodies intrude gabbros and dykes of the sheeted complex in the Visnes area along the main shear zone. They are texturally and mineralogically different from the biotite diorites of the Dyrnes area. Unlike the latter, they do not contain biotite, nor do they contain any of the "spherules" found in the Dyrnes diorites. They are quite homophanous, and have a creamy colour in the field, considerably lighter in colour than the gabbros. They are medium to coarse grained, and are quite altered and weathered.

In thin section, these diorites are distinctive. All plagioclase has been altered to

grey-black clay mineral assemblages. There are abundant large tremolite-after-pyroxene pseudomorphs (Plate 2.34), although some relict clinopyroxene persists. There is also some talc and serpentine alteration, although this is not as abundant as amphibole. As the alteration assemblages suggest, these diorites are more mafic than the surrounding rocks. This is verified geochemically, as they contain up to 15 wt.% MgO (Scott, 1985).

The alteration mineralogy of the diorites is similar to the high Mg-dykes, i.e. they have undergone incipient actinolite-tremolite facies metamorphism, with limited development of serpentine and talc. Geochemically their relationship can be verified by their mutually high MgO-Cr-Ni, low TiO2 chemistry, as shown by Pedersen (1987).

These diorites illustrate several important field relationships. As mentioned, the alteration pattern present in these diorites is different from that in the surrounding country rocks (Visnes dykes, pillow lavas and gabbros). However, while the latter rocks are heavily mineralized with Fe-Cu-Zn sulfides of the nearby Visnes massive sulfide deposit, the diorites are not, even though these intrusions are situated only several hundred meters from the main Visnes orebody. Therefore, like the high-Mg dykes of Feoy, intrusion of the diorites likely post-dated: (1) formation of the Visnes dykes, pillow lavas and gabbros; (2) seafloor alteration of these rocks, and (3) formation of the Visnes massive sulfide deposit. Also, there must have been an episode of alteration/metamorphism subsequent to intrusion of the diorites. This is consistent with interpretation of field data from earlier sections.

2.4.3: Clinopyroxene-phyric intrusion

In the Feoy area, a small gabbroic intrusion cuts all other rock types. It is texturally distinct in its preponderance of large phenocrysts of clinopyroxene, and shows a distinct layering or banding parallel to the margins of the intrusion. The intrusive boundary itself is clearly defined and abrupt, with well developed chilled margins. Pedersen (1987) has demonstrated the ensimatic arc affinity of this gabbro, although he suggests that it has a somewhat more calc-alkaline affinity than other rocks in the area. There are, however, broad geochemical similarities between this gabbro and rocks of the high-Mg suite (diorites and dykes), and so a possible relationship between the two cannot be dismissed.

2.5: Sediments

A small outcrop of highly deformed sedimentary rocks occurs near Digermulen, Visnes. These sediments most likely constitute part of the base of the Torvastad Group (Pedersen and Hertogen, 1987) (see Figure 2.1). They are creamy coloured felsic pyroclastic rocks to green coloured mafic, plagioclase-fragmental sandstones which have been intensely deformed and stretched parallel to the north-south shear zone which truncates them in Digermulen Cove. In this same area, an adit was sunk into the shear zone adjacent to the sediments, and there is abundant quartz-chlorite veining and associated pyrite. The presence of such

mineral assemblages along these large shear zones indicates that a period of deformation and hydrothermal alteration occurred after formation of these volcaniclastic sediments.

Pedersen and Hertogen (1987) have indicated that these sediments are derived from rocks of the clinopyroxene-phyric intrusion discussed in Section 2.4.3. This would put a maximum relative age on the deposition of the basal parts of the Torvastad Group of sediments at 470 +9/-5 Ma. In light of this evidence, it is possible that the ubiquitous conjugate shear zones in the area are not, as had been previously suggested (Sturt, 1978; Sturt and Thon, 1980), older oceanic shear zones that formed contemporaneously with massive sulfide deposition; rather they may be late, possibly post-emplacement shear zones. Alternately, they may indeed be older oceanic shear zones that were simply reactivated subsequent to, or during, ophiolite emplacement.

2.6: Epidotites

"Epidotites" in the study area are defined as rocks composed of 100% coarse crystalline epidote, which are believed to have formed from primary crystallization of aqueous magmatic or deuteric fluids (Pedersen and Malpas, 1984; the present study).

"Epidosite", on the other hand, is a term used to describe highly altered basalt

dykes and pillow lavas, with a secondary groundmass alteration assemblage of epidote, quartz and chlorite (Heaton and Sheppard, 1977; Aldiss, 1978; Richardson et al., 1987; also see Section 2.2.1). While epidote may occupy up to 80% of the groundmass in epidosites, distinction between epidotite and epidosite can be achieved on the basis of their whole rock chemistry. Figure 2.2 illustrates the chemical disparities between "epidotites" and "epidosites" of the study area, along with "epidosites" from Cyprus (Aldiss, 1978) and ideal epidote compositions from Deer et al. (1962). As expected, the "epidotites" plot closer to the field for ideal epidote compositions than do the "epidosites".

Epidotite "segregations" in coarse hornblende gabbro are seen on Feoy (see Section 2.2.3). These segregations are composed of circular patches of coarse crystalline epidote (crystals are up to 3cm in length). The epidotite grades quickly outwards into megacrystic hornblende-plagioclase assemblages, and then into background varitextured gabbro (see Plates 2.17 and 2.18). In thin section, these epidotites are composed of nearly 100% coarse, euhedral epidote crystals with interstitial quartz and occasionally albite (Plate 2.35). This appears to be an igneous texture, and along with the gradational contact of the segregations with the surrounding pegmatite provides convincing evidence for formation by cooling of a volatile-rich melt.

Epidotite is also found in association with Type 1 plagiogranite and biotite-diorite in the Fiskdammen and Dymes areas (as discussed in Sections 2.2.1 and 2.2.4).

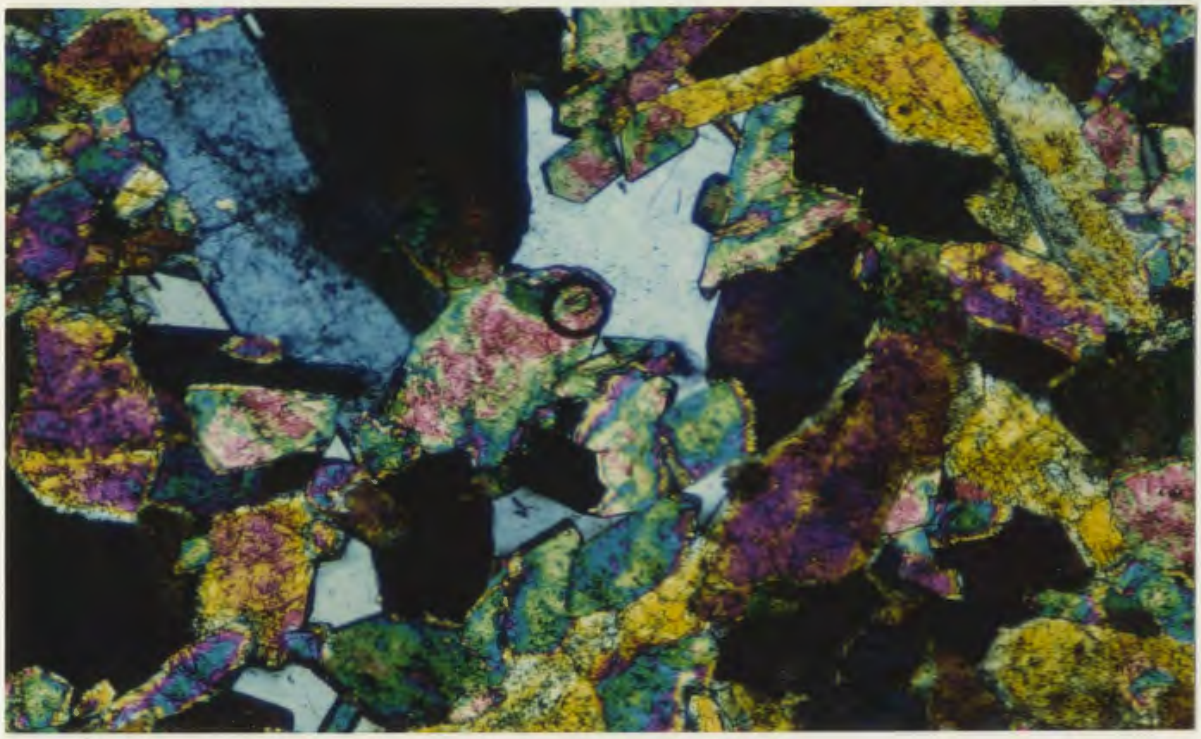

Plate 2.35: Photomicrograph of epidotite "segregation" in gabbro pegmatite from the Feoy area. Note the relatively fresh, coarse grained and euhedral epidote crystals in an unaltered interstitial quartz matrix (magnification: 40X; cn).

Figure 2.2 (a and b): Comparison of epidotites of the study area with "epidosites" from Troodos (data from Aldiss, 1978), and with ideal epidote (data from Deer et al., 1963) compositions (circles represent ideal epidote compositions; triangles represent epidotite compositions; stars represent Visnes epidotites; squares represent Troodos epidosites).

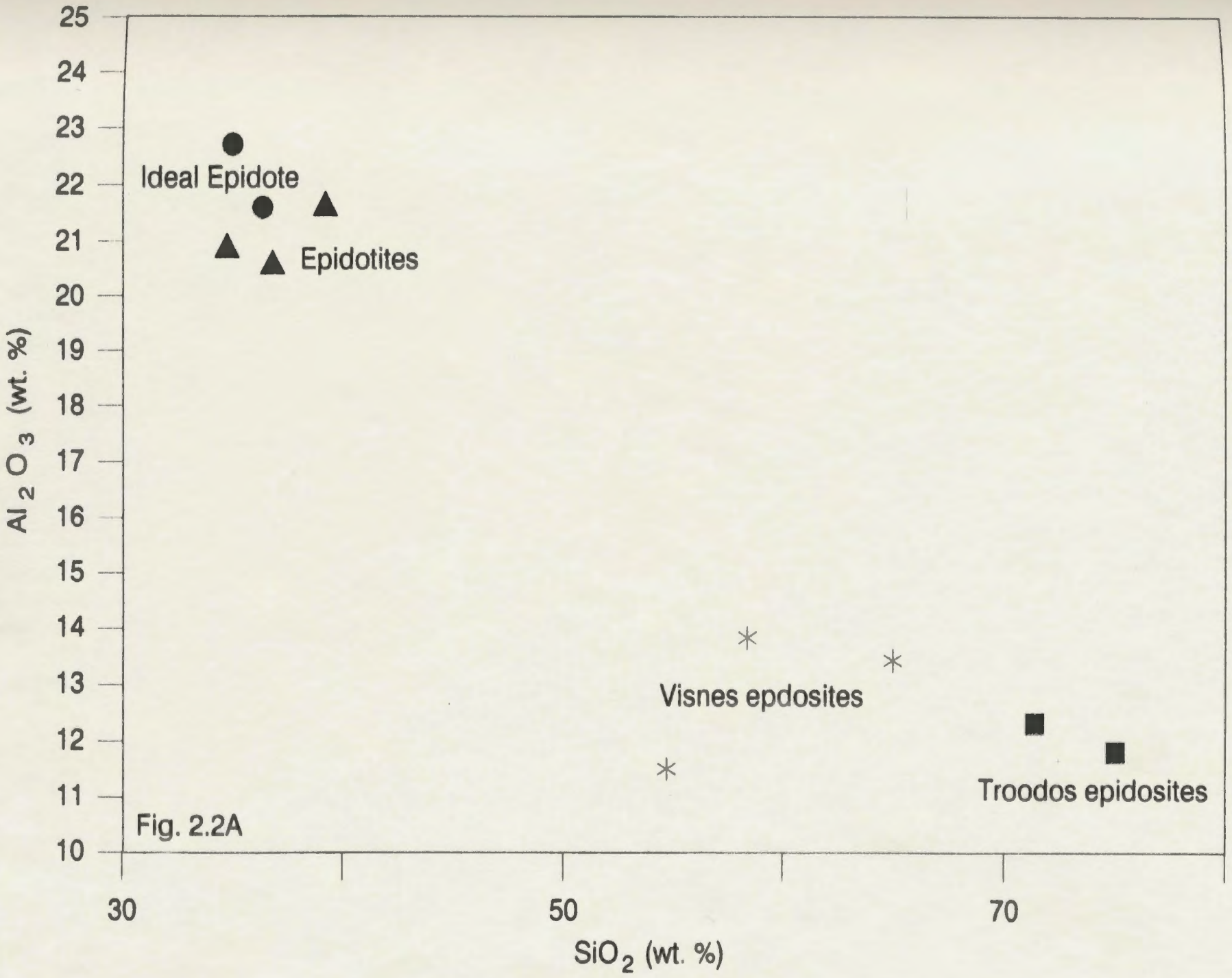
25
24
23
22
21
20
19
18
17
16
15
14
13
12
11
10
Ideal Epidote
Epidotites
Visnes epdosites
Troodos epidosites
Fig. 2.2A
30
50
70
Al_2O_3 (wt. %)
SiO_2 (wt. %)

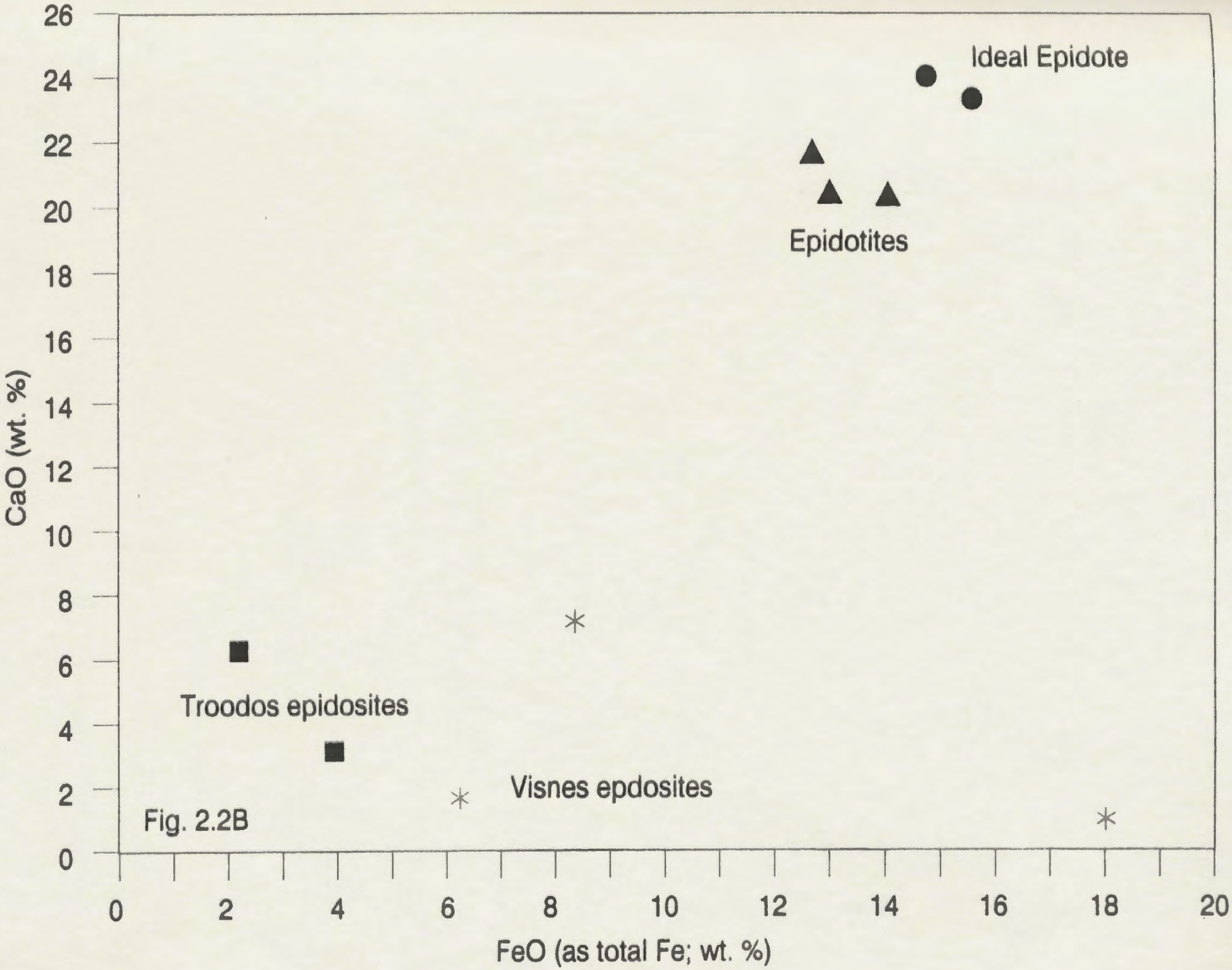
Ideal Epidote
Epidotites
Troodos epidosites
Visnes epdosites
Fig. 2.2B
CaO (wt. %)
FeO (as total Fe; wt. %)
0
2
4
6
8
10
12
14
16
18
20
22
24
26

Field relationships in these areas suggest that the epidotite and Type 1 plagiogranite were co-genetic, both rock types having formed from a residual, water saturated magma.

There are several other epidotite occurrences of interest in the study area. As mentioned, in the Dyrnes and Fiskdammen areas, large "streamers" of epidotite run parallel to the strike of the sheeted dykes, and in these areas the streamers are closely associated with selectively altered and mineralized dykes (see Plate 2.1 and Section 2.2.1). Dykes cut by these streamers are completely altered to "epidosite".

Some of the epidotite veins cutting gabbros and sheeted dykes contain "rinds" of euhedral pyrite cubes (Figure 2.3). Also, three epidotite rock samples were analysed for major oxides and trace elements (Table 2.1), and one of these samples (sample 22EPDT) contains anomalous concentrations of Cu, Zn, Ni and Cr. These features suggest that fluids which crystallized the epidotites also carried metals in solution through the country rocks, and that sulfides actually precipitated directly from these fluids. The high concentrations of Ni and Cr in particular in sample 22EPDT is testament to the extremely corrosive nature of the hydrothermal fluid, since these metals are considerably less mobile than the base metals Cu, Pb and Zn. Table 2.2 summarizes epidotite and epidote occurrences in the study area.

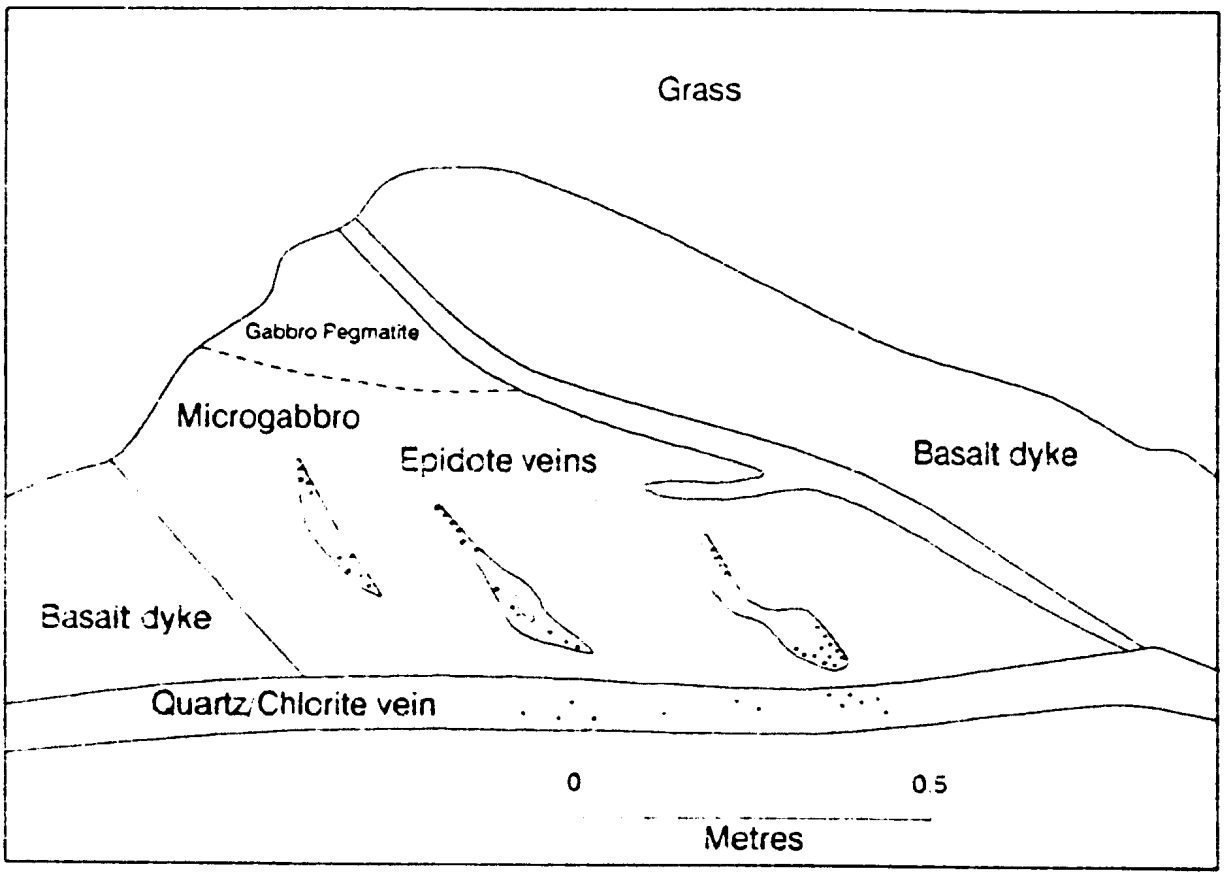

Figure 2.3: Sketch of epidotite vein containing a "rind" of euhedral pyrite cubes(pyrite cubes are represented by black dots). From an offshore skerrie in the Visnes region.

Table 2.1: Comparison of whole rock major oxide, Cu, Zn, Ni and Cr analyses of the Visnes epidotites with "epidosites" from Troodos and Visnes, and with ideal epidote analyses from Deer, Howie and Zussman (1962) (data for Troodos rocks is from Aldiss, 1978).

sample	SiO2	TiO2	Al2O3	FeO	MgO	CaO	Na2O
Epidotites of the Visnes region							
21EPDT	35.1	1.12	20.7	14.4	2.5	20.6	0.03
22EPDT	37.9	0.64	20.5	13.22	2.51	20.7	0.32
48EPDT	39.1	0.52	21.7	12.88	0.09	22.15	0.07
"Epidosites" from Visnes							
17	55.4	1.64	11.5	18.14	4.75	1.82	3.13
15	58.1	1.64	14.1	8.51	3.47	7.12	4.26
12	65.5	1.2	13.5	6.16	2.98	1.8	6.15
"Epidosites" from the Troodos ophiolite							
TM13	75.69	0.15	11.58	3.95	0.55	3.58	3.57
TM112	72.18	0.37	12.21	2.59	2.22	6.56	1.88
Ideal epidote mineral analyses							
Epidote-1	36.12	0.11	22.77	15.41	0.72	23.61	
Epidote-2	37.01	0.01	21.62	15.78	0.68	23.11	

Sample	Cu	Zn	Ni	Cr
21EPDT	30	19	3	0
22EPDT	363	61	61	101
48EPDT	6	0	0	0
17	0	32	0	0
15	3	19	0	0
12	4	93	0	0

In summary then, field data suggest that the epidotite netveins and streamers represent conduits or discharge zones for hydrothermal fluids which circulated around an underlying volatile-rich magma. Epidotite "segregations" in pegmatitic gabbros, and their association with Type 1 plagiogranites, illustrate the deuteric origin of these particular rocks, and provide direct evidence for the deuteric nature of at least part of the hydrothermal system. Discharge of these fluids from the magma chamber into the overlying sheeted dykes (through veins and microfractures, along dyke margins, and through the dykes themselves), along with probable mixing of these fluids with circulating hydrothermal fluids, was responsible for intense alteration and formation of local "epidosite" zones, and also contributed to formation of sulfides in these rocks.

These field observations are unique in that they illustrate the importance of a direct magmatic, deuteric fluid influence on zones of intense alteration and mineralization in the Visnes dykes. The oxygen isotopic tenor of the epidotites, and by inference the magmatic hydrothermal fluids, is discussed in Chapter 6.

Table 2.2: Epidote/epidotite occurrences in the Visnes area

Epidotite
- as large xenoliths in mafic dykes, along with plagiogranite
- as segregations in gabbro
- as streamers running parallel to the strike of the sheeted dykes
- as matrix along pillow lava margins
- as rims or rinds around plagiogranite xenoliths and spherules

Epidote
- as groundmass assemblage in all rocks affected by sub-seafloor alteration (spilitization), along with other typical spilitic alteration minerals.
- in the more intensely altered Visnes dykes (the epidosites), epidote is the main mineral
- as netveins cutting all rocks of the VHLC
- as veins with rinds of pyrite cubes

2.7: Late metamorphism and deformation features in the study area

The high-Mg dykes, Type 2 plagiogranites and diorites of Feoy are altered, deformed, brecciated and cross-cut by shear zones. Therefore, they must have undergone a period of metamorphism and tectonic activity which post-dates these and all other rock types in the area (since these are the youngest rocks in the study area).

While the rocks of the VHLC and associated Visnes massive sulfide deposit are also affected by this metamorphism and deformation, they had clearly been emplaced and then subsequently affected by seafloor alteration (spilitization) about 20m.y. prior to intrusion of the high-Mg dykes, Ni-sulfides, Type 2 plagiogranites and diorites of Feoy. This is clear because, as discussed earlier (see Sections 1.7 and 2.2):

1- geochronologic data date rocks of the VHLC at 493Ma, and about 470Ma for the aforementioned Feoy rock types;

2- field and petrographic data from the latter rock types show that there is no evidence of the seafloor alteration which is so prevalent in the older rocks of the VHLC.

This late, possibly post-emplacement (D2) deformation resulted in either new formation, or reactivation of old large scale shear zones as conjugate sets on a regional scale, along with development of a shear zone-parallel biotite overprint on a regional scale.

The post-emplacement nature of shear zone activity is recorded in the Digermulen area of Visnes (see Figure 2.1). In this area a large north-south striking shear zone appears to form a conjugate

set with the orebody-hosted northwest-southeast shear zone. The shear zone in Digermulen contains disseminated pyrite, and cuts volcaniclastic sediments of the Torvastad Group. These sedimentary rocks have been shown to be the volcanic equivalents to the clinopyroxene-phyric intrusion on Feoy (Pedersen, 1987), the latter having been dated at 470 +9/-5Ma (Dunning and Pedersen, 1987). The West Karmoy Igneous Complex is a post-emplacement granitic pluton which cuts the Karmoy ophiolite, and it is dated at ca. 450Ma (Priem and Torske, 1973). Given a considerable period of tectonic quiescence following intrusion of the clinopyroxene-phyric stock, which allowed for the development of a sedimentary basin before tectonic activity commenced, then the development (or reactivation) of these shear zones likely occurred very late in the evolution of the Karmoy ophiolite. It is possible that the shear zones may be related to intrusion of the granitic pluton, since the age limitations on this latest shear zone activity puts them close to the age of this pluton.

Other late metamorphic features include:

1- alteration of the high-Mg dykes and associated diorites to amphibole-chlorite assemblages (see Section 2.2);

2- development of a biotite overprint on the Type 2 plagiogranites, and a strong schistosity defined by actinolite and tremolite in all rock samples from in or near the shear zones;

3- features such as in situ brecciation (Types A and B breccias; see Chapter 4), tourmalinization (see Chapter 4), and complete reworking of the Feoy and Visnes sulfides (see Chapters 3 and 4) are all related to this late metamorphic episode, since they are contained within these shear zones;

As mentioned, whether these shear zones are solely a product of this late metamorphism, or represent later reactivation of previously formed oceanic shear zones, cannot be adequately assessed.

2.8: Summary and discussion of field relationships and petrology

Although there has been complex structural reworking and metamorphism within the study area during several periods, basic field relationships and petrographic studies still yield abundant information about the timing and separation of ore-forming, magmatic and metamorphic events. Based on these observations, the following summary and conclusions can be made.

1- An extensive sheeted dyke complex and associated gabbros, Type I plagiogranites and pillow lavas (the VHLC) are clearly the first formed of all rock units in the study area.

2- These rocks are characterized by epidote and quartz netveining, a regional pattern of extensive seafloor alteration (spilitization), and variable amounts of Fe-Cu-Zn mineralization. Within this area of regional alteration are smaller, more discrete zones of very intense alteration ("epidosite zones"), quartz and epidote "streamers", and more intense sulfide mineralization.

3- The pervasive regional scale alteration (spilitization) of these rocks probably occurred as a result of large scale circulation of hydrothermal fluids, probably dominated by seawater.

4- Local "epidosite zones" represent extreme alteration of pre-existing lithologies by the passage of more corrosive hydrothermal fluids which likely had a more direct magmatic origin. Associated epidotite veins and streamers correspond to "upflow zones" for hydrothermal fluids. Deuterically formed epidotite patches (segregations) associated with gabbro pegmatites and plagiogranites represent a magmatic source region for at least part of the hydrothermal system.

5- Regional scale alteration by seawater combined with local zones of intense alteration by ascending, magmatic hydrothermal fluids could well account for the overall patterns of alteration and massive sulfide occurrence in the Visnes region, and indeed corresponds very well with field relationships in the area.

6- There is evidence that immiscibility between plagiogranite, diorite, and epidotite played an important role in late stage magmatism at the spreading center. Also, subsequent to formation of these rocks, these was a renewal of basic magmatism, since epidotite and plagiogranite xenoliths are incorporated in large basic dykes in the Dymes area.

7- The high-Mg dykes and associated Ni-sulfides, diorites, gabbros, and Type 2 plagiogranites formed later than the rocks of the VHLC, and have escaped the period of spilitization (and associated Fe-Cu-Zn sulfide mineralization) which affected these earlier rocks. They are not netveined by epidote and quartz, as are earlier formed rocks. On the other hand, they have been altered to tremolite-actinolite facies assemblages during a subsequent metamorphic episode. Since the earlier formed rocks are dated at 493Ma, and the later formed rocks are dated at 485 +/-2Ma (Dunning and Pedersen, 1987), then spilitization and formation of the Visnes massive sulfide deposit must have occurred between these time periods. The study area therefore records at least two separate and distinct periods of alteration/metamorphism: early seafloor alteration of the VHLC, and; later tremolite-actinolite facies metamorphism and associated shear zone formation, affecting all rocks of the study area.

8- Finally, it is concluded from field data that the conjugate system of greenschist-facies shear zones in the area is probably a much later-formed feature than originally thought, and may not be related to formation of the Visnes sulfides at an oceanic spreading center, as has been suggested by earlier writers (eg., Sturt, 1979). Since these shear zones cut sediments of the

Digermulen group (maximum age, 470 +9/-5Ma, after Dunning and Pedersen, 1987) and in places contain remobilized pyrite (on Visnes) and Ni-sulfides (on Feoy), then these shear zones appear to be the youngest structural features in the area, possibly a post-emplacement (M2) feature, and are responsible for deformation of both the Visnes and Feoy sulfide deposits.

Chapter 3: The Visnes Fe-Cu-Zn massive sulfide deposit

3.1: Introduction

The study area contains two sulfide deposits, the Visnes Fe-Cu-Zn sulfide deposit and the Feoy Fe-Cu-Ni-PGE sulfide deposit. Chapters 3, 5 and 6 are concerned only with the Visnes deposit and associated country rocks; chapters 4 and 7 are concerned only with the Feoy deposit and associated country rocks. While both deposits occur within similar rock types (gabbroic, subvolcanic and volcanic rocks of the uppermost portions of the Karmoy Ophiolite Suite), and are in close proximity to one another (see Fig. 1.1), data from this chapter indicate that they are mineralogically and texturally quite distinct from one another. These data, combined with geological, geochemical and isotopic data presented in subsequent chapters, can be shown to be a function of their formation from quite different geological processes in different tectonic environments.

This chapter documents the geology and petrology of the Visnes deposit. This is followed in Chapters 5 and 6 by examination of associated country rock alteration as well as discussion of possible origins of the alteration and mineralization associated with the Visnes sulfides.

3.2: Historical perspective

In 1865 a Cu-rich sulfide seam was discovered in outcrop at Gronnevik, Visnes, and full scale mining commenced several years thereafter. By 1895 the mine shaft had reached a depth of 730m below sea level, and 1.8 million tons of Cu ore had been extracted. During this prosperous era, up to 70% of Norway's Cu export came from Visnes; indeed Visnes was one of northern Europe's largest Cu mines.

Visnes was somewhat of a unique mining community at the time. Although workers were local Norwegians, the owners were all Belgian and French, with much of the export going to these countries. There was little in the way of local control over profits, although this did not seem to concern the Norwegians, since the mining company had their own health and community services, complete with a hospital, school and police force.

During the years 1865-1895, 0.85 million tons of Cu-rich concentrate was exported. The Rodklev main shaft operated from 1899-1972, and extracted 2.8 million tons of ore. A smelting operation produced powdered Cu, Zn-oxide and Sulfur in 9 large ovens from 1872-1877 (Plate 3.1).

Today things are relatively subdued around Visnes. However, many relics testify to the activity of bygone days; on the rocks stretching out seawards there are remains of gunposts, trenches and bunkers which bear witness to the German occupation during

Plate 3.1: A view of the remains of the old smelting house in the Visnes area.

Plate 3.2: Hand sample of massive, banded pyrite-sphalerite-chalcopyrite ore from Visnes Kobberverk.

World War 2. In the Fransehagen area, beautiful old bridle paths still remain which were probably used to transport ore material in horse-driven carts. The mine sites themselves remain, albeit somewhat weathered by time and the elements, and they are filled in with rubble, or are flooded with seawater and barred up.

It has been rumoured that the Statue of Liberty in New York was built from Cu extracted from Visnes. In 1985, Cu from the Statue was analysed, and the origin confirmed by matching of trace elememts.

3.3: Structural and stratigraphic relationships

The Visnes ore zone is structurally controlled by shear tectonics; in fact the Visnes Kobberverk sits directly on a major greenschist facies shear zone which dips steeply (75-90 degrees east) and strikes northwest to north-northwest. The ore zones were originally composed of six cigar shaped to irregular bodies arranged en echelon (Geis, 1962)

Many smaller mineralized shear zones can be seen in the Visnes and Feoy areas, such as at Digermulen, Kvaloy and Sandholmen (see Figure 2.1). All of these occurrences are of disseminated to semi-massive pyrite and occasional trace amounts of chalcopyrite.

As mentioned, the mine itself has been closed for many years now, so that unfortunately

structural and geological maps and cross-sections of the orebodies were unavailable during this study, other than descriptions found in old mine reports.

Petrographic analysis of the sulfides indicates that there has been near complete reworking of the sulfides, and extensive modification by circulating hydrothermal solutions (see following sections). While the country rocks do contain disseminated sulfides, as mentioned the main orebodies are contained within a conjugate system of regional, large scale shear zones. Primary precipitation textures are almost totally absent in the Visnes sulfides (see following sections), and banding on a microscopic and macroscopic scale is now a dominent feature of the Visnes sulfide bodies.

Stratigraphically, the host rocks for the Visnes sulfides are mainly oceanic basaltic rocks of the Visnes Sheeted Dyke Complex (see Chapters 2 and 5), along with pillow lavas and lesser amounts of gabbros; this makes the Visnes deposit somewhat similar to the volcanic-exhalative deposits of the classical Cyprus type (Lydon and Galley, 1987), although metamorphism and shear tectonics have obliterated any primary sulfide textures in the Visnes sulfides (see following sections). This is in contrast to the host rocks for the nearby Feoy Ni-sulfide deposit (see Chapters 4 and 7), which are high-Mg dyke rocks of an arc-basin affinity (Pedersen, 1987).

3.4: Metal content of the Visnes sulfides

The Visnes occurrence is mainly a Cu-Zn deposit, although in some zones Zn is more

abundant than Cu. It is therefore classed as a Fe-Cu-Zn (in order of abundances) sulfide deposit, and because it occurs along shear zones within ophiolitic sheeted dykes, it is similar to many other such occurrences within the Appalachian-Caledonian mountains (ex., deposits of the Lokken, Trondheim and Joma areas of Norway, and the Bathurst, New Brunswick, and Ducktown, Tennessee deposits of North America; Bjorlykke et al., 1980; Foslie, 1926; Craig et al., 1984). There is significant Au in the Visnes sulfides, and during peak production years the byproduct Au may have paid for much of the production costs. The orebody is similar to the classic deposits of the Troodos ophiolite of Cyprus, although its localization within sheeted dykes rather than pillow lavas and sediments is atypical of Cyprus-type deposits. However, this may well be a result of later remobilization of the sulfides during deformation. Typical of Cyprus-type deposits, galena is present only in trace amounts in this orebody.

In general the ore is characterized by a predominance of pyrite; pyrrhotite has not been seen in any of the samples analyzed optically, although it has been reported to occur in trace amounts (Craig et al., 1984). On the scale of the orebody, sulfur varies from 25-45 wt.% (average of 35%); Cu varies from 0.5 to 3 wt.% (average of 1.7%); Zn varies from $<$0.5-2 wt.% (average of 1.4 wt.%), while Pb is always negligible (from 0-0.1 wt.%) (Per Singsaas et al., 1958).

Table 3.1. gives whole rock sulfide analyses for selected samples from the Visnes mine dump.

Table 3.1: Whole rock geochemical analyses of selected ore samples from the Visnes massive sulfide deposit.

Sample	Sulfur (wt.%)	Cu (wt.%)	Pb (ppm)	Zn (wt.%)	Mo (ppm)	Ni (ppm)
V-2	32.9	0.95	6ppm	22.5	41	0
V-9	35.1	1.45	0ppm	26.2	43	0
V-15	42.9	10.9	14ppm	3.2	61	0
V-22	27.2	0.71	0.54	26.6	35	0
V-28	43.1	1.1	284ppm	8.2	58	51

3.5: Ore petrology and geology

The Visnes deposit exhibits several gross similarities to other ancient Cu-Zn volcanogenic sulfide deposits. These are:

1- a preponderance of pyrite as the main sulfide mineral, with trace to no pyrrhotite;

2- a Cu/Zn ratio in excess of unity, although Zn may locally predominate;

3- a paucity of Pb;

4- a lack of any barite or other sulfate minerals which are so ubiquitous in modern day sites of sulfide precipitation (Lydon and Galley, 1987; Oudin, 1983; Hayman et al., 1984).

The sulfides of Visnes can be divided into 4 groups. These are: massive banded pyrite-sphalerite-chalcopyrite (Plates 3.2 and 3.3); massive pyrite and sphalerite (Plates 3.4 and 3.5); disseminated to semi-massive pyrite with minor chalcopyrite; minor stringer sulfides in gabbro (see Plates 2.19 and 2.20).

The most abundant sulfide type is the banded ore. This is 85-100% sulfide, with pyrite as the main component, and lesser amounts of chalcopyrite and sphalerite. It is invariably coarse grained (grains up to 0.4cm wide) and exhibits well developed triple point or annealed grain boundaries in thin section (Plate 3.6). These can be interpreted as metamorphic recrystallization features (Rockingham and Hutchinson, 1980; Ramdohr, 1980).

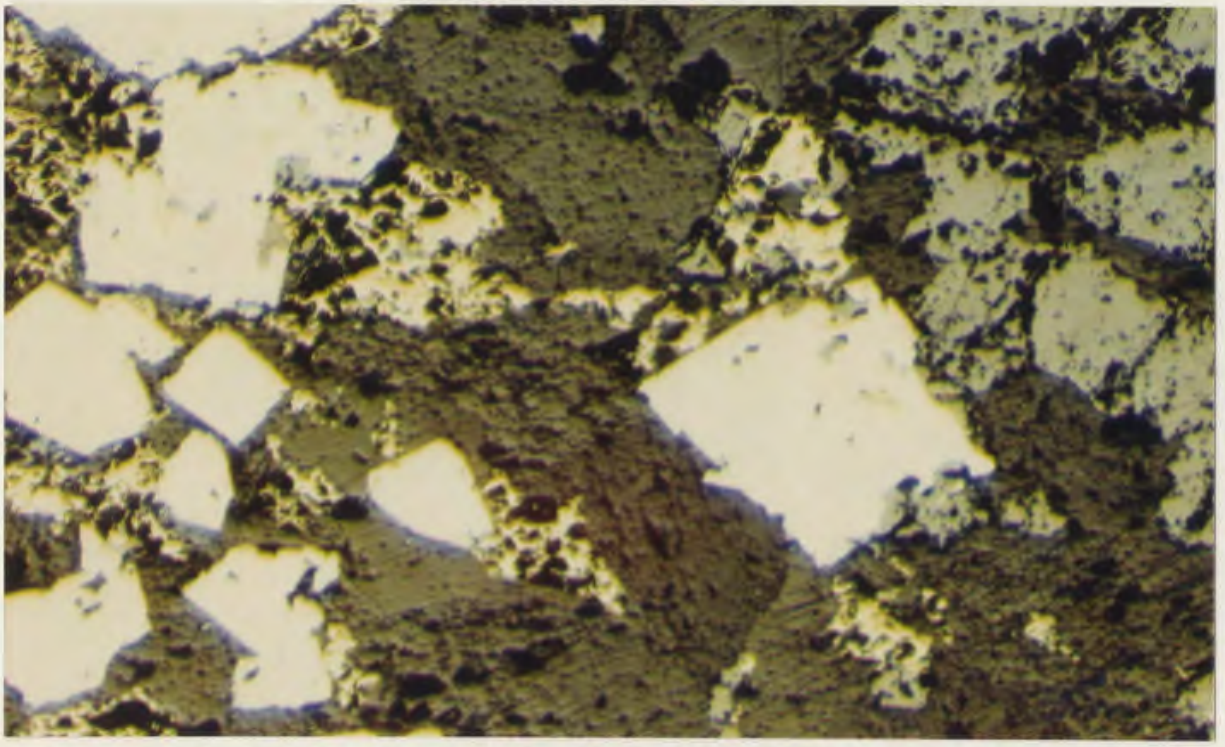

Plate 3.3: Photomicrograph of sample in Plate 3.2. Note pyrite cubes (white) with interstitial chalcopyrite (yellow) and sphalerite (grey) (magnification: 10X; reflected light, rl).

Plate 3.4: Hand sample of massive, banded pyrite-sphalerite ore from Visnes Kobberverk.

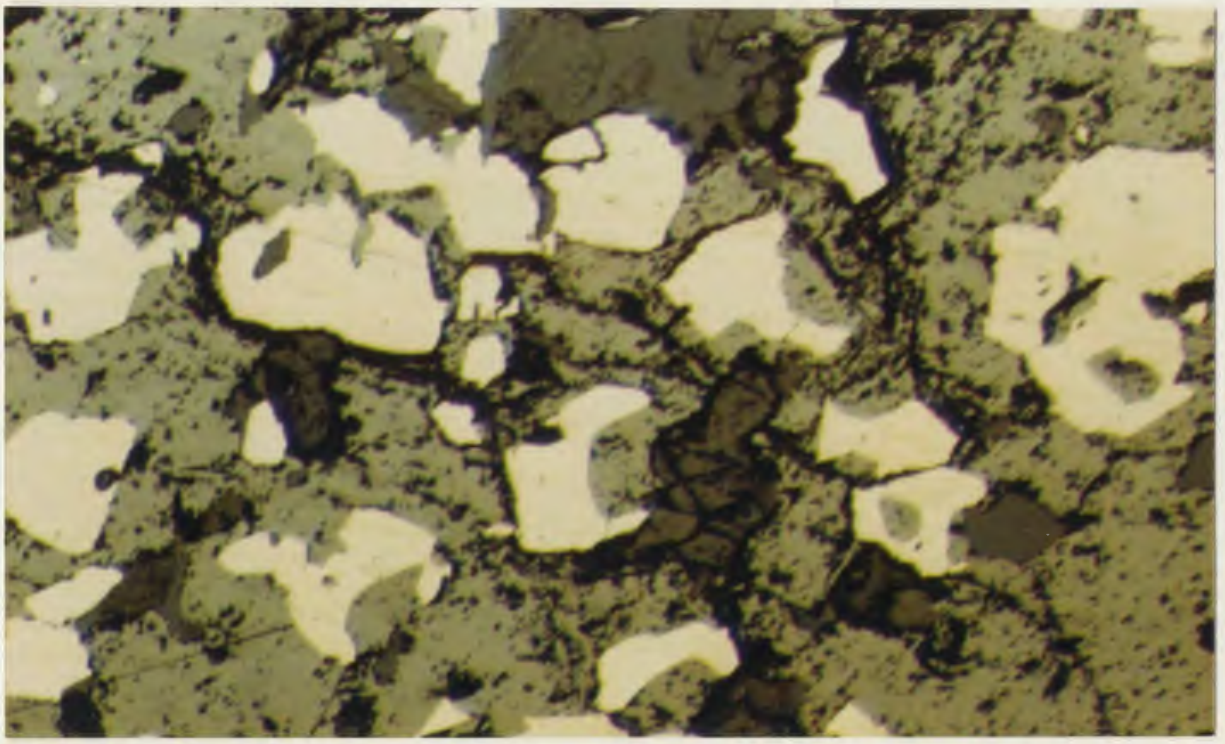

Plate 3.5: Photomicrograph of sample in Plate 3.4. Note the embayment of pyrite cubes (white) by sphalerite (grey) (magnification: 10X; rl).

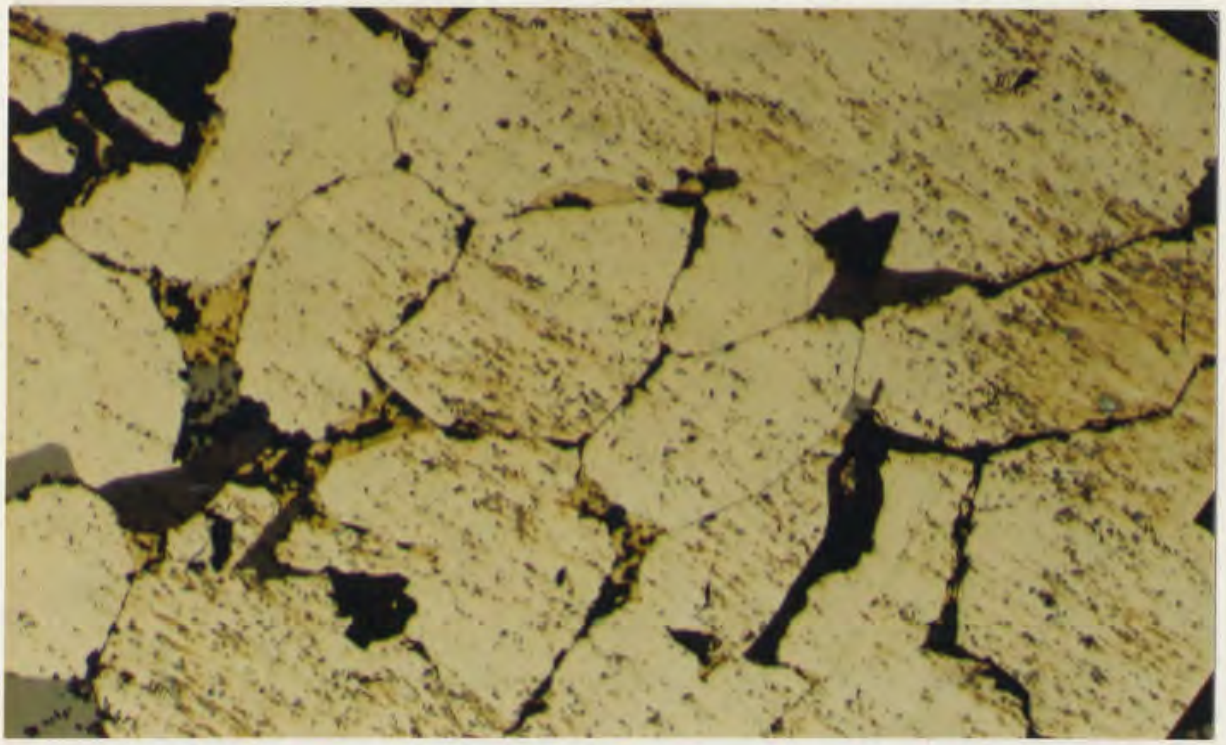

Plate 3.6: Annealed texture in massive pyrite from Visnes Kobberverk. Note yellow interstitial chalcopyrite (yellow) (magnification: 10X; rl).

Banding is usually on a centimeter or decimeter scale, and is restricted to the main orebodies in the Visnes and Rodklev shafts. It is possible that this banding may reflect a retention of primary sedimentary metal zonations during later deformation. However, sphalerite and chalcopyrite might be expected to be easily mobilized during such deformation (Ramdohr, 1980), and may have migrated into parallel layers or cracks. Several samples contain >95% massive pyrite or sphalerite. In such samples the pyrite is generally fresh and strongly annealed, except where it remains as euhedral, individual crystals where there is significant interstitial gangue. The massive sphalerite samples are completely recrystallized, and may simply be samples of a larger sphalerite band in pyrite. Sphalerite in these cases exhibits a strong tectonic fabric (Plate 3.7).

Disseminated pyrite and very minor disseminated chalcopyrite are present along many of the smaller shear zones in the area. Such occurrences are without exception shear zone controlled, where pyrite occupies up to 30% of the host chlorite schist. In one sample, the host rock is ferro-actinolite schist (Plate 3.8). These mineralized zones cut all rocks in the study area, and show no stratigraphic or lithologic preference. There is no evidence of any increase in pyrite-chalcopyrite dissemination with progression towards the main orebody.

The last type of sulfide occurrence associated with the Visnes deposit is a small zone of stringer pyrite-chalcopyrite veins (1-2cm wide) in melanocratic gabbro on one of the nearby skerries (see Plates 2.19 and 2.20). This occurrence is small enough not to warrant being labelled a major stockwork or "discharge" zone; indeed it may well

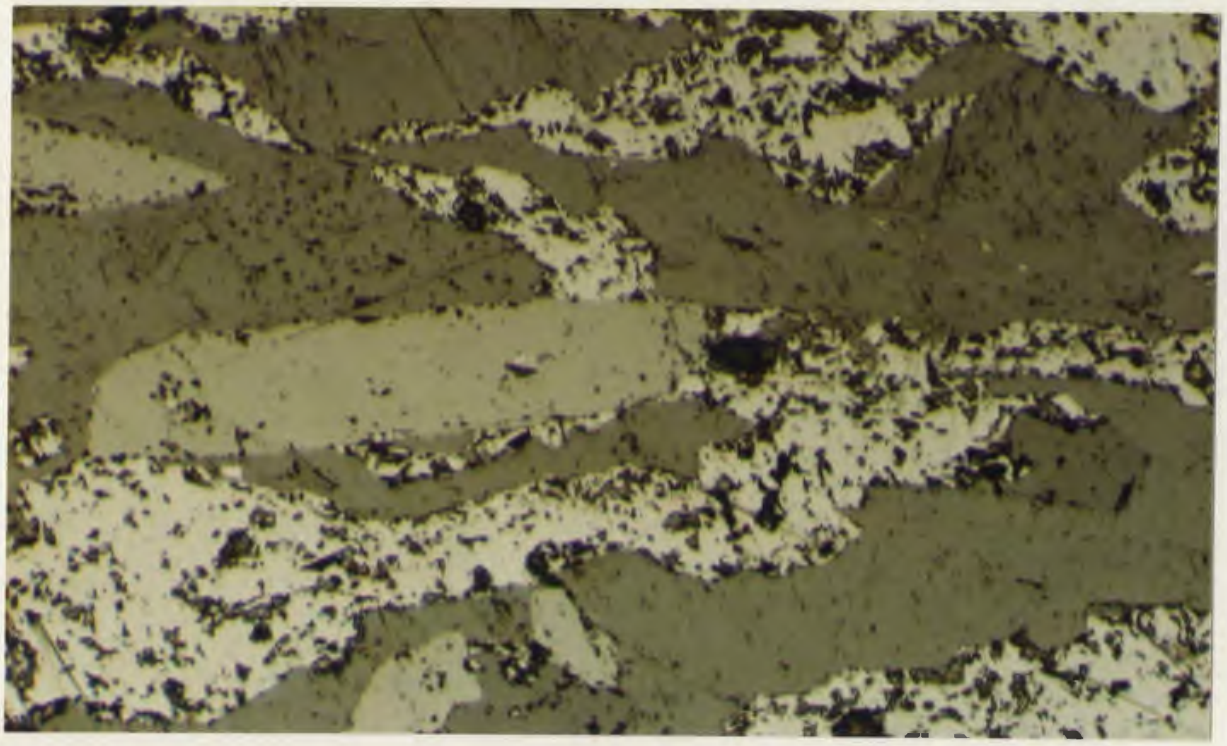

Plate 3.7: Tectonic fabric in massive sphalerite ore from Visnes Kobberverk. Sphalerite is light grey, and is strongly alligned from left to right (magnification: 10X; rl).

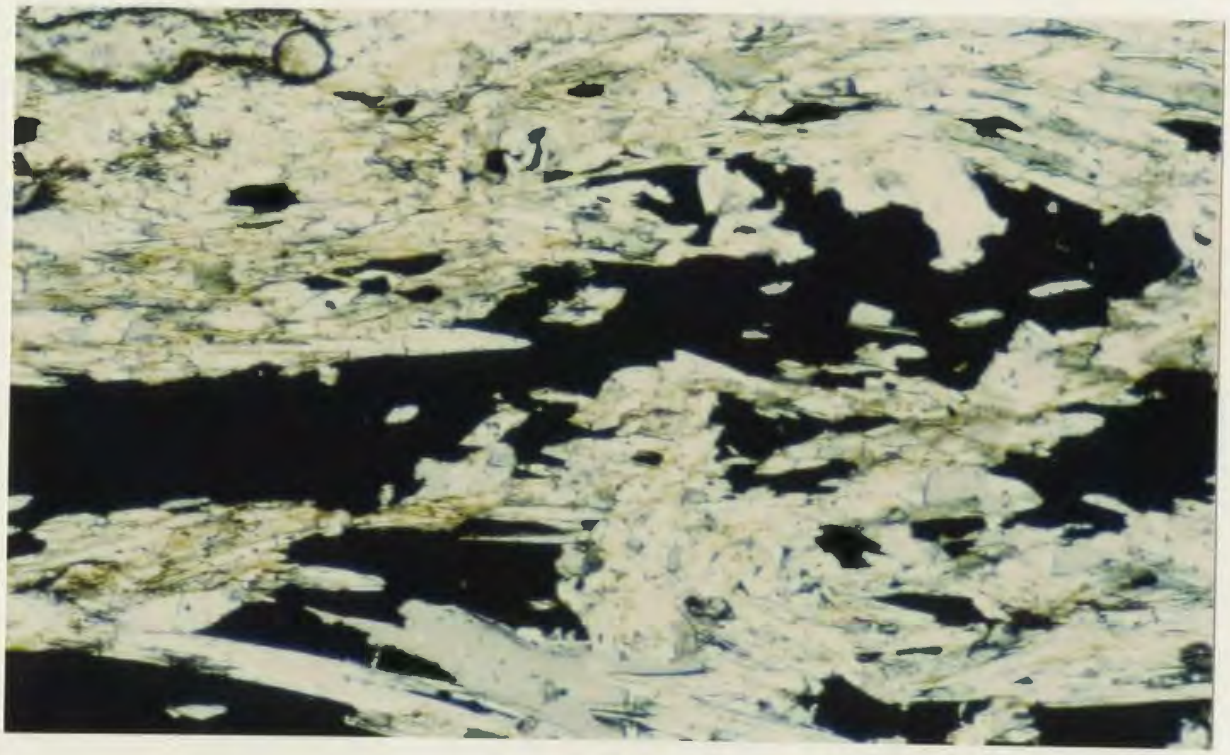

Plate 3.8: Actinolite-pyrite schist. Taken from main shear zone in Visnes Kobberverk (magnification: 10X; ppl).

represent metamorphic sulfide remobilization along fractures. The possibility remains however, that such veins may constitute part of a larger stockwork zone analogous to similar "feeder zones" for the main sulfide deposit, as seen in the Cyprus and Bett's Cove ophiolites.

Petrographic analysis of sulfide textures and mineralogy in these ore types is given below.

Pyrite

Pyrite exhibits a wide grain size distribution even within a single thin section, from fine (<0.5mm) to coarse grained (up to 0.75cm in pyrite porphyroblasts). It is usually subhedral and coarse grained. Where there is abundant interstitial chalcopyrite or sphalerite, the pyrite is often rich in inclusions of these sulfides. It is usually quite fresh when massive, with well developed annealing texture (see Plate 3.6). However, where associated with quartz and amphibole gangue, the pyrite is sometimes strongly corroded or altered. Pyrite illustrates several features indicative of its metamorphic modification:

1- the association of metamorphic gangue assemblages of quartz-actinolite-calcite with lesser albite;

2- the strong annealing texture in massive pyrite;

3- the corroded nature of the pyrite when associated with amphibole or quartz in schistose rock samples;

4- grain growth of pyrite around older pyrite grains in strongly annealed pyrite

groundmass;

5- cataclastic pyrite is replaced by chalcopyrite, and corroded and cut by quartz vein networks.

Because of the extent of recrystallization, it is not possible to qualify the physical nature (either crystalline or as a colloidal sediment) of the pyrite prior to deformation and metamorphism. The observation of grain growth in one sample, the complete lack of any primary sedimentary or colloidal features, and the presence of relatively unfractured, large pyrite porphyroblasts might suggest (according to Ramdohr, 1980) that there was already a relatively coarse grained pyrite component before metamorphic coarsening of grain size.

There is no evidence for any sedimentary sulfide textures in this deposit (such as framboidal or colloform pyrite), with the exception of small amounts of "Vasskis". This amorphous, Fe-rich silicate-sulfide "mud" (Plate 3.9) may represent the original seafloor sulfide precipitate; it is also recorded from several other Norwegian and Canadian massive sulfide deposits (Vokes, 1980; Stevens, 1980; Grenne et al, 1979). Apart from this however, all evidence of the primary chemical precipitation of the sulfide has been obliterated.

Chalcopyrite

On the scale of the orebody chalcopyrite is more abundant than sphalerite, but is present

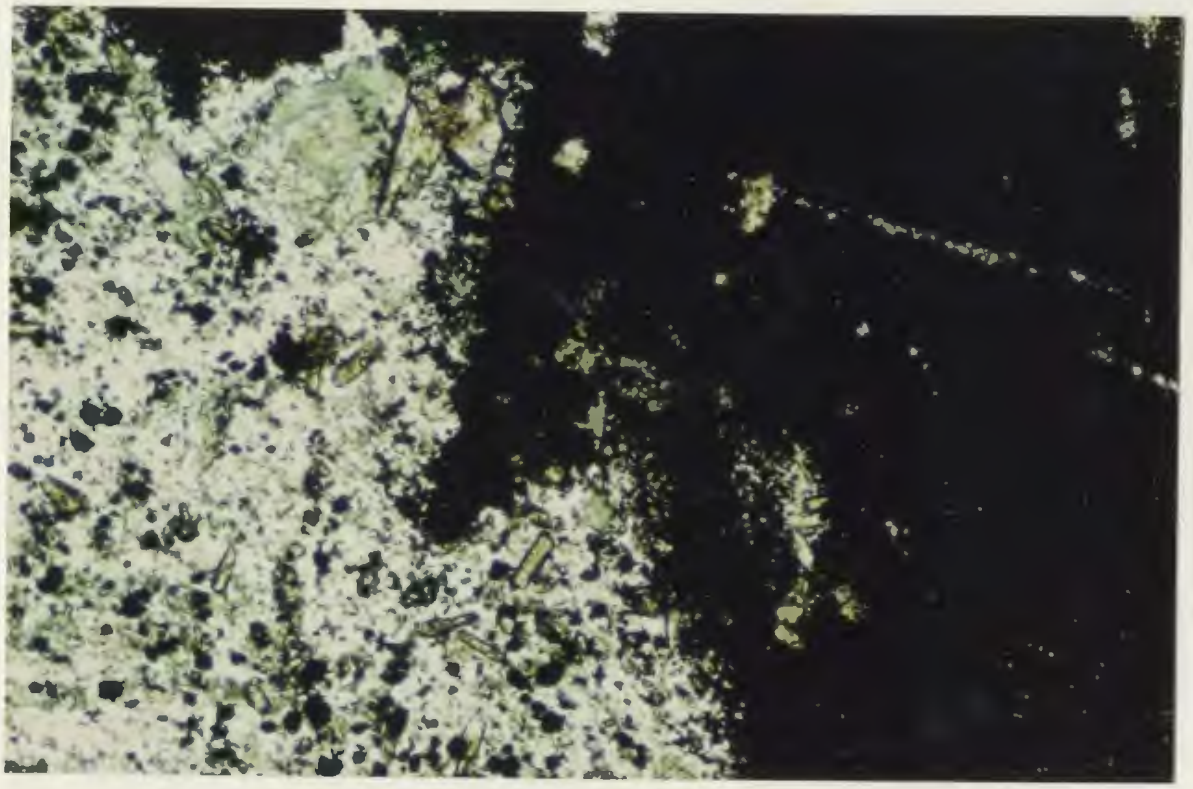

Plate 3.9: Fe-rich "Vasskis" (black material), which is thought to represent ancient seafloor chemical precipitates from "black smokers". The Vasskis is contained in a highly altered, silicified basalt dyke sample in this section (magnification: 3.2X; ppl).

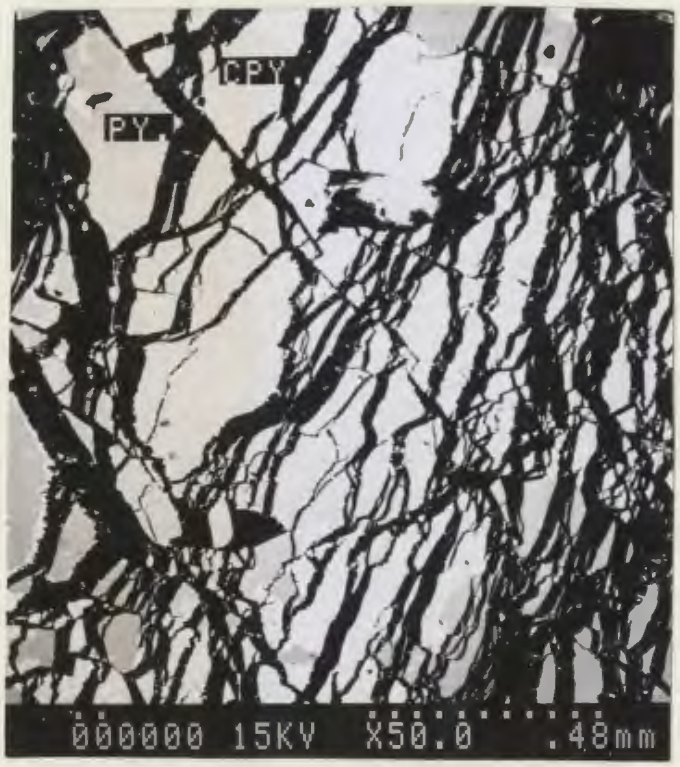

Plate 3.10: Pyrite (py)-chalcopyrite (cpy) assemblages intensely veined and corroded by quartz. The chalcopyrite may have replaced the pyrite along cracks (py is darker grey, cpy is lighter grey) (magnification and scale at base of photograph).

in thin sections in varying amounts. The chalcopyrite occurs interstitial to, or as inclusions in pyrite, except in one sample (Plate 3.10) where chalcopyrite has replaced pyrite along fractures.

Intergrowths of chalcopyrite with sphalerite are commonly observed, as well as abundant inclusions of one in the other. Chalcopyrite inclusions in sphalerite have been called "chalcopyrite disease" (Barton and Skinner, 1979), and may be a function of the solid solution of chalcopyrite-sphalerite at elevated temperatures of formation. Alternately, Eldridge et al. (1983) invoke replacement processes as a means of producing such textures. It is possible that replacement processes have taken place here (it is, unfortunately, difficult to say whether Plate 3.10 represents replacement or simple fracture filling by chalcopyrite), although in light of the upper greenschist facies biotite-actinolite signature of this area, it seems likely that temperatures in excess of those required for chalcopyrite-sphalerite solid solution (Barton and Skinner, 1979) were achieved on at least one occasion.

Sphalerite

Sphalerite may locally constitute up to 80% of the samples of banded ore, and occurs as discrete bands with calcite (+/-ferroactinolite). It is always reddish-brown in hand samples, and shows good internal reflections under the reflecting microscope. In some samples sphalerite is strongly deformed, and clearly wraps around brittle-deformed pyrite

masses. It forms distinct folds in one other sample (Plate 3.11). Owing to its susceptability to solution or plastic flowage during deformation, sphalerite is most often recrystallized completely. Sphalerite occurs also as intergrowths with chalcopyrite, and as inclusions in pyrite.

Galena

Galena was observed in only two samples, and then only in trace amounts as interstitial matrix to pyrite cubes (Plate 3.12).

3.6: Summary

The Visnes orebody is a large Fe-Cu-Zn sulfide deposit which is stratigraphically situated in the uppermost portions of the Karmoy Ophiolite. It has been extensively reworked and altered by subsequent periods of deformation and metamorphism, so that primary sulfide textures are all but absent, with the possible exception of the presence of minor amounts of "Vasskis". Despite its modifications, the deposit exhibits mineralogical, structural and stratigraphic similarities to the volcanic-exhalative deposits of the Troodos Ophiolite in Cyprus. It is also similar to numerous other ophiolitic sulfide deposits of the Norwegian Caledonides and the Appalachians of North America.

It is one of two main sulfide deposits in the study area. On the nearby island of Feoy, a small Fe-Cu-Ni-PGE-sulfide deposit occurs within highly magnesian dykes of an arc-

Plate 3.11: Hand sample of highly deformed, folded sphalerite layer (brown) in calcite.

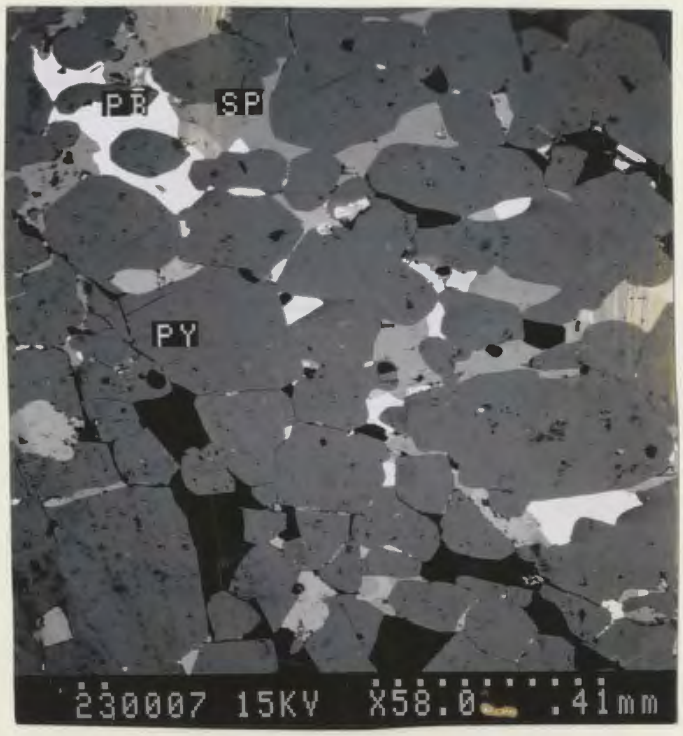

Plate 3.12: Photomicrograph of trace amounts of galena (Pb) in massive pyrite and sphalerite (sp) (magnification and scale at base of photograph).

basin affinity. While the two deposits are situated fairly close together, they can be shown to be unrelated to one another; these distinctions are more clearly made in Chapter 4 after an examination of the geology and petrology of the Feoy deposit.

Chapter 4: The Feoy Fe-Cu-Ni-PGE sulfide deposit

4.1: Introduction

The Feoy area is host to a small Ni-sulfide deposit which sits along a major shear zone within a country rock assemblage of isotropic and varitextured gabbro, sheeted tholeiitic and high-Mg dykes, and minor plagiogranitic dykes. The high-Mg dykes are the only rocks which are internally mineralized with Ni-sulfides (see Plate 2.30). However, later metamorphism and deformation has resulted in remobilization of the Ni-sulfides along shear zones.

A number of breccia samples and quartz-tourmaline vein assemblages were collected from the old Feoy mine dump (see Figure 2.1). The breccia occurrence itself must be below the surface, as is the sulfide deposit, since no outcrops of this type were observed, and such samples are only found around the mine shaft. The breccia samples illustrate some interesting relationships between the Ni-sulfides and later metamorphism and deformation, since some samples contain milled Ni-sulfide fragments in a matrix of chlorite, calcite, tourmaline and quartz. They are considered important in interpretation of the nature of later metamorphism, deformation and hydrothermal activity, and are therefore discussed in some detail in this chapter and in Chapter 8.

The Feoy sulfide deposit is an anomalous occurrence in several respects:

1- the occurrence of Cu-Ni-sulfides within Phanerozoic ophiolite complexes is

relatively rare, and;

2- such occurrences are themselves only seldom as enriched in PGE's as this deposit. The only other deposit comparable in terms of age, size, PGE enrichment, and tectonic environment of formation known by this writer is the Lillefjellklumpen (Lfk) deposit of northwestern Norway (Gronlie, 1988).

Therefore, attempts will be made in this chapter to thouroughly document the ore geology and petrology of this deposit. In Chapter 7, the origin of this deposit and its host rocks, as well as its classification with respect to other Ni-sulfide occurrences, is discussed.

4.2: Ore geology and petrography

Ni-sulfide mineralization appears to be mainly shear zone controlled, and according to old mine reports occurs in several massive sulfide lenses parallel to the shear zone walls. The entire deposit is quite small, probably not containing much more than 100,000 metric tons of sulfide; only 37,000 tons were produced during the active mining period at the turn of the century (Boyd and Nixon, 1985). Unfortunately, structural and geological maps of the sulfide body were unavailable.

Average grades for the Ni-sulfides are (after Foslie and Johnson-Host, 1932): 2.1% Cu, 2.63% Ni, 0.031% Co, with average Cu/Ni at 0.56, Co/Co+Ni at 0.06, and Pt/ Pt+Pd at 0.275. This deposit is unique with respect to other such ophiolitic Ni-sulfide deposits

in its high concentrations of PGE's, and it is clearly distinct from the nearby Visnes deposit, the latter which contains no PGE's or Ni-sulfides (see Chapter 3). Average grades of Pt and Pd are 1.12 and 2.97 g/t respectively. These are contained within an interesting array of Platinum Group Minerals (PGM's) in the Ni-sulfide and gangue, as opposed to as solid solution in the sulfide (see Cabri and Naldrett, 1984).

The sulfides are mainly 95-100% massive, fine grained pyrrhotite, chalcopyrite and pentlandite. Minor minerals include pyrite, magnetite, hematite, chromite, ilmenite, violarite, cubanite, mackinawite, and PGM's. There are some disseminated interstitial Ni-sulfides in high-Mg dykes which occur along the shear zone near the orebody, and these may represent orthomagmatic Ni-sulfides which were trapped as interstitial liquids between crystallizing silicates in cooling silicate/sulfide melt (see Plate 2.30).

The ore mineralogy of the Feoy deposit is examined in order of abundances in hand samples and thin sections.

Pyrrhotite

Pyrrhotite is the main sulfide mineral, and constitutes up to 70% of the massive ore samples. It is generally fine to medium grained (up to 0.5mm) and is of the monoclinic (Fe1-xS) variety. The pyrrhotite exhibits ubiquitous 3-point grain boundaries in all samples as a result of later recrystallization. In some of the more massive, mono-mineralic pyrrhotite samples, this feature may conform to the ideal dihedral, or

120 degree, interfacial angle (Plate 4.1). Because of the strongly deformed nature of the sulfides, it is assumed that this feature represents a slow heating process during progressive metamorphism (hence the development of pyrite porphyroblasts). It should be noted, however, that such a texture could also be achieved by slow cooling of massive pyrrhotite after its deposition from an initial monosulfide solid solution (mss), with conformity of the interfacial angles to ideality (120 degrees) being directly related to the number of mineral phases in the cooling sulfide melt (Vaughn and Craig, 1982). Because of the intense deformation which affects these sulfides, the former explanation is preferred here.

Some pyrrhotite has been hydrothermally altered to marcasite, although the majority of the pyrrhotite is relatively fresh. Exsolution of pentlandite as "flames" along cleavage planes in the pyrrhotite is quite common in these samples, albeit on a minor scale (Plate 4.2).

In several samples pyrrhotite exhibits strong cataclastic textures, or "Durchbewegung" structure (Vokes, 1969) (Plate 4.3). In such samples magnetite is also quite common, suggesting that alteration of the pyrrhotite during metamorphism occurred under elevated fO2 conditions. This is elsewhere supported by the presence of abundant hematite (Plate 4.4). However, at least some of the magnetite is primary, since it does not rim the pyrrhotite in thin section, and occurs in some places as euhedral to rounded, fresh grains. The appearance of magnetite at high temperatures may have ensured an elevated pyrrhotite/pyrite ratio in this deposit (Stanton, 1978).

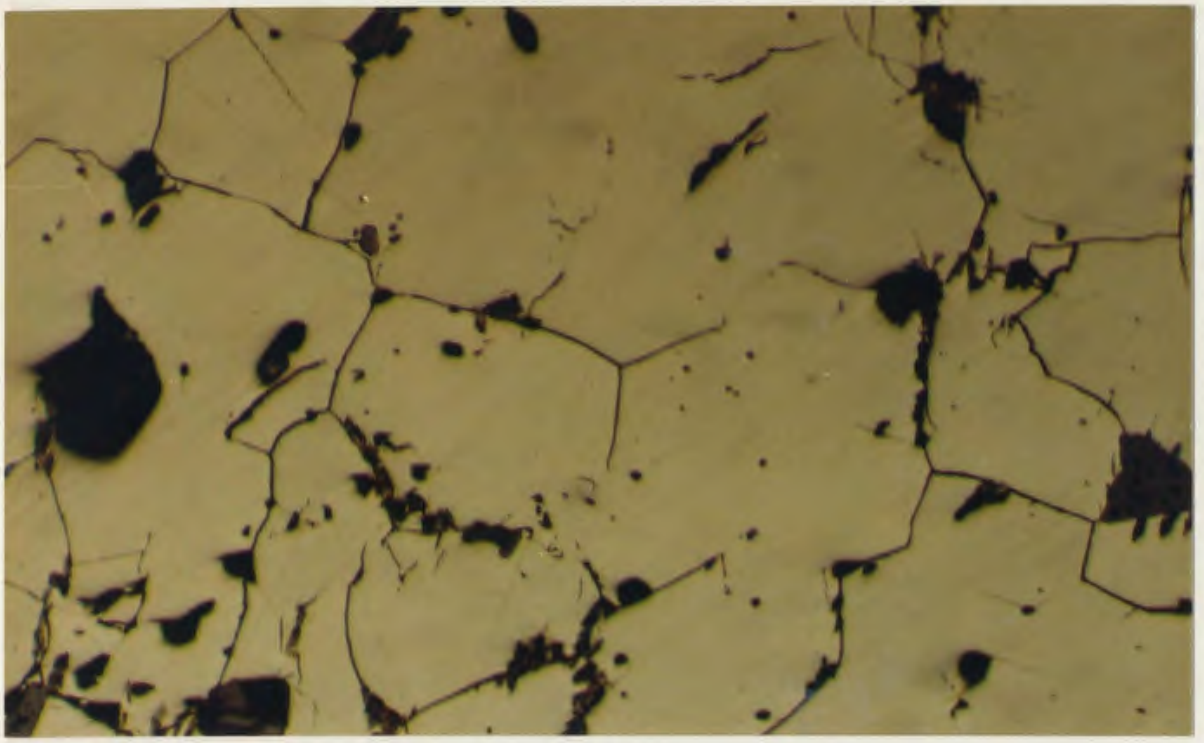

Plate 4.1: Well developed annealed texture (with triple point grain boundary angles approaching 120 degrees) in massive, pyrrhotite ore from the Feoy area (magnification: 10X; reflected light, rl).

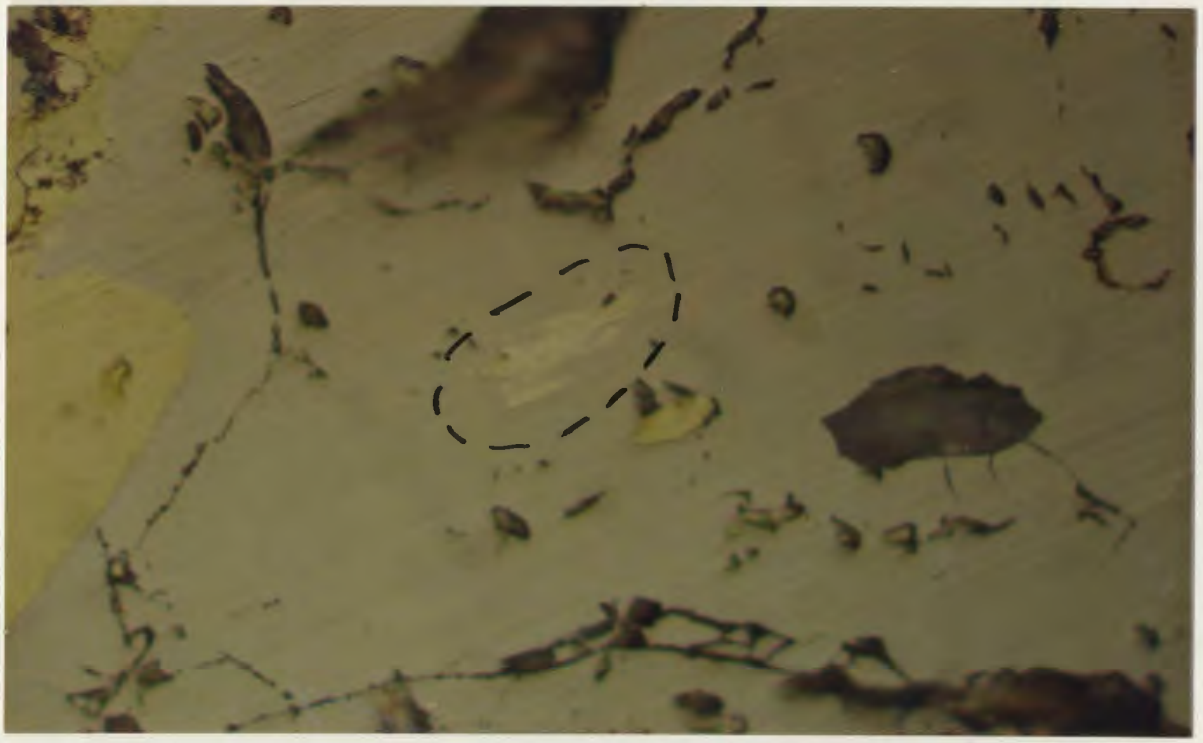

Plate 4.2: Exsolution "flames" of pentlandite (cream coloured) in massive pyrrhotite (grey) and chalcopyrite (yellow) (magnification: 40X;rl).

Plate 4.3: "Durchbewegung" texture, illustrating cataclastic deformation of pyrrhotite (white), along with abundant amphibole (black) (magnification and scale at base of photograph).

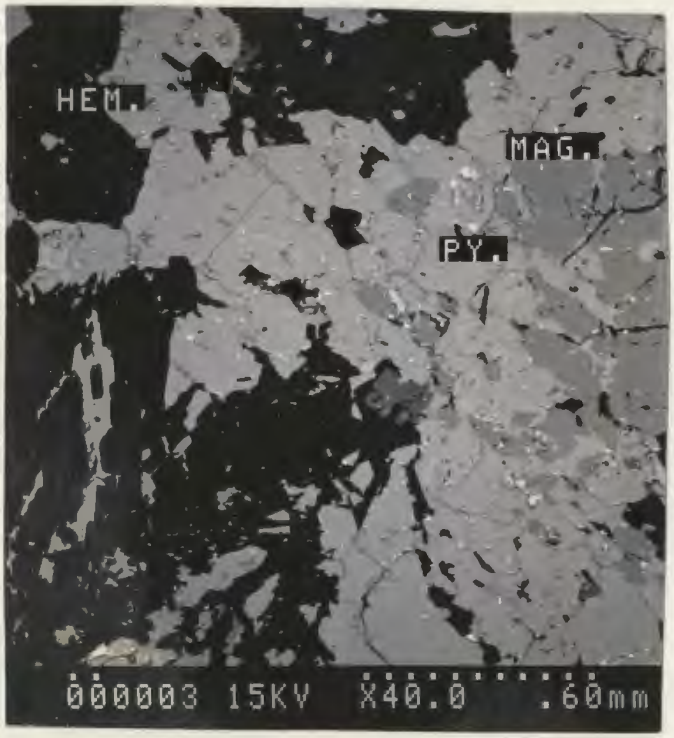

Plate 4.4: Magnetite (dark grey), pyrite (light grey), and hematite (black) in massive pyrrhotite ore from Feoy. The magnetite has formed as a result of the decomposition of pyrite, while the hematite is an alteration product of magnetite (magnification and scale at base of photograph).

Pyrrhotite occurs as minor exsolution blebs in the chalcopyrite; according to Stanton (1978), this feature is indicative of its formation under very high temperatures.

As mentioned, pyrrhotite occurs as an interstitial sulfide phase, along with pentlandite, in some of the high-Mg dykes in the area (see Plate 2.30). The sulfides are interstitial to actinolite and tremolite, the latter which are alteration products of clinopyroxene. The presence of these interstitial sulfides may be interpreted as having resulted from trapping of sulfide liquids during primary crystallization of silicates from a co-magmatic silicate-sulfide melt (see Chapter 7).

Chalcopyrite

Chalcopyrite is present in all samples in variable amounts, from $<$2-30% of each sample, and occurs as different textural varieties.

In the massive ore samples, chalcopyrite is most abundant as an interstitial phase to the pyrrhotite. In some of the more deformed samples, remobilized chalcopyrite often occurs interstitial to foliated amphibole (Plate 4.5).

Chalcopyrite "segregations" were also observed. These are almost pure chalcopyrite patches within massive pyrrhotite that are neither interstitial nor banded. Such segregations might be expected during separation of a Cu-rich phase in a sulfide melt, with conversion of mss to iss (Stanton, 1978).

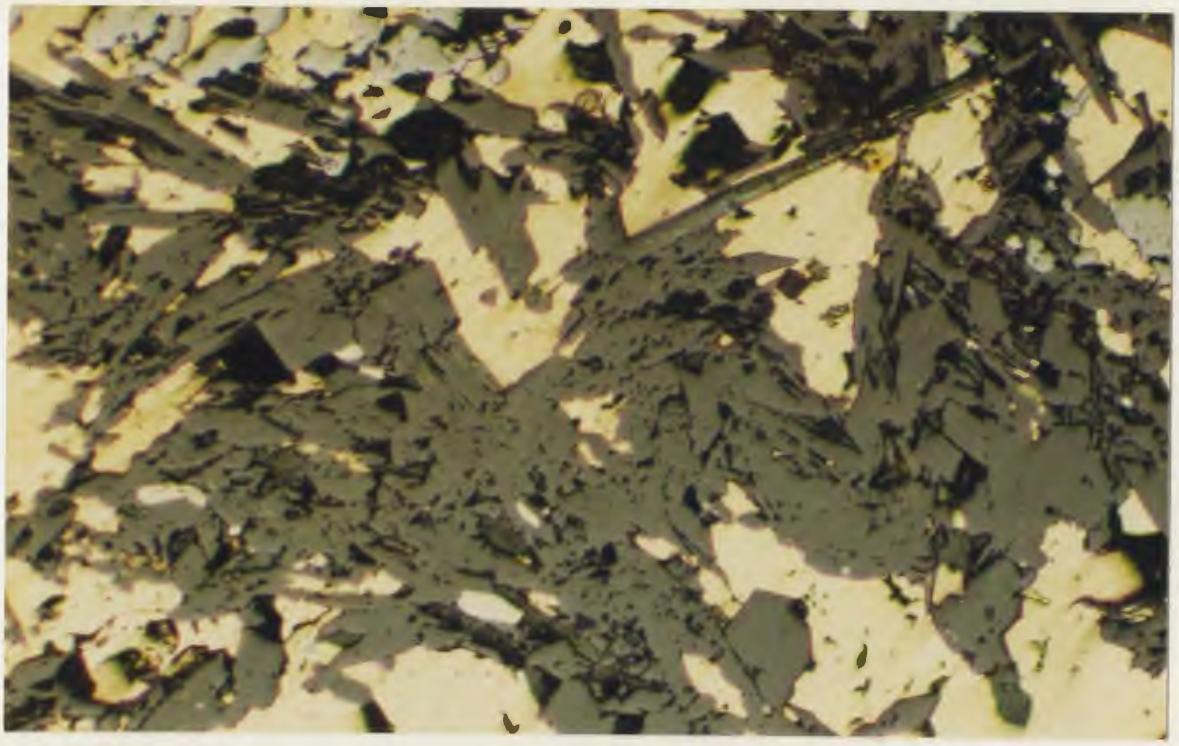

Plate 4.5: Remobilized chalcopyrite (yellow) interstitial to amphibole in highly deformed pyrrhotite-chalcopyrite ore sample from Feoy (magnification: 3.2X; rl).

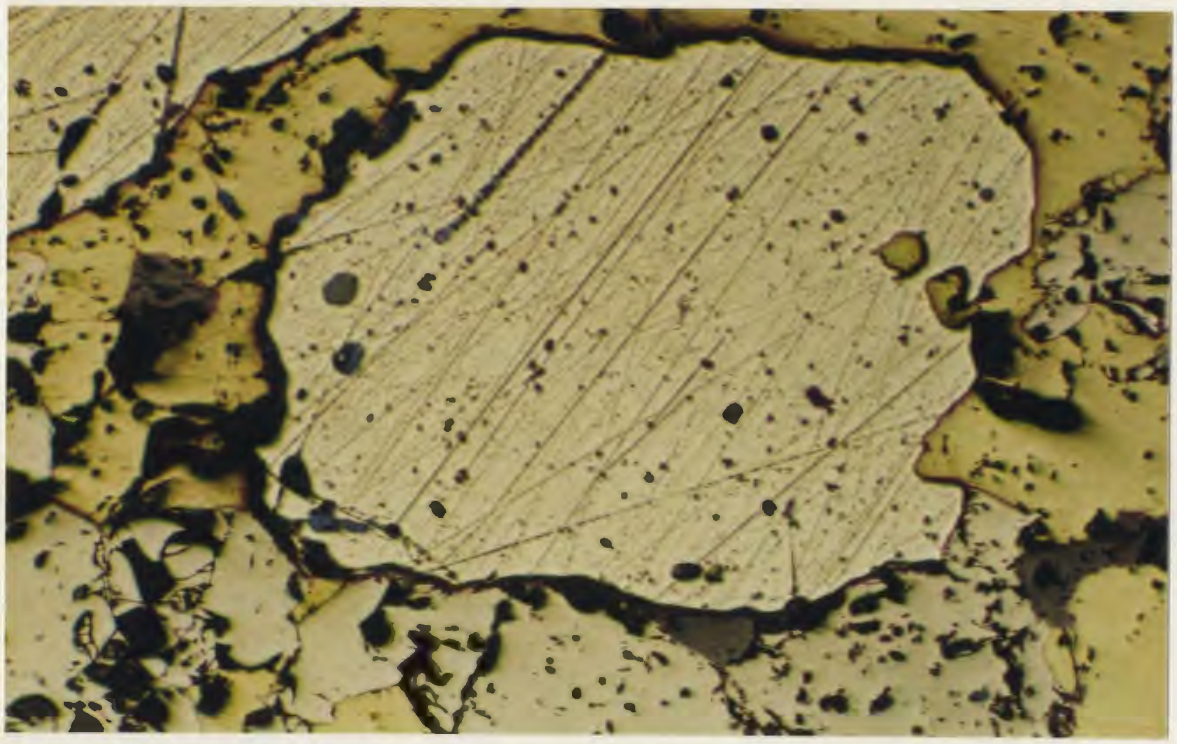

Plate 4.6: Pyrite porphyroblast rimmed and corroded by chalcopyrite (yellow) and magnetite (dark grey). Note the inclusions of chalcopyrite and magnetite in the pyrite porphyroblast (magnification: 3.2X; rl).

The remobilized nature of chalcopyrite is quite obvious in many samples, as it forms distinct bands parallel to the amphibole overprint in deformed ore. In such samples, chalcopyrite is also seen to rim (along with magnetite) highly corroded pyrite porphyroblasts (Plate 4.6). Chalcopyrite and magnetite also occur as inclusions within these same porphyroblasts. This feature can be interpreted as replacement or alteration of the pyrite which post-dated porphyroblast formation.

Pentlandite

Pentlandite is abundant in the Feoy Ni-sulfides, occupying from 3 to 25% of the samples in thin section. Although at temperatures approaching its parent silicate/sulfide liquidus, pyrrhotite can certainly accomodate considerable Ni in solid solution or in mss (0-11%; Yund and Kullerud, 1966), it is suggested that upon equilibration during cooling of mss, all of the Ni is either taken up by a later precipitating pentlandite phase, or is exsolved as "flames" of pentlandite within crystallographic axes of the earlier formed pyrrhotite (Skinner, pers. comm.) (see Plate 4.2), such that at low temperatures there can be no "Ni-pyrrhotite" as is suggested by earlier writers (eg. Ramberg, 1968). Attempts were made in this study to determine the distribution of Ni in the massive ores. Ni was initially determined on a scanning electron microscope to be present as free pentlandite grains, as flames of pentlandite in pyrrhotite, and as solid solution in pyrrhotite. Upon closer observation of this "Ni-pyrrhotite" however, minute flames of pentlandite were always observed in the pyrrhotite. Therefore, it appears that pentlandite represents the only Ni-rich phase in these sulfides.

The pentlandite occurs as cracked, occasionally euhedral octahedrons (Plate 4.7), but mainly as xenomorphic chain-like veinlets or rims around the pyrrhotite, owing to its precipitation at a later stage than the pyrrhotite (Plate 4.8). This also accounts for the abundant exsolution of pentlandite flames in pyrrhotite. The blocky, free pentlandite grains are usually medium to coarse grained owing to their precipitation at unusually high temperatures.

The pentlandite is variably altered to violarite and bravoiite (Plate 4.9; also see Plate 4.8). The resultant texture is highly distinctive, with dirty grey fractured rims and fresh, creamy coloured pentlandite cores, the outline of which follows the shape of the fractures. The alteration to violarite corresponds to a loss of Ni up to 10 wt%.

Minor Minerals

There is very little primary pyrite present in the Feoy deposit; pyrite occurs as large, highly embayed, inclusion-rich porphyroblasts which are variably altered and rimmed by magnetite and chalcopyrite.

Magnetite is present in variable but minor amounts, up to 3% in some samples. It occurs as two distinct textural types in these sulfides: some samples contain subhedral grains or blebs of magnetite rimmed by chalcopyrite; magnetite also occurs as a product of the decomposition (oxidation) of pyrite (see Plates 4.4 and 4.6). In these latter occurrences, magnetite rims and is included in the pyrite, along with chalcopyrite (see Plate 4.6). It

Plate 4.7: Blocky, altered pentlandite crystals (dark grey, at center, labelled PH) in massive pyrrhotite-chalcopyrite (labelled CPY) ore from Feoy (magnification and scale at base of photograph).

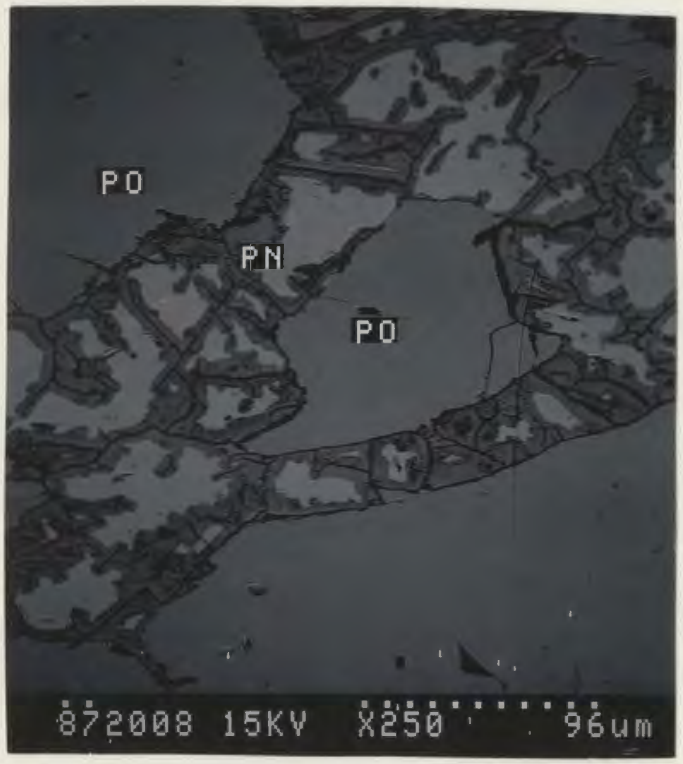

Plate 4.8: Highly altered pentlandite veins (dark grey with cream coloured cores) cutting and rimming massive pyrrhotite (light grey) (magnification and scale at base of photograph).

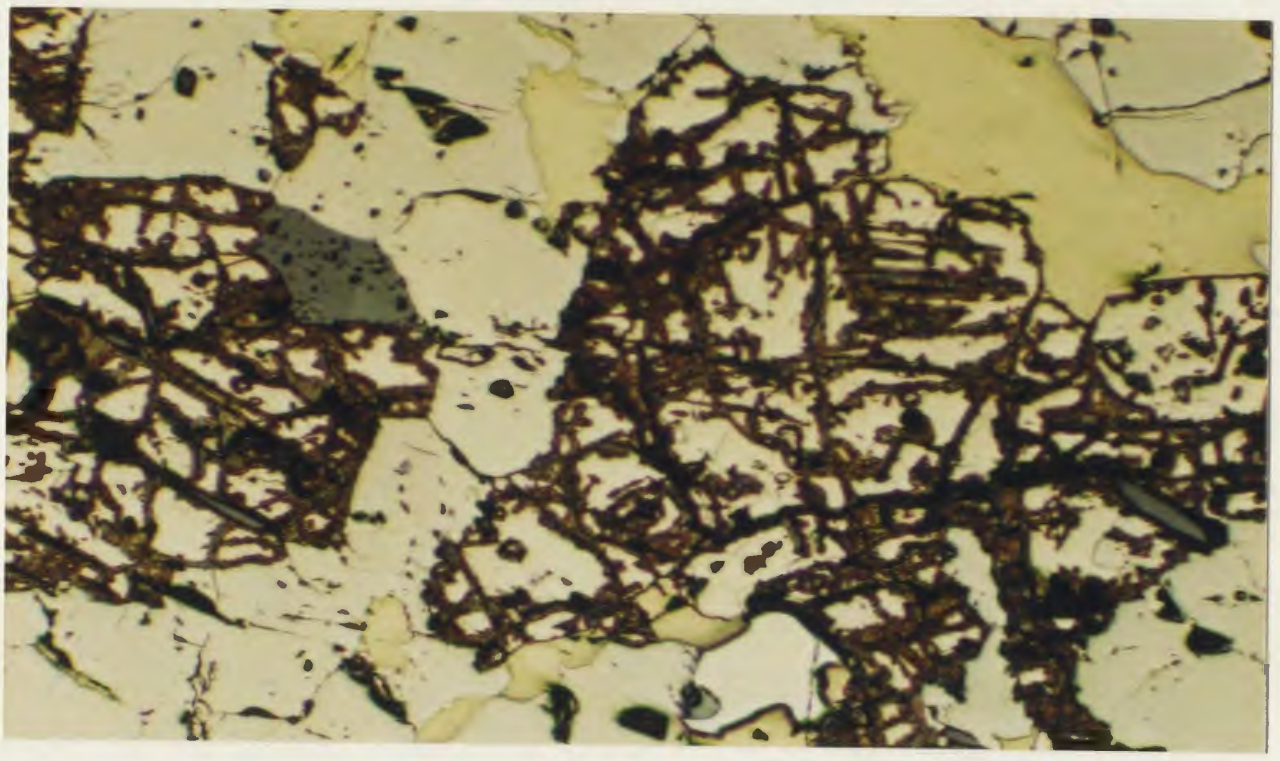

Plate 4.9: Pentlandite which has been heavily altered to violarite. The dark brown violarite rims fresh, cream coloured cores of pentlandite. The surrounding material is pyrrhotite (white) and chalcopyrite (yellow) (magnification: 10X; rl).

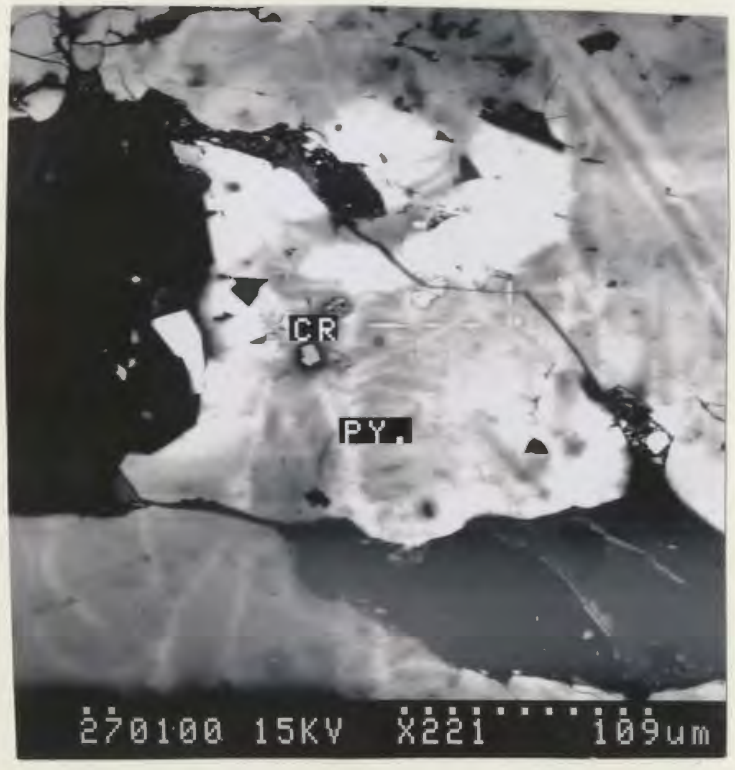

Plate 4.10: Tiny grain of chromite (Cr) in a pyrite (PY) grain. This is in a massive pyrrhotite (darker grey at base of photo) ore sample from Feoy (magnification and scale at base of photograph).

seems clear that the former variety represents primary formation from a sulfide melt with coalescence of chalcopyrite after its exsolution from iss, while the latter variety represents a product of the alteration of pyrite.

Hematite is seen in small amounts as a product of hydrothermal alteration of magnetite (see Plate 4.4), since it is quite common as rinds along cross-cutting quartz/calcite veins in the sulfide.

Chromite and ilmenite are present in only trace amounts as small euhedral grains within the pyrrhotite (Plate 4.10), and occasionally also within the pyrite; these bear witness to the high temperature nature of this deposit. The paucity of chromite attests to very low fO2 conditions during probable formation of the sulfides from a silicate/sulfide melt, so that most of the chromium in the initial melt must have partitioned into the silicate fraction.

Violarite is a common alteration product of pentlandite, and indeed has extensively replaced pentlandite in the Feoy Ni-sulfides (see Plates 4.8 and 4.9); in some samples the alteration is complete.

Mackinawite was found in one sample only as very small, pinkish-red to grey inclusions in pentlandite and pyrrhotite. Cubanite was also identified in one thin section as pink lamellar inclusions, intergrown with pyrrhotite, in chalcopyrite.

Platinum Group Minerals (PGM's)

Although evidently mobilized and reconcentrated during later metamorphism, deformation and hydrothermal activity, the PGE tenor of this deposit is considered to reflect primary PGE enrichment in a host silicate/sulfide melt(s) (See Chapter 7). All sulfide samples were analysed by quantitative electron microscopy for PGM's, which are easily recognizable in a scanning electron microscope (SEM) because of the brightness induced by their high atomic numbers.

In total, five PGM phases were recognized by this author. All of these were present in trace amounts as minute sub to euhedral grains that were in places associated with late chalcopyrite veins and metamorphic silicates, and in other places with massive pyrrhotite and pentlandite. PGM's do not seem to show preference for any particular sulfide or silicate species. Samples on average contained 1 to 3 grains of PGM's, although some are devoid of PGM's. All PGM's found are tellurides, although Ramberg (1968) has recorded the presence of native Pt from a hand sample from Feoy.

Two of the five PGM species identified microscopically were analysed on a SEM using a semi-quantitative stoichiometric method. These results indicate that the analysed grains of Pt-Pd-Bi-Te and Hg-Pd-Te were actually Michenerite, (Pd,Pt)BiTe, and Temagamite, Pd3HgTe3. Table 4.1 is a list of the analysed PGE grains and their probable names, while Plates 4.11 to 4.15 are scanning electron photomicrographs of some of the PGM's observed.

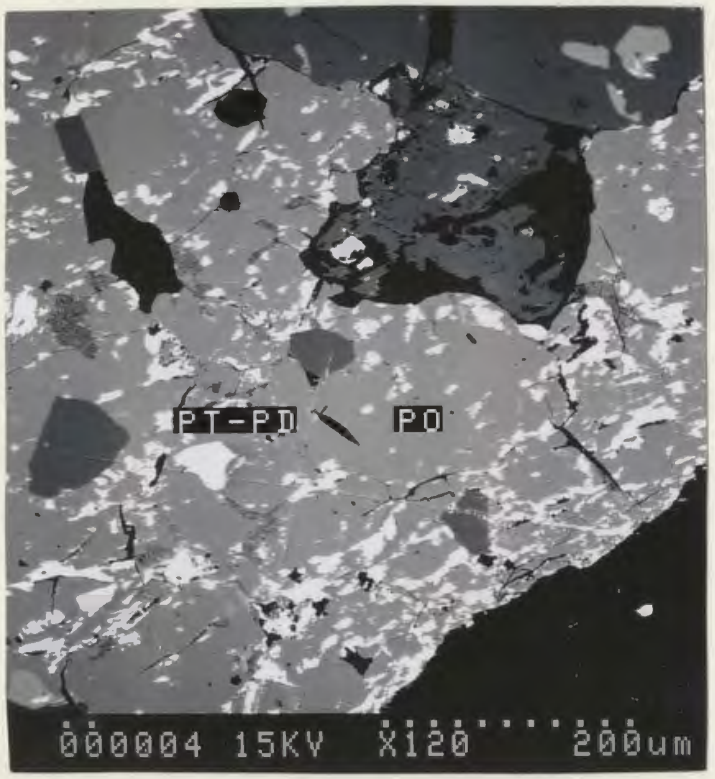

Plate 4.11: A scanning electron photomicrograph of a Platinum Group Mineral (PGM), probably michenerite (PT-PD), in massive pyrrhotite (PO) from Feoy (magnification and scale at base of photograph).

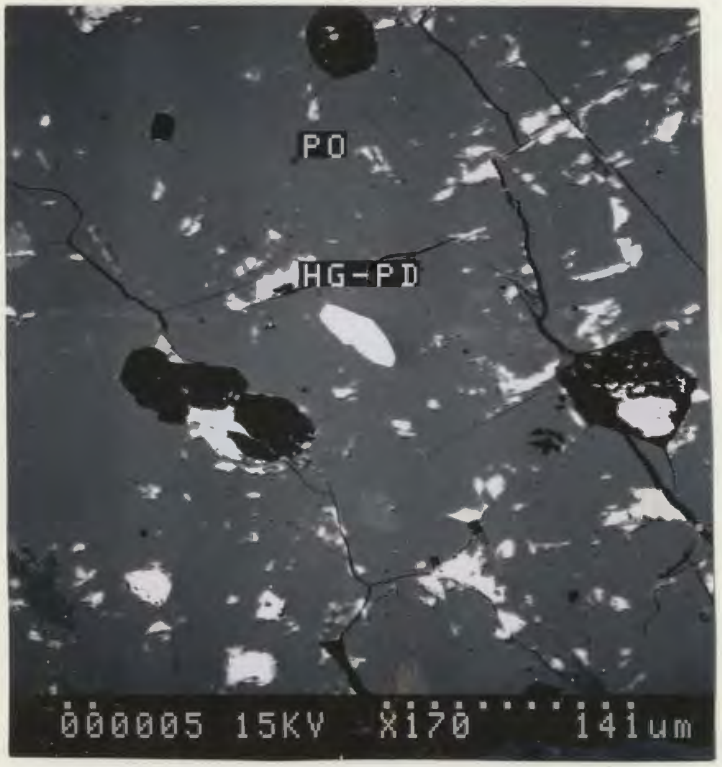

Plate 4.12: A euhedral grain of temagamite (Pd3HgTe3, labelled HG-PD in photo) in massive pyrrhotite (PO) from Feoy (magnification and scale at base of photograph).

Plate 4.13: Temagamite grain (bright white, at center, labelled HG-PD-TE) in highly deformed amphibole (black)-pyrrhotite (white, labelled PO) assemblage (magnification and scale at base of photograph).

Plate 4.14: Michenerite (PD-BI-TE) grain in massive pyrrhotite (PH) from Feoy (magnification and scale at base of photograph).

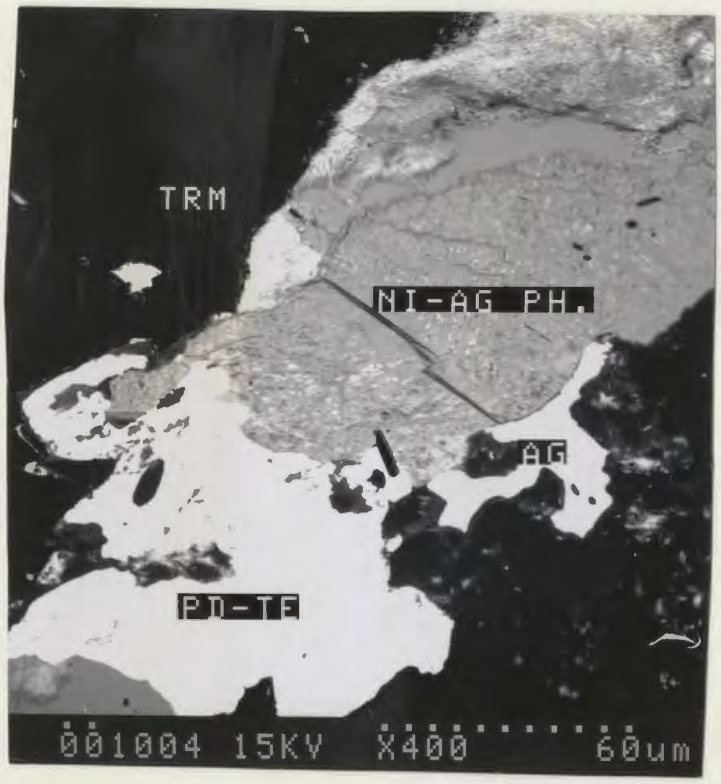

Plate 4.15: Kotulskite (PdTe, labelled PD-TE) and probable hessite (Ag2Te, labelled NI-AG PH and AG) grains in tourmaline-pyrrhotite assemblage from Feoy (magnification and scale at base of photograph).

Plate 4.16: Photograph of Type A breccia from the Feoy mine dump. Note the large, rounded tourmalinite fragment at right, and the sub-rounded, massive pyrrhotite fragment at left (brown). At the top of this sample is an elongate fragment of Type 2 plagiogranite. The matrix material is chlorite and calcite. Note pen for scale.

Table 4.1: Platinum Group Minerals found in the Feoy Ni-sulfides.

Composition	Possible name
Pt,Pd,Bi,Te	Michenerite, (Pd,Pt,Ni)(Bi,Sb)Te
Pd,Bi,Te	Michenerite
Pd,Hg,Te	Temagamite, Pd3HgTe3
Pd,Te	Kotulskite, PdTe
Ag,Te	Empressite, AgTe; Stutzite, Ag5Te3 or Hessite, Ag2Te
Ag,Fe,S	Unknown
Pt	Native Pt (after Ramberg, 1968)

Also found was one grain of a Ag-telluride within an assemblage of tourmaline, pentlandite and Pd-telluride (see Plate 4.15). The Ag-telluride is probably hessite (Ag2Te), since similar grains of hessite have been recorded from other Ni-sulfide deposits (Rowland and Berry, 1951), and most other Ag-tellurides are generally associated with lower temperature auriferous deposits (Ramdohr, 1980).

4.3: Metamorphic and deformation features associated with the Feoy Ni-sulfides

Brecciation and associated tourmaline formation, plastic deformation and remobilization, alteration and leaching of the Feoy sulfides all occurred during a period of metamorphism, deformation and hydrothermal activity which post-dated intrusion of the high-Mg dykes and formation of the associated Ni-sulfides This section deals with some of the effects of this late episode on the Feoy Ni-sulfide deposit.

4.3.1: Breccias

The occurrence of breccias and quartz-tourmaline vein assemblages along shear zones in the Feoy mine area is considered to represent cataclastic deformation and hydrothermal activity which accompanied late metamorphism (see Chapter 8). Breccia and vein samples were taken from the mine dump on Feoy, and of 20 breccia samples collected, two types can be recognized in hand samples. Type A breccia contains a tri-lithologic assemblage of rounded tourmalinite fragments (these are fragments composed of >90% tourmaline,

which have undergone varying degrees of dissection by chlorite and calcite matrix), plastically deformed and remobilized, sub-rounded, massive Cu-Ni-sulfide fragments, and Type 2 plagiogranitic fragments (Plates 4.16 and 4.17). There are also some heavily tourmalinized and mineralized (with chalcopyrite and pyrhhotite) high-Mg dyke fragments present. These fragments are set in a matrix of coarse crystalline metamorphic chlorite, minor tourmaline, and calcite. There is no quartz in this breccia type, although coarse grained quartz-tourmaline veins are also found along the same shear zone (Plate 4.18). The cement material in this breccia has clearly formed from hydrothermal fluids, as the chlorite, tourmaline and calcite are all coarse crystalline, and are intergrown with one another. This is contrasted with a "rock flour" matrix, which is chaotic, non-crystalline cement material that is found in breccias which have formed as a result of tectonic activity (Sillitoe, 1985).

The presence of tourmaline in the breccia cement indicates that there was a boron-rich component to these hydrothermal fluids. The occurrence of tourmaline as tourmalinite fragments in the breccia as well suggests that tourmaline formation occurred both before and during brecciation, i.e. tourmalinization was a prolonged process during this hydrothermal activity. It may be that tourmalinites which formed in the early stages of hydrothermal activity were later incorporated as fragments during brecciation and continued boron-rich fluid circulation.

Type B breccia is composed of fine grained, milky, and sometimes colloform-banded (due to open space filling) calcite-quartz-chlorite assemblages (Plate 4.19). The cement

Plate 4.17: Type A breccia sample. The black areas at far left and far right are zones of tourmalinization. Close observation of the cement material in this sample reveals abundant tourmaline in the matrix.

Plate 4.18: Quartz-tourmaline vein assemblages from the Feoy mine dump. Large (up to 3cm long), black, radially disposed tourmaline crystals are intergrown with coarse grained quartz in these samples.

Plate 4.19: Photograph of Type B breccia from the Feoy mine dump. Note the massive pyrite fragments in a quartz-calcite (minor chlorite) matrix.

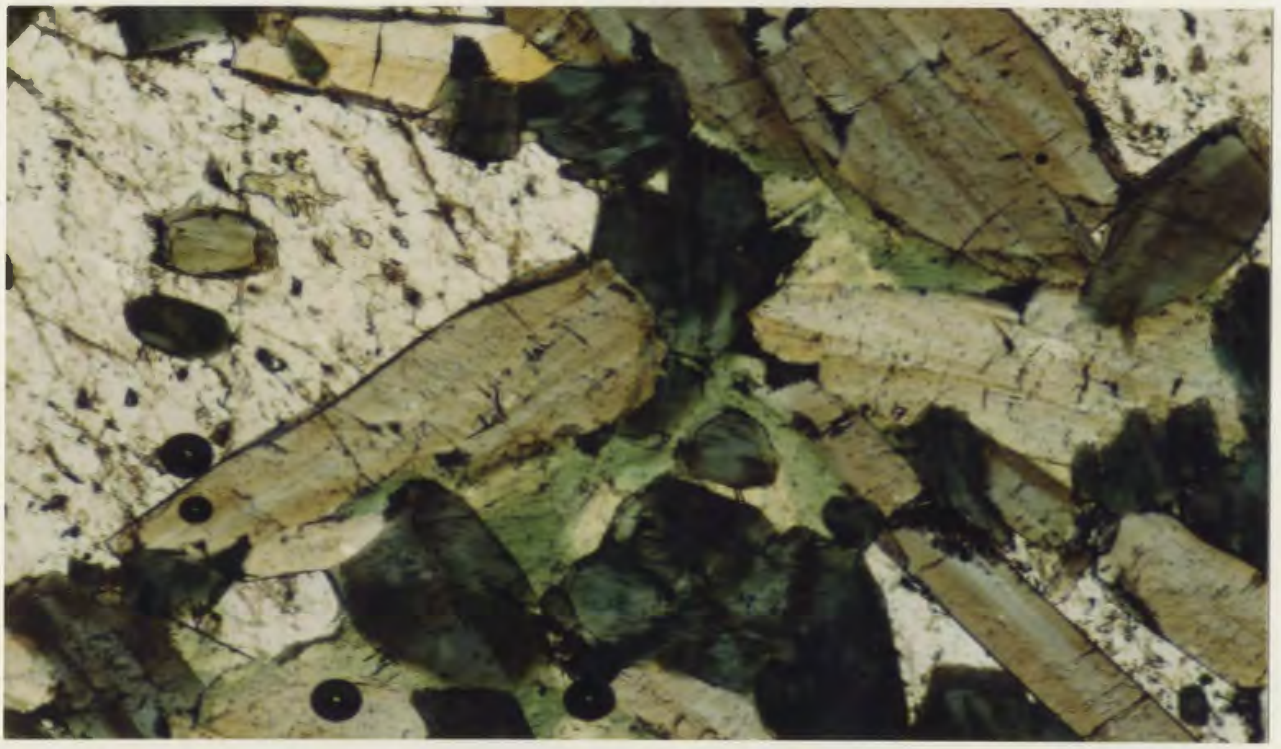

Plate 4.20: Fresh, euhedral tourmaline crystals (dark and pale blue) set in a matrix of calcite (white) and chlorite (light green). Note the growth lines in the tourmaline at upper right (magnification: 20X; ppl).

material in this breccia type is also considered to have formed from hydrothermal fluids rather than from tectonic activity, because of the presence of quartz-calcite-chlorite intergrowths in the matrix, and also because of the absence of any "rock flour"component.

This breccia contains sub-rounded fragments of massive, fine grained and colloform banded pyrite. This type of sulfide is not seen in any of the massive Ni-sulfide samples or in Type A breccia, nor does it resemble any of the Visnes-type sulfides. Also, it was found to have an isotopically unique signature (sulfur isotope ratio of 17 per mil), quite unlike either the Feoy or Visnes sulfides. It is difficult to say whether the pyrite in this breccia is truly fragmentary, or whether it actually precipitated from hydrothermal fluids accompanying Type B breccia formation.

The presence of Type 2 plagiogranite and high-Mg dyke fragments in Type A breccia is significant (the surrounding country rock is also plagiogranite and high-Mg dykes). It suggests that brecciation was in general an in situ feature, with little upward or downward displacement of the fragmented country rock. Sillitoe (1985) has demonstrated that although there is normally some small downward displacement component to many non-tectonic breccias, there need not necessarily be any appreciable vertical displacement of fragments during brecciation, except in the case of breccias produced as a result of tectonic movement or thrusting. He has also shown that there can be considerable and abrupt changes in temperature of formation, pressure, host rock lithology, discharge velocity, and morphology of the breccia within a single breccia occurrence.

There are considerable differences in the lithology and morphology of breccia Types A and B. However, both breccia types are always found together, and are both localized along a shear zone which cuts the Ni-sulfide body in the vicinity of the mine dump. Likewise, both breccia types have a "hydrothermal cement" matrix as opposed to a "rock flour" matrix. Also, both contain coarse crystalline tourmaline as well as tourmalinite fragments. This evidence, coupled with data from Sillitoe (1985) which show that there can be abrupt lithologic and morphologic changes within a single breccia occurrence, suggests that the Types A and B breccias from the study area may have formed at the same time by the same mechanisms (see Chapter 8).

4.3.2: Tourmaline and tourmalinite

Tourmaline is found in the Feoy area as tourmalinite fragments in Type A breccias, as course crystalline quartz-tourmaline vein assemblages in the shear zones, and filling fractures in the country rocks surrounding the Ni-sulfide deposit (see Chapter 2).

The distribution of tourmaline is problematic, and tourmaline-breccia relationships suggest that there was more than one period of tourmalinization, or that tourmalinization was a prolonged process during breccia formation. Firstly, the Type A breccia contains milled, rounded fragments of tourmalinite (see Plate 4.16). These are composed of $>90\%$ tourmaline with minor calcite and remobilized sulfides. This tourmaline is fine grained, sub- to euhedral tourmaline of the black schorl/dravite ($Fe > Mg$) variety. In places the fragments are veined and dissected by chalcopyrite and calcite, indicating

remobilization of the latter during deformation. This tourmalinite clearly pre-dated brecciation, as it is incorporated as fragments in the breccia. However, the matrix of the breccia also contains non-fragmental, euhedral tourmaline within a metamorphic chlorite-calcite assemblage (Plate 4.20), indicating that tourmalinization was an ongoing process during brecciation.

Elsewhere in the mine dump another interesting tourmaline fragment was found, and yields information supporting the pre-brecciation nature of some of the tourmaline. This sample is a tourmalinite, as in the Type A breccia fragments, but has been strongly deformed, so that a pronounced schistosity and kink banding are well developed (Plate 4.21). At the same time the tourmaline is quite altered and corroded.

In thin section, some Type A breccia samples contain radially disposed tourmaline, or tourmaline "suns" (see Plate 4.28) that have been interpreted as products of replacement of pre-existing minerals (Deer et al., 1962). Some of the amphiboles in the high-Mg dyke samples are also replaced by tourmaline "suns". On the other hand, the tourmalinites and the coarse crystalline vein tourmaline are clearly not replacement products, so that there is evidently both primary and secondary (replacement) tourmaline in these rocks.

Tourmaline "suns" are usually quite turbid, and are in some places sulfide-inclusion rich (see Plate 4.28), while tourmaline from vein assemblages is always quite fresh, and never contains inclusions (see Plate 4.24). Where tourmaline overgrows amphibole, remobilized sulfides are commonly present along cleavage planes or growth lines in the tourmaline

(Plate 4.22).

The tourmalinite fragments exhibit several interesting textures. In some samples, tourmaline is subhedral to irregular, and is strongly foliated (see Plate 4.21). In other samples, tourmaline is sub- to euhedral, fine to medium grained and generally randomly orientated (Plate 4.23). This type is always fresh and inclusion-poor. In sulfide-rich samples, tourmaline crystals are often broken or shattered by sulfides or calcite (Plate 4.24), while in other such samples euhedral, unaltered tourmaline sits in an interstitial sulfide matrix, with significant separation bewteen tourmaline crystals (Plate 4.25).

Both the early and late formed tourmaline exhibit optical zoning on a moderate scale, with blue-green colour variations possibly corresponding to variations in Na, Mn, and Ti (see Table 8.2) from cores to rims.

About 400m south along the coastline from the mine dump, there is an outcrop of well exposed dykes of both the Visnes and high-Mg type. Although the dykes are relatively fresh and unaltered, they contain abundant coarse (up to 3cm long, 1cm wide) black tourmaline crystals along microfractures which are copious in these rocks (see Plates 2.31 and 2.32). In the context of the nearby tourmaline- bearing breccias, this feature suggests that boron-rich hydrothermal circulation which post-dated all rocks in the area was not localized to shear zones alone, but rather that it was more widespread and diffuse, and permeated through microfractures in the surrounding country rocks.

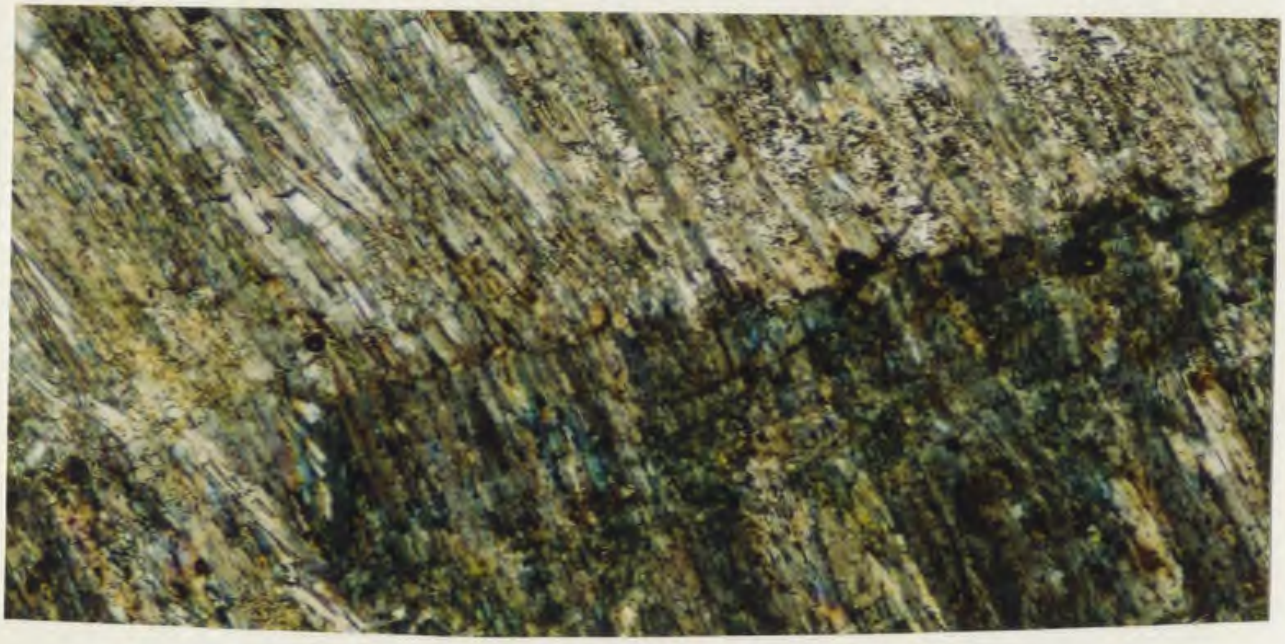

Plate 4.21: Schistose tourmalinite fragment. Sample consists of 100% tourmaline which has been deformed and metamorphosed to tourmaline schist. Note the dark band in the center of the photograph, which is a kink band (magnification: 20X; cn).

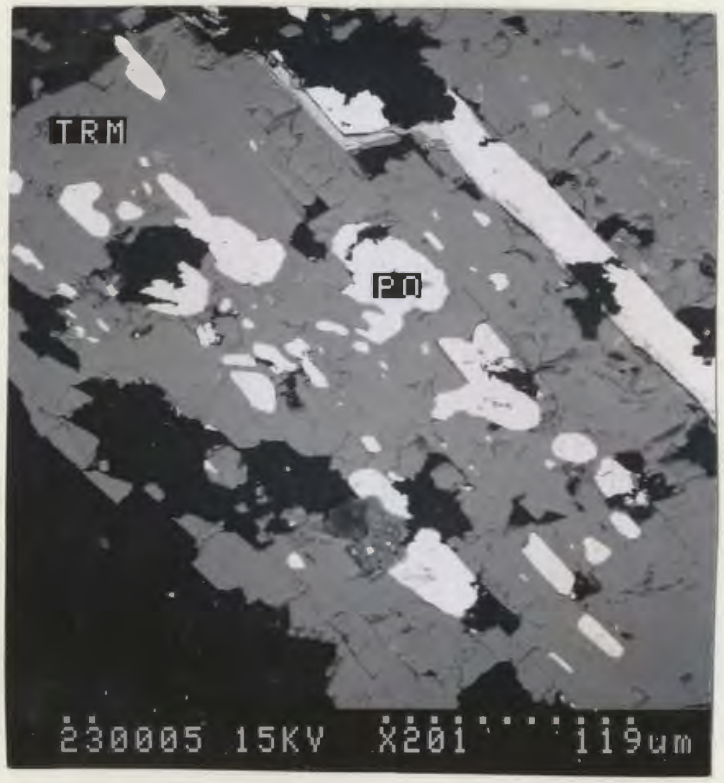

Plate 4.22: Pyrrhotite (PO) along growth lines in tourmaline (TRM) (magnification and scale given at base of photograph).

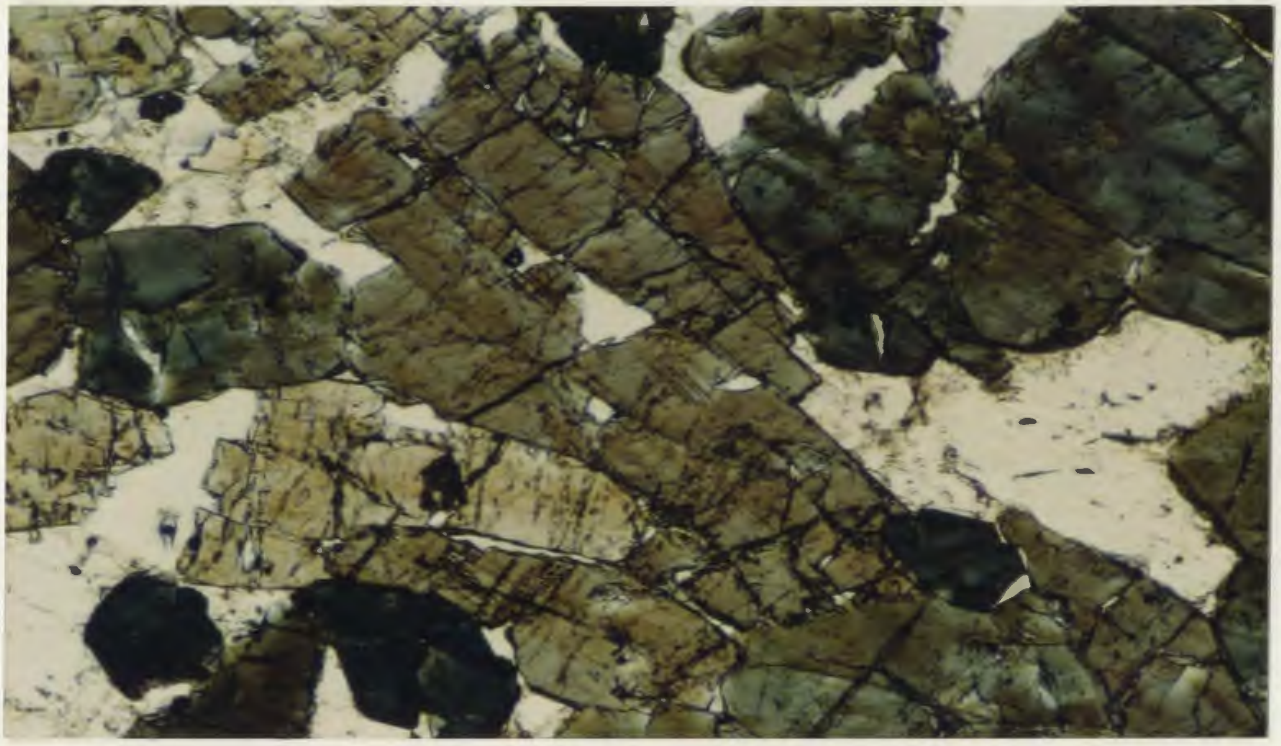

Plate 4.23: Randomly orientated tourmaline from tourmalinite sample (magnification: 20X; ppl).

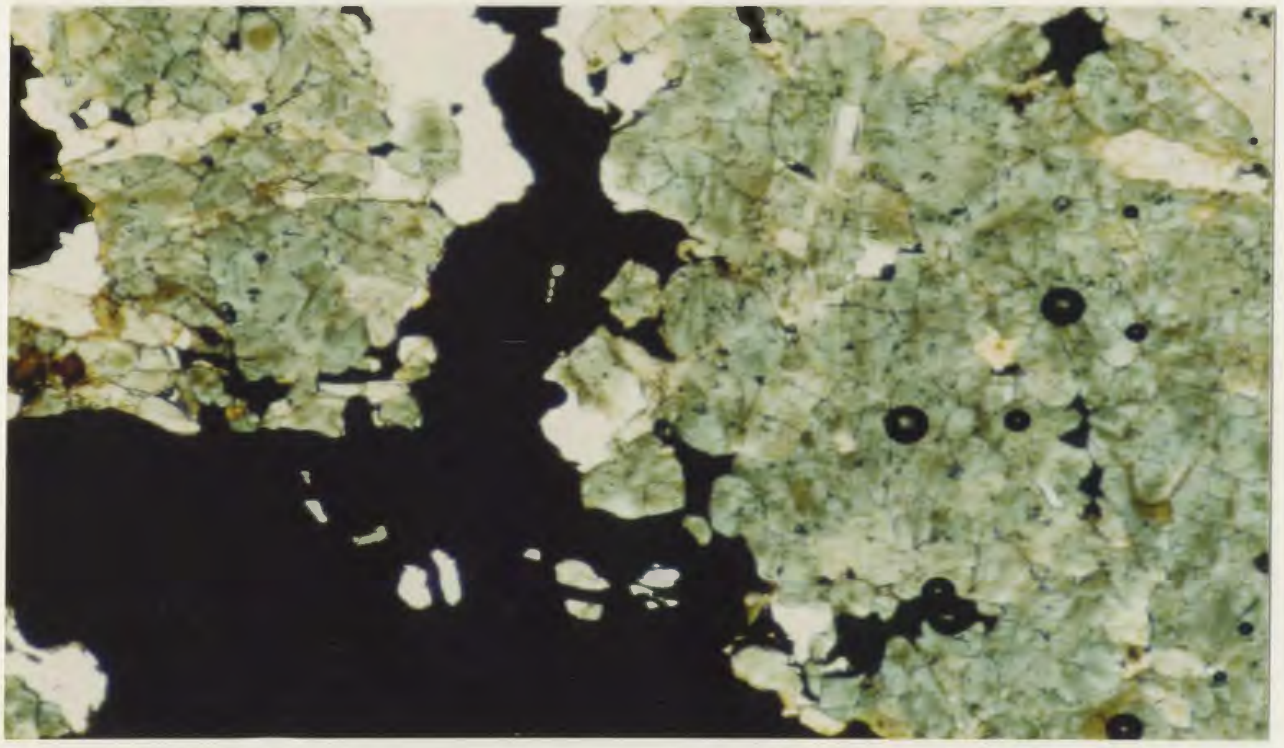

Plate 4.24: Tourmaline (green) from tourmalinite sample being dissected by pyrrhotite and chalcopyrite (black) (magnification: 20X; ppl).

Plate 4.25: Fresh, euhedral tourmaline (TRM) set in a matrix of chalcopyrite (CPY) and pyrrhotite (magnification and scale at base of photograph).

Plate 4.26: Massive pyrrhotite-chalcopyrite ore sample from Feoy. Note the highly deformed nature of this sample, with strong chalcopyrite banding. Pen top for scale.

4.3.3: Leaching of PGE's from the Feoy Ni-sulfides

PGE mobility in both silicates and Ni-sulfides, as a result of post-magmatic hydrothermal processes, has been demonstrated by several writers (Keays et al., 1982; Rowell and Edgar, 1986; Stumpfl, 1987). While there is little doubt that most significant PGE concentrations in basic-ultrabasic rocks must primarily be a result of the presence of an immiscible sulfide or oxide melt, it had long been assumed that such magmatophile PGE's were chemically inert and resistant to hydrothermal alteration.

Recently there has been an abrupt change in attitude about the role of hydrothermal fluids not only in later modification of pre-existing deposits, but also in the primary concentration of the PGE's themselves. For example, the Pt-rich pegmatites of the Bushveld Intrusion (South Africa) are now suggested to be products of infiltration metasomatism of PGE-rich chromite by late magmatic chloride solutions (Irvine et al., 1983). This fluid facilitated solution of Pt from the chromite, while leaving behind the less soluble Pd, Ru, Rh and Ir; this may account for the Pt-rich nature of the Bushveld deposits.

While infiltration metasomatism may be a plausible alternative for formation of the Bushveld deposits, such a fluid phase is not necessary in sulfide bodies like the Feoy deposit, since a sulfide fraction will adequately concentrate any PGE's present in a silicate/sulfide partial melt (Naldrett and Duke, 1980; also, see Chapter 7). Also, MacMillan et al. (1985) have shown that, contrary to suggestions of Irvine et al. (1983),

low temperature hydrothermal fluids (as opposed to high temperature, magmatic hydrothermal fluids in the case of the Bushveld deposit) are also capable of leaching not just Pt, but in fact all PGE's from Ni-sulfide deposits.

In the Feoy sulfides, all fresh, unaltered samples of massive Ni-sulfides contain high contents of PGE's (see Table 7.2, samples F-41, F-31, F and F-b), even those that are highly metamorphosed and completely recrystallized. On the other hand, equally metamorphosed and recrystallized samples that are also highly altered and corroded by hydrothermal fluids (samples F-7, F-10, F-11, F-19, F-35, F-36, and JS-b) have highly erratic PGE abundances. Sample F7 (see Table 7.2) is an extensively altered sample that illustrates complete loss of all PGE's. Since only those samples that have been altered by hydrothermal fluids have erratic PGE abundances, then it is clear that such fluids were responsible for the remobilization of PGE's within the Feoy sulfides.

The economic implications of such hydrothermal modification of PGE-rich sulfide deposits are self-evident.

4.3.4: Metamorphic textures in the Feoy Ni-sulfides

As is the case in the Visnes deposit (see Chapter 3), recrystallization of the Feoy Ni-sulfides appears to be complete, as all samples show well developed annealed textures (see Section 4.3 and Plate 4.1). Many ore samples, especially those rich in the more brittle magnetite, exhibit classic cataclastic textures. Massive pyrrhotite-chalcopyrite--

magnetite ores rich in actinolite gangue exhibit excellent "Durchbewegung" structure (see Plate 4.3). This was defined by Vokes (1969) as minor brecciation which grades into complete cataclasis of both ore and gangue minerals.

The formation of small (up to 0.5cm) pyrite porphyroblasts is indicative of post-formational metamorphism of the Ni-sulfides (see Plate 4.6). In the study area, pyrite porphyroblasts have formed at the expense of pyrrhotite (see Plate 4.6).

In many ore samples, chalcopyrite and pyrrhotite have been remobilized during deformation. Chalcopyrite has coalesced into bands in the massive pyrrhotite ore, giving it a streaked appearance (Plate 4.26), and has also been remobilized into veins in the breccia samples.

Actinolite overprints on the sulfides and high-Mg dykes are often incipiently altered to tourmaline of the schorl/dravite, Fe-rich variety (Plate 4.27). Tourmaline "suns" occur in some samples (Plate 4.28), and these are suggested to be products of feldspar or amphibole replacement followed by radial growth of tourmaline on the relict minerals (Deer et al., 1962).

Pyrite porphyroblasts in the massive pyrrhotite samples are highly corroded by chalcopyrite, and are rimmed by magnetite as well; this must have occurred subsequent to porphyroblastic growth of pyrite during metamorphism. The magnetite itself is in places altered to hematite as a result of low grade hydrothermal alteration or even

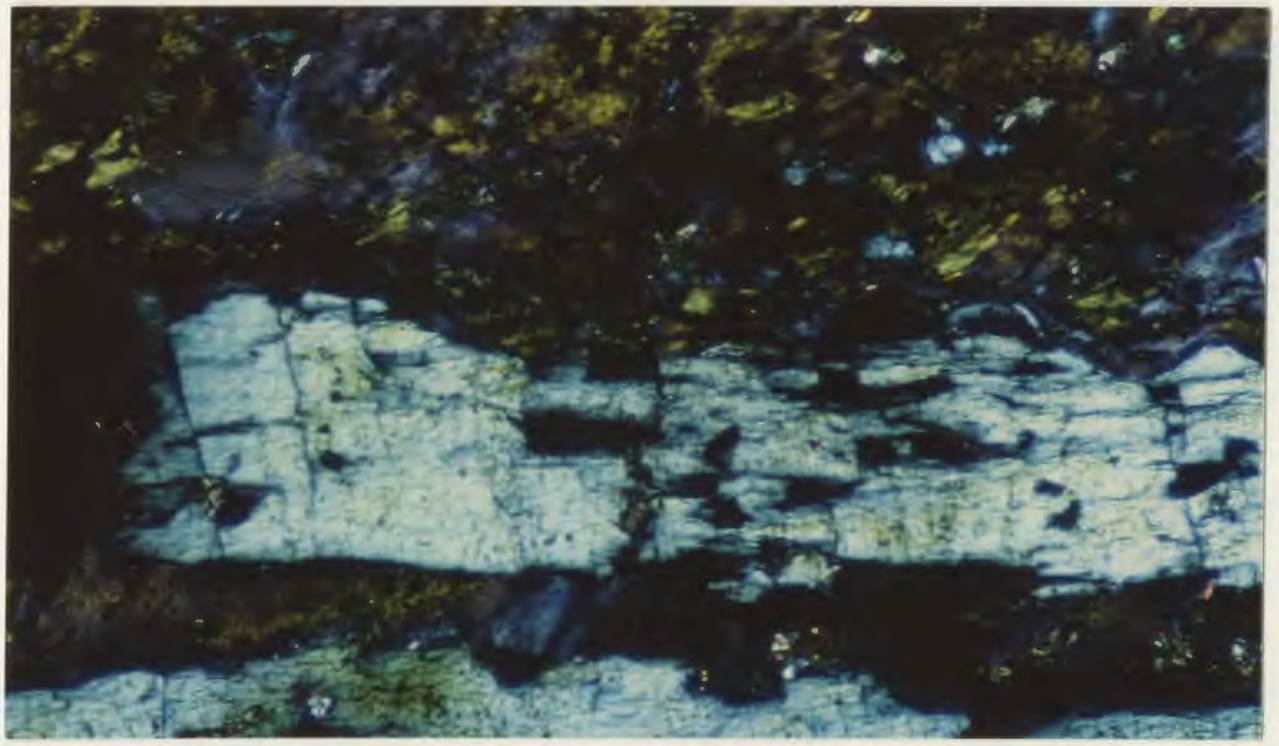

Plate 4.27: Photomicrograph of amphibole porphyroblast being replaced by tourmaline (blue-white). From high-Mg dyke sample from Feoy (magnification: 20X; cn).

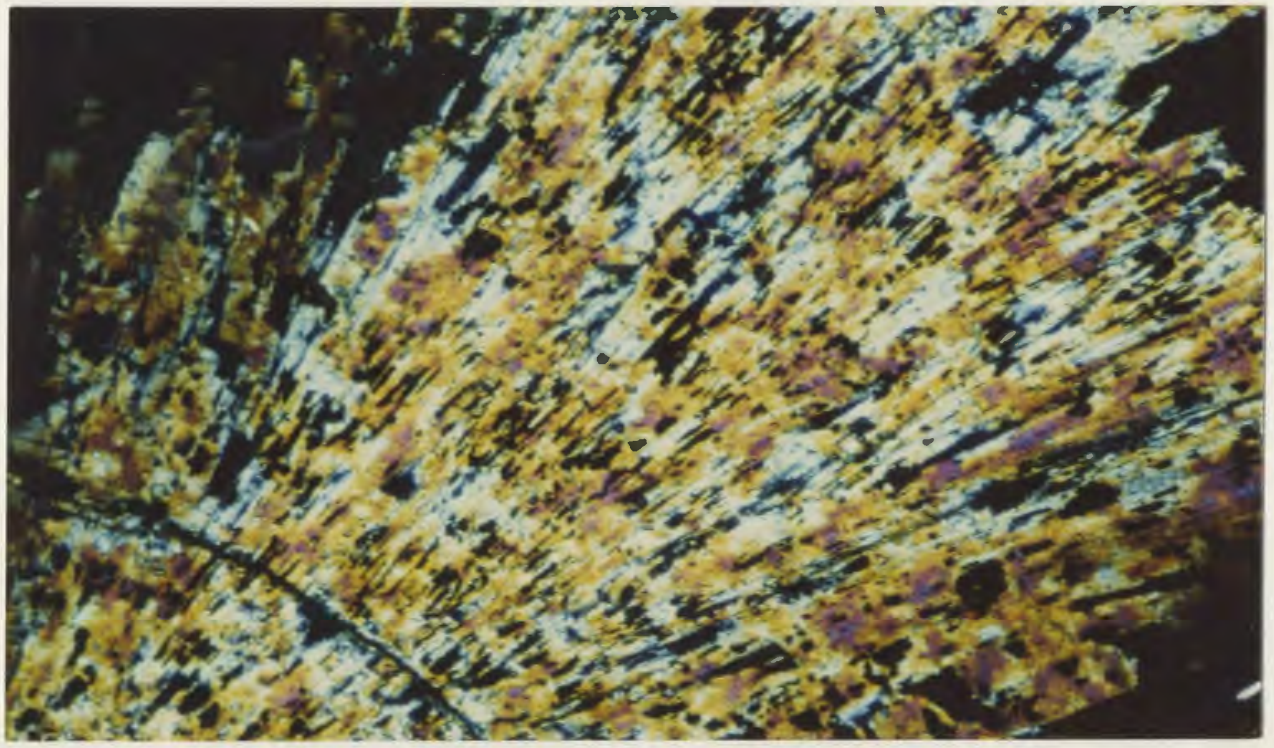

Plate 4.28: Tourmaline "sun", from Type A breccia sample from Feoy. Note abundant inclusions of pyrrhotite in the tourmaline (magnification: 20X; cn).

meteoric weathering.

Finally, all pentlandite is variably altered to violarite. However, it is possible that this may also have occurred during primary precipitation of the Ni-sulfides, since violarite alteration can occur equally well at low or very high temperatures.

4.4: Comparison of the Feoy and Visnes deposits

The two sulfide deposits in the study area are situated about 1/2km apart (see Fig. 1.1), and both deposits are contained within shear zones cutting the uppermost parts of the Karmoy Ophiolite. As a result, they were previously felt to be genetically related to one another (Scott, 1985). It is now clear, however, that they are quite dissimilar in both mineralogy and structure, and that these differences probably are a function of their formation by different geological processes in distinctly different geological environments.

The Visnes deposit (see Chapter 3) contains elements of typical ophiolitic, Cyprus-Type massive Fe-Cu-Zn sulfide deposits which are currently felt to be ancient analogues of present day "black smoker" deposits. Mineralogically, structurally, and stratigraphically, the Feoy deposit has been shown to be different in the following ways:

(1) metal content- the Feoy deposit contains predominently Fe-Cu-Ni-PGE-rich sulfides, as opposed to Fe-Cu-Zn-rich sulfides in the Visnes deposit;

(2) mineralogy- Feoy contains predominently pyrrhotite-chalcopyrite-pentlandite-PGM assemblages, as opposed to pyrite-chalcopyrite-sphalerite in the Visnes deposit;

(3) structure- Feoy is a very small (<20,000 tonnes) massive sulfide deposit, with very little evidence of sulfide-gangue mineral veining or "stockwork zones". This is in distinct contrast to the Visnes deposit, which is characterized by extensive sulfide-silicate-carbonate veining both on a local and regional scale;

(4) stratigraphy- the Ni-sulfides are only found along one local shear zone on the Island of Feoy, and are associated with high-Mg dykes and tourmaline breccias. In contrast, the Visnes sulfides occur along several large shear zones within a country rock assemblage of sheeted dykes and pillow lavas.

While there is little doubt that the Visnes deposit is similar to other volcanogenic massive sulfide deposits found all along the Appalachian-Caledonian Mountain System, data presented in this chapter and in Chapter 3 suggests an entirely different formational history for the Feoy deposit. Data given in the preceeding sections, and listed again below, are consistent with formation of the Feoy sulfides from a PGE-enriched sulfide melt in association with a basic, highly magnesian subvolcanic intrusion:

(1) essential mineralogy- pyrrhotite-pentlandite-chalcopyrite-PGM-sulfide deposits are uncommon, and the vast majority of such mineral assemblages are found in orthomagmatic Ni-sulfide deposits (see Chapter 7);

(2) accessory mineralogy- the presence of primary magnetite, chromite, ilmenite and PGM's all point to a very high temperature origin for the deposit. Indeed most authors would consider these primary magmatic minerals (see Chapter 7);

(3) mineral textures- "exsolution flames" of pentlandite in pyrrhotite, exsolution blebs of pyrrhotite in chalcopyrite, and "segregations" of chalcopyrite in pyrrhotite, are all considered very high temperature features (Stanton, 1978), and most likely result from conversion of mss to iss in a primary sulfide melt. Also, the presence of interstitial sulfides in a silicate host is strong evidence for magmatic sulfide precipitation from a co-magmatic silicate melt;

(4) the paucity of any Ni-sulfide veining or "stockwork zone", the lack of any disseminated Ni-sulfides outside the immediate mine dump area, and the highly localized, massive nature of the deposit itself are all non-specific evidence for a non-hydrothermal origin of the Feoy Ni-sulfides.

Part B: Major oxide, trace element, PGE, oxygen and sulfur isotope chemistry

Chapter 5: Alteration geochemistry of the Visnes dykes

5.1: Introduction and literature review

The relationship between alteration and mineralization in the study area is not surprising, since many writers consider hydrothermal alteration (spilitization) of sub-volcanic and volcanic ophiolitic rocks and formation of volcanogenic massive sulfide deposits to be one and the same process (eg., Stevens, 1980; Alabaster and Pearce, 1985; Saunders and Strong, 1985; Constantinou, 1987; Richardson et al., 1987; Nehlig, 1989; Richards and Cann, 1989; Butterfield, et al., 1990; etc.). Assuming that such relationships are indeed real, then the following section deals with the nature and extent of geochemical alteration in the Visnes dykes.

Spilitization of seafloor volcanic rocks and dykes is characterized by the following physical and chemical changes (Amstutz, 1974):

1- a low grade mineralogy that completely, or nearly so, masks the original basaltic textures and mineralogy, and;

2- an apparent and/or real increase in Na2O, with a real decrease in CaO, and often K2O, relative to unaltered basalts.

Many authors have discussed the effects of spilitization on the major and trace element chemistry of basalts (eg., Cann, 1970; Hart et al., 1974; Coish, 1977; Seyfried et al., 1978; Ludden and Thompson, 1979; Hellman et al., 1979; Furnes et al., 1980; Stevens,

1980; Stephens et al., 1984; Cann et al., 1985/86; Richardson et al., 1987; Hudson, 1988; Butterfield et al., 1990; etc.). Some consistencies are evident in these studies, such as the behavior of Na2O, CaO, K2O, Sr, Ba, and FeO. Strong and Saunders (1987) have documented the "immobility" of Zr, TiO2 and Cr in basalts of the Bett's Cove area of Newfoundland during spilitization, and suggest a genetic link between intense spilitization of basalts and formation of the Bett's Cove massive sulfide deposit. Likewise, Stevens (1980) demonstrated the immobility of Ti, Y, Si, Al, Fe and P within sheeted dykes and volcanics of the Swedish Caledonides, although he found Zr, Ni and Cr to be somewhat mobile in this case. Leaching of base metals from the volcanic pile by convecting hydrothermal fluids was shown by Stevens (1980) and Richardson et al. (1987) to be responsible for formation of large massive sulfide deposits.

With these considerations in mind, alteration of the Visnes dykes is described in terms of relative gain or loss of material.

5.2: Alteration geochemistry

Appendix 3 is a compilation of major oxide and selected trace element data for dykes of the sheeted complex (the Visnes dykes), and high-Mg dykes of Feoy. In order to assess the chemical changes during alteration, it is necessary to compare these dykes to unaltered dykes, as well as to true spilites, from similar environments.

Data from Appendix 3 are plotted in Figures 5.1 and 5.2. Major oxides and trace

Figures 5.1.1 to 5.1.10: Major oxides (in wt. %) versus Na2O/Na20+CaO for: 1- the Visnes dykes (denoted by asterix- unshaded); 2- the high-Mg dykes of Feoy (denoted by crosses- darkly stippled field); 3-typical unaltered island arc tholeiites (data from Basaltic Volcanism Study Project, 1981) (denoted by circles- intermediate stippled field); 4- the field for 231 spilitized basalts of an island arc tholeiitic nature (data from Stevens, 1980) (denoted by squares- lightly stippled field); 5- an average of 66 typical unaltered MORB samples (data from Engel et al., 1965; Cann, 1969; Engel and Engel, 1970; Shido et al., 1971) (denoted by triangles); 6- the average compositions of 32 typical unaltered boninites (data from Hamlyn and Keays, 1986) (denoted by inverted triangles).

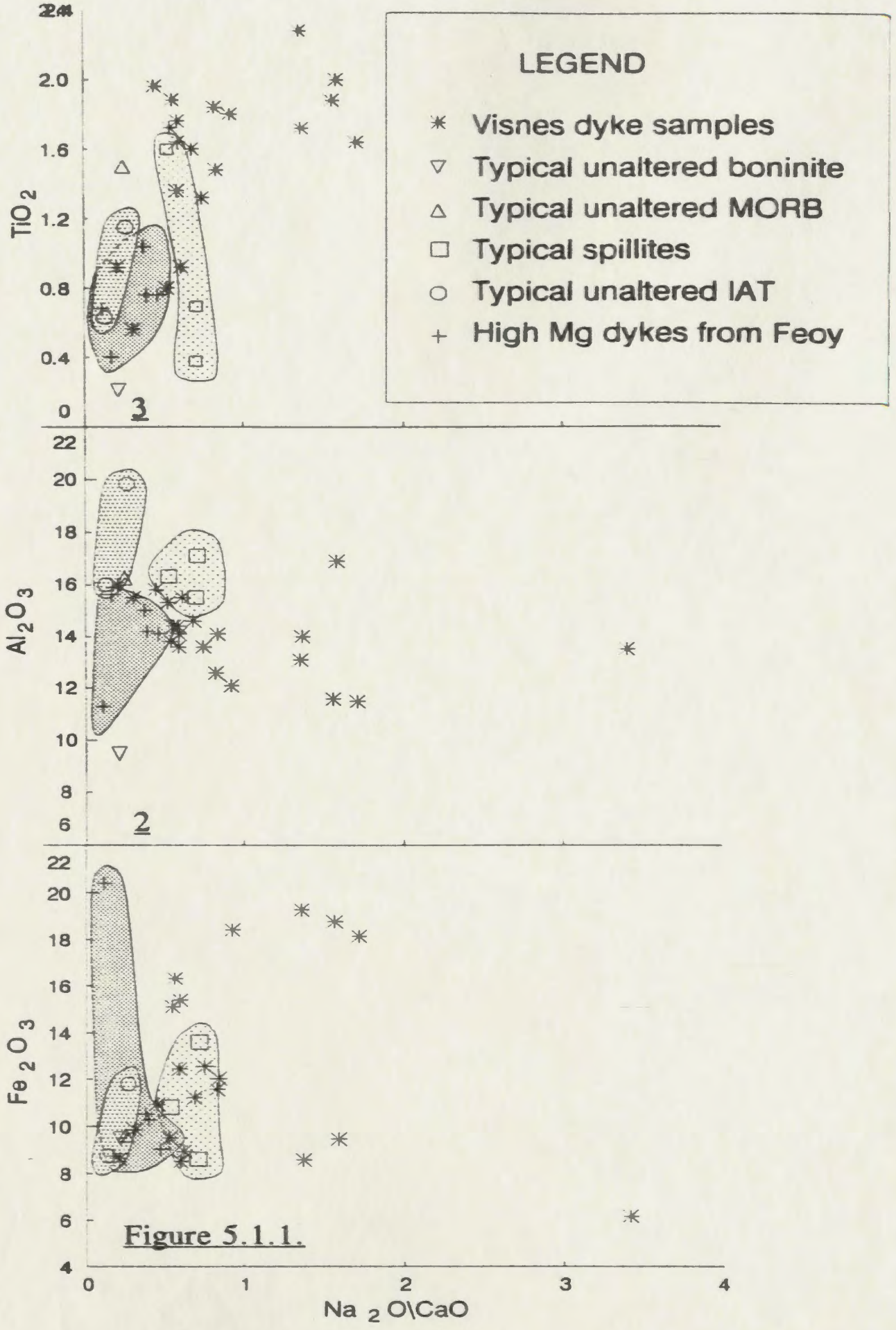
LEGEND
Visnes dyke samples
Typical unaltered boninite
Typical unaltered MORB
Typical spillites
Typical unaltered IAT
High Mg dykes from Feoy
TiO2
Al2O3
Fe2O3
Na2O\CaO
3
2

Figure 5.1.1.

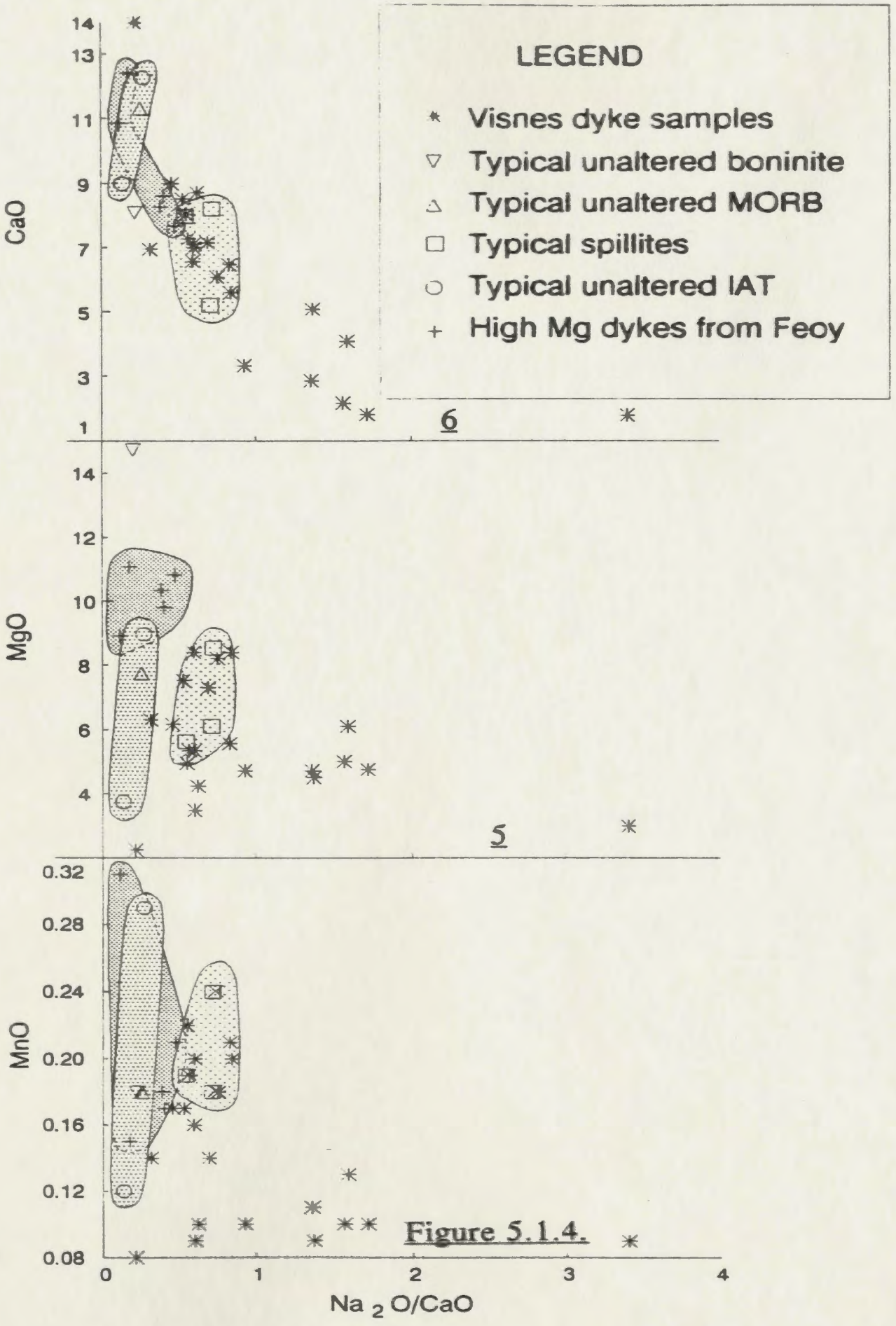
LEGEND
Visnes dyke samples
Typical unaltered boninite
Typical unaltered MORB
Typical spillites
Typical unaltered IAT
High Mg dykes from Feoy
CaO
MgO
MnO
Na 2 O/CaO
6
5

Figure 5.1.4.

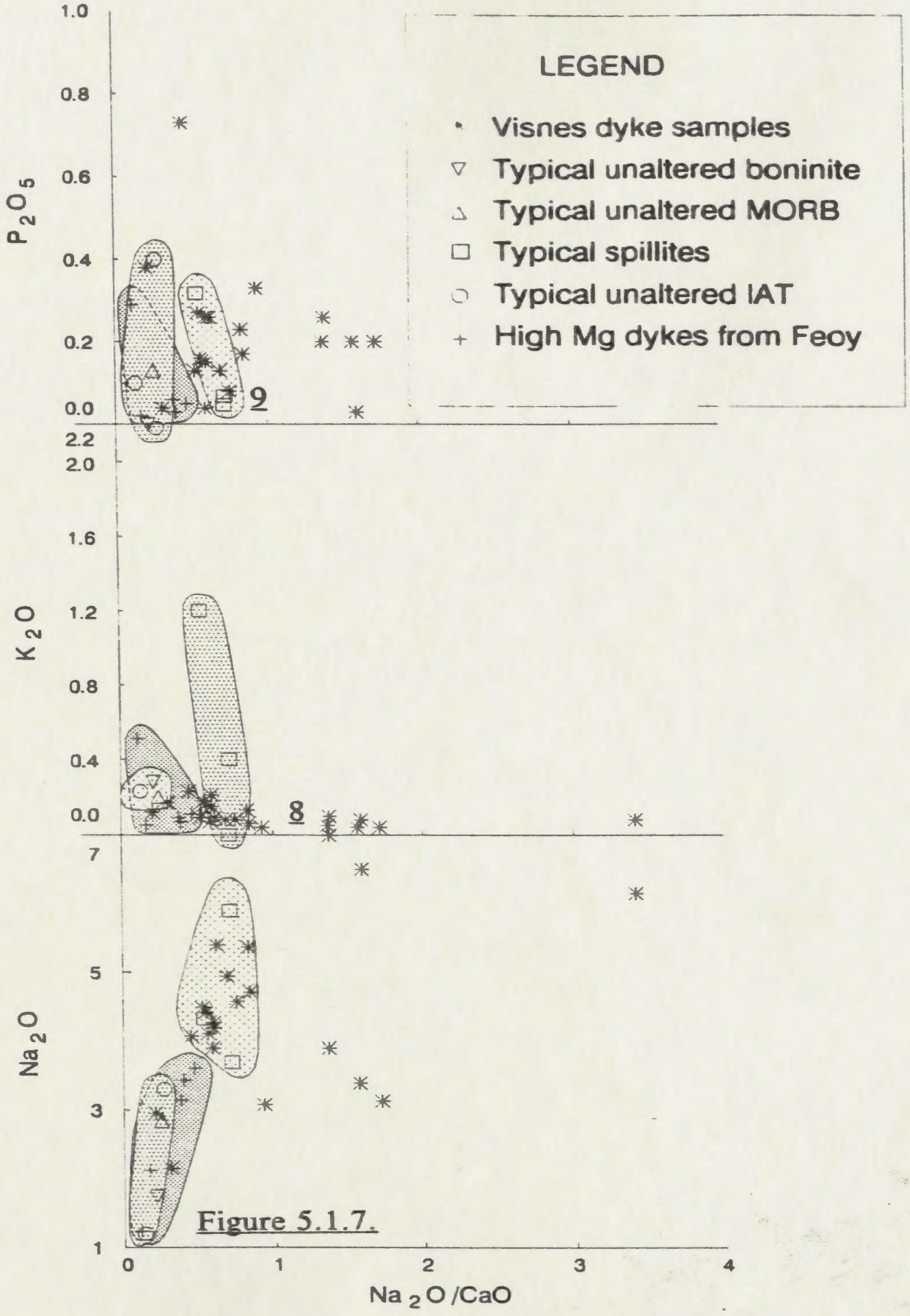
LEGEND
Visnes dyke samples
Typical unaltered boninite
Typical unaltered MORB
Typical spillites
Typical unaltered IAT
High Mg dykes from Feoy
P2O5
K2O
Na2O
Na2O/CaO
9
8
1.0
0.8
0.6
0.4
0.2
0.0
2.2
2.0
1.6
1.2
0.8
0.4
0.0
7
5
3
1
0
1
2
3
4

Figure 5.1.7.

Figures 5.2.1 to 5.2.8: Trace elements (in ppm) versus Na2O/Na2O+CaO for rock suites 1 through 6 in Figure 5.1 (symbols as in Figure 5.1).

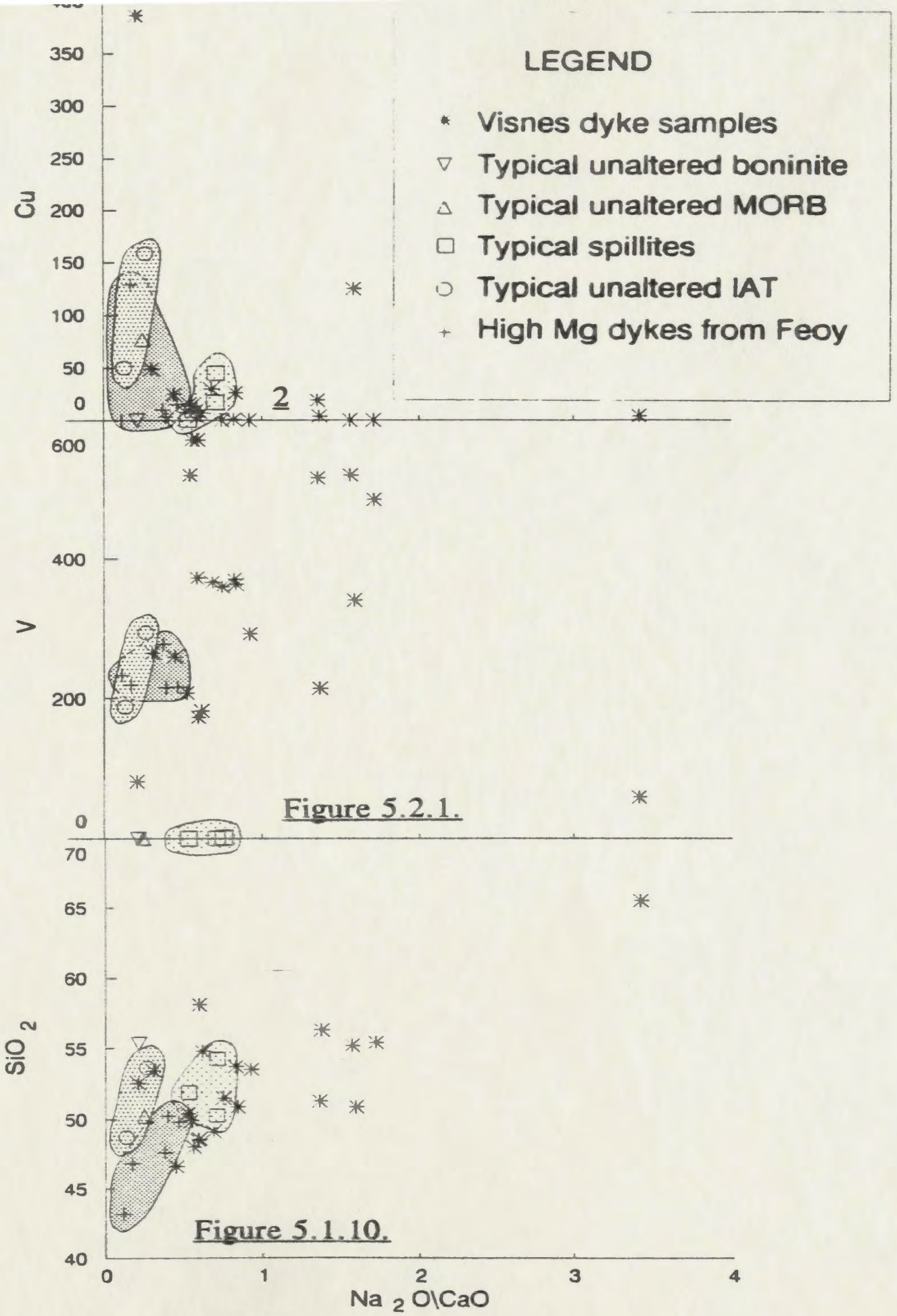

Figure 5.2.1.

Figure 5.1.10.

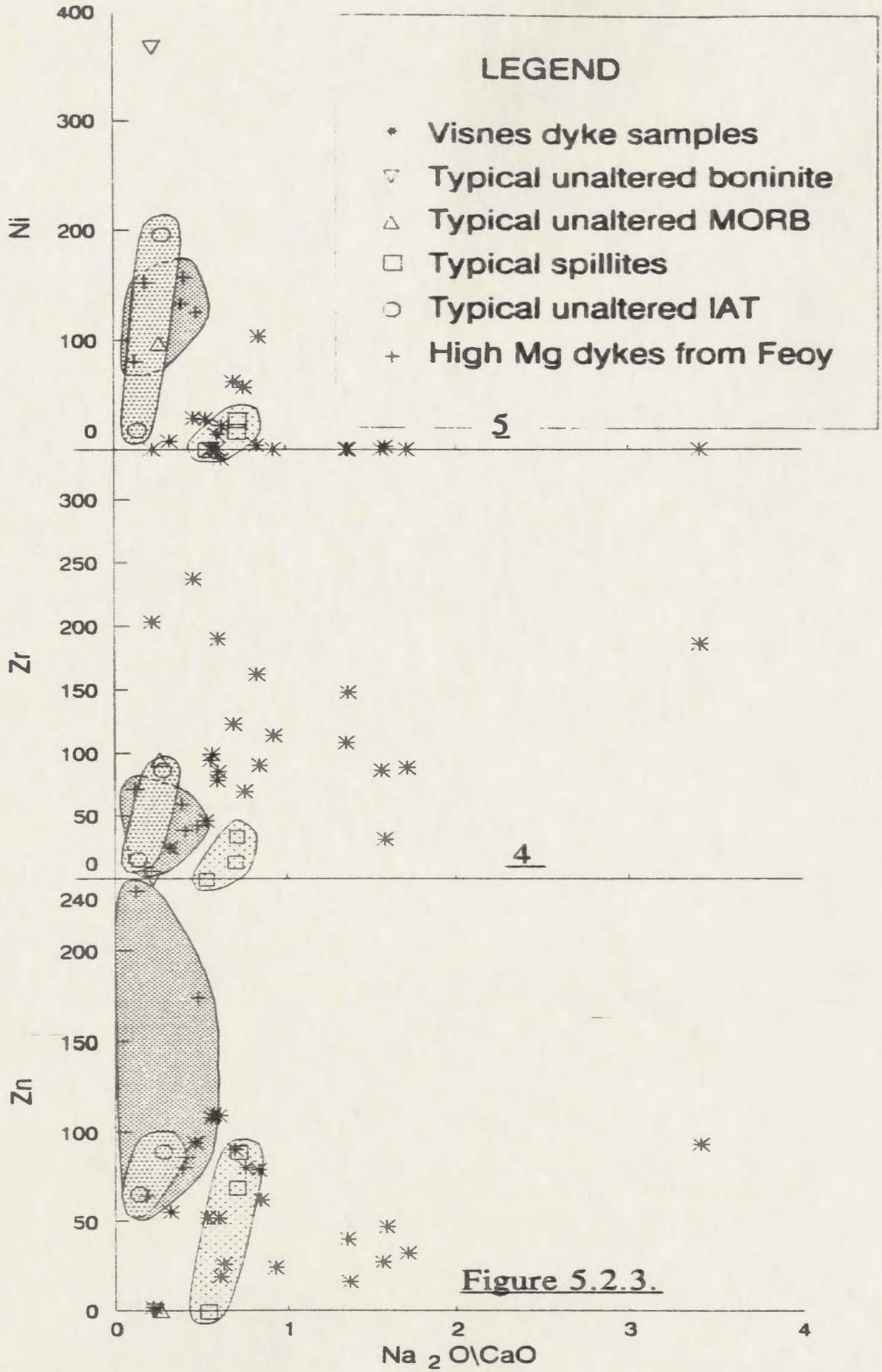
LEGEND
Visnes dyke samples
Typical unaltered boninite
Typical unaltered MORB
Typical spillites
Typical unaltered IAT
High Mg dykes from Feoy
5
4
Ni
Zr
Zn
Na 2 O\CaO
400
300
200
100
0
250
150
50
240
1
2
3
4

Figure 5.2.3.

elements are plotted against Na2O/CaO. This index has been chosen to assess the effects of alteration since Na2O and CaO mobility during spilitic alteration of basalts has been well documented (Bachinskii, 1977; Stevens, 1980; Mottl, 1983; Stevens et al., 1984; Strong and Saunders, 1986; etc.).

The Visnes dykes have geochemical and rare earth element (REE) similarities to both island arc (IAT) and mid-ocean ridge (MORB) basalts (Pedersen, 1982, 1987). Therefore, comparison of the Visnes dyke rock samples to representative samples from these environments is reasonable. Figures 5.1.1 to 5.1.10 plot Na2O/CaO+Na2O vs. major oxides. The Visnes and high-Mg dyke samples are compared to: (1) the field of typical unaltered IAT (data is from Basaltic Volcanism Study Project, 1981); (2) the average compositions of 66 typical unaltered MORB (data is from Engel et al., 1965; Cann, 1969; Engel and Engel, 1970; Shido et al., 1971); (3) the average compositions of 32 typical unaltered boninites (data is from Hamyln and Keays, 1986), and; (4) the field for 231 true spilitized basalts of an IAT affinity (data is from Stevens, 1980). The following features are noteworthy:

1- the Visnes dykes show considerable overlap with the field for true spilites in all cases;

2- in no case does the field for spilites overlap significantly with the field for the high-Mg dykes of Feoy, and there is little to no overlap between the field for the high-Mg dykes of Feoy and the distribution of the Visnes dykes. On the other hand there is considerable overlap in nearly all cases between the field for unaltered IAT and the field for the high-Mg dykes of Feoy;

3- relative to the field for unaltered IAT and MORB, the Visnes dykes show enrichment in Na2O, Fe2O3 (as total Fe) and TiO2; depletion in K2O, CaO, MnO and Al2O3; moderate depletion in MgO, and variable changes in P2O5 and SiO2.

Figures 5.2.1 to 5.2.10 plot the trace elements Nb, Sr, Zr, Cr, Ni, V, Cu, Zn vs. Na2O/CaO. Data for V, Nb and Sr were unavailable from the spilites, MORB, and boninite sources. The following features are noteworthy:

1- in all cases where the field for true spilites is shown, there is considerable overlap between this and the distribution of the Visnes dykes. The exception to this is Zr, which is more enriched in the Visnes dykes relative to the field for spilites. This suggests once again that the Visnes dykes have undergone spilitization;

2- in all cases except V, Zr and Cu, there is little or no overlap between the field for the high-Mg dykes of Feoy and the distribution of the Visnes dykes, while there is nearly complete overlap between the field for unaltered IAT and that for the high-Mg dykes of Feoy. Assuming that at least some trace elements would have been mobilized during seafloor alteration (spilitization), as appears to have been the case with the Visnes dykes and the field for true spilites, then these data suggest that the high-Mg dykes of Feoy have escaped spilitization;

3- relative to the field for unaltered IAT, the Visnes dykes show: an overall enrichment in Zr and V; depletion in Cr, Ni and Cu; moderate overall depletion in Zn and Sr, and; no change in Nb.

4- relative to the field for unaltered MORB, the Visnes dykes show depletion in Cr, Ni and Cu, and show no change in Zr.

In summary, Figures 5.1 and 5.2 support earlier suggestions (from Section 2.2) that the Visnes dykes have undergone spilitization during sub-seafloor hydrothermal circulation, while the later high-Mg dykes of Feoy have escaped this period of alteration. In comparison with unaltered IAT and MORB, spilitization of the Visnes dykes appears to have resulted in a relative loss of K2O, CaO, MnO, Al2O3, MgO, Cr, Ni, Cu, Zn, Pb and Sr from the rocks; a relative gain of Na2O, Fe2O3, TiO2 and Zr. P2O5 and SiO2 appear to have acted in a variable manner relative to IAT and MORB. However, because of the variability in primary geochemistry of the different rock types, the changes suggested above must be considered relative ones at best.

It is interesting to note that in Figure 5.2.8 and 9, there is a general relationship between increasing Na2O/CaO+Na2O and decreasing Cu and Zn concentrations. The most heavily altered of the Visnes dyke samples are from the "epidosite zones" (for eg., samples 12, 15, 17 in Appendix 3), and these are usually the most severely Cu and Zn depleted. Richardson et al. (1987) have suggested that epidosites from the Troodos ophiolite represent "root zones" for ore-forming hydrothermal fluids. The highly altered and metal-depleted nature of epidosite samples from the study area suggests that these rocks might also have represented root zones for hydrothermal fluids responsible for formation of the Visnes sulfide deposit.

Chapter 6: The origin and oxygen-isotopic tenor of epidotites and Type 1 plagiogranites

6.1: Literature review

Studies on the origin of plagiogranites and epidotites within ophiolites are rare (Aldiss, 1978; Heaton and Sheppard, 1977; Taylor, 1979, 1980; Sheppard, 1978; Pedersen and Malpas, 1984; Kelley et al., in prep.). Aldiss (1978) demonstrated the critical role that water saturation in the residual melt played in plagiogranite formation in the Troodos ophiolite of Cyprus. He suggested that an initially tholeiitic magma became progressively Fe-enriched during differentiation, until water saturation caused an increase in fO_2, thereupon resulting in Fe-Ti-O2 fractionation. A corresponding decrease in the liquidus temperature of plagioclase might allow for separation of a plagiogranitic melt from the varitextured gabbro matrix. Aldiss (1978) also suggested that vigorous discharge of an aqueous magmatic phase may have been responsible for alteration of the overlying sheeted dykes and pillow lavas of Troodos, resulting in the formation of "epidosites" (see Section 2.2).

Pedersen and Malpas (1984) have modelled formation of the (Visnes) Type 1 plagiogranites as a result of filter pressing of a differentiated interstitial liquid from the varitextured gabbros (see Chapters 1 and 2). The depletion of the hydro-magmatophile elements K, Rb and Ba could not be adequately explained by this model, and so they suggested loss of these elements from the system by auto-metasomatic processes

involving volatile evolution. Evidence of such loss was given by the presence of epidotites and sericite alteration. These writers recognized the primary nature of the epidotite in the study area, and its essentially co-genetic relationship with the plagiogranites.

A third model for formation of ophiolitic plagiogranites and epidotites is that of Taylor (1980). He combined field and oxygen-isotopic data from granophyres and rhyolites in several ancient and modern spreading centers, all of which have been subject to the action of convecting meteoric fluids. These are compared with plagiogranites of an oceanic (seawater influenced) environment, such as the Troodos plagiogranites. Firstly, it is shown how the two different types of acid rocks are mineralogically, texturally and stratigraphically identical to one another, except for the absence of K-feldspar in oceanic plagiogranites, and their depletion in Rb with respect to granophyres and rhyolites (Figure 6.1). Taylor (1980) used whole rock oxygen isotopic data to show that continental or sub-aerial granophyres, which have a significant K-feldspar component, form as a result of direct or indirect, late stage assimilation of meteoric water by a fractionally crystallizing gabbroic melt. He suggested that direct assimilation might result from diffusion of meteoric water along fracture zones; indirect assimilation would occur from incorporation of meteoric water altered roof rocks into the magma chamber. Assimilation of such material would provide the necessary influx of K2O into an essentially K2O-depleted melt. The result of this assimilation would be to produce a K2O-rich rock, or a rhyolite or granophyre. Since meteoric water is enriched in Rb relative to seawater, then assimilation of meteoric water would result in the formation

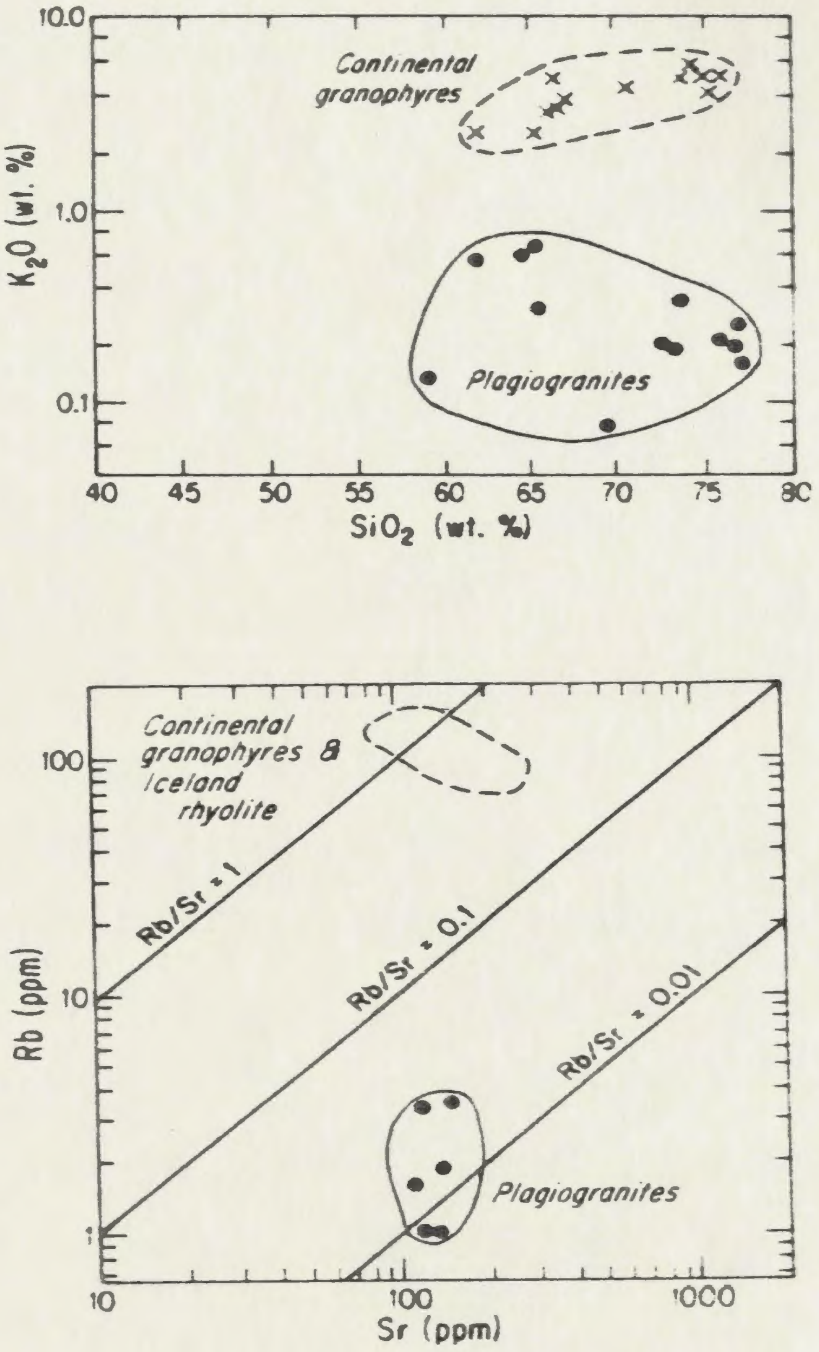

Figure 6.1: Comparison of continental granophyres with plagiogranites (data from Coleman and Peterman, 1975).

of rocks relatively rich in Rb (Coleman and Peterman, 1975), such as continental granophyres.

Conversely, assimilation by a gabbroic melt of seawater altered roof rocks would provide an influx of Na and H2O, but very little K or Rb to the melt. Interaction of the residual melt with this Na-H2O enriched material would produce rocks reflecting this elevated Na-H2O activity, such as plagiogranites and epidotite segregations. As a result, such rocks should possess oxygen isotopic signatures consistent with a seawater origin.

Heaton and Sheppard (1977) offered O/H isotope evidence for seawater hydrothermal alteration of the ophiolitic rocks of the Troodos massif, Cyprus. Temperatures of 0 to 250 degrees Celsius are suggested for formation of the spilitic alteration assemblages in the volcanic rocks and upper regions of the Troodos sheeted complex, while epidote bearing vein assemblages from gabbro pegmatites, plagiogranites and sheeted dykes record temperatures of 350 to more than 500 degrees. Where temperatures were greater than 500 degrees, a deuteric water component may have been present, although these writers suggest that this was ultimately of seawater origin. This corresponds well with suggestions of Taylor (1980) that both the epidote veins and plagiogranites of Troodos formed from incorporation of seawater into a residual magma.

Kelley et al. (in prep.) provide fluid inclusion evidence of highly saline brines which formed at temperatures in excess of 450-600 degrees Celsius; these authors suggest that late stage exsolution of such brines from a hydrous, residual melt may well have been

responsible for formation of epidotites, as well as local zones of intense hydrothermal alteration.

Richardson et al. (1987) recognized the importance of "epidosites" in Troodos as "root zones" for convecting, ore-forming hydrothermal fluids driven by an underlying magma chamber. However, these writers do not recognize a magmatic water influence on formation of an evolved hydrothermal fluid, as suggested by Aldiss (1978), Taylor (1980), Kelley et al. (in prep.), and this writer. This is perhaps because clearly deuteric epidotite "segregations"(see Chapter 2), which provide a link between magmatic fluids and overlying epidosite zones, have not been documented from the Troodos area as they have in Visnes.

In conclusion, while there is clearly a paucity of data on epidotite and plagiogranite formation in ophiolites, some features of this data are common:

1- most writers are aware of the importance of a volatile-rich residual magma in formation of plagiogranites and epidotites;

2- the magmatic water component responsible for epidotite formation is probably of seawater origin, the seawater having been incorporated into the magma chamber by assimilation of seawater altered roof rocks. Assimilation may also have been responsible for plagiogranite formation;

3- evolved, epidote-forming hydrothermal fluids were responsible for alteration of sheeted dykes to epidosite zones in the Troodos ophiolite, and were also responsible for formation of the Cyprus-type massive sulfides. There is disagreement as to whether this

hydrotnermal fluid was directly magma influenced or not.

With these considerations in mind, the oxygen isotopic tenor of Type 1 plagiogranites and epidotites from the study area is examined.

6.2: Oxygen isotopes from epidotites and Type 1 plagiogranites

Five whole rock epidotite and plagiogranite samples were analysed for oxygen isotope ratios (delta 18O); results are given in Table 6.1 along with data of Heaton and Sheppard (1977) from plagiogranites, gabbro pegmatites, epidote veins, and sheeted dykes in the Troodos ophiolite. Because the epidotites from the Visnes region are 98-100% epidote, then these samples are equivalent to mineral separates; the isotopic tenor of the Type 1 plagiogranites may not, however, be an accurate representation of the isotopic tenor of plagioclase, since the latter is much more susceptible to oxygen isotopic exchange during alteration than is quartz (Taylor, 1979). Notwithstanding such limitations, the isotopic tenor of these essentially cogenetic magmatic products has been investigated.

The Visnes epidotites have isotopic signatures quite similar to epidote from veins in the Troodos plagiogranites and gabbros, while whole rock oxygen isotope (delta 18O) values of the Visnes (Type 1) plagiogranites are somewhat enriched relative to the Troodos plagiogranites. However, quartz separates from associated gabbro pegmatites in Troodos give values of +7.6 per mil, which are identical to values obtained from Type 1 plagiogranites in the present study.

Table 6.1: Oxygen isotopic data from selected rocks of the Troodos Ophiolite (data for the Troodos samples are from Heaton and Sheppard, 1977), and from the Visnes region.

Sample	delta 18O (whole rock) (data is in per mil notation)	delta 18O (mineral) (data is in per mil notation)
Troodos		
11-1 plagiogranite	+4.4	0.00 (epidote)
49-plagiogranite	+5.3	
92-plagiogranite	+5.0	
gabbro	+6.2	+3.8 (epidote)
35-2 gabbro		+1.6 (epidote)
79-gabbro		+7.6 (quartz)
33-1 sheeted dyke		+3.4 (epidote)
32 sheeted dyke	+5.8	+0.9 (epidote)
Visnes region		
C-12 epidotite		+1.57
05-04 epidotite		+2.33
05-5 plagiogranite	+7.98	
05-2 plagiogranite	+7.56	
22-5 Visnes dyke (epidotized)	+5.07	

Although there is a distinct lack of published data on mineral-H2O fractionations for epidote which hinders geothermometric studies, epidote veins in the Troodos plagiogranites are believed to have formed from seawater hydrothermal fluids in excess of 500 degrees Celsius (Heaton and Sheppard, 1977). Epidotites of the Visnes region have quite similar oxygen-isotopic signatures to the Troodos epidotites, and as such similar temperatures of formation can be inferred for these epidotites. This supports suggestions that the epidotites of Visnes formed from magmatic, deuteric fluids. However, because of the lack of published data, the possibilty exists that the isotopic tenor of epidote from both Visnes and Troodos may reflect of the poor 18O fractionating capacity of epidote in general.

In general terms then, the low oxygen isotope values for the Visnes epidotites may be explained in any of the following ways:

1- formation from high temperature (350-500 degrees) alteration processes in the region of the magma chamber. This is consistant with data from Richardson et al. (1987), and accounts well for epidosite formation;

2- formation from low S18O seawater influx into the magma by assimilation of seawater altered roof rocks. This accounts well for both field relationships (which suggests their formation from deuteric fluids) and for the isotopic tenor of the Visnes epidotites, and is considered the most plausible explanation by this author;

3- from the low oxygen-isotopic fractionation capacity of epidote in general, regardless of source or temperatures of formation. Due to the lack of available data on isotope fractionation in epidote, this possibility cannot be adequately assessed.

As for the isotopic signatures of the Type 1 plagiogranites, which are about 2.5 per mil higher than seawater-hydrothermally altered plagiogranites of the Troodos ophiolite, there can be several explanations:

1- the "seawater imprint" from the Troodos plagiogranites is detectable as a function of 18O exchange during alteration of the plagioclase component of the plagiogranites. Since such alteration is not as intense in the Visnes plagiogranites, then it may be that the albite component of the Visnes plagiogranites has retained a magmatic (igneous) signature despite the presence of seawater during its crystallization;

2- plagiogranites of Troodos are on average between 66-76wt.% SiO2, while the Visnes plagiogranites contain 75-79wt.% SiO2 (see Table 6.2). This corresponds to a significant modal increase in quartz in the Visnes plagiogranites. Quartz preferentially fractionates 18O relative to 16O, and retains its original isotope signature much better than does plagioclase (quartz from gabbro pegmatites in Troodos have S18O about +7.6 per mil). Therefore, one might expect this absolute SiO2 increase in the Visnes plagiogranites to correspond to a variation in S18O, assuming similar formational histories;

3- the third alternative is that the Visnes plagiogranites are indeed representative of normal unaltered igneous rocks. Because of the intense alteration of the other rock types, and because of their close relationship to epidotites, however, this is likely not the case.

6.3: Summary

In conclusion, it is evident that the isotopic tenor of the epidotites and Type 1

Table 6.2: Major oxide analyses of Type 1 plagiogranites from the Visnes region, along with analyses from Aldiss (1978) for plagiogranites from the Troodos ophiolite in Cyprus.

sample	SiO2	TiO2	Al2O3	FeO*	MnO	MgO	CaO
Type 1 plagiogranites							
46TRN	75.5	0.2	9.3	1.85	0.05	0.04	5.34
73TRN	68.9	0.32	13.9	3.87	0.05	0.84	3.2
18TRN	79.1	0.2	11.1	0.78	0.01	0.05	1.06
51TRN	75.8	0.2	8.74	4.14	0.03	0.05	7.96
47TRN	76.8	0.24	10.2	3.04	0.02	0.09	3.34
Plagiogranites of the Troodos ophiolite							
TM33	77.02	0.09	13.66	2.24	0.01	0.42	3.1
TM89	71.02	0.38	12.32	5.39	0.07	0.71	1.98

Sample	Na2O	K2O	P2O5	LOI	Total
46TRN	3.74	0.04	0.02	2.12	98.2
73TRN	5.89	0.21	0.02	0.97	98.17
18TRN	6.13	0.07	0.01	0.24	98.75
51TRN	1.23	0.04	0.03	0.67	98.89
47TRN	4.25	0.04	0.03	0.38	98.43
TM33	3.09	0.68	0.01		100.32
TM89	6.4	0.12	0.07		98.46

plagiogranites from the study area is quite similar to that of epidote veins and plagiogranites from the Troodos ophiolite in Cyprus. The low S18O ratios of the epidotites of the study area, coupled with their primary deuteric nature, suggests that they formed from a magma which was rich in seawater derived fluids. This is consistent with Taylor (1980), and to a lesser degree can be supported by the isotopic tenor of the Type 1 plagiogranites.

Data from this chapter, coupled with field evidence from Chapter 2, are significant in that they focus attention on the importance of magmatic deuteric processes in formation of an evolved hydrothermal fluid. Assimilation of seawater into the magma chamber(s) may ultimately have been responsible for formation of the magmatic hydrothermal fluids in Visnes. Field data suggest that ascent of this magmatic fluid through the overlying Visnes dykes was responsible for formation of epidosite zones, the latter which are believed to represent root zones for associated overlying massive sulfide deposits (Richardson et al, 1987). By inference, one can see the possibly strategic role of magmatic hydrothermal fluids in the evolution of both the Visnes and the Cyprus massive sulfide deposits.

Chapter 7: PGE's, trace elements, sulfur isotopes, and their relationships to the petrogenesis of the Feoy Ni-sulfides and their host rocks

7.1: Introduction

The vast majority of PGE-rich sulfide deposits are felt to be of an orthomagmatic origin (Naldrett and Barnes, 1986), although there are some authors that advocate hydrothermal alteration of ultrabasic rocks as a means of forming PGE-rich deposits (ex., Keays et al., 1982; Rowell and Edgar, 1986; Stumpfl, 1987). The Feoy deposit has been shown (see Chapter 4) to contain the essential elements of an orthomagmatic, PGE-rich Ni-sulfide deposit, although it has undoubtedly been modified by later hydrothermal and metamorphic events.

It has long been known that the composition of magmatic sulfide deposits is strongly controlled by the composition of the co-magmatic silicate melt in terms of the base and precious metal reservoir initially available for scavenging by the sulfide melt. Recently, the importance of other factors such as the tectonic setting and degree of partial melting, the relative volumes of silicate and sulfide melt (or the "R factor", after Naldrett and Barnes, 1986), the interaction of this melt with country rock during ascent, and the internal changes that occur within the melt during cooling, have been emphasized (Naldrett and Duke, 1980; Hamlyn and Keays, 1986; Naldrett and Barnes, 1986). Therefore, since the sulfides of the Feoy area appear to be genetically related to the host high-Mg dykes, then any meaningful analysis of the sulfides of the area must be

accompanied by similar analysis of these dykes. In this respect, a discussion of the sulfide and high-Mg dyke geochemistry is offered in the following sections.

Petrogenetic modelling of co-magmatic sulfide-silicate deposits through the use of PGE's is a relatively recently developed technique (eg., Naldrett and Duke, 1980; Hamlyn and Keays, 1986), and unfortunately there is a fairly small number of similar PGE-rich deposits worldwide from which to make comparisons with Feoy. Therefore, it is constructive to review some of the literature on petrogenetic PGE-modelling of these magmatic sulfide deposits before attempting to analyse data from the Feoy sulfides. Firstly however, classification of the Feoy Ni-sulfide deposit with respect to other Ni sulfide occurrences is discussed.

7.2: Classification of the Feoy Ni-sulfide deposit

Naldrett (1981a) has presented a comprehensive classification scheme for all available data on Ni-sulfide deposits. Table 7.1 is a modification of this classification, and some examples of the various deposit types are given, including some relevant Norwegian occurrences (data for Norwegian deposits other than Feoy are from Boyd and Nixon, 1985; data for Feoy are from the present study).

Although the effects of later metamorphic and hydrothermal episodes can be shown to have profoundly modified Cu-Ni-sulfides in several areas (Panayiotou, 1985; McMillan

Table 7.1: Classification of Ni-sulfide deposits from various geological environments (modified after Naldrett, 1981a).

Setting	Examples	References
1- Astrobleme related noritic intrusions	-Sudbury	(Naldrett, 1981a)
2- Intrusions in cratonic areas	-Noril'sk, Siberia, USSR	(Glazkovsky and Gorbunov, 1974)
	-Minnamax, Duluth, Minnesota	(Mainwaring and Naldrett, 1977)
3- Archean komatiites	-Kambalda, Australia	(Ross and Hopkins, 1975
	-Pipe, Manitoba	(Naldrett and Cabri, 1976)
4- Tholeiitic volcanics in Precambrian greenstone belts	-Pechanga, USSR	(Gorbunov, 1968)
	-Montcalm, Ontario	(Naldrett, 1981a)
5- Synorogenic, generally tholeiitic intrusions of Phanerozoic age	-Rona, Norway	(Boyd and Mathieson, 1979)
a- ophiolite related	-Feoy	(present study)
	-Lillefjellklumpen	(Gronlie, 1988)
	-Lyngen, Norway	(Boyd and Nixon, 1985)
	-Ste, Norway	(Boyd and Nixon, 1985)
6- Setting uncertain	-Stillwater, Montana	(Naldrett, 1981a)
	-Bushveld, South Africa	(Naldrett, 1981a)
	-Espedalen, Norway	(Naldrett et al., 1979; Heim, 1981)

et al., 1984; also, see Chapters 4 and 8), there seems little doubt that most of the Ni-sulfide deposits hosted by basic-ultrabasic igneous and volcanic rocks have ultimately formed from cooling of a silicate/sulfide melt(s) (Naldrett, 1981a; Cabri and Naldrett, 1984). Such deposits are characterized by a predominance of pyrrhotite, chalcopyrite and pentlandite in variable amounts, with pyrrhotite being the main sulfide component; PGM's may or may not be present. Direct evidence for a primary magmatic origin of Ni-sulfides can be present in several forms:

1- the presence of immiscible sulfide droplets in volcanic rocks;

2- the presence of an interstitial sulfide phase in igneous or volcanic host rocks, and;

3- the stratigraphic position of the sulfide deposit within plutonic or volcanic rocks.

Paragenetically, the suggested order of crystallization from such a silicate/sulfide melt would be (after Yund and Kullerud, 1966):

silicates - magnetite (possibly Ti-rich) + ilmenite + chromite - Fe-Cu-Ni-rich monosulfide solid solution (mss) - pyrrhotite - chalcopyrite, pentlandite (as exsolution in pyrrhotite, and as free pentlandite grains) - PGM's, telurides, etc.

It should be noted that not all PGE-rich deposits form from a sulfide/silicate melt. There are PGE-rich chromitite deposits (eg., the Unst Ophiolite, Scotland; the Bushveld, South Africa), and other sulfide deposits which may have concentrated PGE's as a result of the activity of chloride-rich aqueous magmatic fluids (Stumpfl, 1987). Still other writers provide evidence for formation of PGE-rich Ni-sulfide deposits from hydrothermal alteration of mafic/ultramafic country rocks (MacMillan et al., 1984).

The Feoy deposit fulfills 2 and 3 of the criteria outlined above (see Chapter 4), in that there is evidence for interstitial Ni-sulfides in host silicate rocks, and in that the deposit is situated within subvolcanic rocks.

The Feoy deposit can be classified as a syn-orogenic Ni-sulfide body (Barnes et al., 1987: also see Table 7.1). It is shown in the present study (see Sections 2.2 and 7.3) to have been magmatically emplaced during the later stages of development of the Karmoy ophiolite in a supra-subduction zone environment. Field and petrographic evidence for the orthomagmatic origin of the Feoy Ni-sulfides, and for its distinction from the Visnes sulfide deposit, was discussed in Chapters 2, 3, 4 and 6, and is again summarized below:

1- mineralogically, the Feoy deposit meets all criteria for typical orthomagmatic massive Ni-sulfides, with a preponderance of massive pyrrhotite, chalcopyrite and pentlandite as the main sulfides (see Section 4.3). Also there is evidence of a zone of disseminated Ni-sulfides interstitial to silicates in the high-Mg dykes (see Chapter 2). These rocks are interpreted as "trapped sulfide liquids in a crystallizing silicate melt" (Naldrett, 1979);

2- primary Ni-sulfides are restricted to the main massive Ni-sulfide deposit along a shear zone, and are found as an interstitial phase to silicate minerals in the high-Mg dykes. There is no evidence of primary Ni-sulfides in any of the other rock types in the area, nor is there any evidence of Ni-sulfide veins or other features which might indicate a hydrothermal origin for these sulfides.

3- nowhere in this deposit is there any evidence for mineralization of the Visnes Fe-Cu-Zn sulfide types. Likewise, there are no Ni or PGE-rich sulfides in the Visnes

deposit.

4- as the high-Mg dykes themselves have been shown to have formed late in the evolution of the Karmoy ophiolite (see Chapters 1 and 2), then so to must have the Ni sulfides.

Sulfur isotopes and PGE patterns from selected Feoy Ni-sulfide samples are discussed in Section 7.4, and also support an orthomagmatic origin for the Feoy sulfides.

7.3: Petrogenetic considerations from other Ni-sulfide deposits

The occurrence of Cu-Ni-sulfides in ophiolitic terranes is not at all well documented, indeed magmatic (as opposed to hydrothermal) ore deposits within such rock types are predominantly of the chromite-ilmenite association. It is evident then, that special conditions must be met before separation of a magmatic sulfide component can occur in such environments.

The Feoy, Lillefjellklumpen and Bruvann deposits of Norway, along with one of the Tilt Cove deposits of Newfoundland, and the gabbro-related deposits of the Troodos area of Cyprus all represent ophiolitic or ophiolite-related deposits of Ni-sulfides and arsenides. Of these 5 deposits, two of them (the Troodos and Tilt Cove deposits) are arsenide-rich deposits structurally controlled along serpentinized fault zones, and neither deposit contains the textural and mineralogical signatures typical of orthomagmatic Ni

deposits (Stanton, 1978). The Troodos occurrence has recently been interpreted in terms of hydrothermal alteration and leaching of mafic-ultramafic plutonic rocks (Panayiotou, 1985), and it is suggested that based on the stratigraphic, structural and lithologic similarities between this and the Tilt Cove deposit, the latter deposit may also have formed from hydrothermal alteration of mafic-ultramafic rocks. These Ni-sulfide and arsenide deposits are not enriched in PGE's, undoubtedly because the ability of a hydrothermal fluid to effectively leach and concentrate PGE's from consolidated rock is relatively minimal in comparison to a sulfide melt scavenging PGE's from a co-magmatic silcate melt.

Unfortunately, not all truly magmatic sulfide deposits in ophiolitic terranes are PGE-rich. While the Feoy and Lillefjellklumpen deposits are PGE-rich, the Bruvann deposit in the Rana mafic intrusion of northern Norway is a large magmatic Ni-sulfide deposit in a similar type of environment which has very low abundances of PGE's (see Table 7.2). The two main questions that arise, therefore, are:

1- what controls magmatic sulfide formation in such environments, and;

2- what controls the PGE tenor of these deposits?

Subsidiary to these questions are other concerns such as the origin of the sulfur (mantle derived, country rock derived, or some combination thereof), the petrogenesis of the co-magmatic host rock, and the physico-chemical changes that may have affected the magma during its ascent. It is shown in the following sections that the PGE ratios, sulfur isotopes and host rock geochemistry of the Feoy deposit can be used to successfully

resolve these questions.

Most of the world's major Ni-sulfide deposits are formed in continental settings, while ophiolitic complexes are dominated by oxide mineralization within the plutonic ultramafic assemblages. Rarer still is the occurrence of such ophiolite related sulfide deposits that are also enriched in PGE's.

One of these, the Lillefjellklumpen Ni-Cu-PGE deposit is situated in gabbros and greenstones of the Seve-Koli Nappe Complex in the Grong area, northeast of Trondheim, Norway (Gronlie, 1988). Eruptive sequences in the area are interpreted as ensimatic island arc, formed to the west of the Fenno-Scandian continent during Lower to Middle Ordovician times (Reinsbakken, 1980). The sulfide deposit probably represents a magmatic sulfide segregation related to an ensimatic gabbro body, later remobilized during a tectonic event and redeposited in its present position (Gronlie, 1988). The analogous nature of this deposit to both the sulfides and co-magmatic host rocks (the high-Mg dykes) of Feoy are self-evident.

There are several possible reasons for the paucity of PGE-rich, magmatic sulfide deposits in ophiolites. Thayer (1976) suggested that in the crystallization of a mafic-ultramafic silicate melt, the Ni and PGE's would partition favourably into the mafic phases, so that in the absence of a co-magmatic oxide or sulfide melt (which would effectively scavenge all PGE's from the silicate portion of the melt) the PGE's would become widely distributed in the silicates. Of course, any chromite, ilmenite and magnetite present with

the crystallizing silicates would be expected to be enriched in PGE's, and indeed it appears that this may well be the case in some ophiolites (eg., Tilt Cove, Newfoundland, and Leka, Norway; Strong and Vokes, respectively, pers. comm.). Since most ophiolitic complexes are barren of significant oxide or sulfide deposits, then the fate of the PGE's in most cases is wide distribution into disseminated oxides and other mafic minerals.

Alternately, if fO2 or fS2 conditions are adequate then an oxide or sulfide melt will form, and such a melt will effectively scavenge or partition most of the PGE's from the silicate melt into the oxide or sulfide melt. However, what of the ophiolite related oxide and sulfide deposits, of orthomagmatic origin, which are not enriched in PGE's (eg., Troodos, Cyprus, and Bruvann, Norway)? Clearly, in such cases the original partial melt must have been depleted in PGE's, or else the PGE's were somehow lost from the system before formation of the oxide or sulfide melt (barring any later leaching of the deposits by hydrothermal fluids).

Naldrett and Barnes (1986) have suggested that the "R factor", or the ratio of silicate to sulfide melt, is also a critical factor in the concentration of PGE's, and that variability in R can account for variations in the concentration of PGE's within deposit types. For example, the PGE-rich Sudbury deposit is associated with a very large mafic intrusive complex (Naldrett, 1981a), and therefore had formed from a magma with a large R factor, while the PGE-poor Bruvann deposit of Norway (Boyd and Mathieson, 1979) would have been produced from a magma with a low R factor. In both cases, however, use of the R factor in determination of the PGE tenor of a deposit assumes that the

concentration of PGE's in the original partial melt was not a limiting factor. Obviously then, if the original melt was depleted in PGE's, then whether or not any later-separating sulfide melt had a large or small R factor would make little difference in terms of the absolute PGE concentrations in the deposit.

Another possible reason for the paucity of ophiolitic magmatic sulfides could be that there was simply not as much sulfur in the Phanerozoic mantle as there was in Archean and Proterozoic mantle material. Nearly all of the major Ni-sulfide occurrences are at least Precambrian in age, and in fact those with purely mantle derived sulfides (such as the Sudbury and komatiitic deposits, with mantle sulfur isotope values of near 0 per mil) are confined to the Archean and early Proterozoic (Naldrett, 1981a). The only major deposit which is of Phanerozoic age, which has sulfur isotope values indicative of large scale assimilation of a foreign, country rock sulfur component (i.e., with variable isotopic values, but usually highly positive), and which is also associated with a continental setting, is the Noril'sk deposit of the Soviet Union. Accordingly then, pre-Phanerozoic deposits such as Sudbury, and the komatiitic deposits of Australia, have mantle isotopic values of -0.2 to +5.9 per mil and 4.4 to 6.2 per mil respectively (Naldrett, 1981a; Naldrett and Barnes, 1986). On the other hand, the much younger Noril'sk deposit (Triassic gabbro hosted) has isotopic values of +7 to +17, indicative of assimilation of large quantities of country rock sulfur (Godlevskii and Grinenko, 1963).

However, a simple Proterozoic or Archean mantle source, or an influx of foreign sulfur,

may not always ensure the formation of a sulfide melt. It can now be shown with some confidence that in many cases, regardless of the origin of the sulfur, special conditions must prevail before the conditions for sulfide segregation are met. Irvine (1975) has shown that in mafic-ultramafic melts contaminated by felsic material there is a dilution factor which favours separation of magmatic sulfides. In continental settings, it is more likely that inclusion and melting of more felsic material is occurring. If there is an intrusion of a refractory mantle diapir into felsic crust, then the diapir might be expected to assimilate large volumes of felsic crustal material upon melting. This could make the melt more felsic, and such a process has been shown to favour sulfide immiscibility and Ni-PGE concentration in several respects (Irvine, 1975):

1- as the melt is being made more felsic, the effective fO2 is lowered, the fS2 is raised, and the segregation of sulfides becomes possible. Polymerization of the silicate melt would result in precipitation of orthopyroxene instead of olivine, thereby decreasing the available lattice sites for Ni and PGE's. Therefore these elements would become more concentrated in the sulfide melt;

2- the possible assimilation of sulfur-rich country rock might increase the sulfur content of the melt, or might induce sulfur saturation in a previously Sulfur-undersaturated melt.

Such processes can be modelled in geochemical and isotopic terms: assimilation of felsic material effectively reduces the maficity of the initial magma, and it has been shown that the Cu/Cu+Ni ratios of sulfide deposits increase with decreasing maficity (Wilson and Anderson, 1959; Naldrett and Cabri, 1976; Naldrett and Duke, 1980); the assimilation

of a foreign sulfur component can be monitored by variation of isotope values from normal mantle values (0 per mil).

Accordingly, continental magmatic sulfide deposits, where large scale assimilation of sulfur-rich crustal material has occurred, have high Cu/Cu+Ni ratios and variable isotopic values. Thus, Noril'sk and Sudbury have quite high Cu/Cu+Ni ratios, while komatiitic deposits (highly MgO rich rocks with little or no evidence of assimilation) have typically low Cu/Cu+Ni ratios (Naldrett, 1981a) (see Table 7.2).

In all deposits, however, the parent magma was of a relatively MgO-rich, mafic-ultramafic nature. Whatever compositional variations occur after crustal assimilation, there is evidence from all major deposits to support this statement (Naldrett, 1981a).

Assimilation accounts well for the Sudbury and Noril'sk deposits, but cannot account for komatiitic or ophiolite-related Ni-sulfide deposits. Komatiitic deposits show no evidence of assimilation of crustal material, although they are without exception pre-Phanerozoic in age, and therefore may have had access to good (i.e., undepleted) mantle sulfur reservoirs. Ophiolitic deposits, on the other hand, are generally Phanerozoic (the vast majority of ophiolites are from late Precambrian to Mesozoic in age), and the deposits discussed here show no isotopic evidence of assimilation of a significant foreign sulfur component (Boyd and Mathieson, 1979; present study). How then does one account for the formation of sulfide deposits in these areas?

In the case of komatiite associated deposits, the answer is relatively straightforward. One is dealing with highly MgO-rich (and therefore probably Ni-rich) melts that are believed to have formed from advanced partial melting of an undepleted and previously unmelted (Barnes et al., 1985), pre-Phanerozoic mantle which was therefore probably rich in mantle sulfur. It has been shown (Naldrett and Duke, 1980; Campbell et al., 1983) that the Pt+Pd/Os+Ir+Ru ratios of Ni-sulfides can be related to the source region of the co-magmatic host rock. When partial melting of an undepleted mantle occurs, Pt and Pd will partition preferentially into the melt over Os, Ir and Ru, while the latter elements prefer to remain in the mantle residuum (Hamlyn and Keays, 1985). The amount of PGE's and mantle sulfide which are taken into this "first stage" melt will obviously depend on the degree of partial melting of the mantle, so that the lower the degree of partial melting, the higher will be the Pt+Pd/Os+Ir+Ru ratio in the melt. In the case of komatiites, partial melting is quite extensive, so that most of the mantle sulfide component, and most of the mantle PGE's, will be extracted. The result will be formation of a MgO-rich, ultramafic melt with a PGE-rich Ni-sulfide component of pure mantle origin.

Since most or all of the mantle PGE's were extracted in komatiite Ni-sulfide generation, the Pt+Pd/Os+Ir+Ru ratios for such deposits would not be as high as for those deposits which formed from lesser degrees of first stage partial melting, such as the Bruvann deposit (Boyd and Nixon, 1985), since in the latter case much of the mantle Os, Ir and Ru would have remained in the mantle residuum (see Figure 7.3 for the PGE patterns for Bruvann). Also, the fact that little or no assimilation has occurred in komatiitic

deposits (which would have facilitated earlier separation of the sulfide melt), coupled with the fact that komatiitic melts are generally believed to have formed from rapid ascent from their mantle source region (Hudson, 1986; Cowden et al., 1986; Keays et al., 1982), may have ensured that the exsolution of a significant sulfide melt from a silicate melt was delayed until quite late in the evolution of the magma, giving rise to the association of Ni-sulfide deposits with volcanic to sub-volcanic komatiites.

But what of the late Precambrian and Phanerozoic ophiolite and ophiolite-related deposits (Bruvann and Lillefjellklumpen)? Firstly, it is necessary to qualify the source of sulfur in these deposits. Boyd and Mathieson (1979) have shown that the Bruvann Ni-sulfides formed from a mantle derived sulfur source, with isotopic values at 0.7 to 2 per mil. There may have been a minor country rock sulfur component, and if so, this had little effect. Unfortunately, no isotopic data is available for the Lillefjellklumpen deposit. Both of these deposits are relatively young compared to other deposits of Archean and Proterozoic ages (Lillefjellklumpen is Lower to Middle Ordovician, while Bruvann is dated at 400Ma by Roddick, 1977), and therefore any possible mantle derived sulfur source would not be as enriched in sulfur as the mantle sources for the older deposits which had not undergone previous melting episodes.

Secondly, one must identify the source region for the co-magmatic silicates. In the case of Bruvann, the low Cu/Cu+Ni ratio of the sulfides indicates a high-MgO parent silicate melt for the sulfides, while the fairly high Pt+Pd/Os+Ir+Ru ratio (which is indicated by the steep slope for Bruvann in Figure 7.3) indicates only moderate to low degrees of

partial melting of a first stage or previously unmelted source. Barnes et al. (1987) have shown that the initial liquid at Rana (Bruvann) was not depleted in highly incompatible elements such as Cs, Rb and the LREE's, and therefore was likely derived from a fertile, non-depleted mantle. This is in agreement with the interpretation of the PGE patterns for this deposit, and contrasts with the interpretation of high degrees of first-stage partial melting for komatiitic deposits, the latter which have lower Pt+Pd/Os+Ir+Ru ratios, and shallower slopes in Figure 7.3.

Hamlyn et al. (1985), Naldrett and Barnes (1986) and Hamlyn and Keays (1986) have all examined the possibilities for sulfur saturation in first stage and second stage (already depleted) melts. It is concluded in these studies that average first stage melts are sulfur saturated at the point of their extraction from the mantle. Such melts are depleted in PGE's for two main reasons: (1) Low to moderate degrees of first stage partial melting of fertile mantle would only partially extract the mantle sulfur component, leaving behind a significant sulfide fraction in the mantle residuum. This mantle sulfide residue would be enriched in PGE's; (2) These first stage partial melts would become quickly depleted in PGE's in the early stages of fractional crystallization during ascent, because sulfur saturation would ensure co-precipitation of the magmatic sulfides (Hamyln and Keays, 1986). Consequently, later separation of any subsequent sulfide fractions during ascent of this partial melt would be expectedly low in PGE's.

Because of initial sulfur saturation however, such first stage melts would have the capacity to form relatively large magmatic sulfide deposits. Therefore,the largest and

most PGE-enriched Ni-sulfide deposits in ophiolitic terranes would be found in rocks where high degrees of first stage partial melting (thus ensuring extraction of most PGE's and mantle sulfides from a fertile mantle) had occurred.

Any subsequent (second stage) partial melt produced from an already depleted mantle would have access to the residual mantle sulfides, and these sulfides would be highly enriched in all PGE's. Therefore, a second stage melt would be PGE-rich. Also, second stage melts have been shown to be undersaturated in sulfur (Hamyln and Keays, 1986; Hamyln et al., 1985), and therefore are less likely to lose their PGE's during ascent of the partial melt by early precipitation of sulfide fractions. If sulfur saturation was attained in such melts, however (perhaps because of country rock assimilation or fractional crystallization), the resultant deposits would undoubtedly be small but PGE-rich. Also, the sulfides would have a PGE distribution which reflected a depleted mantle source (that is, low Pt+Pd/Os+Ir+Ru ratios, and a relatively shallow slope in Figure 7.3), and would have a co-magmatic host rock geochemistry which supported this mechanism of formation. The Lillefjellklumpen deposit has Pt+Pd/Os+Ir+Ru ratios indicative of such a mechanism of formation (see Figure 7.3); the co-magmatic host rocks have been suggested to have affinity to ensimatic island arc, and indeed the deposit is also quite small and PGE-rich (Gronlie, 1988).

Thus it is clear that special conditions must be met in order to form PGE-rich magmatic sulfide deposits in ophiolitic terranes. That such deposits are extremely rare suggests that these physico-chemical (adequate fS2 conditions) and compositional (adequate

concentrations of PGE's in the initial partial melt) conditions are in fact rarely achieved in magma chambers within ophiolite complexes. The Feoy sulfide deposit and its co-magmatic host rocks therefore represent an exception, and so the following sections will attempt to delineate the special conditions that must have existed for its formation.

7.4: The geochemistry, PGE and sulfur-isotopic signature of the Feoy Ni-sulfides and their host rocks

7.4.1: Sulfur isotopes

Figure 7.1 is a histogram of average sulfur isotope values for several major Ni-sulfide deposits (after Naldrett, 1981a). These are compared with data from the Feoy Ni-sulfides obtained during this study (the absolute values for sulfur isotope ratios are also given in Figure 7.1). It is evident that most values, including those from Feoy, plot very close to 0 per mil, which is to be expected for sulfides from truly magmatic sources. Samples from the Feoy deposit are fresh, massive, metamorphosed pyrrhotite-chalcopyrite assemblages, and indicate the following:

1- there is a total delta 34S range of only 0.9 per mil, from 3.0 to 3.9 per mil;

2- the range for pyrrhotite is 0.9, while that for chalcopyrite is 0.4 per mil;

3- the delta 34S (pyrrhotite-chalcopyrite) is very small, with a minimum of 0.2 and a maximum of 0.3 per mil.

While there are only a limited amount of data presented here, the following conclusions

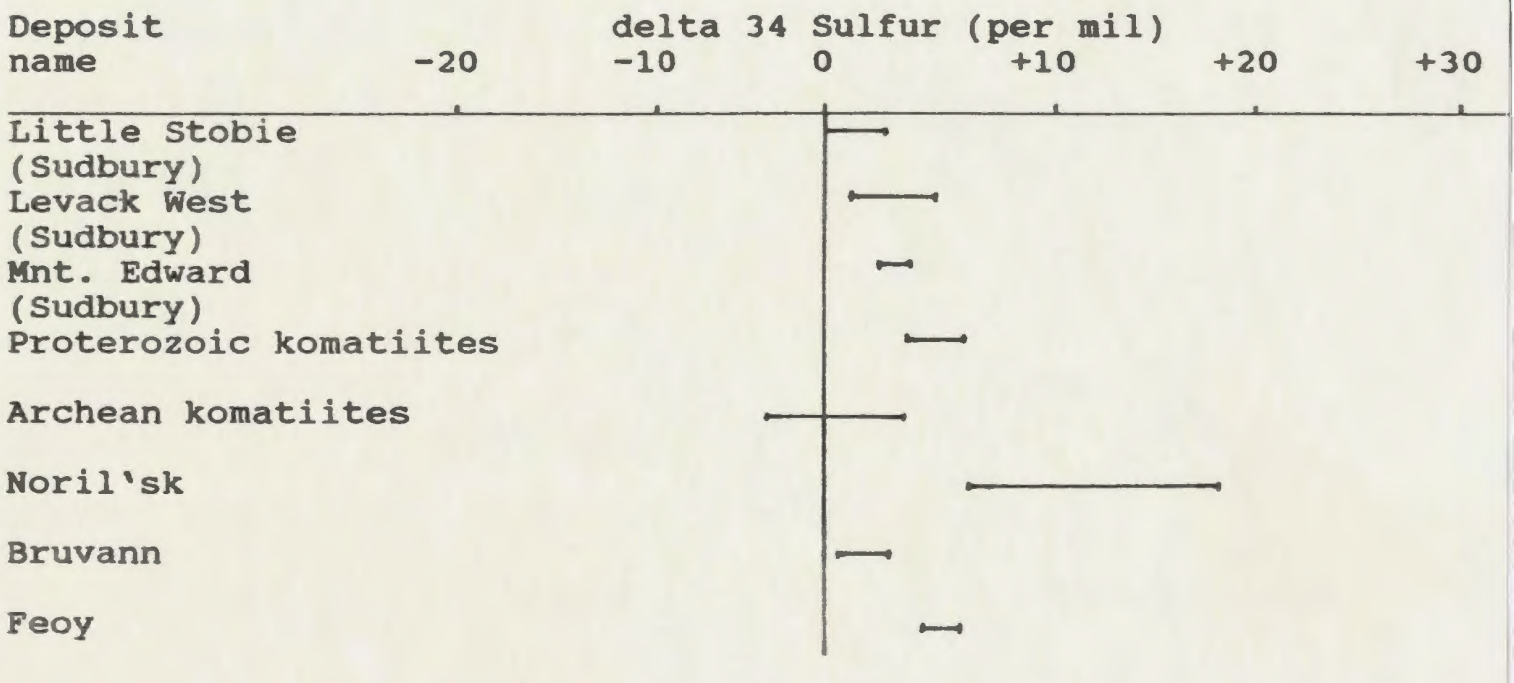

Figure 7.1: Histogram of average sulfur isotope values from selected orthomagmatic Ni-sulfide deposits (after Naldrett, 1981a; data for Bruvann is from Boyd and Mathieson, 1979; data for Feoy is from present study). The absolute values for sulfur isotope ratios of the Feoy samples are given below:

Sample	Sulfur isotope values
F33-cpy	3.3 per mil
F11-cpy	3.7
F35-cpy	3.7
F35-po	3.9
F33-po	3.0
F24A-po	3.7
F24A-cpy	3.5

can be made from existing isotope data:

1- all samples plot very close to mantle sulfur values (0 per mil). The consistently low nature of their isotope values suggests that the Feoy Ni-sulfides formed from a magmatic, mantle-derived sulfur source. Deviation of sulfur isotope ratios from 0 per mil in magmatic sulfide deposits might be explained in terms of metamorphism or hydrothermal alteration, assimilation of a foreign sulfur component into the melt, or mantle isotopic heterogeneity;

2- there is negligible isotopic fractionation between sulfide species, which may indicate an isotopically homogeneous source of sulfur, although isotopic fractionation may be temperature/redox controlled ultimately. This also supports an orthomagmatic origin for the sulfides;

3- the Feoy Ni-sulfides were extensively recrystallized and variably altered during later metamorphism and deformation. However, since all samples still retain sulfur isotope signatures consistent with an orthomagmatic sulfide origin, then it is suggested that neither recrystallization nor alteration has significantly affected the original sulfur isotope composition of the Feoy sulfides. The possibility remains, however, that the narrow range of sulfur isotopes observed in these samples may have been partially a result of later metamorphism.

Assimilation of a foreign sulfur component was suggested for the Noril'sk deposit to acount for variation of the isotopic signature from 0 per mil, and also to account for the large size of the deposit. This may have occurred to a small extent in the Feoy sulfides, since the country rock in the area does indeed contain significant amounts of

disseminated sulfides from the earlier-formed Visnes sulfide deposit.

However, another possible source of sulfur for the Feoy Ni-sulfide deposit could have been from reduced seawater sulfate (Malpas, pers. comm.). Above a subduction zone, any sulfate in seawater would be reduced to sulfur, and this might enrich a partial melt in sulfur. If this was the only source of sulfur for the Feoy deposit, then these sulfides might be expected to have a seawater sulfur-isotopic signature. On the other hand, if there was addition of only small amounts of reduced seawater sulfate to a melt which already contained a small mantle sulfide component, then the resultant sulfide deposit might have sulfur isotope values intermediate between seawater (generally highly positive) and mantle (0 per mil). Such a mechanism might equally well explain the small deviation (3 per mil) of the Feoy sulfur isotope values from mantle sulfur values of 0 per mil. The data presently available cannot be used to distinguish between these sources.

7.4.2: Ore geochemistry

Table 7.2 is a compilation of geochemical data for the Feoy deposit, along with selected Ni-sulfide deposits from Norway and other areas. Data from Feoy and other Norwegian deposits have been collected in this study, and also from Boyd and Nixon (1987). Data for other deposits are from Naldrett and Duke (1980). Also included are PGE abundances for the co-magmatic silicate host rock (the high-Mg dykes) of the Feoy sulfides. Unless otherwise indicated, data were collected during this study.

Table 7.2: The geochemistry of massive Ni-sulfide samples from Feoy, along with data from several other Ni-sulfide deposits (data sources are the same as in Figure 7.1).

Sample	Os (ppb)	Ir (ppb)	Ru (ppb)	Rh (ppb)	Pt (ppb)	Pd (ppb)	Au (ppb)
FEOY							
F-41	155.2	279.5	282.5	353.3	1044.9	2530.1	23.4
F-41b	152.4	275.4	285.3	358.5	1038.8	2587.6	24.2
F	150.7	208.1	330	422.2	1943.3	2140.4	158.8
F-b	110.8	201.9	347	415.6	1874.4	2077.8	94.9
JS-b	241.1	272.8	395.2	400.6	587.1	4116.3	13.1
F-36	239.2	325.6	399.9	445.4	821.2	3623.1	18.1
F-36b	265.5	376.3	481	519.8	957.5	4201.8	16.5
F-11	71.48	120.58	208.37	143.2	857.27	4117.04	10.62
F-35	250.19	339.01	507.61	362.26	443.94	3971.4	245.15
F-35b	337.5	346.4	582.1	428.9	432.5	4458.1	274.6
F-10	0.6	0.9	1.7	5.1	3561.4	6388.8	224.1
F-10b	1.2	0.8	1.4	3.9	3413.8	6465.7	368.6
F-31	93.8	188	213.7	267.6	323.3	2004.3	42.6
F-31b	156	225.6	285.3	357.5	386.6	2680.6	66.2
F-7	1.8	2.1	3.1	2.9	4.1	25	1.4
F-19	254.2	268.7	415	421.2	567.9	4405	6
15-Visnes	0.01	0.01	0.1	0.01	0.01	0.6	1.7
43-highMg	0.01	0.01	0.6	0.4	5.3	6.7	8.2
Bruvann		6	6.9	2	52	70	1010
Lillefjel	139	170	189	214	1799	3068	219
Komatiite	402	219	803		<730	1314	402
Komatiite	380	320	1980	800	4130	15530	460
Sudbury 1	29	62	120	120	1930	2120	862
Sudbury 2	46	110	250	300	2130	3170	860
Noril'sk	950	1500	1500	2240	13700	36000	1600
C1-Chond	514	540	690	200	1020	545	152

Table 7.2 (continued) Values Normalized to C1-Chondrite

sample#	Os	Ir	Ru	Rh	Pt	Pd	Au
FEOY							
F-41	0.302	0.516	0.41	1.767	1.02	4.64	0.154
F	0.293	0.385	0.478	2.11	1.91	3.93	1.04
F-b	0.216	0.374	0.503	2.08	1.84	3.81	0.62
F-31	0.183	0.35	0.31	1.34	0.317	3.68	0.28
15-Visnes	0.01	0.01	0.02	0.01	0.01	1	1.1
43-highMg	0.01	0.01	0.1	0.2	0.52	12.3	5.4
Bruvann		0.01	0.01	0.01	0.051	0.128	6.645
Lillefjel	0.27	0.315	0.274	1.07	1.764	5.63	1.44
Komatiite	0.78	0.406	1.164		0.716	2.41	2.645
Komatiite	0.74	0.593	2.87	4	4.05	28.5	3.03
Sudbury-1	0.056	0.115	0.174	0.6	1.89	3.89	5.67
Sudbury-2	0.09	0.204	0.36	1.5	2.09	5.82	5.66
Noril'sk	1.85	2.78	2.174	11.2	13.43	66.06	10.53

Sample	Pt+Pd/ Os+Ir+Ru	Ni (ppm)	Cu (ppm)	Cu/Cu+Ni
FEOY				
F-41	4.98	21584	11055	0.34
F-41b	5.09			
F	5.93	24229	14880	0.38
F-b	5.99			
JS-b	5.17			
F-36	4.61	22650	41218	0.65
F-36b	4.61			
F-11	12.42	3994	190119	0.98
F-35	4.03	21906	44563	0.67
F-35b	3.86			
F-10	3109.44	18585	41825	0.69
F-10b	2905.74			
F-31	4.72	23219	30625	0.57
F-31b	4.61			
F-7	4.16			
F-19	5.31	22805	15221	0.4
15-Visnes	6.01			
43-highMg	20.01			
Bruvann		9%	2.1%	0.19
Lillefjel	9.8	4%	1.2%	0.33
Komatiite		12.1%	0.84%	0.07
Komatiite	7.3	15.5%	3.71%	0.19
Sudbury 1	19	3.83%	4.41%	0.54
Sudbury 2	13	4%	3.6%	0.47
Noril'sk	13	7.6%	10.9%	0.59

Data from the ore samples are based on the assumption that rock samples are composed of 100% Ni and Cu-sulfides. The method of stating Ni and Cu in 100% sulfides is discussed by Naldrett (1981a), and is designed to eliminate discrepancies in PGE abundances caused by variations in the amount of sulfide in a given sample. It assumes an average of 38% sulfur in the sulfide, with the remaining % being taken up by Ni and Cu as pure pentlandite, (Fe,Ni)9S8, and chalcopyrite, CuFeS2, with Ni in the pentlandite at 36%. For the PGE diagrams, the PGE values given in Table 7.2 are considered to represent their concentrations in 100% sulfides, as selected samples were >98% sulfides. These samples are normalized against equivalent elemental concentrations in C1-chondrite, after Naldrett and Duke (1980).

Cu, Ni, Pt and Pd relations

Figures 7.2a and 7.2b show the relationships between Cu, Ni and Pt/Pt+Pd for rocks of the Feoy deposit along with data from other Ni-sulfide deposits. Sources of this data are from the present study, from Panayiotou (1985), and from Naldrett (1981a).

Figure 7.2a is a histogram of Cu/Cu+Ni ratios for the Feoy sulfides and other deposits. From Table 7.2, it is clear that the Feoy sulfides have highly variable Cu/Cu+Ni ratios, from 0.34 to 0.98. All of the Feoy sulfide samples have been completely recrystallized and deformed during later metamorphism and deformation, and have also been variably altered by hydrothermal and meteoric fluids (see Chapter 4). Therefore, an attempt is made to determine whether this variability in the Cu/Cu+Ni

Figures 7.2.a and 7.2.b: Cu, Ni, Pt and Pd relations for sulfides of the Feoy deposit, compared with data for Ni-sulfides from various other environments (data for all deposits except Visnes is from Naldrett, 1981a). Fields for Fig. 7.2b are from Panayioutou (1985).

Figure 7.2.a

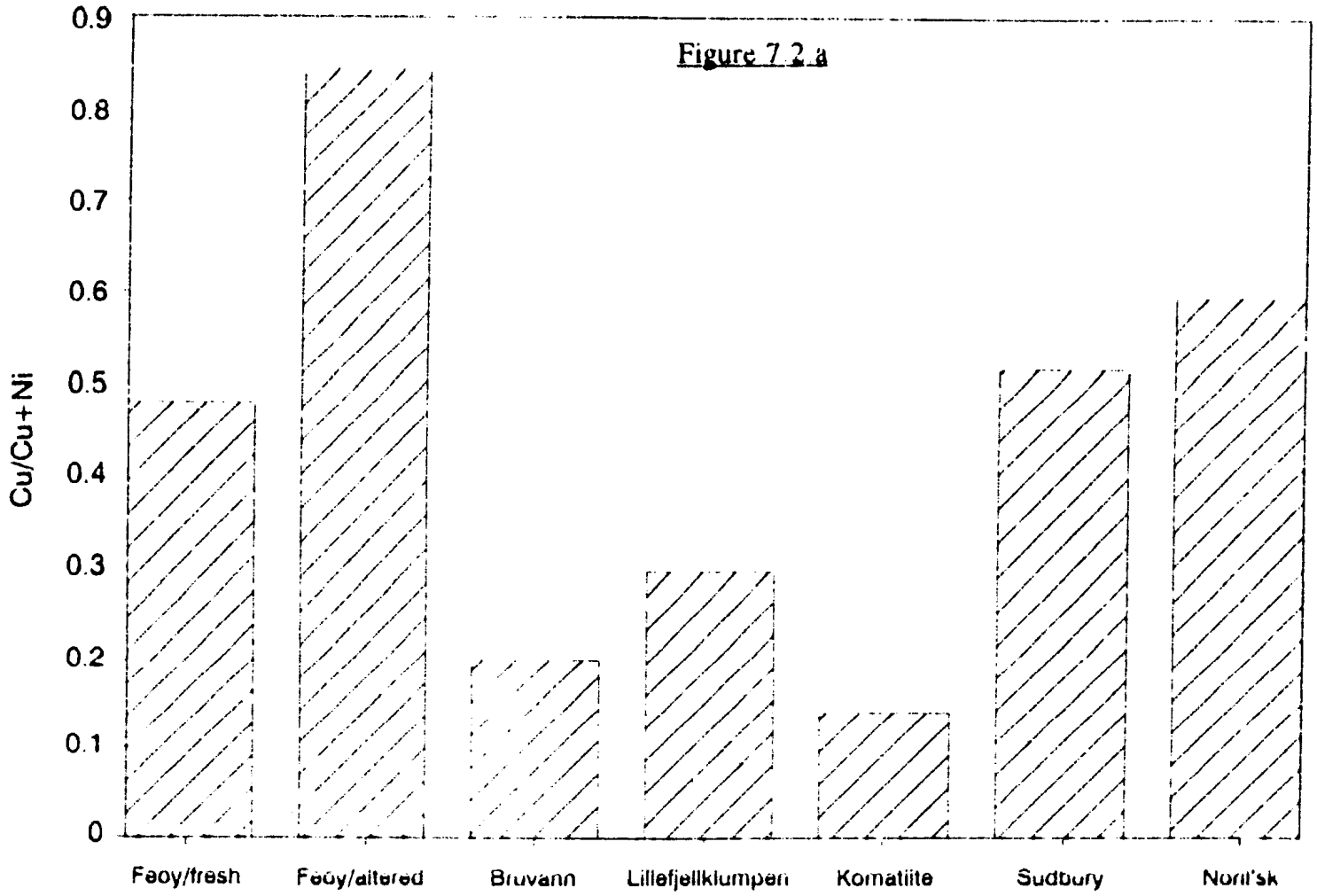
0.9
0.8
0.7
0.6
0.5
0.4
0.3
0.2
0.1
0
Cu/Cu+Ni
Føoy/fresh
Føoy/altered
Bruvann
Lillefjellklumpen
Komatiite
Sudbury
Noril'sk

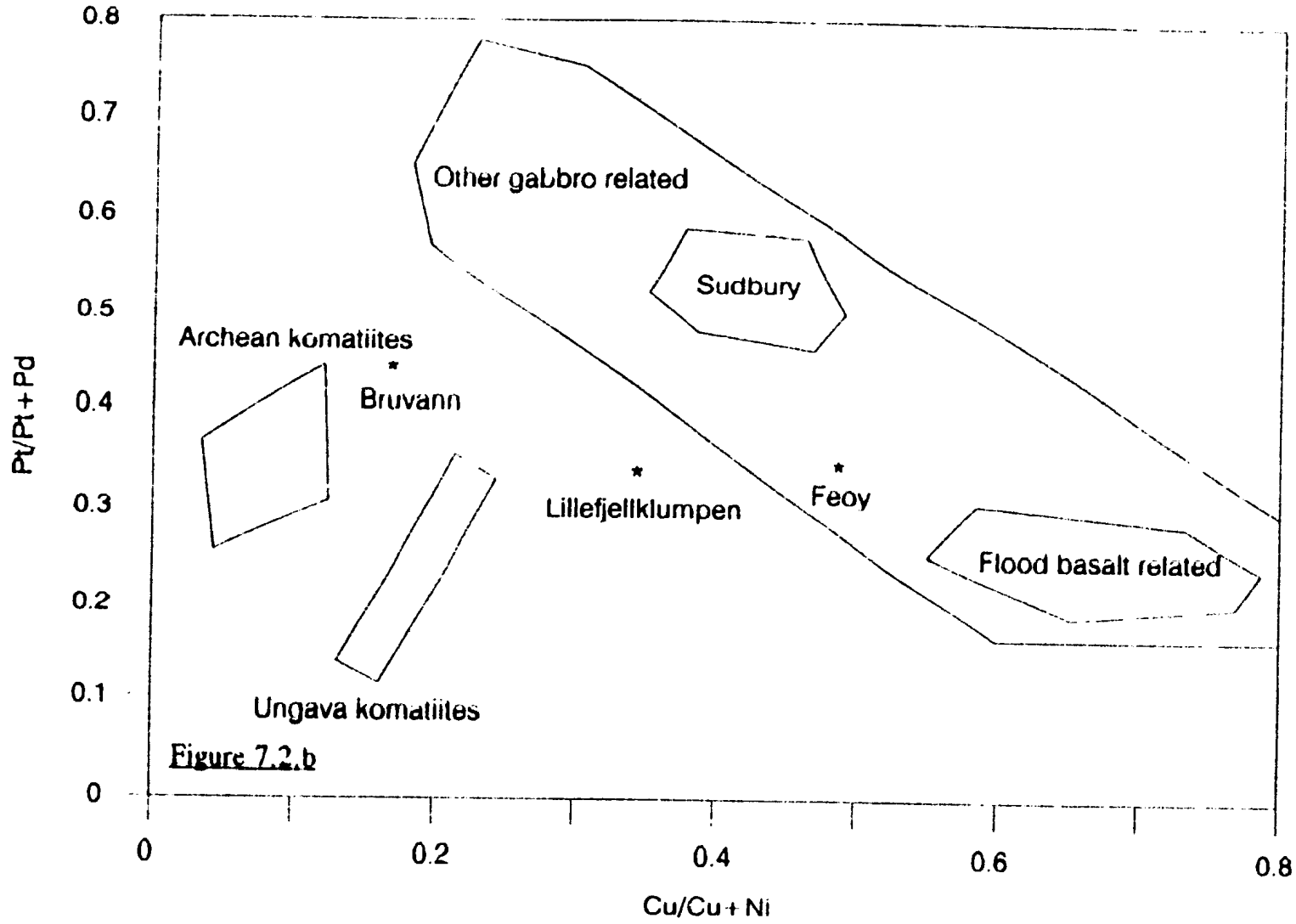
0.8
0.7
0.6
0.5
0.4
0.3
0.2
0.1
0
Pt/Pt+Pd
Other gabbro related
Sudbury
Archean komatiites
Bruvann
Lillefjellklumpen
Feoy
Flood basalt related
Ungava komatiites
0
0.2
0.4
0.6
0.8
Cu/Cu+Ni

Figure 7.2.b

ratios corresponds to variations in the intensity of hydrothermal alteration in the samples. Accordingly, the relatively fresh samples (samples F41, F, Fb, F31) are grouped separately from those that are extensively altered (samples F10 and F11).

Cu/Cu+Ni ratios for the unaltered samples vary from 0.34 to 0.57, with an average of 0.43; Cu/Cu+Ni ratios for the heavily altered samples vary from 0.69 to 0.98, with an average of 0.84. Clearly, the hydrothermally altered samples have considerably higher Cu/Cu+Ni ratios than relatively unaltered samples. This is in agreement with data from Paktunc (1987), which examines variations in Cu/Cu+Ni ratios from Ni-sulfides of the St. Stephen intrusion in New Brunswick in terms of metamorphism and remobilization of the sulfides.

Lillefjellklumpen is similar to Feoy in terms of its inferred tectonic environment of formation in an arc environment (Gronlie, 1988), and the sulfides are remarkably similar in terms of their position within an ophiolite and their PGE enrichment (see Table 7.2). Accordingly, its Cu/Cu+Ni ratio is quite close to that of the fresh Feoy samples at 0.33. The Cu/Cu+Ni ratios for both Feoy and Lillefjellklumpen are consistant with the expected Cu/Cu+Ni ratio for the relatively MgO-rich co-magmatic host rocks that are present in these areas. This is based on suggestions of Wilson and Anderson (1959) that the Cu/Cu+Ni ratio will increase with decreasing maficity of the initial partial melt. The Cu/Cu+Ni ratio for Bruvann is somewhat low for the peridotitic co-magmatic host rocks that are present in this deposit (Boyd and Mathieson, 1979).

In Figure 7.2b, the fresh Feoy sulfide samples plot in the field for gabbro related deposits, and very close to the Lillefjellklumpen deposit. The Bruvann deposit, although not PGE-rich, has a Pt/Pt+Pd ratio higher than that for both Feoy and Lillefjellklumpen.

PGE abundances

Figures 7.3a and b illustrate chondrite-normalized PGE abundances for the Feoy, Lillefjellklumpen and Bruvann deposits of Norway, along with average abundances for komatiite-hosted, Noril'sk and Sudbury deposits. Only those samples from Feoy that appeared relatively fresh and unaltered in thin section were used in Figure 7.3 (samples F41, F, F-b, F31). Also, only the highest (sample F41) and the lowest (sample F31) abundances of PGE's in these samples are plotted in order to show the total range of patterns for the Feoy sulfides. Data sources for Lillefjellklumpen and Bruvann are from Barnes et al., (1987); data for Feoy were obtained during the present study; data sources for other deposits are from Naldrett (1981a). Several features are noteworthy. Firstly, for the Feoy deposit, PGE abundances are less than chondritic values for Os, Ir and Ru in all cases; about 2 times chondrite for Rh; between 0.3 and 2 times chondrite for Pt; between 4 and 6 times chondrite for Pd, and from 0.15 to 1 times chondrite for Au. The average Pt+Pd/Os+Ir+Ru ratio for the Feoy sulfides is 5.41.

Secondly, relative to other deposits the Feoy deposit is most similar to the Lillefjellklumpen deposit and the field for komatiites, both in absolute and relative abundances. The intermediate to low Pt+Pd/Os+Ir+Ru ratios for the Feoy and

Figures 7.3.a and 7.3.b: C1-chondrite normalized PGE patterns for the Feoy sulfides, along with patterns for other Norwegian Ni-sulfide deposits, and patterns for Ni-sulfides from various other tectonic environments (data for Norwegian deposits other than Feoy is from Barnes et al., 1987; data for Feoy is from the present study; data for all other deposits is from Naldrett and Duke, 1980).

Figure 7.3.a

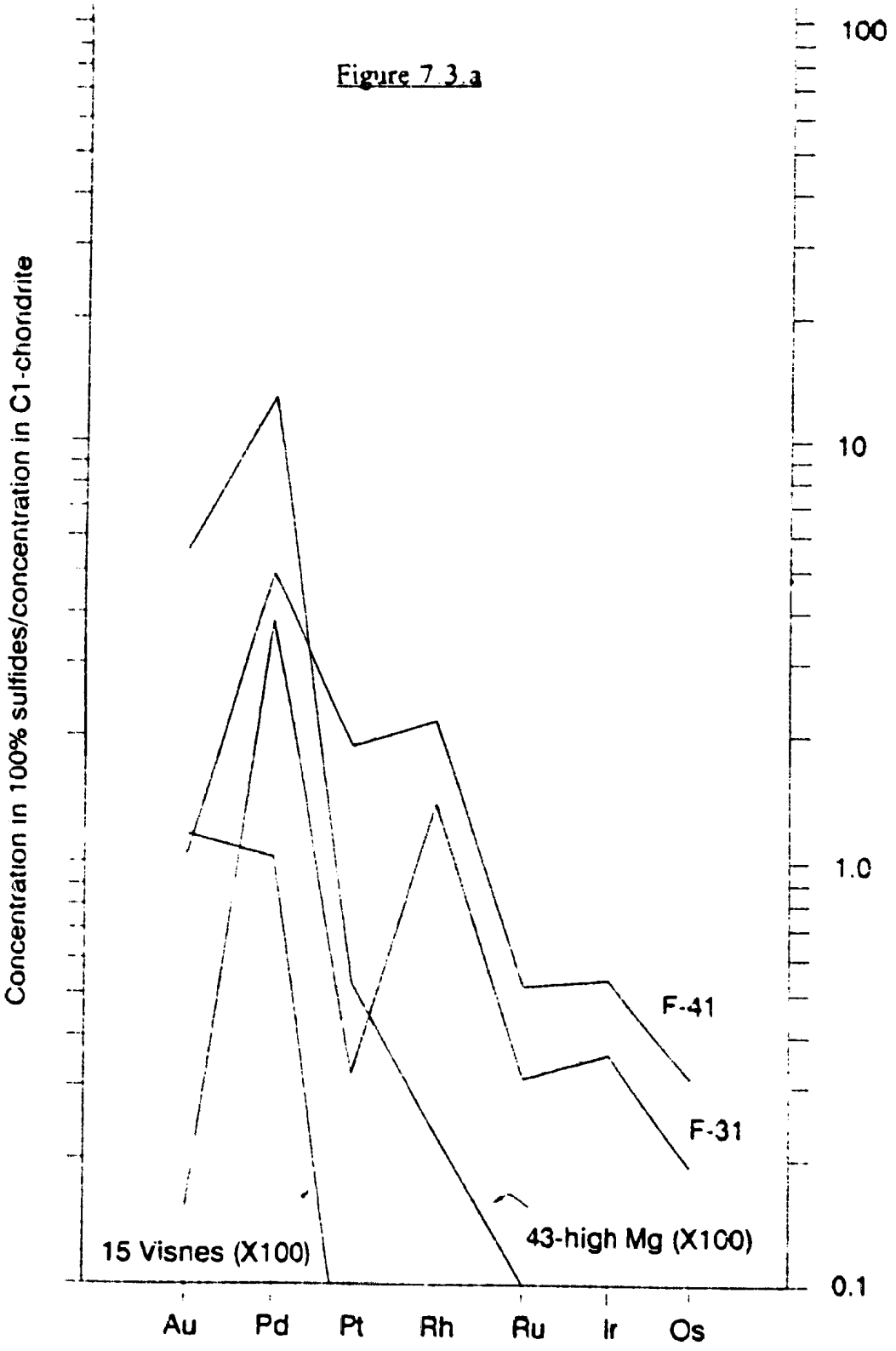
Concentration in 100% sulfides/concentration in C1-chondrite
100
10
1.0
0.1
F-41
F-31
15 Visnes (X100)
43-high Mg (X100)
Au
Pd
Pt
Rh
Ru
Ir
Os

Figure 7.3.b

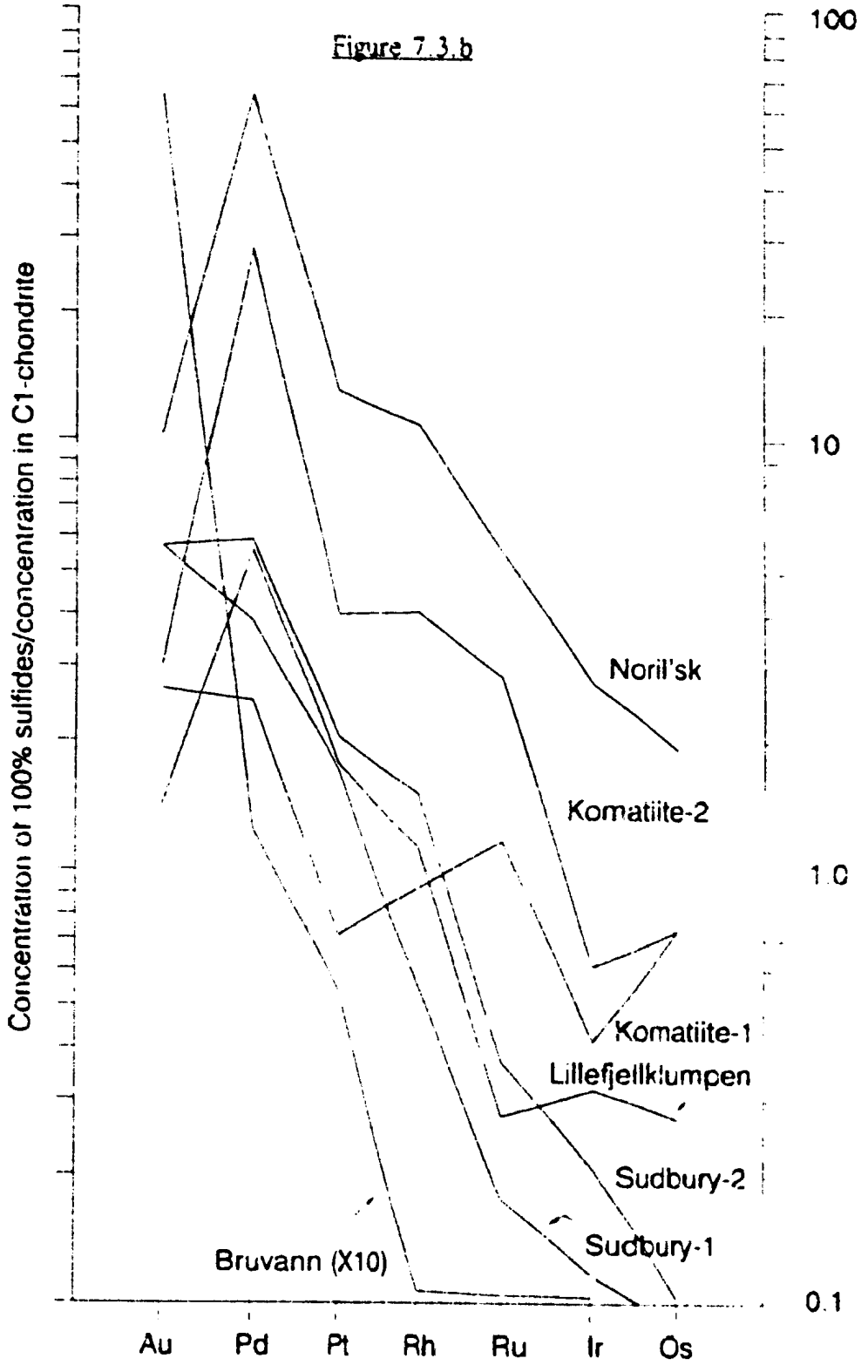
Concentration of 100% sulfides/concentration in C1-chondrite
100
10
1.0
0.1
Noril'sk
Komatiite-2
Komatiite-1
Lillefjellklumpen
Sudbury-2
Sudbury-1
Bruvann (X10)
Au
Pd
Pt
Rh
Ru
Ir
Os

Lillefjellklumpen deposits are indicative of their origins from second stage partial melting, or partial melting of a depleted mantle. This is in agreement with REE and other geochemical data from the high-Mg dykes of Feoy, and from volcanic rocks of the Nord-Trondelag region (the host rocks for the Lillefjellklumpen deposit; Reinsbakken, 1980) which suggest that the co-magmatic host rocks formed from partial melting above a subducting oceanic plate (Pedersen, 1987; Reinsbakken, 1980)).

The field for the Sudbury deposits has a steeper slope with higher (>10) Pt+Pd/Os+Ir+Ru ratios than Feoy or Lillefjellklumpen. The Bruvann deposit has the steepest slope, and the lowest absolute abundances of PGE's.

7.4.3: Co-magmatic host rock geochemistry

The geochemistry of magmatic Cu-Ni-sulfides is directly related to the geochemistry of the co-magmatic silicate host rocks, and therefore a brief analysis of the nature of the host rocks in the Feoy area is warranted.

Figure 7.4 illustrates the Pd-Ir tenor of a high Mg-dyke sample from the vicinity of the Feoy sulfide deposit (sample 43-high Mg), as well as a sample from the Visnes dykes of the sheeted complex (sample 15-Visnes) for comparison. This diagram illustrates the dependence of the PGE content on the environment of formation of the partial melt (fields for MORB and low-Ti lavas from Hamyln et al., 1985). MORB lavas, which form

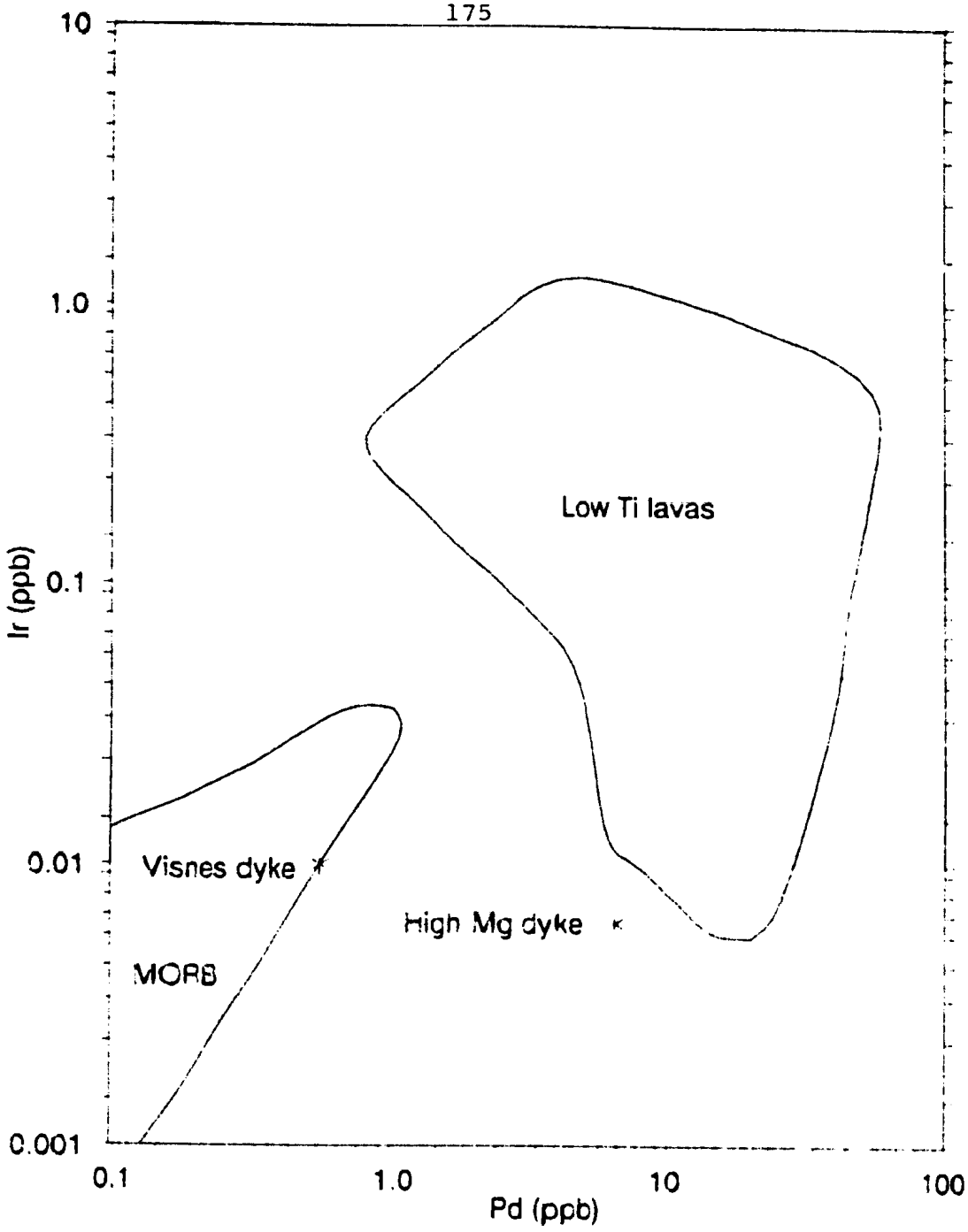

Figure 7.4: Pd-Ir relations for high-Mg and Visnes dyke samples from the study area, along with fields for typical MORB and low-Ti Lavas (data for MORB and low-Ti Lavas fields from Hamyln et al., 1985).

from relatively undepleted mantle, have on average much lower Pd-Ir abundances than do the low-Ti (boninitic) melts, the latter which form from a previously melted, and therefore depleted, but PGE-rich residuum. The high-Mg dykes of Feoy plot well within the field for low-Ti lavas, consistent with their chemistry (see Table 5.1). The Visnes dykes, alternately, are an order of magnitude more depleted in Pd, as would be expected from dykes of a lower-Mg, non-boninitic nature (see Appendix 3).

Figure 7.3a plots these same two dyke samples on PGE diagrams, along with the fields for the Feoy Ni-sulfide samples. In order to facilitate comparison of PGE patterns, the abundances for the basalt dyke samples have been multiplied by a factor of 100. It can be seen that although the high-Mg dyke sample contains about 3 orders of magnitude less PGE's (which corresponds to a partition coefficient, Dsul/Dsil, for the PGE's between the co-magmatic silicate melt and the sulfide melt of approximately 1000), the relative patterns for both the Feoy sulfides and the high-Mg dyke sample are somewhat similar, with a fairly steep positive slope from Os to Pt, an even steeper slope from Pt to Pd, and a sharp drop from Pd to Au. Such patterns are not observed in the Visnes dyke sample. This lends support to earlier suggestions (see Chapter 2) that the high-Mg dykes are the co-magmatic host rocks for the Feoy sulfides.

The Feoy sulfide Pt+Pd/Os+Ir+Ru ratio is 5.41, but the same ratio for the high-Mg dyke sample is 19.4. This difference exists because the partitioning of Os, Ir and Ru into any crystallizing silicate is somewhat greater than for Pd and Pt (which are more "incompatible", with a lower Dsul/Dsil). Therefore, any fractionation occurring during

ascent, cooling and eventual sulfide formation from the magma would invariably have the effect of depleting the silicate melt in Os, Ir and Ru, thereby increasing its Pt+Pd/Os+Ir+Ru ratio.

7.5: Summary and discussion

Geochemical and isotopic data presented in this chapter are consistent with field and petrologic data from Chapter 4 in that they all support an orthomagmatic origin for the Feoy Ni-sulfides and PGM's. The host silicate rocks for the Feoy deposit appear to be highly magnesian basaltic rocks of an arc-basin affinity (the geochemistry of these basaltic rocks is discussed in detail by Pedersen, 1987). In these respects the Feoy deposit, while spatially quite close to the Visnes orebody, records an entirely different genetic and geotectonic history.

The Feoy deposit has been geochemically modelled by comparison of selected PGE abundances with data from other orthomagmatic Ni-sulfide deposits throughout the world. It has been shown that the PGE signature of the sulfide deposits under consideration is a direct function of the nature of the source region for the host rocks. In all cases where second stage partial melting (Feoy and Lillefjellklumpen) or advanced first stage partial melting (the komatiitic deposits) had occurred, and sulfur saturation had been achieved, the melt has produced a PGE-rich sulfide deposit, since all or most of the mantle sulfide and PGE's had been extracted. In the case of moderate to low degrees of first stage

partial melting, however, resultant sulfide deposits are PGE-poor (eg., Bruvann).

The very small size of the Feoy and Lillefjellklumpen deposits suggests a large R factor, so that the small amount of sulfide melt would have had a relatively large volume of silicate melt from which to extract PGE's. However, it is suggested here that in this case the R factor is of secondary importance after the primary geochemical nature of the co-magmatic host rock. In fact, the silicate/sulfide ratio may actually result from the nature of the source region of the co-magmatic host rock just as does the PGE tenor of the associated deposit. For example, it is logical to assume that if there were a larger amount of magmatic sulfide (or a lesser volume of silicate magma) present, and therefore a smaller R factor, then the PGE concentration of the Feoy deposit would be effectively decreased, since there would be more sulfide and less silicate from which to scavenge PGE's. However, because of the very nature of the parent magma, itself a second stage melt, then it was only capable of forming a very small volume of magmatic sulfide at best. Also, such a small concentration of magmatic sulfide in a magma already enriched in PGE's would necessarily result in the formation of a small, but PGE-rich deposit. In other words, the R factor does not control, but is an associated feature of the deposit, since the only deposit that could possibly form from such a melt (barring assimilation) would be one with a very large R factor.

Accordingly, it might be expected that wherever there is evidence of magmatic sulfides in co-magmatic host rocks of a second stage (depleted) nature, such as the high-Mg dykes of Feoy, then such sulfides would very likely be rich in PGE's. This might prove

attractive as an exploration tool, were it not for the very low volume of sulfide to be expected from such environments. Of course the ideal situation in exploration would be when some kind of enrichment process had occurred during intrusion of second stage melts.

While the only such deposits known to this author appear to be the Feoy and Lillefjellklumpen deposits, confirmation of this theory must await data from similar environments. However, it is intriguing that of all the Ni-sulfide deposits of an ophiolite-related nature in the Norwegian Caledonides, Cyprus and Newfoundland, only those of a truly magmatic nature (i.e. this excludes Tilt Cove and Troodos), and which are clearly associated with second stage mantle melts, are enriched in PGE's (Feoy and Lillefjellklumpen).

Chapter 8: Major oxide and oxygen isotope chemistry and the origin of tourmaline and breccia occurrences in the Feoy area

8.1: Introduction: the origin of tourmaline

Tourmaline occurs in several geologically distinct environments, the most common of which are:

1- granites;

2- placer deposits;

3- evaporites;

4- seafloor chemical precipitates.

Since tourmaline occurrences in the study area are either 100% "tourmalinite" fragments, tourmaline replacement of amphibole, or coarse crystalline vein tourmaline, with no evidence of either evaporitic or placer types of sediment, geotypes 2 and 3 can be discounted here. The question is then, is the tourmaline related to submarine exhalative processes, or rather to an acid intrusion of some sort.

Taylor and Slack (1984), and Appel (1985) have demonstrated the textural, chemical and isotopic differences between granitic and sedimentary exhalative types of tourmaline. Using methods outlined in these studies, as well as from Slack (1980), it is possible to determine the origin of tourmaline from the study area. For the purposes of clarity and comparison, the data supplied in this section is presented in a similar format to that of Taylor and Slack (1984), since the latter study deals with other Norwegian sulfide-tourmaline associations which bear some similarity to

the study area.

8.2: Tourmaline field relationships

In an environment such as the study area, where ophiolitic mafic-ultramafic rocks and associated seafloor exhalative and orthomagmatic sulfide deposits are the main rock types, it would be easy to assume that tourmaline had its origin in a seafloor exhalative type of environment, especially considering the proximity of the Visnes massive sulfide deposit. However, several field relationships of the tourmaline in the study area do not support this conclusion. Firstly, there is no tourmaline found in the Visnes massive sulfides (see Chapter 3). Secondly, tourmaline is only found in and around the shear zones. These are related to metamorphism and deformation which post-dated intrusion of the high-Mg dykes and associated Ni-sulfides, since these shear zones cut the latter rock types. Consequently, tourmalinization cannot be related to formation of the Visnes massive sulfides.

8.3: Major element chemistry

11 tourmaline-rich samples were used to obtain electron microprobe analyses for 23 tourmaline crystals. Data for these samples is given in Table 8.1, in comparison with data from Taylor and Slack (1984), for tourmaline from massive sulfide deposits in the Norwegian Caledonides and the Appalachians of North America. The following features are noteworthy:

1- tourmaline from the study area is all characterized by relatively low Na2O, MgO, Al2O3 and CaO;

Table 8.1: Electron microprobe analyses of tourmaline from the Feoy area (data from the present study), along with data from selected massive sulfide related tourmaline occurrences (data are from Taylor and Slack, 1984).

Sample	Na2O	MgO	Al2O3	SiO2	K2O	CaO	TiO2
Feoy							
Rim	2.77	6.64	29.76	37.75	0.03	0.47	0.19
Rim	2.8	6.59	29.19	36.99	0.03	0.69	0.34
Rim	2.9	6.65	29.32	36.61	0.04	0.72	0.36
F-54	2.8	5.65	28.12	39.07	0.04	0.7	0.52
F-54	2.78	5.55	27.57	38.58	0.02	0.72	0.7
F-43	2.42	6.55	29.48	37.55	0.03	0.57	0.25
F-43	2.7	6.86	29.31	37.67	0.01	0.58	0.32
F-43	2.38	6.32	28.89	37.09	0.04	0.59	0.33
Trm	2.99	6.56	30.2	36.27	0.03	0.48	0.11
JS-2	3.22	5.94	26.6	34.56	0.02	0.73	0.61
JS-2	2.94	6.1	27.83	32.13	0.08	0.53	0.23
JS-2	2.7	5.57	25.37	34.71	0.06	0.72	0.86
F-6D	3	6.29	30.03	35.54	0.03	0.36	0.07
F-6D	2.62	5.96	28.86	34.53	0.03	0.29	0.11
F-6D	2.82	6.35	28.32	36.24	0.02	0.68	0.38
F-6B	2.63	6.28	29.92	36.53	0.02	0.31	0.2
F-6B	2.6	6.69	28.49	35.31	0.02	0.6	0.52
F-7B	2.88	6.46	27.15	28.59	0.03	0.54	0.43
F-7B	3.04	6.87	28.87	35.01	0.02	0.49	0.27
F-7B	2.75	6.98	26.16	36.09	0.02	1.32	0.44
F-24	3	6.52	28.25	36.07	0	0.36	0.12
F-40A	3	4.67	29.03	34.64	0.02	0.18	0.04
F-40A	2.97	5.01	29.35	35.35	0.03	0.18	0.08
Elisabeth	2.81	11.51	34.01	39.01	0.06	0.6	0.31
Ely	2.33	11.92	32.22	38.05	0.02	1.54	1.54
Bleikvassli	1.63	10.71	35.61	38.61		1.18	0.2
Black Hawk	1.95	10.01	34.01	37.61	0.1	1.95	0.26

Table 8.1: (continued)

Sample	Cr2O3	MnO	FeO	NiO	Total
Feoy					
Rim	0.02	0.03	10.17	0.05	87.86
Rim	0.02	0.04	10.48	0.04	87.21
Rim	0.01	0.09	9.79	0	86.47
F-54	0	0.03	13.96	0.04	90.91
F-54	0	0.04	13.95	0.01	89.93
F-43	0.04	0.02	9.91	0.01	86.82
F-43	0.08	0.11	10.04	0.05	87.73
F-43	0.16	0.04	9.97	0.02	85.82
Trm	0	0.09	8.29	0.12	85.14
JS-2	0.04	0.07	12.09	0.09	83.95
JS-2	0.04	0.05	10.88	0	80.81
JS-2	0.07	0.07	14.03	0	84.16
F-6D	0.03	0.07	9.49	0.03	84.94
F-6D	0	0.11	10.58	0.03	83.12
F-6D	0	0.04	10.01	0.05	84.89
F-6B	0.02	0.06	9.59	0.02	85.58
F-6B	0.01	0.03	9.61	0.04	83.92
F-7B	0.04	0.05	10.49	0.11	76.77
F-7B	0.18	0.07	8.58	0.05	83.45
F-7B	0.18	0.04	9.65	0.07	83.7
F-24	0.02	0.06	10.66	0.01	85.06
F-40A	0.02	0.04	11.2	0	82.84
F-40A	0	0.03	11.41	0	84.42
Elisabeth			2.13		91.01
Ely			3.02		90.65
Bleikvassli			0.98		89.47
Black Hawk			3.15		86.51

Chemical end members of the tourmaline group (from Taylor and Slack, 1984).

Mineral	Ideal composition
Schorl	$NaFe^{3+}Al_6B_3Si_6O_{27}(OH, F)_4$
Elbaite	$Na(Li, Al)_3Al_6B_3Si_6O_{27}(OH, F)_4$
Dravite	$Na(Mg_3Al_6B_3Si_6O)_{27}(OH, F)_4$
Buergerite	$NaFe^{3+}Al_6B_3Si_6O_{30}F$
Tsilaisite	$NaMn_3Al_6B_3Si_6O_{30}F$
Liddicoatite	$Ca(Li, Al)_3Al_6B_3Si_6O_{27}(OH, F)_4$
Uvite	$CaMg_3(Mg,Al_5)B_3Si_6O_{27}(OH, F)_4$

2- the concentrations of K2O, TiO2, CrO2, MnO and NiO are all low, and some are below the limits of detection;

3- the low Al2O3 precludes the presence of any elbaite component here, and the MgO-FeO contents indicate that all samples are near the schorl endmember in the schorl-dravite solid solution series (Deer et al., 1962; note that the chemical compositions for the Schorl-dravite solid solution are included in Table 8.1).

Compared with tourmaline occurrences elsewhere in the Caledonian-Appalachian orogen, the following variations are noted:

1- tourmaline from the study area is on average similar to other occurrences in its SiO2, K2O and TiO2 contents;

2- tourmaline from the study area is on average enriched in Na2O and depleted in CaO relative to other occurrences. This is reflected in a higher Na2O/Na2O+CaO ratio for the tourmaline of Feoy;

3- tourmaline from the study area is clearly enriched in FeO and depleted in MgO relative to other areas. Consequently, FeO/FeO+MgO ratios are significantly higher than ratios for all other massive sulfide-related deposits of tourmaline.

Figure 8.1, and Table 8.1 outline the marked chemical disparities between tourmaline of the study area and tourmaline from other sulfide related occurrences in the Norwegian Caledonides. This data is compared with data from granite related tourmaline from Portugal and England (data from massive sulfide deposits is from Taylor and Slack, 1984; data from granites is from Neiva, 1974, and Power, 1968). In Figure 8.1, the Feoy tourmaline plots in the lower range of

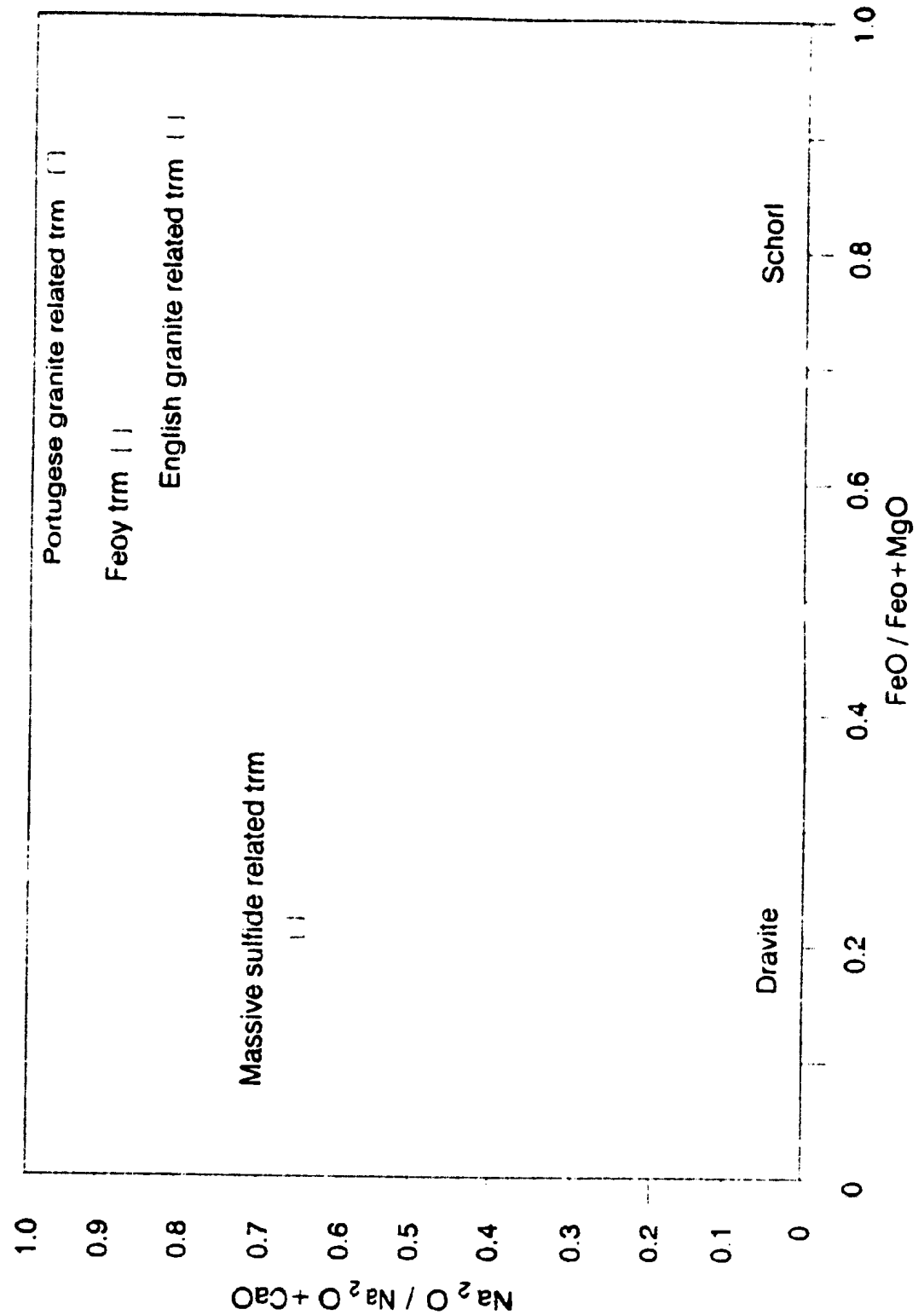

Figure 8.1: Chemical disparity between tourmaline from Feoy and tourmaline from massive sulfide and granite related environments (data for all areas except Feoy are from Taylor and Slack, 1984).

schorl compositions in terms of FeO/FeO+MgO, and is more closely related to the granite related tourmaline in this respect, although it is not dissimilar to tourmaline from the Blackhawk (Maine) and Ore Knob (North Carolina) mines.

Although not plotted here, schorl tourmaline has been recorded from the Vassfjell massive sulfide deposit in the Trondheim District of Norway (Greene et al., 1980). This deposit is an ophiolite related occurrence, and along with the tourmaline from the study area represents the only known occurrence of schorl tourmaline from this type of environment. Unfortunately, the origin of this tourmaline has not been discussed.

In terms of its Na2O/Na2O+CaO ratios, the Feoy tourmaline is clearly dissimilar to all massive sulfide related tourmaline, and is intermediate bewteen tourmaline of the Portugese and English granites, thereby putting the Feoy tourmaline well within the field of average granite related tourmaline.

8.4: Oxygen isotopes

Oxygen isotopes from tourmaline and quartz in granite related and massive sulfide related occurrences are distinctly different, and these differences can be used to qualify the origin of the Feoy tourmaline occurrence. Three tourmaline separates and three quartz separates were analysed from vein and breccia samples in the Feoy area, taken mainly from the area of the mine dump. Their oxygen-isotopic tenor is reported in Table 8.2.

Table 8.2: Chemical disparities between tourmaline from Feoy and tourmaline from granite related (Portugese granite data from Neiva, 1974; English granite data from Power, 1968) and massive sulfide related (data from Taylor and Slack, 1984) environments.

Chemical parameter	Massive sulfides	Portugese granites	English granites	Feoy trm
# of samples	15	18	17	23
FeO/FeO+MgO	0.21	0.86	0.91	0.65
Na2O/Na2O+CaO	0.66	0.97	0.82	0.88

Table 8.3: Oxygen isotope values of tourmaline and quartz from Feoy.

Sample #	del 18O (trm)	del 18O (qtz)	Range of del 18O qtz-trm
F-54	+7.55 per mil		
F-9	+6.53		
F-40A	+6.4		
F-24		+10.16	
F-6		+9.44	
F-61		+10.24	
			minimum of 1.89
			maximum of 3.84
			probable= 2.40

Note: Isotopic values are the ratios of heavy (18O) to light Oxygen (16O) relative to the international standard SMOW (Standard Mean Ocean Water) of 0 per mil.

* All six mineral separates are from trm bearing vein and breccia samples. However, trm sample F-54 is vein associated trm, and is 1 per mil heavier than trm samples F-9 and F-40A, the latter which are samples of the tourmalinite fragments in Type A breccia. All 3 quartz separates are from trm bearing vein assemblages, and so sample F-54 may be more isotopically representative of hydrothermal fluids, and of del 18O (qtz-trm), than are F-9 or F-40A. For the purposes of completeness, however, the whole range of possible del 18O (qtz-trm) are given. The most representative trm sample, F-54, is paired with an average del 18O (qtz) of 9.95 per mil to give a probable del 18O (qtz-trm) of 2.4 per mil.

Figures 8.2 and 8.3: Oxygen isotope relations for tourmaline and quartz assemblages from the study area, along with data from massive sulfide and granite related environments (data from all areas except Feoy from Taylor and Slack, 1984).

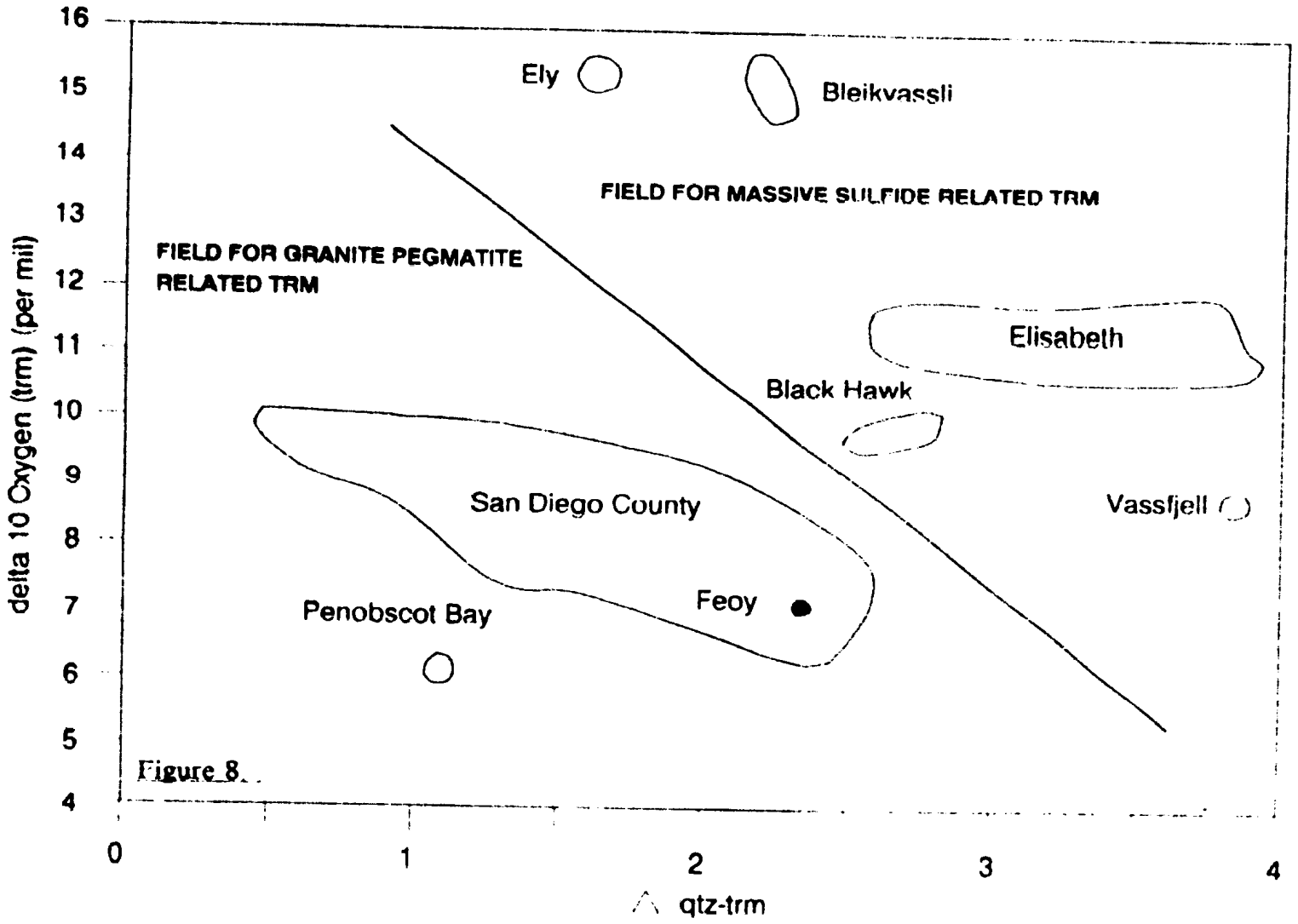
16
15
14
13
12
11
10
9
8
7
6
5
4
delta 10 Oxygen (trm) (per mil)
Ely
Bleikvassli
FIELD FOR MASSIVE SULFIDE RELATED TRM
FIELD FOR GRANITE PEGMATITE RELATED TRM
Elisabeth
Black Hawk
San Diego County
Vassfjell
Feoy
Penobscot Bay
0
1
2
3
4
qtz-trm

Figure 8.

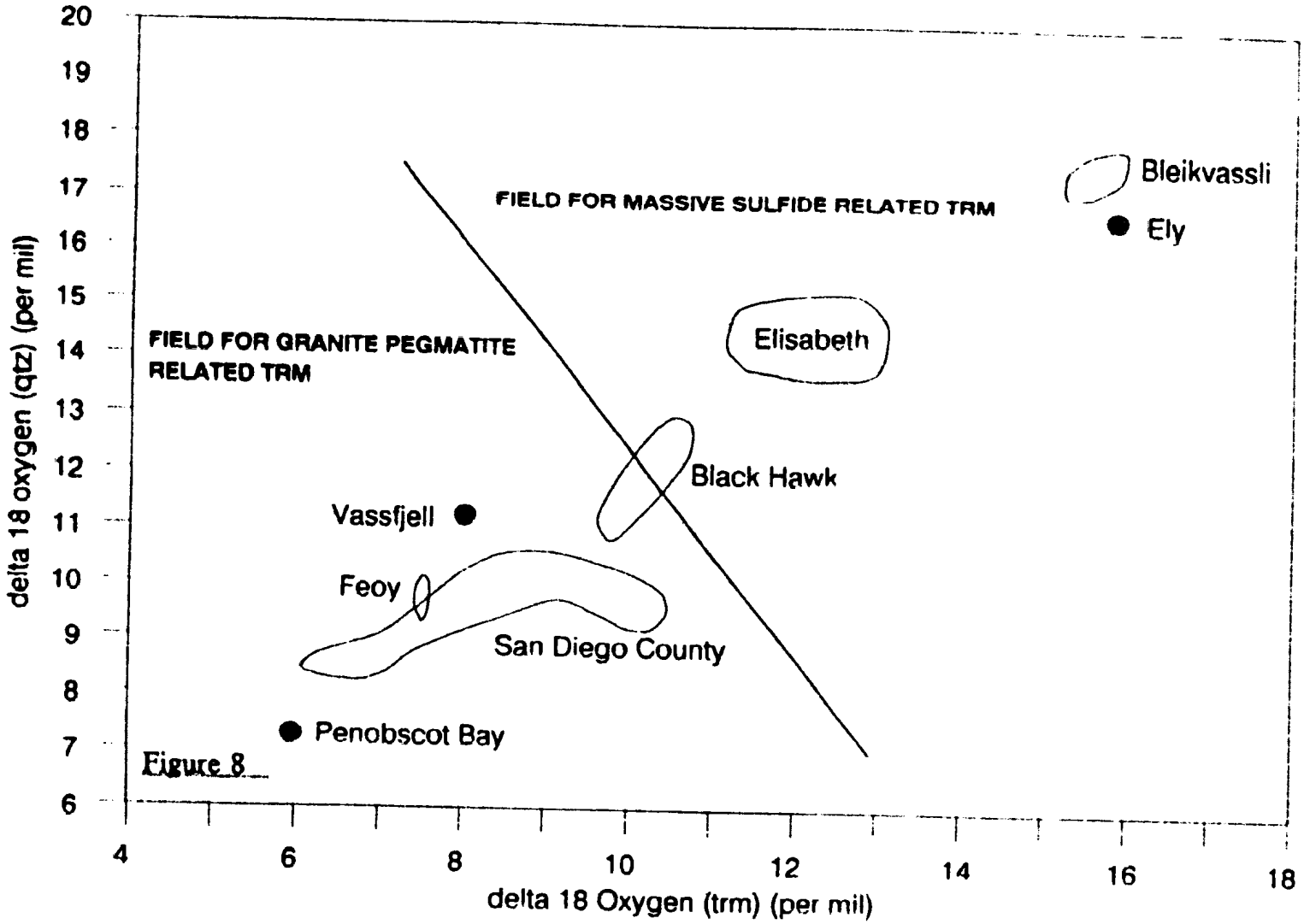
20
19
18
17
16
15
14
13
12
11
10
9
8
7
6
delta 18 oxygen (qtz) (per mil)
FIELD FOR MASSIVE SULFIDE RELATED TRM
FIELD FOR GRANITE PEGMATITE RELATED TRM
Bleikvassli
Ely
Elisabeth
Black Hawk
Vassfjell
Feoy
San Diego County
Penobscot Bay
4
6
8
10
12
14
16
18
delta 18 Oxygen (trm) (per mil)

Figure 8

Figure 8.2 plots delta 18O (tourmaline) against delta 18O (quartz) for some pegmatitic and massive sulfide related deposits, as well as for the Feoy tourmaline. It has been shown (Garlick and Epstein, 1966; Slack and Taylor, 1984) that quartz is relatively resistant to isotopic exchange during metamorphism; the linear relationship exhibited here between the various deposits demonstrates the probable isotopic stability of tourmaline as well as quartz during metamorphism. It also suggests that variations in the isotopic signatures of the different deposits reflect differences in the thermal and/or isotopic nature of the hydrothermal fluid itself. In the study area, it appears that the isotopic integrity of tourmaline was indeed maintained throughout metamorphism, since earlier formed (deformed) tourmaline (samples F-9 and F-40A, which are tourmalinite fragments in Type A breccia) samples are only 1 per mil lighter than later formed (undeformed) tourmaline (sample F-54, which is a sample of coarse crystalline vein tourmaline).

A second feature evident from Figure 8.2 is that all the Feoy tourmaline plots much closer to the isotopically distinct pegmatite group than to massive sulfide related tourmaline.

Figure 8.3 plots delta 18O (tourmaline) vs. delta 18O (quartz minus tourmaline) for those deposits plotted in Figure 8.2. Once again it is evident that for the minimum and probable delta 18O (quartz-tourmaline) values of the Feoy tourmaline-quartz samples, they are most closely related to granite-pegmatitic tourmaline, although some similarity to the Black Hawk (massive sulfide related) tourmaline is also observed.

In summary, it is clear that tourmaline from the study area, although exhibiting some textural

similarities to the Blackhawk massive sulfide related tourmaline occurrence, is chemically and isotopically distinct from most massive sulfide related tourmaline deposits in the Appalachians and Caledonides. Indeed, in these respects the Feoy tourmaline is much more closely related to granite, pegmatite and aplite hosted tourmaline occurrences. Likewise, field data suggests that there is no relationship between the tourmaline occurrence and the Visnes massive sulfides.

The only other possible option for the environment of origin of the Feoy tourmaline, having ruled out placer, evaporitic and seafloor precipitate deposits, is a granitic environment. Data from the breccia occurrence in the Feoy area offers support to this suggestion, and is discussed in the following section. The geology and petrology of this breccia was discussed in Chapter 4, and therefore the following discussion only involves features which are pertinent to its origin.

8.5: The origin of the Feoy breccia

The occurrence of a tourmaline-bearing breccia pipe within arc related rocks of the Feoy area is an intriguing addition to the problem of tourmaline formation. The term "breccia pipe" is used here instead of "stockwork" or "fault breccia" for several reasons. Firstly, a true massive sulfide related "stockwork" zone, as exemplified in the Cyprus and Bett's Cove ophiolites (Lydon, 1987; Saunders, 1985), contains angular, unmilled fragments of mineralized, highly altered wall rock (in both cases pillow lava), and sits below a massive sulfide zone of exhalative origin. Such stockworks are characterized by intense silicification and pyrite-chalcopyrite veining which in some places reaches ore grade. None of these features are present in the Feoy

breccias. Likewise, "fault breccias", or breccias resulting from simple movement along fault zones, are characterized by angular, highly unsorted and irregular fragments set in a matrix of clastic silt to sand sized material, termed "rock flour" (Sillitoe, 1985). This "rock flour" is an essential component of all fault or tectonic breccias, but is conspicuously absent from the Feoy breccias. On the contrary, the Feoy breccias are characterized by open space breccia filling with hydrothermal cement matrix, as opposed to a rock flour matrix in tectonic breccias (otherwise known as fault gouge or collapse breccia). Also, it is important to note that tectonic brecciation, or the production of dilatent fault zones during ophiolite emplacement, cannot account for the close relationship between brecciation, chlorite-calcite-quartz precipitation, and the consistantly bi-, or possibly tri-lithologic nature of the breccia fragments (Sillitoe, 1985). That is, breccia fragments are composed of tourmalinites, Type 2 plagiogranites, and also high-Mg basalts.

These features, along with the localization of brecciation to one small area of Feoy (in which Ni-sulfides, high-Mg dykes and Type 2 plagiogranite dykes are also abundant), suggest that this breccia is part of a "breccia pipe" in its truest sense.

Sillitoe (1985) has provided an exhaustive study on breccia pipe occurrences in volcano-plutonic arcs, and has been able to qualify 6 main breccia types; these are outlined in Table 8.4. All of these breccia types, excluding tectonic breccias, have been explained by a combination of one or more of the following mechanisms (after Sillitoe, 1985):

1- localized dissolution and upward removal of rock by fluid released from a cooling magma;

2- release of volatiles from magma with material carried physically upward;

Table 8.4: General characteristics of ore related breccias in volcano-plutonic arcs (after Sillitoe, 1985).

Breccia category	Deposit type	Geometry	Diameter (m)
Magmatic hydrothermal	Isolated pipes	Single or multiple pipes	50-300, locally >1000
	Porphyry	Single or multiple pipes, irregular bodies	up to 2000m
Phreatic	Epithermal	Pipelike but commonly irregular	up to 500m
	Porphyry	Pipes, pebble dykes	up to 500m
	Kuroko	Sheets, lenses	up to 1000m long
Phreatomagmatic	Porphyry	Diatreme	1000-3000m
	Epithermal	Diatreme	1000-3000m
Magmatic	Porphyry	Diatreme	500-5000m
	Epithermal	Diatreme	500-5000m
Intrusion	Intrusion related deposits	Irregular patches	up to 100m
Tectonic	Any deposit	Steep tabular bodies	up to 50m wide

Table 8.4: (continued)

Breccia category	Fragment form	Rock flour matrix
Magmatic hydrothermal	Angular-subrounded locally rounded	Locally present (<30%)
	Angular to rounded	Commonly present (>50%)
Phreatic	Angular to rounded	Commonly present (<50%)
	Angular to rounded	Commonly present (up to 100%)
	Angular to rounded	Present (<30%)
Phreatomagmatic	Subrounded to rounded	Present (<90%)
	Subrounded to rounded	Present (<90%)
Magmatic	Subrounded to rounded	Present
	Subrounded to rounded	Present
Intrusion	Angular	Absent
Tectonic	Angular to rounded	Present (up to 100%)

3- downward movement of magma by shrinkage or withdrawal;

4- development of a vapour bubble on the roof of a stock or pluton by accumulation of exsolved fluids.

Upon examination of the scheme presented in Table 8.4, it becomes evident that there are problems in classifying the Feoy breccia pipe. It is clearly not a tectonic breccia for reasons discussed above. Neither is it an intrusion breccia, since such a breccia is the result of intrusion of a melt into country rock, and requires a matrix of igneous material.

Magmatic, phreatomagmatic and phreatic breccias all require a significant rock flour matrix, but this is not present in the Feoy breccia. While magmatic-hydrothermal breccias allow for the possibility of no rock flour in the matrix, and for the presence of rounded fragments, such mechanisms imply high temperature hydrothermal fluids along with the presence of an underlying hydrous granitic or similar type of intrusion. Indeed, fluid inclusion data from many intrusion-related breccia pipes indicate fluid temperatures in the range of 310-470 degrees Celsius (So and Shelton, 1983). Unfortunately, the breccia matrix in the Feoy rock samples is either pure chlorite (Type A breccia), or chlorite with fine grained, milky quartz and calcite (Type B breccia), neither type which yielded any samples suitable for fluid inclusion studies. Tourmaline samples were also checked optically for fluid inclusions, but because of their dark color and relatively fine grain size, they were unsuitable for such studies. In this respect, breccia pipe formation as a result of magmatic-hydrothermal activity cannot be ruled out.

While there is no direct evidence from the breccia pipe of tourmaline-bearing granitic fragments,

there is still abundant evidence which strongly supports an origin of the breccia pipe and associated tourmaline from granitic intrusion related processes. Firstly, the isotopic and chemical signature of the tourmaline strongly suggests a granitic origin for the tourmaline.

Secondly, the morphology (and to a lesser extent the lithology) of the breccia pipe provides convincing evidence for its formation as a result of intrusion related processes; the absence of rock flour and incipient silicification or mineralization, the roundness of the fragments, and the hydrothermal cement matrix virtually precludes the possibility of brecciation as a result of tectonic or stockwork related activity. Therefore, the only alternative is that brecciation occurred from intrusion related activity.

Thirdly, the WKIC to the north is a large granitic pluton which contains black tourmaline of the schorl/dravite variety along the margins. Intrusion of the WKIC is also accompanied by large scale shearing in the country rocks. The WKIC is dated at 450Ma by Rb/Sr methods (Priem and Torske, 1973), a date which is younger than intrusion of the clinopyroxene-phyric stock on Feoy (which is dated at 470 +9/-5Ma by Dunning and Pedersen, 1987). Allowing for a significant period of tectonic and/or magmatic quiescence, with inter-arc or arc basin deposition of the volcaniclastic equivalents to this clinopyroxene-phyric stock before the initiation of metamorphism, deformation and associated brecciation, then the onset of such activity would correspond remarkably well with intrusion of this granite.

In summary then, it is quite possible that the onset of late metamorphism, along with development of regional scale shear zones, was a direct result of intrusion of the WKIC.

Associated brecciation need not have commenced until the granite intrusion had ascended to relatively shallow crustal levels, at which stage it would have already exsolved a considerable boron-rich aqueous phase (Strong, pers.comm.), and would have had ample time to form tourmaline-rich roof rocks prior to their subsequent brecciation (these being the tourmalinite fragments in Type A breccia). Continued exsolution of a magmatic, boron-rich aqueous phase during brecciation would ensure formation of fresh new tourmaline vein assmblages in addition to incorporation of tourmalinite fragments in the breccia (which explains the two types of tourmaline found in the study area).

Locally, explosive discharge of boron-rich fluids from a crystallizing granitic pluton would have been through country rocks composed of high-Mg dykes, the Ni-sulfide deposit, Type 2 plagiogranites and diorites in the Feoy area. Therefore, these are the rock fragments which one might expect to find in the breccia pipe, as indeed is the case. This explains the spatial relationship between Ni-sulfides and tourmaline.

Chapter 9: Conclusions

The preceeding chapters have illustrated the complex interrelationships between mineralization, alteration, deformation and magmatism in the evolution of the Karmoy Ophiolite. Sulfide mineralization occurred during two distinct periods of magmatic activity: firstly as a result of hydrothermal activity at a seafloor spreading center; then some 20ma later as a result of precipitation from a sulfur-saturated mafic melt in a supra-subduction zone environment. Patterns of alteration unique to each deposit have been examined, and serve to distinguish petrographically and geochemically between older and younger rock formations. Finally, late deformation has considerably modified both deposits, and it is possible to delineate the nature and probable origin of this activity.

Because of the complexity of geological relationships in the study area involving multiple periods of magmatism, alteration, mineralization and deformation, it is perhaps easier to summarize the main findings of this study in the form of schematic diagrams. These are illustrated and briefly described in Figure 9.1. In addition, the salient conclusions from each chapter are listed below:

1- the geology of the study area is dominated by heavily altered volcanic, subvolcanic, and plutonic rocks of the upper portion of the Karmoy Ophiolite, and records Early Ordovician oceanic spreading and subduction zone activity;

2- a massive Fe-Cu-Zn sulfide deposit (the Visnes deposit) represents a period of seafloor sulfide precipitation which occurred early in the evolution of the Karmoy Ophiolite;

3- a massive Fe-Cu-Ni-PGE sulfide deposit (the Feoy deposit) represents a period of magmatic sulfide formation associated with intrusion of late, highly magnesian dykes. This mineralization appears to be related to supra-subduction zone activity;

4- alteration associated with the Visnes deposit is typical spilitic in nature, and probably resulted from large scale regional convection of seawater-hydrothermal fluids. However, local epidosite zones, epidotites and plagiogranites provide field, petrographic and geochemical data that suggests there may well have been a direct magmatic water influence on alteration and mineralization in the Visnes deposit;

5- a period of alteration which occurred after formation of the Feoy Ni-sulfides has resulted in extensive, and in some samples complete leaching of PGE's from the sulfides. This alteration may have been a post-emplacement event related to regional shear zone formation as well as local formation of tourmaline-bearing breccia pipes;

6- geochemical, isotopic and petrographic analyses of the Feoy deposit suggest that it formed from sulfide precipitation in an already-depleted partial melt during ascent from a mantle origin. Petrogenetic modelling of the co-magmatic host silicate rocks for the Feoy deposit show PGE patterns which are, as expected, also indicative of formation from a second stage melt, or from partial melting of an already-depleted melt;

7- volcaniclastic sediments of the Torvastad Group, which represent a period of arc-basin formation following arc-volcanism late in the evolution of the ophiolite, are themselves quite deformed and cut by shear zones. Therefore, shear zone formation which affects all rocks in the study area must have occurred very late in the evolution of the Karmoy Ophiolite, and is possibly a post-emplacement phenomenon;

8- tourmaline-bearing breccias and tourmalinites occur in the Feoy area. Textural,

isotopic and geochemical analyses of the tourmaline and breccia strongly suggest that they formed as a result of forceful intrusion of a hydrous granitic body into the surrounding country rocks. This may well represent an extension of the West Karmoy Igneous Complex.

Schematic diagrams illustrating the geological events, dates and geotectonic environments of formation of sulfide occurrences in the Karmoy ophiolite.

1a. Formation of the Visnes sulfides, ca. 493 ma., within an island arc environment.

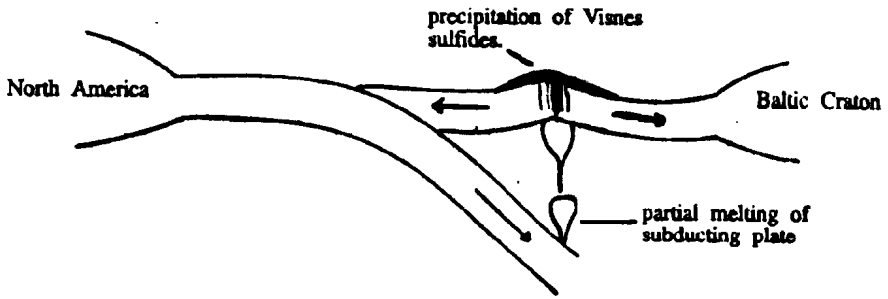

1b. Detailed sketch of the Visnes sulfides zone of formation.

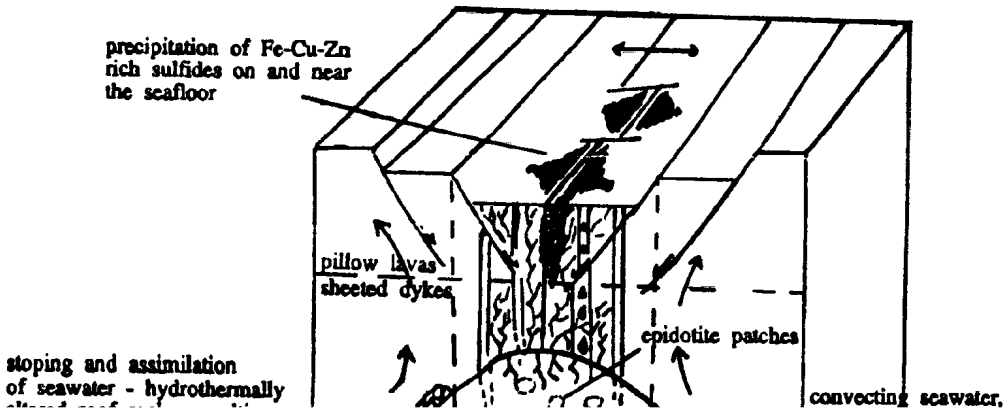

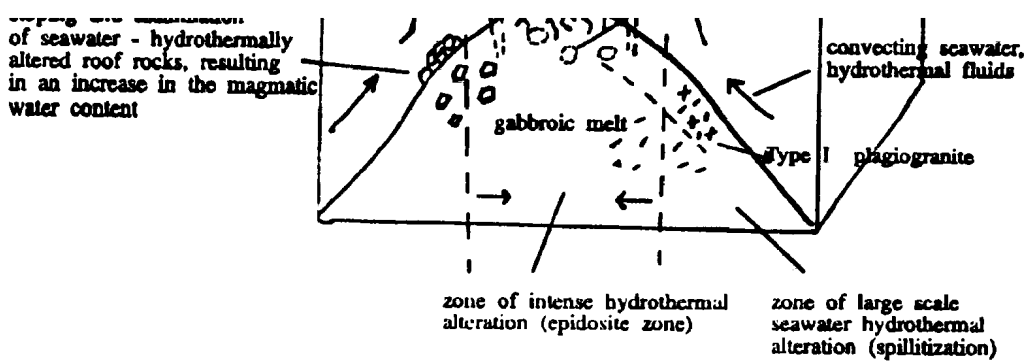

2. Deformation and remobilization of the visnes sulphides.

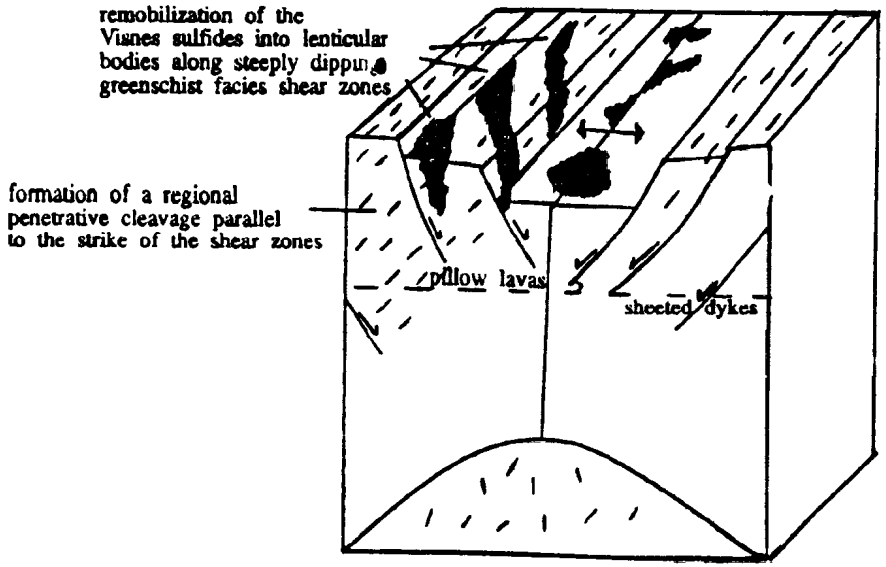

3. Formation of the Feoy sulfides, dated between 485 +/- 2 ma (from the type 2 plagiogranites) and 470 +9 / -5 ma. (from clinopyroxene - phyric intrusions in the area), in an island arc - back arc - arc basin environment.

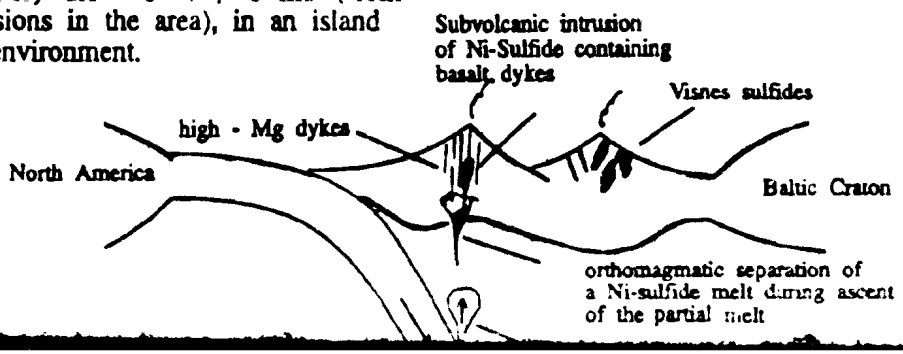

3. Formation of the Feoy sulfides, dated between 485 +/- 2 ma (from the type 2 plagiogranites) and 470 +9 / -5 ma. (from clinopyroxene - phyric intrusions in the area), in an island arc - back arc - arc basin environment.

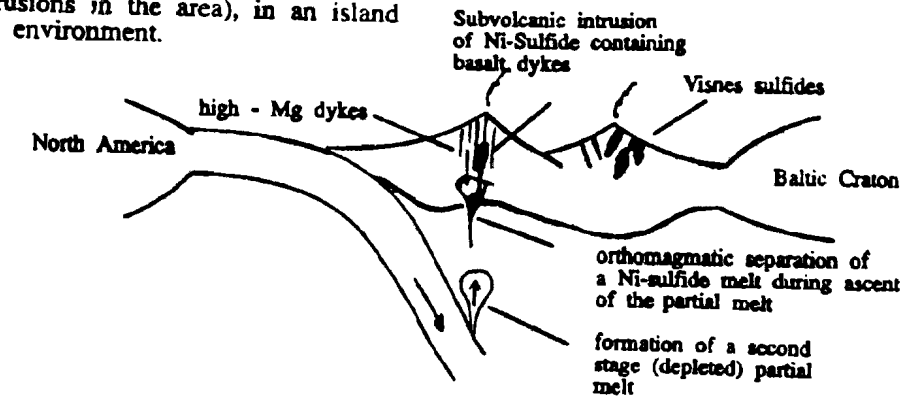

4. Deformation and remobilization of the Feoy sulfides, intrusion of a granitic pluton, and formation of a tourmaline - bearing breccia pipe during emplacement of the Karmoy ophiolite into the continental crust, ca. 450 ma..

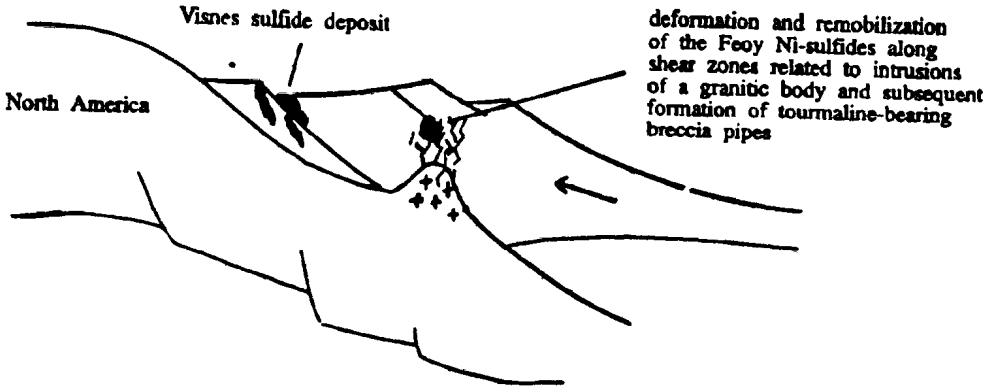

References

Alabaster, T. and Pearce, J.A., 1985. The interrelationships between magmatic and ore-forming hydrothermal processes in the Oman Ophiolite. Econ. Geol., v. 80, no. 1, pp. 1-16.

Aldiss, D.S., 1978. Granitic rocks of ophiolites. Ph.D. dissertation, The Open University.

Amstutz, G.C., 1974. Spilites and spilitic rocks. Springer-Verlag, Berlin, Heidelberg and New York. 482pp.

Appel, P.W.U., 1985. Strata-bound tourmaline in the Archaen Malene Supracrustals, West Greenland. Can. Jnl. Earth Sci., v. 22, pp. 1485-1491.

Bachinskii, D.J., 1977. Alteration associated with metamorphosed ophiolitic cupriferous iron sulfide deposits: Whalesback Mine, Notre Dame Bay, Nfld. Mineral. Deposita (Berl.), v. 12, pp. 48-63.

Barnes, S.J., Boyd, R., Korneliussen, A., Nilsson, L.P., Often, M., Pedersen, R.B. and Robins, B., 1987. Geochemistry of Platinum metals in rocks and ores in Norway. Pilot project. Draft report no. 87-021. pp. 1-50, EEC raw materials program INGU/NTNF.

Barton, P.B.Jr. and Skinner, B.J., 1979. Sulfide mineral stabilities. In Barnes, H.L. (ed.), Geochemistry of hydrothermal ore deposits. Second edition. New York, Wiley, pp. 278-403.

Basaltic Volcanism Study Project, 1981. Basaltic volcanism on the terrestrial planets. Pergammon Press Inc., New York, 1286pp.

Birkeland, T., 1975. Western Karmoy, an integral part of the Precambrian basement of Southern Norway. Nor. Geol. Tidsskr., v. 55, pp. 213-241.

Bjorlykke, A., Grenne, T., Rui, I. and Vokes, F.M., 1980. A review of Caledonian-Appalachian strata-bound sulfide deposits in Norway. Geol. Sur. Ireland, Spec. Paper no. 5. pp. 29-46.

Boyd, R. and Nixon, F., 1985. Norwegian Ni deposits: A review. Geol. Sur. Finland, Bull. 333, Papunen and Gorbunov (eds.), pp. 363-394.

Boyd, R. and Mathieson, C.O., 1979. The Ni mineralization of the Rana Mafic Intrusion, Nordland, Norway. Can. Mineral., v. 17, pp. 287-298.

Butterfield, D.A., Massoth, G.J., McDuff, R.E., Lupton, J.E. and Lilley, M.D., 1990. Geochemistry of hydrothermal fluids from axial seamount hydrothermal emissions study vent field, Juan de Fuca Ridge: Sub-seafloor boiling and subsequent fluid-rock alteration. Jnl. Geophys. Res., v. 95, pp. 12895-12921.

Cabri, L.J. and Naldrett, A.J., 1984. The nature of the distribution and concentration of PGE's in various geological environments. Int. Geol. Cong., 27, Moscow. Proc., v. 10, pp. 17-46.

Campbell, I.H., Naldrett, A.J. and Barnes, S.J., 1983. A model for the origin of the Pt-rich sulfide horizons in the Bushveld and Stillwater Complexes. Jnl. Petrol., v. 24, pp. 133-165.

Cann, J.R., 1969. Spilites from the Carlsberg Ridge, Indian Ocean. Jnl. Petrol., v. 10, pp. 1-19.

Cann, J.R., 1970. Rb, Sr, Y, Zr, and Nb in some ocean-floor basaltic rocks. Earth Planet. Sci. Letts., v. 10, pp. 7-11.

Cann, J.R., Strens, M.R. and Rice, A., 1985/86. A simple magma-driven thermal balance model for the formation of volcanogenic massive sulfides. Earth Planet. Sci. Letts., v.76, pp.123-134.

Coish, R.A., 1977. Ocean-floor metamorphism in the Bett's Cove Ophiolite, Nfld. Contrib. Mineral. Petrol., v. 60, pp. 255-270.

Coleman, R.G. and Peterman, Z.E., 1975. Oceanic plagiogranite. Jnl. Geophys. Res., v. 80, pp.1099-1108.

Constantinou, G., 1987. Massive sulfide deposits. In Troodos 87 Ophiolites and Oceanic lithosphere Symp. Field Exc. Guidebook (eds. C. Xenophontos and J.G. Malpas), pp. 92-113.

Cowan. J. and Cann, J., 1989. Supercritical two-phase separation of hydrothermal fluids in the Troodos Ophiolite. Nature, v.333, no.6170, pp.259-261.

Cowden, A., Donaldson, M.J., Naldrett, A.J. and Campbell, I.H., 1986. PGE's and Au in the komatiite-hosted Fe-Ni-Cu sulfide deposits at Kambalda, Western Australia. Econ. Geol., v. 81, pp. 1226-1235.

Craig, J.R., Ljokjell, P. and Vokes, F.M., 1984. Sphalerite compositional variations in sulfide ores of the Norwegian Caledonides. Econ. Geol., v. 79, pp. 1727-1735.

Crawford, M.L., 1981. Phase equilibria in aqueous fluid inclusions. In Fluid inclusions: Applications to petrology, Short Course Handbook Min. Assoc. Can. (ed. L.S. Hollister), V. 6, pp. 75-100.

Crawford, A.J.; Beccaluva, L. and Serri, G., 1981. Tectono-magmatic evolution of the Western Phillipine-Mariana region and the origin of boninites. Earth Planet. Sci. Letts., v. 54, pp.346-356.

Deer, W.A., Howie, R.A. and Zussman, J., 1962. Rock forming minerals, Vol. 1- Ortho and ring silicates. p.198.

Dunning, G.R. and Pedersen, R.B., 1987. U/Pb ages of ophiolites and arc-related plutons of the Norwegian Caledonides: Implications for the development of Iapetus.

Eldridge, C.S., Barton, P.B.Jr. and Ohmoto, H., 1983. Mineral textures and their bearing on formation of the Kuroko orebodies. Econ. Geol. Mon. 5, pp. 241-281.

Engel, A.E.J., Engel, C.G. and Havens, R.G., 1965. Chemical characteristics of oceanic basalts and the upper mantle. Bull. Geol. Soc. Amer., v. 76., pp. 719-734.

Foslie, S., 1926. Norges Svorelkisforekemster. Nor Geol. Unders., v. 127, 122pp.

Foslie, S., 1938. Betrakringer over Kisforekanstenes dannelse. Nor. Geol. Tidsskr., v. 17, pp. 214-217.

Foslie, S. and Host, M.J., 1932. Platina i sulfidisk Nikkel-malm. Nor. Geol. Unders., v. 137, 71pp.

Franklin, J.M., Lydon, J.W. and Sangster, D.F., 1981. Volcanic associated massive sulfide deposits. Econ. Geol. 75 anniv. vol., pp. 485-627.

Furnes, H., Sturt, B.A. and Griffin, W.L., 1980. Trace element geochemistry of metabasalts from the Karmoy ophiolite, SW Norwegian Caledonides. Earth Planet. Sci. Letts., v. 50, pp. 75-91.

Furnes, H., Thon, A., Nordas, J. and Garmann, L.B., 1983. Trace element geochemistry of metabasalts from some Norwegian ophiolite fragments: Evidence of mineralogical and chemical mantle heterogeneity. Contrib. Mineral. Petrol. v. 79, pp. 295-307.

Garlick, G.D. and Epstein, S., 1966. The isotopic composition of oxygen and carbon in hydrothermal minerals at Butte, Montana. Econ. Geol., v. 61, pp. 1325-1335.

Geis, H.P., 1962. Structural observations on some Norwegian sulfide deposits. Nor. Geol. Tidskr. no. 41.

Glazkovsky, A.A., Gorbunov, G.I. and Sysoev, F.A., 1977. Ore deposits of the USSR. V.I. Smirnov (ed.). Pittman, London. Vol. 2.

Godlevskii, M.N. and Grinenko, L.N., 1963. Some data on the isotopic composition of sulfur in the sulfides of the Noril'sk deposit. Geochem., 35-41.

Gorbunov, G.I., 1968. Geology and origin of the Cu-Ni sulfide ore deposits of Pechanga (Petsano): Nedra, Moscow. 352pp. (in Russian).

Greene, T., Grammeltvedt, G. and Vokes, F.M., 1980. Cyprus-Type sulfide deposits in the Western Trondheim district, Central Norwegian Caledonides. In Panayioutou, A. (ed.),

Ophiolites: Proc. Int. Oph. Symp., 1979, Cyprus. Geol. Sur. Dept., pp. 727-743.

Gronlie, A., 1988. Platinum Group Minerals in the Lillefjellklumpen Ni-Cu deposit, Nord-Trondelag, Norway. Nor. Geol. Tidsskr., v. 68, pp. 65-72.

Hamlyn, P.R. and Keays, R R., 1986. Sulfur saturation and second stage melts: Applications to the Bushveld Platinum metal deposits. Econ. Geol. v. 81, pp. 1431-1445.

Hamlyn, P.R., Keays, R.R., Warrington, E.C., Cameron, W.E., Crawford, A.J. and Waldron, H.M., 1985. Precious metals in Magnesian low-Ti lavas: Implications for metallogenesis and sulfur saturation in primary magmas. Geochim. Cosmochim. Acta, v. 49, pp. 1797-1811.

Hayman, R.M., Koski, R.A. and Sinclair, C., 1984. Fossils of hydrothermal vent worms from Cretaceous ssulfide ores of the Semail Ophiolite, Oman. Science, v. 223, pp. 1407-1409.

Heaton, T.H.E. and Sheppard, S.M.F., 1977. Hydrogen and oxygen isotope evidence for seawater-hydrothermal alteration and ore deposition. Troodos Complex, Cyprus. In Volcanic processes in ore genesis. London inst. min. metall. and geol. soc. pp. 42-47.

Heim, M., 1981. Basement/cover relations in the allochthon at Espedalen (Jotun-Valdres Nappe Complex, SW Norway). Terra Cognita v. 1, 51 (abs).

Hellman, P.L., Smith, R.E. and Henderson, P., 1979. The mobility of the REE's: evidence and implications from selected terrains affected by burial metamorphism. Contrib. Mineral. Petrol., v. 71, pp. 23-44.

Hudson, D.R., 1986. PGM's from the Kambalda Ni deposits, Western Australia. Econ. Geol. v. 81, pp. 1218-1225.

Hudson, K., 1988. Mineralization in the Nipper's Harbour Ophiolite, Nfld. M.Sc. thesis, Dept. of EASC, Memorial Univ. Nfld.

Irvine, T.N., 1975. Crystallization sequences in the Muskox Intrusion and other layered intrusions. II. Origin of chromitite layers and similar deposits of other magmatic ores. Geochim. Cosmochim. Acta, v. 39, pp. 991-1020.

Irvine, T.N., Keith, D.W. and Todd, J.G., 1983. The J-M Pt-Pd Reef of the Stillwater Complex, Montana: II. Origin by double diffusive convective magma mixing and implications for the Bushveld Complex. Econ. Geol., v. 78, pp. 1287-1334.

Keays, R.R., Nickel, E.H., Groves, D.I. and McGoldrick, P.J., 1982. Ir and Pd as discriminants of volcanic exhalative, hydrothermal, and magmatic Ni-sulfide mineralization. Econ. Geol., v. 77, pp. 1535-1547.

Kelley, D.S., Robinson, P.T. and Malpas, J.G., 1991 (in press). Processes of brine generation and circulation in the oceanic crust: Fluid inclusion evidence from the Troodos Ophiolite,

Cyprus. Jnl. Geophys. Res.

Langmhyr, F.G. and Paus, P.E., 1968. The analysis of inorganic siliceous materials by spectrophotometry and the hydrofluoric acid decomposition technique. Part 1. The analysis of silicate rocks. Anal. Chimica. Acta, v.43, pp. 397-408.

Longerich, H.P. and Veinott, G., 1986. Study of precision and accuracy of XRF data obtained in the Dept. of EASC and CERR at Memorial University. Unpublished report.

Lydon, J.W. and Galley, A., 1987. Chemical and mineralogical zonation of the Mathiati alteration pipe, Cyprus, and its genetic significance. Report for the Geol. Sur. Can., pp. 49-68.

Mainwaring, P.R. and Naldrett, A.J., 1977. Country rock assimilation and the genesis of Cu-Ni sulfides in the Waterhen Intrusion, Duluth Complex, Minnesota. Econ. Geol., v. 72, pp. 1269-1284.

Malpas, J.G., 1989. Pers. comm., Dept. of EASC, Memorial Univ. Nfld.

Mottl, M.J., 1983. Metabasalts, axial hot springs, and the structure of hydrothermal systems at mid-ocean ridges. Geol. Soc. Amer. Bull., v. 94, pp. 161-180.

Naldrett, A.J., 1979. Ni-Cu sulfide deposits: Magmatic or hydrothermal? A response and discussion. Econ. Geol. v. 74, pp. 1520-1528.

Naldrett, A.J., 1981a. Ni-sulfide deposits: Classification, composition and genesis. Econ. Geol., 75 anniv. vol., pp. 628-685.

Naldrett, A.J. and Barnes, S.J., 1986. The behavior of PGE's during fractional crystallization and partial melting with special reference to the composition of magmatic sulfide ores. Fortschritte der Mineralogie, v. 64, pp. 113-133.

Naldrett, A.J. and Cabri, L.J., 1976. Ultramafic and related mafic rocks: Their classification and genesis with special reference to the concentration of Ni-sulfides and PGE's. Econ. Geol., v. 71, pp. 1131-1158.

Naldrett, A.J. and Duke, J.M., 1980. Platinum metals in magmatic sulfide ores. Science, v. 208, pp. 1417-1424.

Naldrett, A.J. Hoffman, E.L., Green, A.H., Chen Lin Chou and Naldrett, S.R., 1979. The composition of Ni sulfide ores with particular reference to their content of PGE's and Au. Can. Mineral., v. 17, pp. 403-415.

Nehlig, P., 1989. Supercritical two-phase separation of hydrothermal fluids in the Semail Ophiolite. EOS Trans. Amer. Geophys., v. 70, pp. 1396.

Neiva, A.M.R., 1974. Geochemistry of tourmaline (schorlite) from aplites, granites and

pegmatites from Northern Portugal. Geochim. Cosmochim. Acta, v. 38, pp. 1307-1317.

Oudin, E., 1983. Hydrothermal sulfide deposits of the East Pacific Ridge (21N), Part 1: Descriptive Mineralogy. Marine Min., v. 4, pp. 39-72.

Paktunc, A.D., 1987. Ni, Cu, Pt and Pd relations in Ni-Cu deposits of the St. Stephen intrusion, New Brunswick. In Current Research, Part A, Geol. Sur. Can. Paper 87-1A, pp. 543-553.

Panayioutou, A., 1985. Sulfide and arsenide mineralization associated with the basic and ultrabasic plutonic rocks of the Troodos Ophiolite, Cyprus. Geol. Sur. Dept., Nicosia, Cyprus. pp. 417-447.

Pedersen, R.B., 1982. The Karmoy Ophiolite Plutonic Suite. Cand. Real. thesis, Univ. Bergen, Norway.

Pedersen, R.B., 1986. The nature and significance of magma chamber margins in ophiolites: examples from the Norwegian Caledonides. Earth Planet. Sci. Letts., v. 77, pp. 100-112.

Pedersen, R.B., 1987. Pers. comm., Dept. of Easc, Memorial University of NFLD, St. John's, NFLD.

Pedersen, R.B. and Hertogen, J., 1987. Magmatic evolution of the Karmoy Ophiolite Complex.

Pedersen, R.B. and Malpas, J.G., 1984. The origin of oceanic plagiogranites from the Karmoy Ophiolite, Western Norway. Contrib. Mineral. Petrol., V. 88, pp. 36-52.

Pedersen, R.B., Furnes, H. and Dunning, G., 1987. Norwegian ophiolite complexes reconsidered.

Potter, R.W., 1977. Pressure corrections for fluid inclusion homogenization temperatures based on the volumetric properties of the system NaCl-H2O. Jnl. Res. U.S. Geol. Sur., v. 5, no. 5, pp.603-607.

Power, G.M., 1968. Chemical variation in tourmalines from Southwest England. Mineralog. Mag., v. 36, pp. 1078-1089.

Priem, H. and Torske, T., 1973. Rb-Sr isochron age of Caledonian acid volcanics from Stord, Western Norway. Nor. Geol. Unders., v. 300, pp. 83-85.

Ramberg, I.B., 1968. Kongsfjell-omradets geologi, en petrografisk og strukturell undersokelse i Helgeland, Nord-Norge. Nor. Geol. Tidsskr., v. 53, pp. 433-442. (47).

Ramdohr, P., 1980. The ore minerals and their intergrowths. Toronto, Pergammon Press, 1205pp.

Reinsbakken, A., 1980. Geology of the Skorovass Mine: A volcanogenic massive sulfide deposit

in the Central Norwegian Caledonides. Nor. Geol. Unders., v. 360, pp. 123-154.

Richards, H.G. and Cann, J.R., 1989. Mineralogical zonation and metasomatism of the alteration pipes of Cyprus sulfide deposits. Econ. Geol., v. 84, pp. 91-115.

Richardson, C.J., Cann, J.R., Richards, H.G. and Cowan, J.G., 1987. Metal-depleted root zones of the Troodos ore-forming hydrothermal system, Cyprus. Earth Planet. Sci. Letts., v. 84, pp. 243-253.

Rockingham, C. and Hutchinson, R., 1980. Metamorphic textures in Archaen Cu-Zn massive sulfide deposits. Can. Inst. Min. Bull., April, 1980. pp. 104-112.

Roddick, J.C., 1977. Age of the Rana Massif, North Norway. Fifth Eur. Colloq. Geochron. Cosmschron. and Isotope Geol. Pisa (abstr.)

Ross, J.R. and Hopkins, G.M.F., 1975. Kambalda Ni sulfide deposits. Australasian Inst. Min. Metall. Mon. 5, pp. 100-121.

Rowell, W.F. and Edgar, A.D., 1986. Platinum Group Element mineralization in a hydrothermal Cu-Ni sulfide occurrence, Rathbun Lake, NE Ontario. Econ. Geol., v. 81, pp. 1272-1279.

Saunders, C., 1985. Controls of mineralization in the Bett's Cove Ophiolite. Masters thesis, Dept. of EASC, Memorial Univ. Nfld. 215pp.

Saunders, C.M. and Strong, D.F., 1986. Alteration-zonation related to variations in water/rock ratio at the Bett's Cove ophiolitic massive sulfide deposit, Nfld, Can. Extract from Met. of basic and ultrabasic rocks. Inst. Min. Metall. Conf. Proc. pp. 161-175.

Scott, J., 1985. The geology, petrology and geochemistry of the Visnes region, Karmoy, Southwest Norway. B.Sc. (hons.) thesis, Dept. of Easc, Memorial univ. of Nfld.

Seyfried, W.E.Jr., Mottl, M.J. and Bischoff, J.I., 1978. Seawater-basalt ratio effects on the chemistry and mineralogy of spilites from the ocean floor. Nature, v. 275, pp. 211-213.

Sheppard, S.M.F., 1978. Isotopic evidence for the origins of water during metamorphic processes in oceanic crust and ophiolite complexes.

Sillitoe, R.H., 1972. Formation of certain massive sulfide deposits at sites of seafloor spreading. Trans. Inst. Min. Met., Sect. B, Appl. Earth Sci., v. 81, pp. 141-148.

Sillitoe, R.H., 1985. Ore-related breccias in volcano-plutonic arcs. Econ. Geol. v. 80, pp. 1467-1514.

Singsaas, P. and Skjerlie, J., 1958. Industridepartementet/Bergverkskontoret. G. M. Rapport nr. 225.

Skinner, B.J., 1987. Pers. comm., Dept. of EASC, Memorial univ., Nfld.

Slack, J.F., 1980. Tourmaline- A prospecting guide for massive base-metal sulfide deposits in the Penobscot Bay area, Maine. Maine Geol. Sur., Spec. Econ. Studies Ser. 8, 25pp.

Spooner, E.T., 1977. Hydrodynamic model for the origin of ophiolitic cupriferous pyrite ore deposits of Cyprus. In Volcanic processes in ore genesis. Inst. Min. Metall. and Geol. Soc., pp. 58-71.

Spooner, E.T. and Fyfe, W.S., 1973. Sub-seafloor metamorphism, heat and mass transfer. Contrib. Min. Petrol., v. 42, pp. 287-304.

Stevens, M.B., 1980. Spilitization, elemental release, and formation of massive sulfides in the Stekenjokk volcanites, Central Swedish Caledonides. Nor. Geol. Unders. no. 360, pp. 159-193.

Stevens, M.B., Swinden, S. and Slack, J.F., 1984. Correlation of massive sulfide deopsits in the Appalachian-Caledonian orogen on the basis of paleo-tectonic setting. Econ. Geol., v. 79, pp. 1442-1478.

Strong, D.F. and Saunders, C.M., 1986. Geological setting of sulfide mineralization at Tilt Cove, Nfld. In Current Research, Part A, Geol. Sur. Can. Paper 86-1A, pp. 319-325.

Strong, D.F. and Saunders, C.M., 1987. Ophiolitic sulfide mineralization at Tilt Cove, Nfld: Controls by upper mantle and crustal processes. pp. 1-30.

Strong, D.F., 1988. Pers. comm., Dept. of EASC, Memorial Univ., Nfld.

Stumpfl, E.F., 1987. Distribution, transport and concentration of Platinum Group Elements. Inst. Mineral. Petrol. In Metallogeny of basic and ultrabasic rocks. Gallaher, Ixer, Neary and Prichard (eds.), pp. 379-394.

Sturt, B.A. and Thon, A., 1978a. Caledonides of Southern Norway. In IGCP project 27.

Sturt, B.A. and Thon, A., 1978b. An ophiolite complex of probable Early Caledonian age discovered on Karmoy. Nature, v. 275, pp. 538-539.

Sturt, B.A., Thon, A. and Furnes, H., 1979. The Karmoy Ophiolite, SW Norway. Geol., v. 7, pp. 316-320.

Sturt, B.A., Thon, A. and Furnes, H., 1980. The geology and preliminary geochemistry of the Karmoy Ophiolite, Southwest Norway. Proc. Int. Oph. Symp., Cyprus. pp. 538-554.

Taylor, B.E. and Slack, J.F., 1984. Tourmalines from Appalachian-Caledonian massive sulfide deposits: Textural, chemical and isotopic relations. Econ. Geol. v. 79, pp. 1703-1726.

Taylor, H.P., 1979. O and H isotope relationships in hydrothermal mineral deposits. In Barnes, H.L. (ed.), Geochemistry of hydrothermal ore deposits, second ed., New York Wiley. pp. 236-277.

Taylor, H.P., 1980. Stable isotope studies of spreading centers and their bearing on the origin of granophyres and plagiogranites. Contrib. no. 3190, Div. geol. planet. sci., Cal. Inst. Tech., pp. 9-25.

Thayer, T.P., 1976. Metallogenic contrasts in the plutonic and volcanic rocks of the ophiolite assemblage. GAC Spec. Paper no. 14, pp. 211-219.

Vokes, F.M., 1968. Regional metamorphism of the Paleozoic geosynclinal sulfide deposits of Norway. Trans. Inst. Min. Metall., v. 77, B53-59 (70).

Vokes, F.M., 1969. A review of metamorphism of sulfide deposits. Earth Sci. Rev., v. 5, pp. 99-143.

Vokes, F.M., 1976. Caledonian massive sulfide deposits in Scandinavia: A comparative review. In Handbook of strata-bound and strati-form ores (Wolf, H., ed.), v. 6, ch. 4, Elsevier, pp. 79-127.

Vokes, F.M., 1979. Some aspects of research into the Caledonian strata-bound sulfide deposits of Scandinavia. Nor. Geol. Unders., v. 360, pp. 77-93.

Vokes, F.M., 1988. Pers. comm., Dept. of EASC, Memorial Univ., Nfld.

Vokes, F.M. and Gale, G.H., 1976. Metallogeny related to global tectonics in Southern Scandinavia. Geol. assoc. Can. Spec. Paper no. 14, pp. 413-441.

Von Damm, K.L., 1988. Systematics and postulated controls on submarine hydrothermal solution chemistry. Jnl. Geophys. Res., v. 93, pp. 4551-4561.

Wilson, H.D.B. and Anderson, D.T., 1959. The composition of Canadian sulfide ore deposits. Can. Inst. Min. Metall. Trans., v. 62, pp. 327-339.

Yund, R.A. and Kullerud, G., 1966. Thermal stability of assemblages in the Cu-Fe-S system. Jnl. Petrol., v.7, pp. 454-488.

Appendix 1: Accuracy data for major element analyses of the Visnes dykes.

ACCURACY OF ANALYSES OF MAJOR ELEMENTS

By

ATOMIC ABSORPTION SPECTROPHOTOMETRY

BE-N (BASALT)

OXIDES	PUBLISHED VALUE (WT%)	NO. ANALYSES	MEAN (WT%)	DIFFERENCE OF MEAN PUBLISHED VALUE	STANDARD DEVIATION	RANGE OF VALUES (%)
SiO_2	38.20	6	38.50	+0.30	0.18	38.21-38.67
TiO_2	2.61	6	2.59	-0.02	0.04	2.56-2.64
Al_2O_3	10.07	6	10.02	-0.05	0.09	9.85-10.10
Fe_2O_3T	12.84	6	12.84	0.00	0.11	12.69-12.96
CaO	13.87	6	13.91	+0.04	0.05	13.84-13.96
MgO	13.15	6	13.14	0.03	0.07	13.04-13.27
Na_2O	3.18	6	3.25	+0.07	0.02	3.22-3.28
K_2O	1.39	6	1.46	+0.07	0.007	1.45-1.47
MnO	0.20	6	0.19	-0.01	0.00	0.19-0.19

Appendix 2: Electron microprobe analyses of selected minerals from rock samples in the study area.

	Na	Mg	Al	Si	K	Ca	Ti	Cr	Mn	Fe	Ni	Total
Chlorite (on the basis of 36 oxygens)												
bg	6.3	1.59	3.19	3.88	2.73	4.92	9.35	22.55	2.83	4.26	6.45	
Cl	0.06	9.59	9.15	11.52	0.02	0.05	0.02	0.0	0.29	16.85	0.05	
bc	0.08	15.9	17.29	24.65	0.03	0.06	0.02	0.0	0.38	21.67	0.06	
ac	0.11	17.39	18.75	27.80	0.03	0.07	0.02	0.0	0.38	21.62	0.07	96.24
fm	0.026	3.884	3.312	4.165	0.004	0.009	0.0	0.0	0.048	2.709	0.004	14.163
Hornblende (on the basis of 24 oxygens)												
bg	25.95	2.14	3.34	5.34	2.95	6.06	11.37	20.95	2.98	4.54	6.67	
Cl	0.34	8.46	1.44	25.21	0.05	8.11	0.03	0.02	0.28	10.61	0.04	
bc	0.46	14.02	2.72	53.93	0.06	11.34	0.05	0.03	0.36	13.65	0.04	
ac	0.53	14.73	2.78	53.27	0.07	11.61	0.05	0.03	0.37	13.84	0.05	97.32
fm	0.151	3.324	0.493	8.066	0.009	1.884	0.004	0.0	0.044	1.751	0.004	15.732
Actinolite (on the basis of 24 oxygens)												
bg	23.2	1.35	3.17	4.60	3.83	4.95	10.69	19.54	3.47	4.60	na	
Cl	0.51	10.57	0.13	27.23	0.0	8.62	0.0	0.02	0.14	7.65	na	
bc	0.69	17.52	0.25	58.24	0.0	12.06	0.0	0.03	0.18	9.34	na	
ac	0.76	17.35	0.25	56.82	0.0	12.41	0.0	0.03	0.19	10.04	na	98.36
fm	0.207	3.745	0.041	8.002	0.0	1.873	0.0	0.0	0.021	1.182	na	15.070

na = not analized

Appendix 3: Major and Trace element analyses for the Visnes dykes (1 to 23), the High Mg dykes (24 to 28), and selected basalts from various tectonic environments (29 and 30 are typical unaltered island arc tholeiites, IAT; 31 to 33 are spilites of an island arc nature; 34 is average unaltered MORB composition; 35 is average unaltered boninite composition). Data sources are given in caption for Fig. 5.1. Major elements are given in weight per cent, and Trace elements are in ppm.

sample	Label	SiO2	TiO2	Al2O3	Fe2O3	MnO
1.00	a	53.70	1.84	12.60	11.58	0.21
2.00	a	52.50	0.92	16.00	8.62	0.08
3.00	a	55.20	1.88	11.60	18.76	0.10
4.00	a	60.30	0.24	15.90	8.78	0.11
5.00	a	53.50	1.80	12.10	18.41	0.10
6.00	a	49.90	1.72	13.80	15.09	0.22
7.00	a	51.30	2.28	13.10	19.27	0.11
8.00	a	48.60	1.76	13.60	15.37	0.20
9.00	a	60.30	0.24	15.90	8.78	0.11
10.00	a	56.30	1.72	14.00	8.58	0.09
11.00	a	50.90	2.00	16.90	9.47	0.13
12.00	a	65.50	1.20	13.50	6.16	0.09
13.00	a	53.40	0.56	15.50	9.85	0.14
14.00	a	48.00	1.88	14.40	16.31	0.19
15.00	a	58.10	1.64	14.10	8.51	0.09
16.00	a	48.50	1.36	14.40	12.44	0.16
17.00	a	55.40	1.61	11.50	18.14	0.10
18.00	a	50.40	0.80	15.30	9.50	0.17
19.00	a	49.10	1.60	14.60	11.22	0.14
20.00	a	50.90	1.48	14.10	12.04	0.20
21.00	a	54.80	0.92	15.50	8.93	0.10
22.00	a	51.50	1.32	13.60	12.55	0.18
23.00	a	46.60	1.96	15.80	10.93	0.17
24.00	b	49.80	0.76	14.10	9.03	0.21
25.00	b	43.20	0.68	11.30	20.39	0.31
26.00	b	46.80	0.40	15.60	8.74	0.15
26.00	b	50.20	0.76	14.20	10.28	0.17
28.00	b	47.60	1.04	15.00	10.52	0.18
29.00	c	48.70	0.63	16.00	8.74	0.12
30.00	c	53.60	1.15	19.83	11.80	0.29
31.00	d	50.30	0.38	15.50	8.62	0.18
32.00	d	54.30	0.70	17.10	13.60	0.24
33.00	d	51.90	1.60	16.30	10.80	0.19
34.00	e	50.20	1.50	16.25	9.63	0.18
35.00	f	55.30	0.21	9.47	9.48	0.18

sample	Label	MgO	CaO	Na2O	Na2O/CaO
1.00	a	5.56	6.48	5.37	0.83
2.00	a	2.24	13.98	2.95	0.21
3.00	a	5.00	2.16	3.39	1.57
4.00	a	3.65	1.52	6.60	4.34
5.00	a	4.71	3.32	3.08	0.93
6.00	a	4.95	8.04	4.41	0.55
7.00	a	4.71	2.86	3.90	1.36
8.00	a	5.33	7.00	4.18	0.60
9.00	a	3.65	1.52	6.60	4.34
10.00	a	4.50	5.08	6.99	1.38
11.00	a	6.10	4.08	6.50	1.59
12.00	a	2.98	1.80	6.15	3.42
13.00	a	6.30	6.96	2.16	0.31
14.00	a	5.34	7.28	4.10	0.56
15.00	a	3.47	7.12	4.26	0.60
16.00	a	8.40	6.58	3.90	0.59
17.00	a	4.75	1.82	3.13	1.72
18.00	a	7.50	8.52	4.48	0.53
19.00	a	7.29	7.16	4.94	0.69
20.00	a	8.40	5.60	4.71	0.84
21.00	a	4.23	8.72	5.40	0.62
22.00	a	8.21	6.08	4.57	0.75
23.00	a	6.16	9.00	4.06	0.45
24.00	b	10.83	7.70	3.61	0.47
25.00	b	8.91	10.86	1.24	0.11
26.00	b	11.07	12.40	2.13	0.17
26.00	b	9.80	8.62	3.43	0.40
28.00	b	10.35	8.28	3.14	0.38
29.00	c	3.74	9.00	1.20	0.13
30.00	c	8.96	12.25	3.30	0.27
31.00	d	6.10	5.20	3.70	0.71
32.00	d	8.50	8.20	5.90	0.72
33.00	d	5.60	8.00	4.30	0.54
34.00	e	7.74	11.30	2.84	0.25
35.00	f	14.98	8.09	1.75	0.22

sample	Label	K2O	P2O5	Total	Rb
1.00	a	0.13	0.23	98.89	0.00
2.00	a	0.12	0.38	99.45	2.00
3.00	a	0.04	0.20	100.75	2.00
4.00	a	0.18	0.05	99.92	2.00
5.00	a	0.04	0.33	99.86	0.00
6.00	a	0.18	0.27	100.08	1.00
7.00	a	0.05	0.20	100.47	1.00
8.00	a	0.15	0.15	98.13	0.00
9.00	a	0.18	0.05	99.92	3.00
10.00	a	0.10	0.26	98.38	0.00
11.00	a	0.08	0.03	100.43	0.00
12.00	a	0.08	0.59	99.45	1.00
13.00	a	0.17	0.04	98.52	6.00
14.00	a	0.16	0.16	99.95	3.00
15.00	a	0.21	0.26	99.19	5.00
16.00	a	0.07	0.04	98.68	0.00
17.00	a	0.04	0.20	99.20	0.00
18.00	a	0.09	0.13	100.08	0.00
19.00	a	0.08	0.13	100.45	0.00
20.00	a	0.06	0.17	100.42	0.00
21.00	a	0.09	0.26	100.01	0.00
22.00	a	0.08	0.08	100.27	0.00
23.00	a	0.23	0.73	98.07	3.00
24.00	b	0.11	0.05	98.98	2.00
25.00	b	0.51	0.29	100.28	20.00
26.00	b	0.05	0.02	100.81	0.00
26.00	b	0.07	0.03	100.00	0.00
28.00	b	0.09	0.06	99.50	4.00
29.00	c	0.23	0.10		
30.00	c	2.18	0.40		
31.00	d	0.00	0.05	99.60	
32.00	d	0.40	0.07	99.60	
33.00	d	1.20	0.32	100.20	
34.00	e	0.20	0.13	99.97	
35.00	f	0.28			

sample	Label	Cu	Ni	V	Cr
1.00	a	1.00	4.00	370.00	0.00
2.00	a	386.00	0.00	81.00	0.00
3.00	a	0.00	0.00	520.00	0.00
4.00	a	3.00	0.00	299.00	0.00
5.00	a	0.00	0.00	292.00	0.00
6.00	a	16.00	0.00	520.00	0.00
7.00	a	19.00	0.00	516.00	0.00
8.00	a	10.00	0.00	571.00	0.00
9.00	a	17.00	0.00	315.00	0.00
10.00	a	4.00	0.00	214.00	0.00
11.00	a	125.00	3.00	340.00	0.00
12.00	a	4.00	0.00	59.00	0.00
13.00	a	49.00	8.00	265.00	0.00
14.00	a	14.00	0.00	571.00	0.00
15.00	a	3.00	0.00	173.00	0.00
16.00	a	9.00	14.00	372.00	0.00
17.00	a	0.00	0.00	485.00	0.00
18.00	a	8.00	28.00	208.00	108.00
19.00	a	30.00	62.00	366.00	217.00
20.00	a	26.00	103.00	363.00	342.00
21.00	a	7.00	22.00	182.00	46.00
22.00	a	0.00	57.00	360.00	219.00
23.00	a	25.00	29.00	259.00	32.00
24.00	b	15.00	125.00	216.00	537.00
25.00	b	0.00	81.00	233.00	591.00
26.00	b	129.00	152.00	219.00	532.00
26.00	b	3.00	157.00	215.00	398.00
28.00	b	10.00	133.00	277.00	497.00
29.00	c	50.00	18.00	188.00	15.00
30.00	c	159.00	196.00	294.00	535.00
31.00	d	17.00	17.00		7.00
32.00	d	45.00	27.00		75.00
33.00	d				
34.00	e	77.00	97.00		297.00
35.00	f		367.00		1410.00

sample	Label	Nb	Sr	Zr	Zn
1.00	a	3.00	66.00	162.00	79.00
2.00	a	5.00	487.00	203.00	2.00
3.00	a	5.00	26.00	86.00	27.00
4.00	a	2.00	94.00	44.00	55.00
5.00	a	3.00	99.00	114.00	24.00
6.00	a	5.00	96.00	94.00	108.00
7.00	a	2.00	68.00	108.00	40.00
8.00	a	2.00	91.00	85.00	109.00
9.00	a	5.00	42.00	41.00	67.00
10.00	a	4.00	50.00	148.00	16.00
11.00	a	3.00	53.00	31.00	47.00
12.00	a	5.00	49.00	186.00	93.00
13.00	a	3.00	186.00	24.00	55.00
14.00	a	4.00	101.00	99.00	110.00
15.00	a	3.00	226.00	190.00	19.00
16.00	a	2.00	182.00	78.00	52.00
17.00	a	4.00	26.00	88.00	32.00
18.00	a	4.00	349.00	46.00	52.00
19.00	a	2.00	89.00	123.00	90.00
20.00	a	3.00	55.00	90.00	62.00
21.00	a	5.00	279.00	332.00	26.00
22.00	a	2.00	59.00	69.00	80.00
23.00	a	40.00	539.00	237.00	94.00
24.00	b	3.00	137.00	42.00	174.00
25.00	b	7.00	127.00	71.00	233.00
26.00	b	1.00	125.00	9.00	64.00
26.00	b	3.00	110.00	38.00	86.00
28.00	b	2.00	161.00	59.00	80.00
29.00	c	0.28	135.00	15.00	65.00
30.00	c	3.90	540.00	86.00	89.00
31.00	d			14.00	69.00
32.00	d			34.00	89.00
33.00	d				
34.00	e			95.00	
35.00	f				

Appendix 4: Sample descriptions of selected rock samples used in the present study.

1- Samples used in Table 2.1:

21EPDT- sample of fine to medium grained, moderately altered epidotite taken from an outcrop near the old bridle path in Visnes (see Figure 2.1).

22EPDT- as per 21EPDT, except more extensively altered.

48EPDT- sample taken from the Fiskdammen area of Visnes, from an outcrop containing biotite-diorite. Sample is crosscut by quartz veins and is moderately weathered.

17- fragment of epidosite taken from selectively mineralized dyke in the Fiskdammen area.

15- as per 17 above.

12- zone of intensely altered basalt dykes in the Feoy area. There is extensive mineralization in this outcrop.

2- Samples used in Table 3.1:

V2- sample of metamorphosed, banded cpy-sp-py. Relatively fresh sample.

V9- banded py-sp. Note minor amounts of cpy.

V15- massive py-cpy from drill core in main Visnes deposit.

V22- massive sp sample from mine dump area of Visnes. Highly altered sample.

V28- massive py and minor cpy in quartz gangue from Visnes mine dump.

3- Samples used in Table 6.1:

C12- sample taken from outcrop of siliceous, epidote-rich dykes cutting through zone of brecciation, in the Visnes area. Sample is quite fresh.

05-04- sample of epidotite xenolith in mineralized basalt dyke. Xenolith is cut by chlorite veins.

05-5- plagiogranite sample from same area as 05-04 above (Fiskdammen). Sample is quite fresh, but also quite altered.

05-2- plagiogranite sample from plagiogranite pod in area dominated by basalt dykes and biotite-diorite (Dymes). Plagiogranite may be a large xenolith.

22-5- basalt dyke cutting gabbro. Dyke is heavily mineralized, while the host rock is unmineralized.

4- Samples used in Table 6.2:

46TRN- sample taken from plagiogranite pod in area around Visnes mine dump. Sample is medium grained and relatively fresh.

73TRN- sample taken from plagiogranite ridge in northern Visnes area. Cut by quartz and chlorite veins.

18TRN- as per 73TRN above.

51TRN- sample taken from plagiogranite dyke cutting basalt on one of the nearby offshore skerries in the Visnes area. Sample is quite fresh, and is moderately pyritized.

47TRN- as per 51TRN above.

5- Samples used in Figure 7.1:

F33- sample of massive cpy-po cut by tourmaline vein. Sample is from Type A breccia zone in the Feoy mine area.

F11- sample of massive cpy fragment in Type A breccia from the Feoy mine dump.

F35- sample of massive po with bands of cpy. Sample is relatively fresh.

F24a- sample of massive po and cpy from Type A breccia.

6- Samples used in Figure 7.3:

15Visnes- sample of fresh, unmineralized but quite altered Visnes dyke. From the sheeted dyke sequence seen in the northern Feoy area.

43-high-Mg- sample of high-Mg dyke from the Feoy area. Sample is quite fresh and unmineralized.

F31- sample of massive po with pyrite porphyroblasts and minor cpy.

F41- sample of deformed cpy in massive po with py porphyroblasts. From the Feoy mine dump.

7- Samples used in Table 7.2:

F41- as per F41 above.

F- sample of massive po with banded cpy.

F-b- sample of fresh, massive po with minor amounts of py and cpy.

JS-b- sample of fresh, unaltered massive po from mine dump in Feoy.

F36- massive po with deformed cpy bands.

F11- sample of massive cpy fragment found in Type A breccia.

F35- as per F35 above.

F10- sample of massive po with abundant cpy banding. Sample is quite altered.

F31- as per F31 above.

F7- fragment of rounded, massive po in tourmalinite sample from breccia zone in Feoy. Sample is quite altered and corroded.

F19- sample of massive po.

15Visnes- as per 15Visnes above.

43-high-Mg- as per 43-high-Mg above.

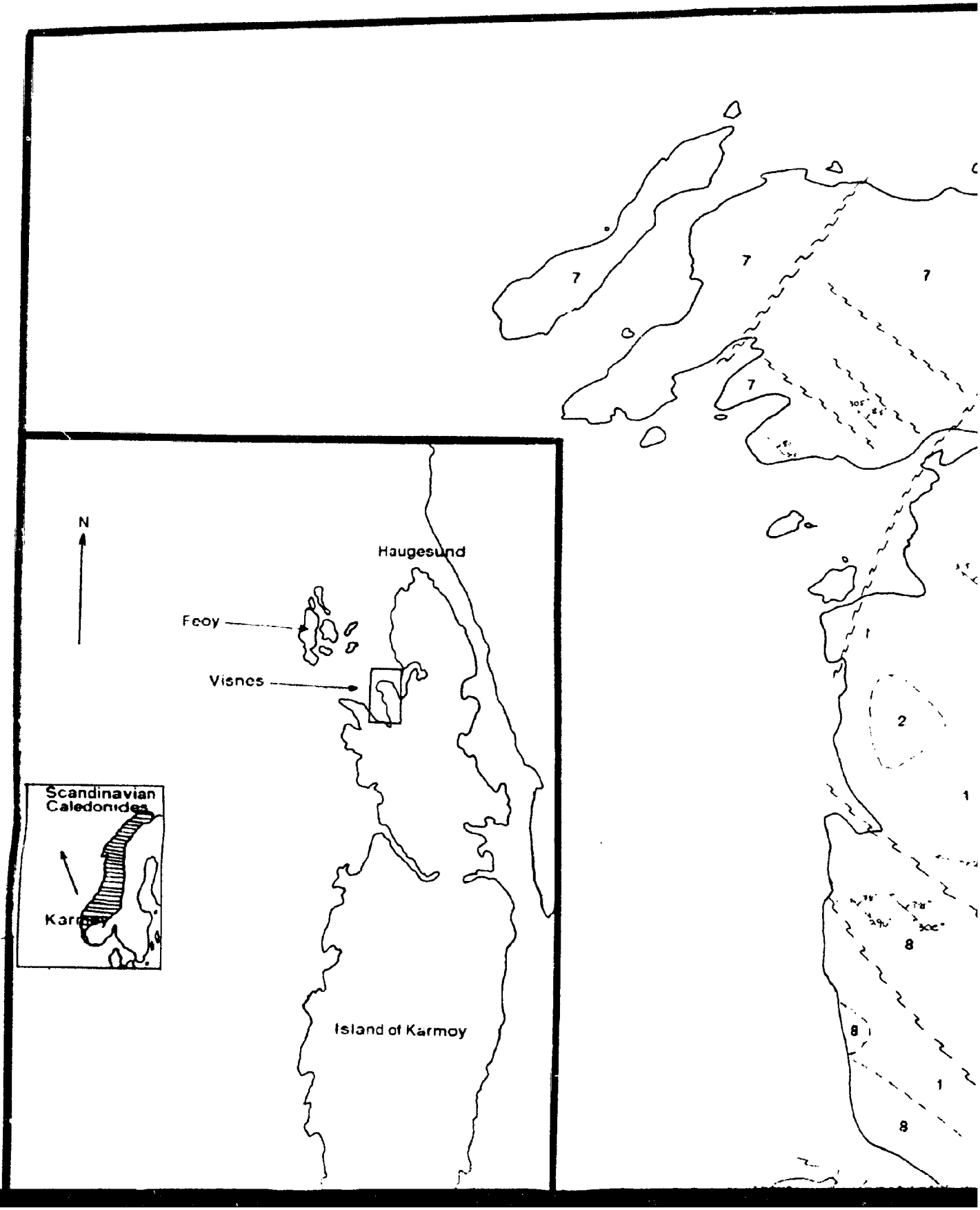
N
Haugesund
Feoy
Visnes
Scandinavian
Caledonides
Island of Karmoy

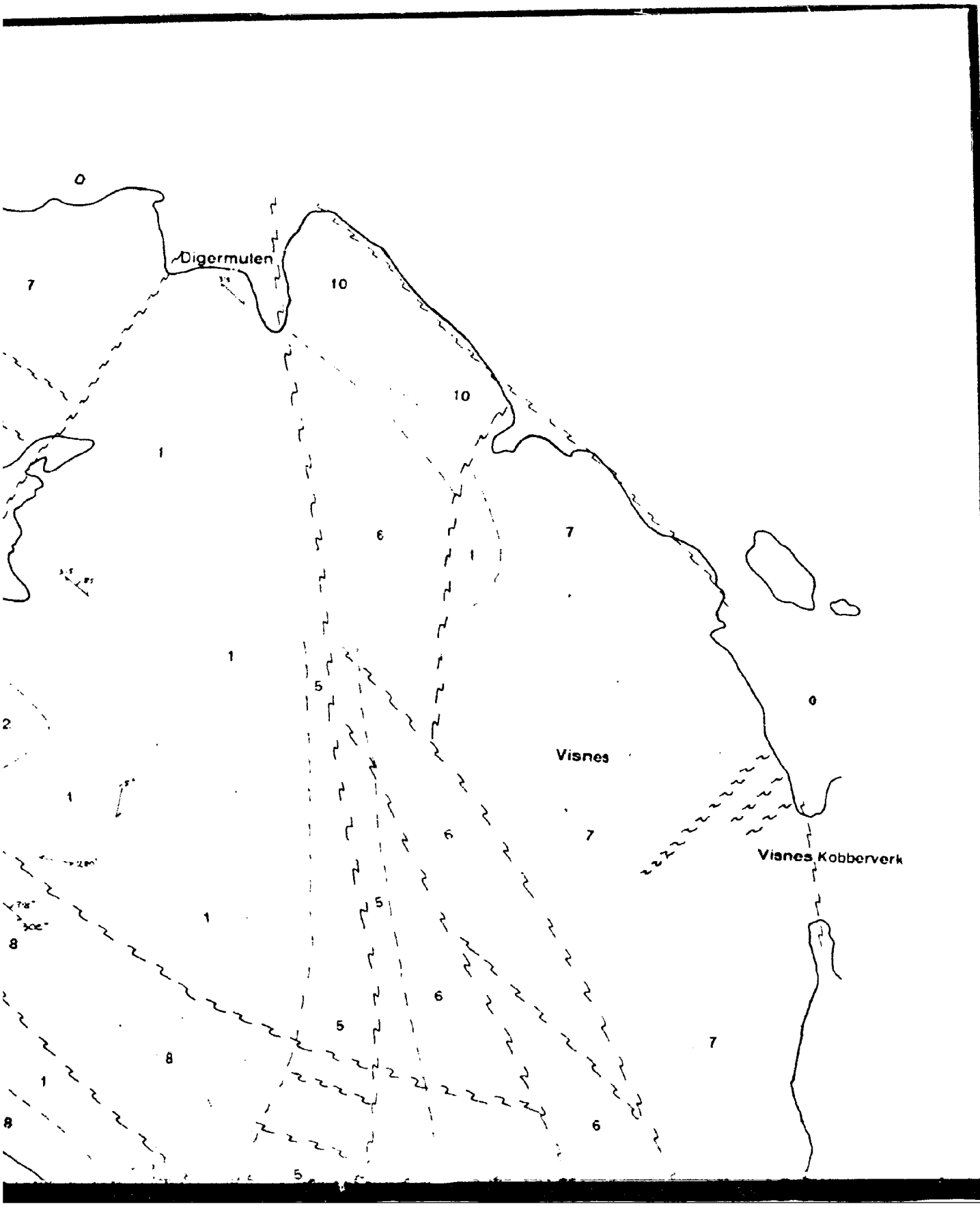
Digermulen
Visnes
Visnes Kobberverk

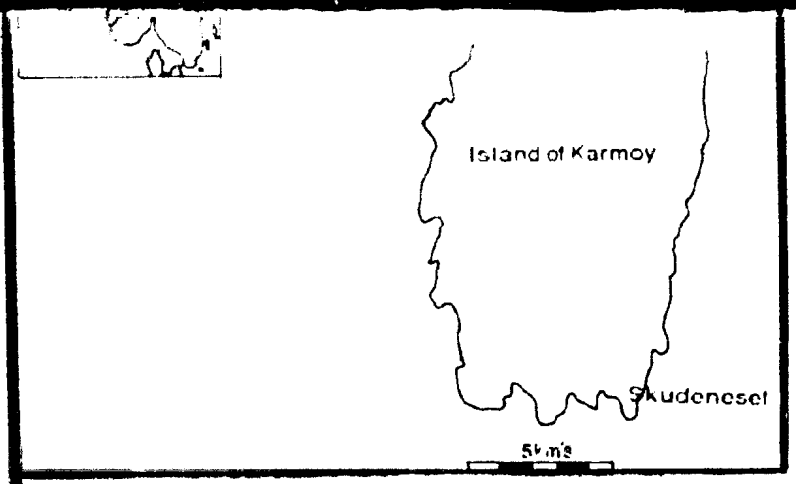

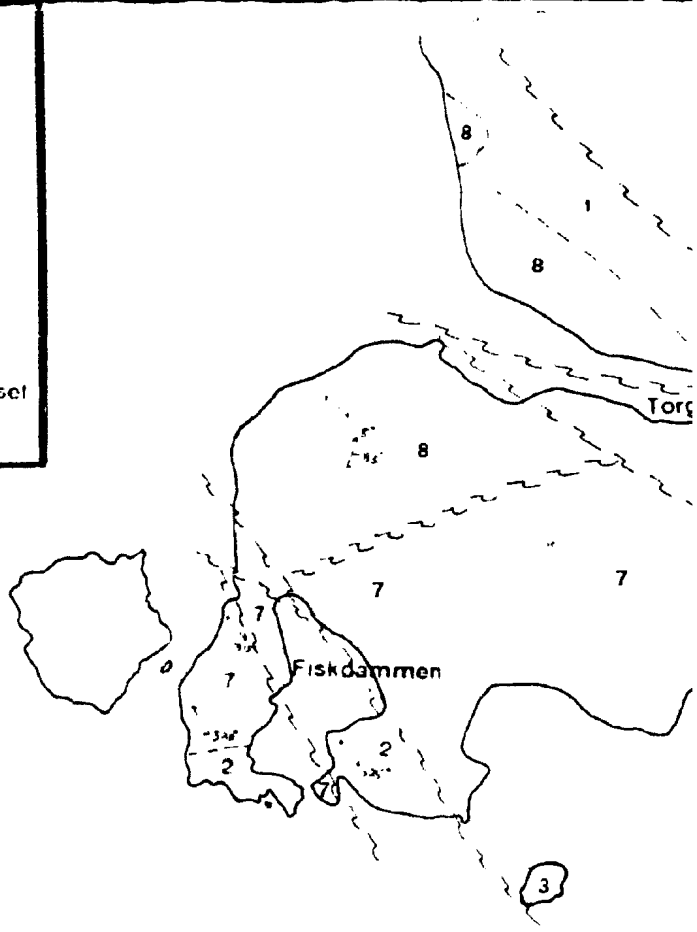

LEGEND

1	Sheeted Dykes (Part of the Visnes High Level Complex)
2	Gabbro
3	Type 1 Plagiogranite
4	Diorite
5	Greenschist
6	Highly altered deformed and recrystallized rocks bordering shear zones
7	Sheeted dykes with Type 1 plagiogranite screens
8	Gabbro with basic dykes
9	Gabbro diorite
10	Deformed volcaniclastic sediments of the Torvastad Group
	Strike-dip of dykes
	Shear zone
	Gradational or unidentified boundary

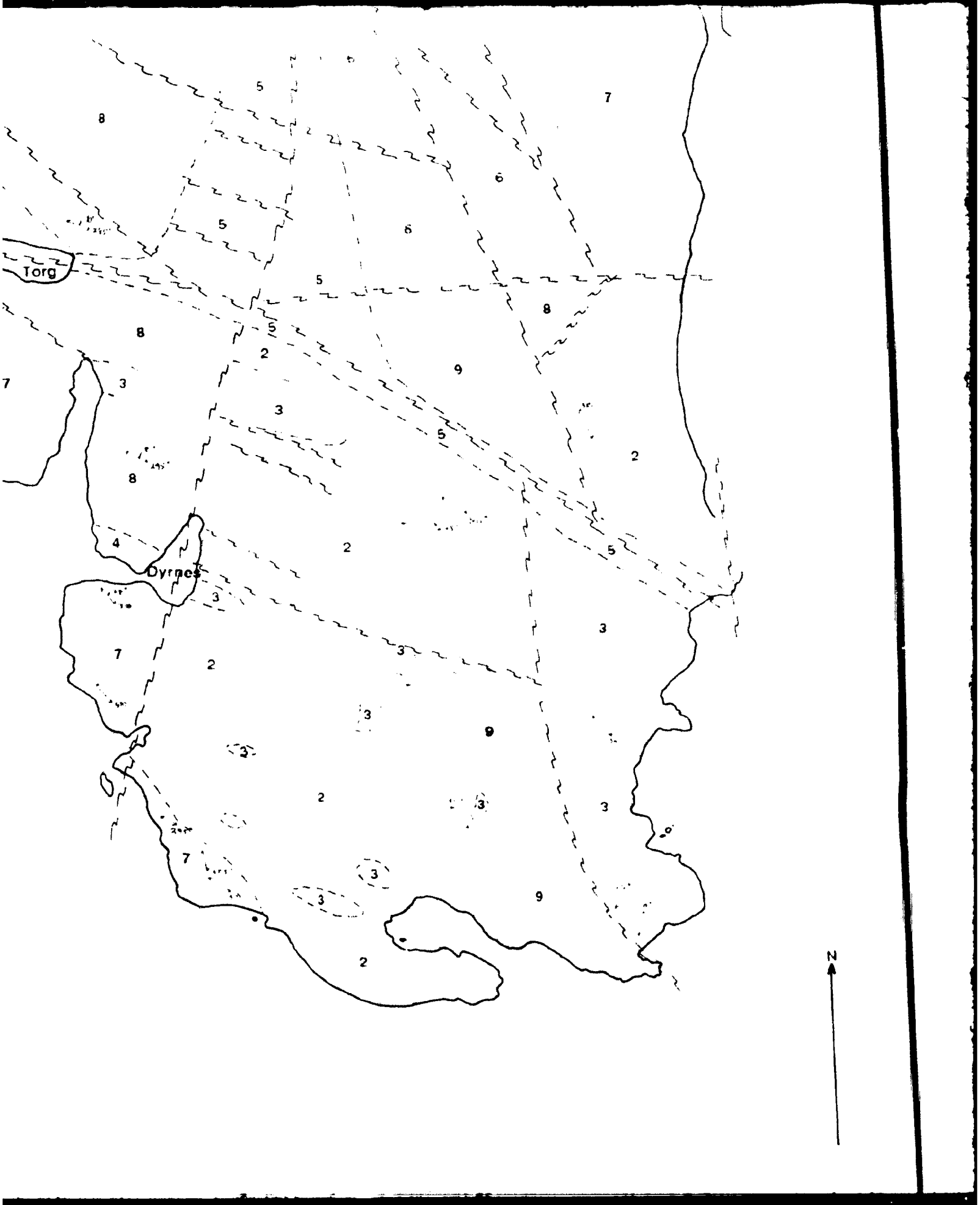
Torg
Dyrnes
N

GEOLOGICA
Compiled by

Scale 1:5000

0 50 100

N

OLOGICAL MAP OF VISNES, KARMOY, SOUTHWEST NORWAY

mpiled by. J L Scott 1991

e 1 5000

50 100 500M